Electronic Supplementary Material (ESI) for Chemical Communications.

Supporting Information

Exogenous Photocatalyst-Free Aryl Radical Generation from Diaryliodonium Salts and use in Metal-Catalyzed C–H Arylation

Jonathan Galicia,[†] Nicholas R. McDonald,[†] Christopher W. Bennett, Jiajun He, Mark D. Glossbrenner, Erik A. Romero*

Department of Chemistry and Biochemistry, University of California San Diego, La Jolla CA 92093-0309

E-mail: earomero@ucsd.edu

Table of Contents

Table of Figures

Table of Tables

Author Contributions: J.G. performed the kinetic investigation of pyridine the substrates in borylation reactions and radical trapping studies. J.H. and J.G. elucidated the LB scope of aryl radical generation from iodonium salts. M.D.G. identified preliminary conditions enabling a Pd-catalyzed photocatalyst-free arylation reactions on aryl pyridine substrates. N.R.M. performed the full optimization, and substrate scopes for the aryl pyridine and iodonium salts. C.W.B. optimized and elucidated the substrate scope for acetanilide-directed arylation reactions presented in the supplementary information. E.A.R. devised and managed the project, performed the computational investigation, and wrote the manuscript. All authors read, commented, and approved the final version of the manuscript.

A. General considerations

Unless indicated otherwise, all reactions were performed under an atmosphere of air. Reactions at elevated temperature were maintained by thermostatically controlled pre-heated aluminum heating block or water baths. Common organic solvents were purchased from Fisher scientific and used without further purification. $Pd(OTFA)_2$ (OTFA = trifluoroacetate) and $Pd(PPh_3)_4$ were purchased from Strem chemicals and used without further purification. Other commercial chemicals were used as received unless otherwise noted.

Silica gel chromatography was performed with Silicycle's silica gel high-purity grade, pore size 60 Å, 230-400 mesh particle size, 40-63 µm particle size or using CombiFlash® Nextgen 300+ from Teledyne ISCO with a high-performance gold silica RediSepRf column (12g HP silica). Thin-layer chromatography (TLC) was carried out on silica gel glass-back plates ($60F_{254}$) using UV light to visualize the separation.

NMR Spectroscopy: ^1H and ^{13}C NMR spectra were recorded on either JEOL ECZ 400, ECZ 402, and ECA 500 MHz NMR spectrometers. ^1H and ^{13}C chemical shifts (δ) are reported in ppm relative to the residual solvent signal ($CDCl_3$: 7.26 ppm for ^1H NMR and 77.16 for ^{13}C; MeOD = 3.31 ppm for ^1H and 53.84 ppm for ^{13}C; DMSO-d_6 = 2.50 ppm for ^1H and 39.52 for ^{13}C NMR). Coupling constants are reported in hertz (Hz). Abbreviations are used as follows: s = singlet, d = doublet, t = triplet, q = quartet, p = pentet, quint = quintet, h = heptet, m = multiplet, dd = doublet of doublets, ddd = doublet of doublets of doublets, dddd = doublet of doublets of doublets of doublets dt = doublet of triplet, dq = doublet of quartet, td = triplet of doublet, dtd = oublet of triplet of doublet, pd = pentuplet of doublet, qd = quartet of doublet, br = broad.

Gas chromatography-mass spectrometry (GC-MS) analyses were conducted on an Agilent 8890 gas chromatograph and a 5977B mass-spectrometer equipped with an EI XTR ion source. Hydrogen was used as the carrier gas and was generated using a Peak Scientific Precision Trace 250cc H_2 generator.

High Performance Liquid Chromatography (HPLC): Separations were conducted on a Shimadzu Nexera LC equipped with a Nexera SPD-40 UV Detector. A Shim-pack GIS C18, 5 µm, 20 x 250 mm preparative column using a gradient of 0-100% MeOH in H_2O.

UV-Vis Spectroscopy. Absorption measurements were collected on an Agilent Cary 60 spectrophotometer using Fisherbrand semi-micro quartz cuvettes. All sample preparation was done under air using commercial MeCN and cuvettes were sealed with Teflon caps for data collection.

Photoredox reactions were performed using a HepatoChem® PhotoRedOx Box TC® (temperature controlled) equipped with an EvoluChem™ 18 W 405, 450, 525 nm LED lamp, 18 W 6200K white LED, or a Kessil PR160L 40 W 390 nm LED lamp.

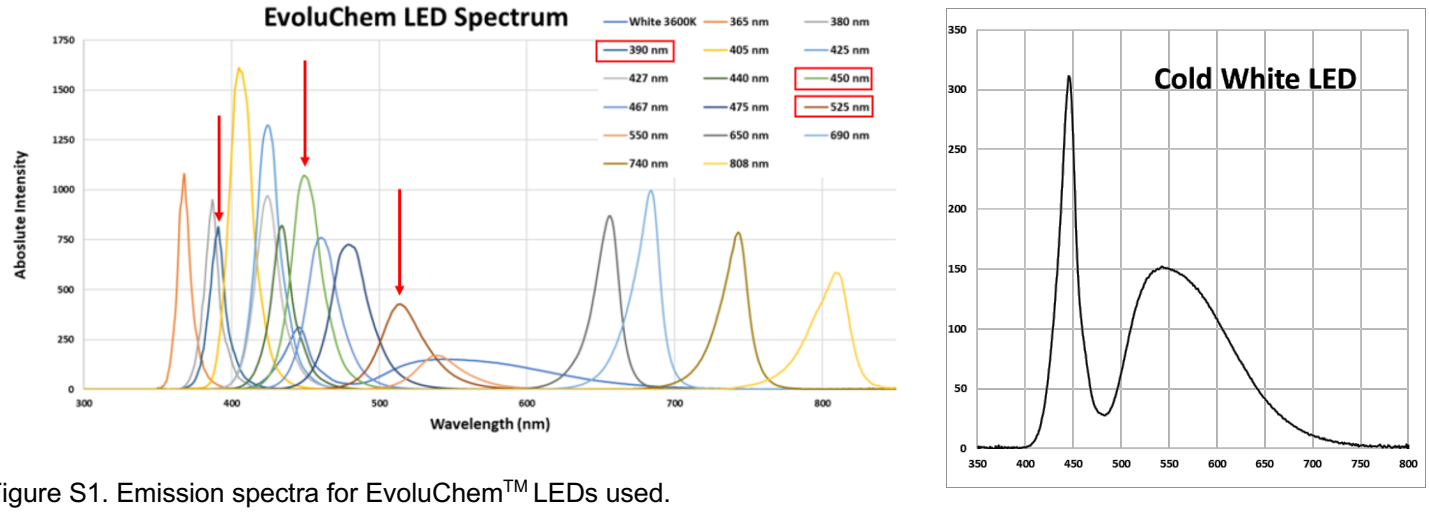

Figure S1. Emission spectra for EvoluChem™ LEDs used.

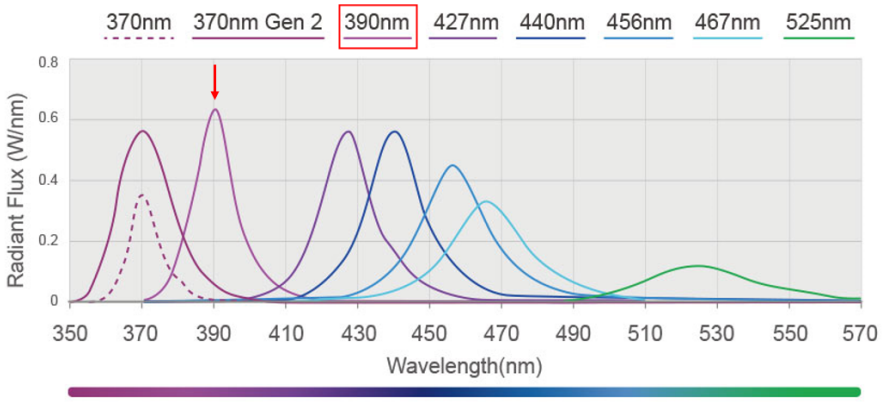

Figure S2. Emission spectra for Kessil PR160L options.

Total arylation determination. Total arylation is defined as percent aryl group incorporation across both mono- and di-arylated products. To quantify total arylation, calibration curves of **4b**, **5b**, **7b**, and **8b** were used and applied to the corresponding mono- and di-arylated 2-arylpyridines and acetanilides. Importantly, when combining mono- and di-arylation yields, the yield for di-arylation was multiplied by 2 to account for the two aryl groups that were added. To validate this approach, we isolated several mono-arylated product variations for both pyridine and acetanilide groups. We found that the yields of mono-arylated products obtained in all cases closely matched that predicted by the GC calibration curves. For example, product **4l** was isolated in a 46% yield, while its approximated GC yield using the calibration curve for **4b** was 41%. Thus, we reasoned that total arylation percentage could be adequately approximated by this strategy to enable the determination of arylation trends.

B. Calibration curves

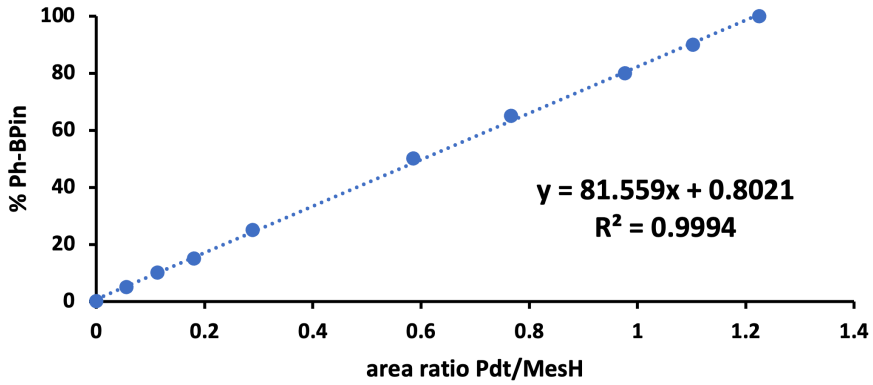

Figure S3. Calibration curve of Ph-BPin (**3**) using mesitylene as the internal standard.

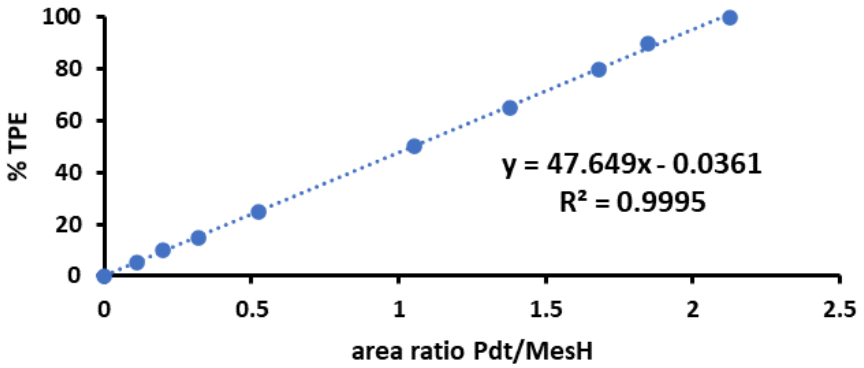

Figure S4. Calibration curve of 1,1,2-triphenylethylene using mesitylene as the internal standard.

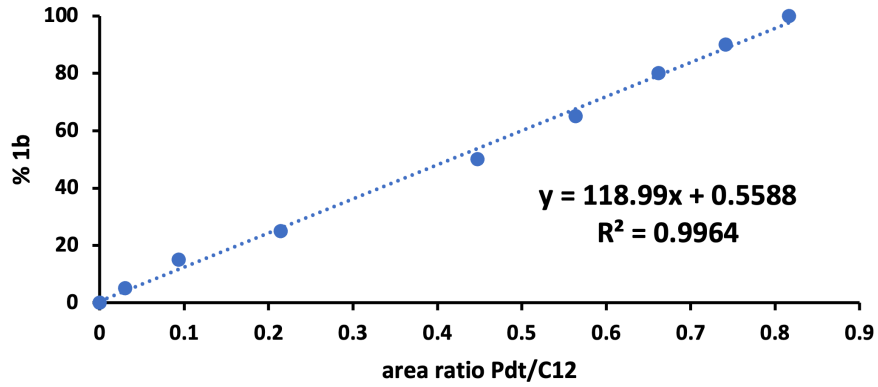

Figure S5. Calibration curve of 2-phenylpyridine (**1b**) using ^{n}dodecane as the internal standard.

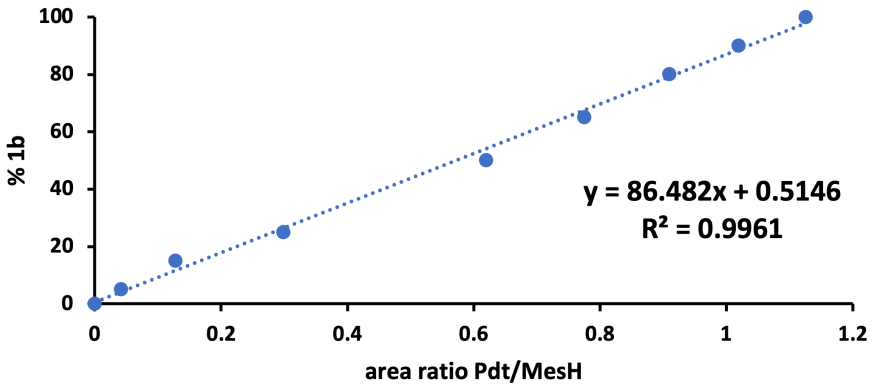

Figure S6. Calibration curve of 2-phenylpyridine (**1b**) using mesitylene as the internal standard.

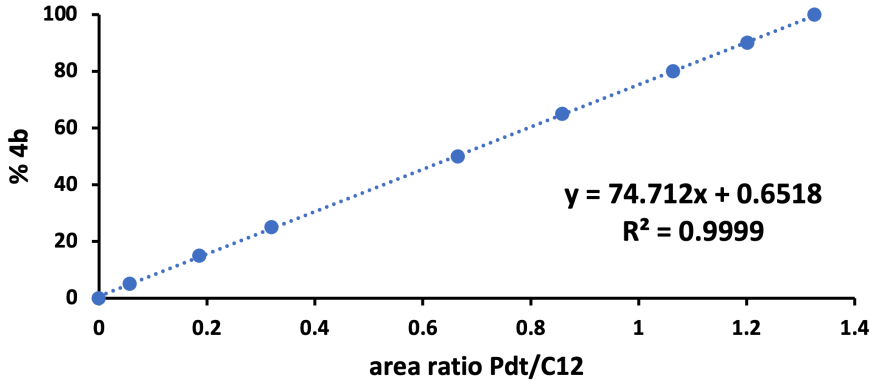

Figure S7. Calibration curve of 2-(2-phenyl)phenylpyridine (**4b**) using *n*dodecane as the internal standard.

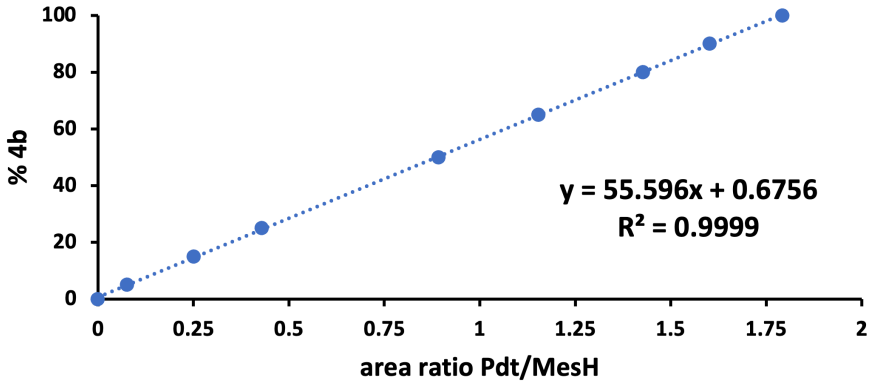

Figure S8. Calibration curve of 2-(2-phenyl)phenylpyridine (**4b**) using mesitylene as the internal standard.

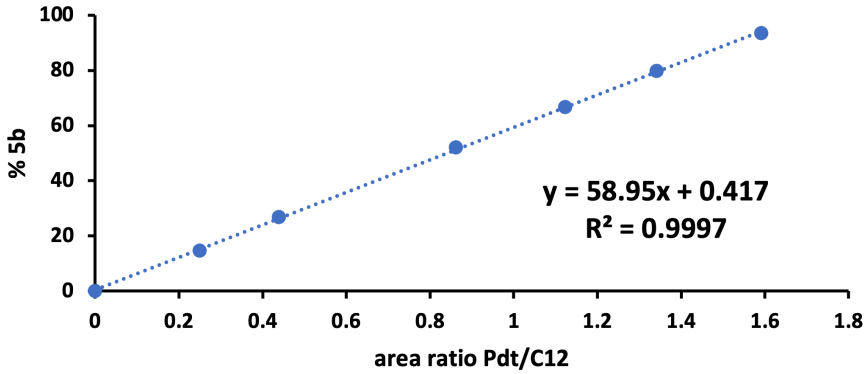

Figure S9. Calibration curve of 2-(2,6-diphenyl)phenylpyridine (**5b**) using *n*dodecane as the internal standard.

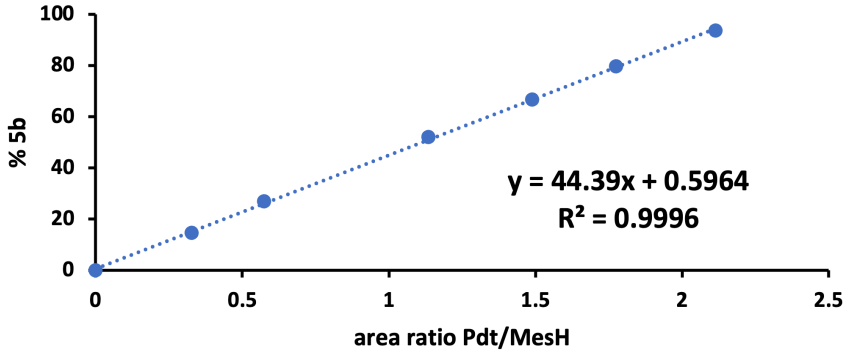

Figure S10. Calibration curve of 2-(2,6-diphenyl)phenylpyridine (**5b**) using mesitylene as the internal standard.

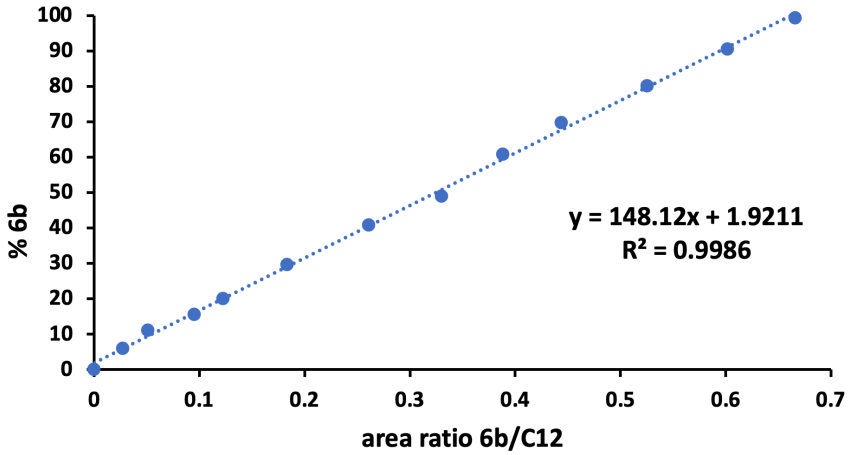

Figure S11. Calibration curve of acetanilide (**6b**) using ⁿdodecane as the internal standard.

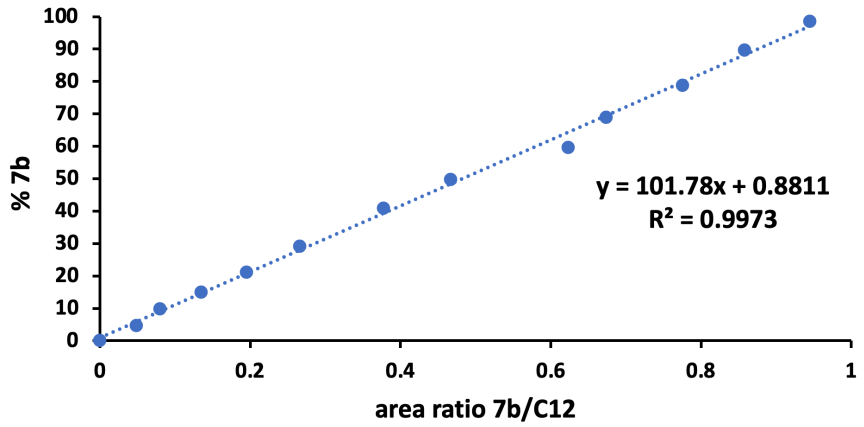

Figure S12. Calibration curve of 2-phenylacetanilide (**7b**) using ^{n}dodecane as the internal standard.

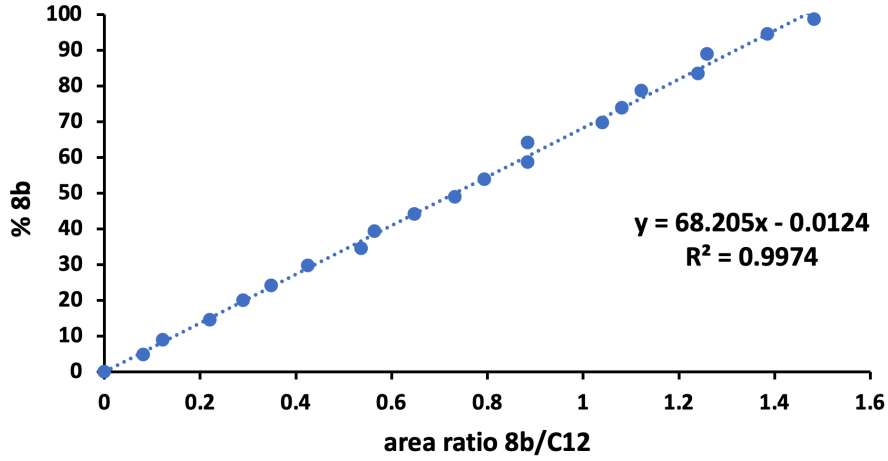

Figure S13. Calibration curve of 2,6-diphenylacetanilide (**8b**) using ^{n}dodecane as the internal standard.

C. Lewis base screening study for aryl radical generation from diphenyliodonium triflate

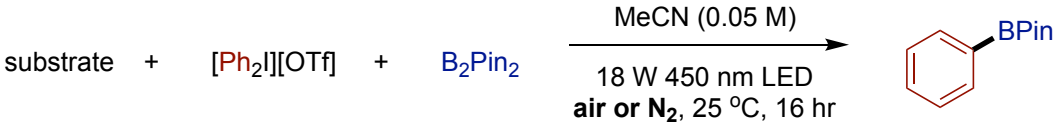

In a N_2 glovebox or under air, a magnetic stir bar, substrate (30 mol%), diphenyliodonium triflate (21 mg, 0.05 mmol, 1.0 eq.), and bis(pinacolato)diboron (25 mg, 0.1 mmol, 2.0 eq.) were added to a 4-mL scintillation vial. Dry, degassed acetonitrile (1 mL, 0.05 M) was added to reactions under N_2, and the vials capped with a Teflon lined screw top cap. The N_2 reactions were removed from the glovebox and all reactions were irradiated by an 18 W 450 nm light at 25 °C for 16 hours. After 16 hours, irradiation was stopped and a 20 µL aliquot was extracted using a microliter syringe and dispensed into a GC vial alongside 50 µL of a 0.04 M mesitylene (0.002 mmol mesitylene, 1 eq. relative to B_2Pin_2) stock solution before dilution to 1.5 mL total volume with EtOAc. This solution was analyzed by GC.

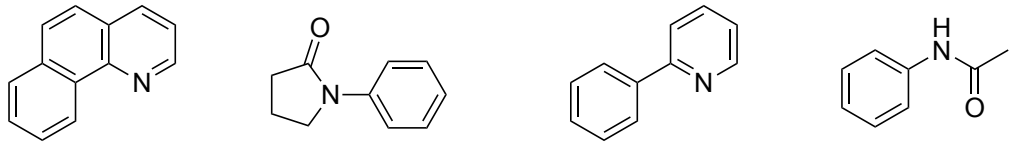

air: 47%
N_2: 56%

air: 20%
N_2: 4%

air: 18%
N_2: 4%

air: 11%
N_2: 22%

Figure S14. Optimizing radical generation under air or N_2. GC yields are given as an average of 2 runs.

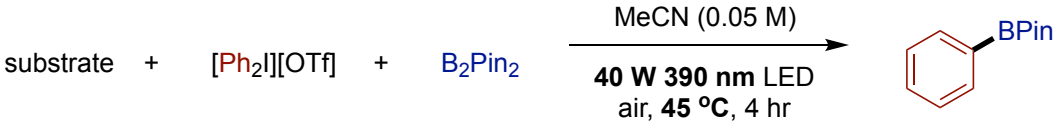

A magnetic stir bar, substrate (30 mol%), diphenyliodonium triflate (21 mg, 0.05 mmol, 1.0 eq.), and bis(pinacolato)diboron (25 mg, 0.1 mmol, 2.0 eq.) were added to a 4-mL scintillation vial. Acetonitrile (1 mL, 0.05 M) was added, and the vials capped with a Teflon lined screw top cap. The reactions were irradiated by a 40 W 390 nm light at 45 °C for 4 hours. After 4 hours, irradiation was stopped and a 20 µL aliquot was extracted using a microliter syringe and dispensed into a GC vial alongside 50 µL of a 0.04 M mesitylene (0.002 mmol mesitylene, 1 eq. relative to B_2Pin_2) stock solution before dilution to 1.5 mL total volume with EtOAc. This solution was analyzed by GC.

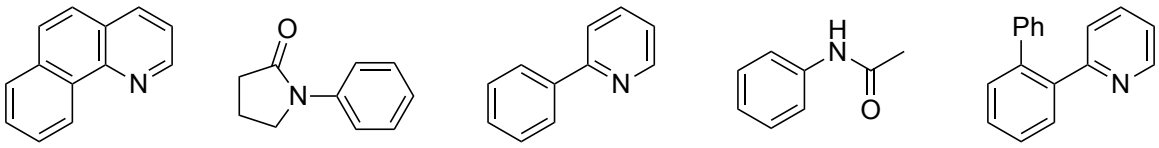

47%

19%

35%

23%

64%[a]

Figure S15. Optimizing radical generation based on LED power, wavelength, and reaction temperature. GC yields are given as an average of 2 runs. [a]Average of 8 runs.

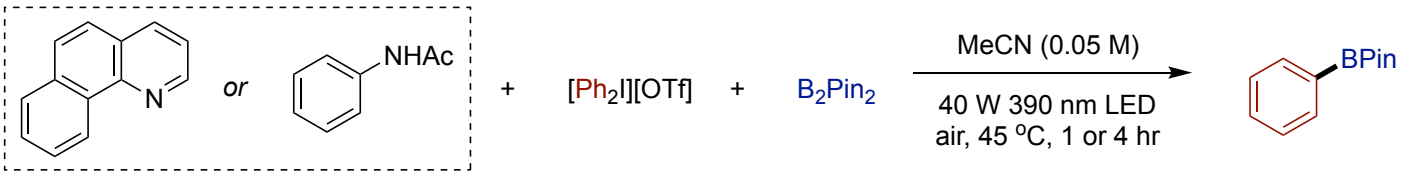

A magnetic stir bar, benzo[*h*]quinoline or acetanilide (mmol), diphenyliodonium triflate (mmol), and bis(pinacolato)diboron (25 mg, 0.1 mmol, 2.0 eq.) were added to a 4-mL scintillation vial. Acetonitrile (1 mL, 0.05 M) was added, and the vials capped with a Teflon lined screw top cap. The reactions were irradiated by a 40 W 390 nm light at 45 °C for 1 or 4 hours (1 hour for benzo[*h*]quinoline and 4 hours for acetanilide. After the noted time, irradiation was stopped and a 20 µL aliquot was extracted using a microliter syringe and dispensed into a GC vial alongside 50 µL of a 0.04 M mesitylene (0.002 mmol mesitylene, 1 eq. relative to B_2Pin_2) stock solution before dilution to 1.5 mL total volume with EtOAc. This solution was analyzed by GC.

Entry	benzo[*h*]quinoline (mmol)	acetanilide (mmol)	[Ph₂I][OTf] (mmol)	GC Yield (%)
1	0.010	-	0.050	26
2	0.015	-	0.050	32
3	0.030	-	0.050	39

4	0.050	-	0.050	51
5	-	0.050	0.050	36
6	-	0.075	0.050	36
7	-	0.100	0.050	43
8	-	0.500	0.050	37
9	-	0.015	0.015	65
10	-	0.015	0.030	55
11	-	0.015	0.050	52
12	-	0.015	0.075	47

Table S1. Investigation of benzo[*h*]quinoline, acetanilide, and diphenyliodonium triflate loading.

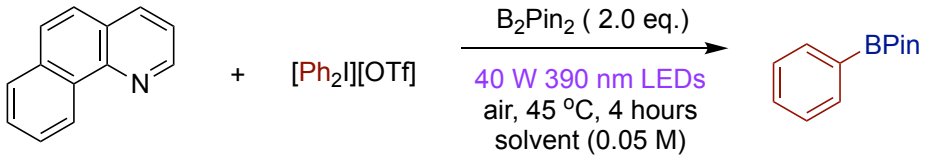

A magnetic stir bar, benzo[h]quinoline (9 mg, 0.05 mmol, 1 eq.), diphenyliodonium triflate (21 mg, 0.05 mmol, 1 eq.), and bis(pinacolato)diboron (25 mg, 0.1 mmol, 2.0 eq.) were added to a 4-mL scintillation vial. Solvent (1 mL, 0.05 M) were added, and the vials capped with a Teflon lined screw top cap. The reactions were irradiated by a 40 W 390 nm light at 45 °C for 4 hours. After 4 hours, irradiation was stopped and a 20 µL aliquot was extracted using a microliter syringe and dispensed into a GC vial outside 50 µL of a 0.04 M mesitylene (0.002 mesitylene, 1 eq. relative to B_2Pin_2) stock solution before dilution to 1.5 mL total volume of EtOAc. This solution was analyzed by GC.

Entry	Solvent	GC Yield (%)
1	Methanol	73
2	THF	17
3	Chloroform	9
4	Acetone	65
5	HFIP:H_2O (4:1)	63
6	Acetonitrile	62

Table S2. Investigation of solvent identity on the borylation reaction using benzo[h]quinoline as activator.

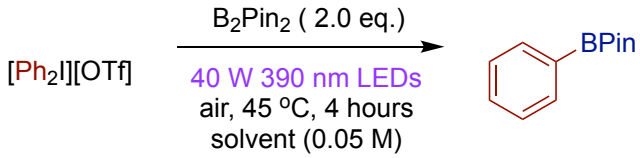

A magnetic stir bar, diphenyliodonium triflate (21 mg, 0.05 mmol, 1.0 eq.), and bis(pinacolato)diboron (25 mg, 0.1 mmol, 2.0 eq.) were added to a 4-mL scintillation vial. Solvent (1 mL, 0.05 M) was added, and the vials capped with a Teflon lined screw top cap. The reactions were irradiated by a 40 W 390 nm light at 45 °C for 4 hours. After 4 hours, irradiation was stopped and a 20 µL aliquot was extracted using a microliter syringe and dispensed into a GC vial alongside 50 µL of a 0.04 M mesitylene (0.002 mmol mesitylene, 1 eq. relative to B_2Pin_2) stock solution before dilution to 1.5 mL total volume with EtOAc. This solution was analyzed by GC.

Entry	Solvent	GC Yield (%)
1	Acetone	7
2	HFIP:H_2O (1:1)	20

Table S3. Investigation of solvent identity on photolysis of **2a** without LB activators.

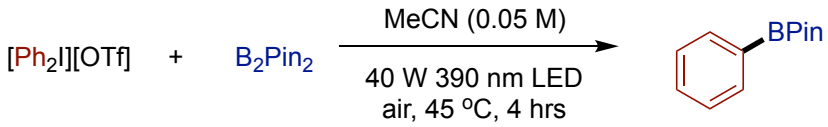

7 run average GC yield: 13 ± 2%

A magnetic stir bar, diphenyliodonium triflate (21 mg, 0.05 mmol, 1.0 eq.), and bis(pinacolato)diboron (25 mg, 0.1 mmol, 2.0 eq.) were added to a 4-mL scintillation vial. Acetonitrile (1 mL, 0.05 M) was added, and the vials capped with a Teflon lined screw top cap. The reactions were irradiated by a 40 W 390 nm light at 45 °C for 4 hours. After 4 hours, irradiation was stopped and a 20 µL aliquot was extracted using a microliter syringe and dispensed into a GC vial alongside 50 µL of a 0.04 M mesitylene (0.002 mmol mesitylene, 1 eq. relative to B_2Pin_2) stock solution before dilution to 1.5 mL total volume with EtOAc. This solution was analyzed by GC.

Entry	GC Yield (%)
1	14
2	15
3	15
4	13
5	11
6	12
7	13

Table S4. Control reactions of the background aryl radical generation in MeCN in the absence of substrate.

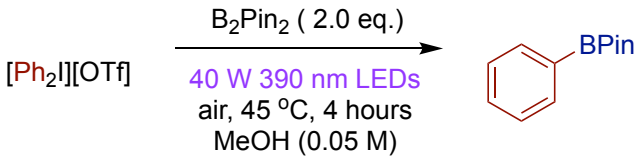

8 run average GC yield: 34 ± 3%

A magnetic stir bar, diphenyliodonium triflate (21 mg, 0.05 mmol, 1.0 eq.), and bis(pinacolato)diboron (25 mg, 0.1 mmol, 2.0 eq.) were added to a 4-mL scintillation vial. Methanol (1 mL, 0.05 M) was added, and the vials capped with a Teflon lined screw top cap. The reactions were irradiated by a 40 W 390 nm light at 45 °C for 4 hours. After 4 hours, irradiation was stopped and a 20 µL aliquot was extracted using a microliter syringe and dispensed into a GC vial alongside 50 µL of a 0.04 M mesitylene (0.002 mmol mesitylene, 1 eq. relative to B_2Pin_2) stock solution before dilution to 1.5 mL total volume with EtOAc. This solution was analyzed by GC.

Entry	GC Yield (%)
1	36
2	37
3	34
4	31
5	38
6	33
7	34

8	30

Table S5. Control reactions of the background aryl radical generation in MeOH in the absence of substrate.

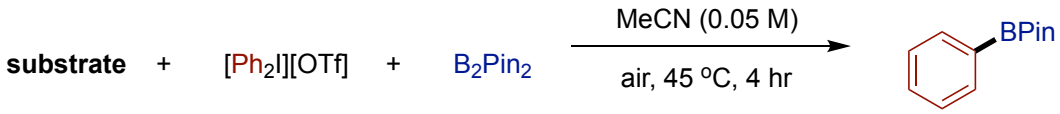

A magnetic stir bar, substrate (30 mol%), diphenyliodonium triflate (21 mg, 0.05 mmol, 1.0 eq.), and bis(pinacolato)diboron (25 mg, 0.1 mmol, 2.0 eq.) were added to a 4-mL scintillation vial. Acetonitrile (1 mL, 0.05 M) was added, and the vials capped with a Teflon lined screw top cap. The reactions were stirred in the dark at 45 °C for 4 hours. After 4 hours, a 20 µL aliquot was extracted using a microliter syringe and dispensed into a GC vial alongside 50 µL of a 0.04 M mesitylene (0.002 mmol mesitylene, 1 eq. relative to B_2Pin_2) stock solution before dilution to 1.5 mL total volume with EtOAc. This solution was analyzed by GC.

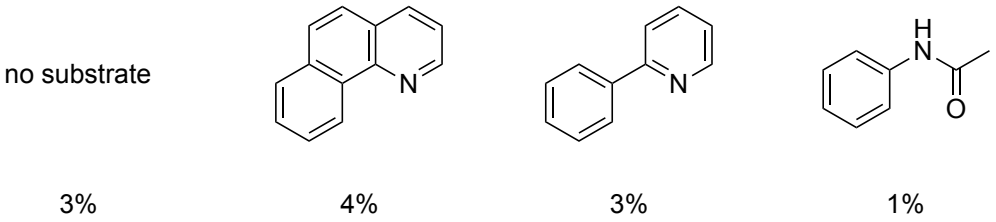

Figure S16. Control reactions conducted in MeCN without irradiation but with heating.

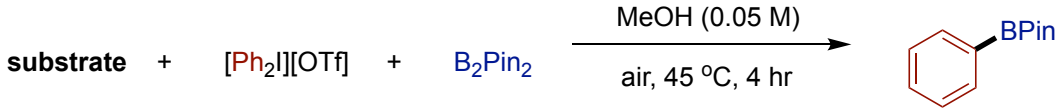

A magnetic stir bar, substrate (1.0 eq.), diphenyliodonium triflate (21 mg, 0.05 mmol, 1 eq.), and bis(pinacolato)diboron (25 mg, 0.1 mmol, 2.0 eq.) were added to a 4-mL scintillation vial. Methanol (1 mL, 0.05 M) were added, and the vials capped with a Teflon lined screw top cap. The reactions were stirred in the dark at 45 °C for 4 hours. After 4 hours, a 20 µL aliquot was extracted using a microliter syringe and dispensed into a GC vial outside 50 µL of a 0.04 M mesitylene (0.002 mesitylene, 1 eq. relative to B_2Pin_2) stock solution before dilution to 1.5 mL total volume of EtOAc. This solution was analyzed by GC.

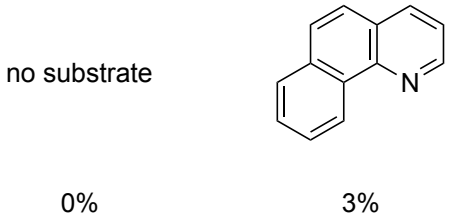

Figure S17. Control reactions conducted in MeOH without irradiation but with heating.

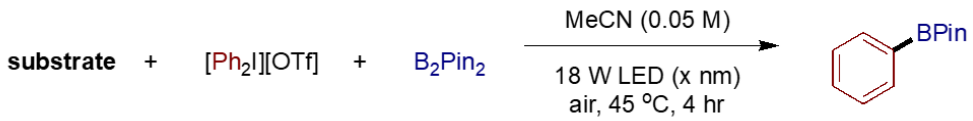

A magnetic stir bar, substrate (0.05 mmol, 1.0 eq.), diphenyliodonium triflate (21 mg, 0.05 mmol, 1.0 eq.), and bis(pinacolato)diboron (25 mg, 0.1 mmol, 2.0 eq.) were added to a 4-mL scintillation vial. Acetonitrile (1 mL, 0.05 M) was added, and the vials capped with a Teflon lined screw top cap. The reactions were irradiated by an 18 W LED at 45 °C for 4 hours. After 4 hours, irradiation was stopped and a 20 µL aliquot was extracted using a microliter syringe and dispensed into a GC vial alongside 50 µL of a 0.04 M mesitylene (0.002 mmol mesitylene, 1 eq. relative to B_2Pin_2) stock solution before dilution to 1.5 mL total volume with EtOAc. This solution was analyzed by GC.

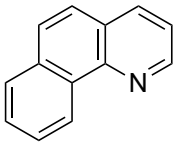

405 nm: 17%
450 nm: 4%
525 nm: 1%
6200K white: 3%

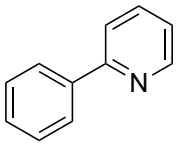

405 nm: 50%
450 nm: 43%
525 nm: 1%
6200K white: 18%

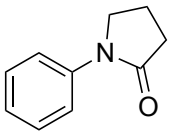

405 nm: 4%
450 nm: 1%
525 nm: 1%
6200K white: 1%

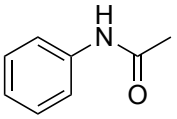

405 nm: 4%
450 nm: 2%
525 nm: 1%
6200K white: 1%

Figure S18. Investigation of light wavelength. GC yields are given as an average of 2 runs.

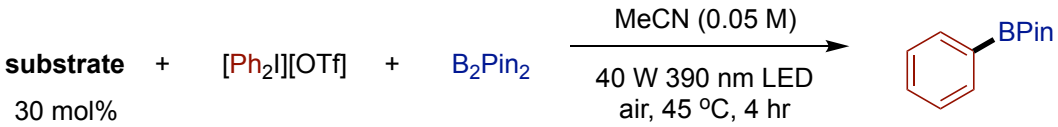

General procedure for substrate Lewis base screen. A magnetic stir bar, substrate (30 mol%), diphenyliodonium triflate (21 mg, 0.05 mmol, 1.0 eq.), and bis(pinacolato)diboron (25 mg, 0.1 mmol, 2.0 eq.) were added to a 4-mL scintillation vial. Acetonitrile (1 mL, 0.05 M) was added, and the vials capped with a Teflon lined screw top cap. The reactions were irradiated by a 40 W 390 nm light at 45 °C for 4 hours. After 4 hours, irradiation was stopped and a 20 µL aliquot was extracted using a microliter syringe and dispensed into a GC vial alongside 50 µL of a 0.04 M mesitylene (0.002 mmol mesitylene, 1 eq. relative to B_2Pin_2) stock solution before dilution to 1.5 mL total volume with EtOAc. This solution was analyzed by GC.

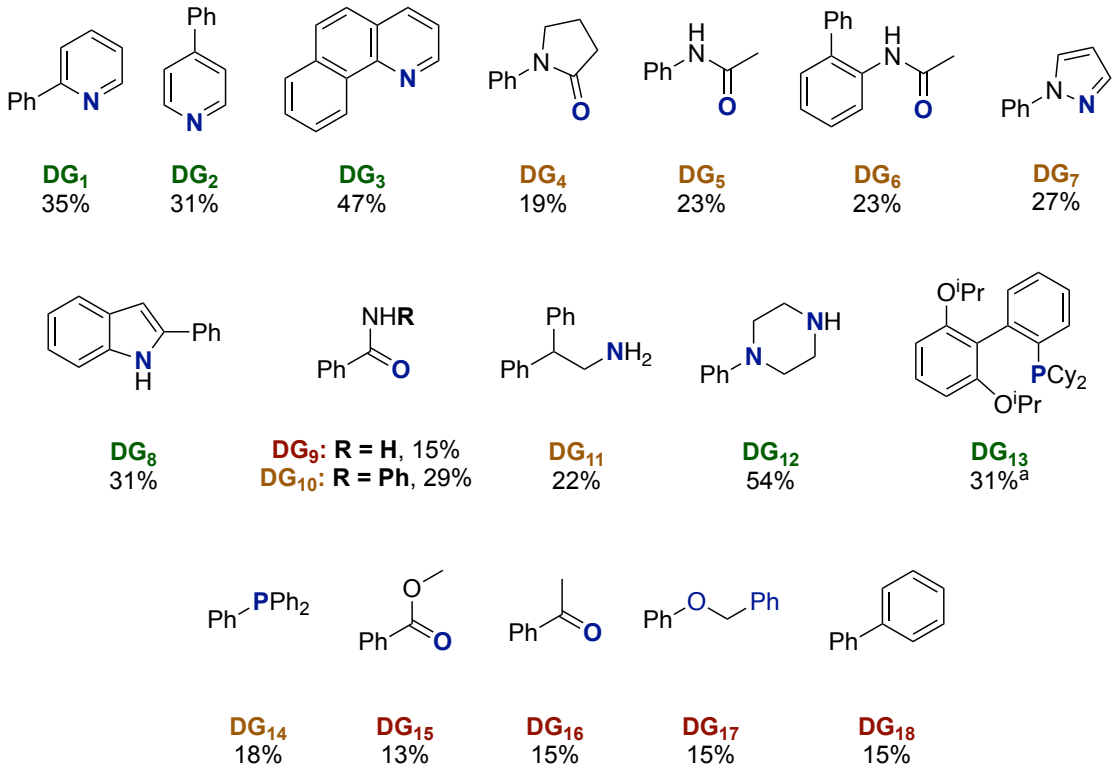

Figure S19. Substrate scope assess the ability of catalytic quantities of Lewis bases to generate aryl radicals from diphenyliodonium triflate in acetonitrile. [a]Performed under N_2.

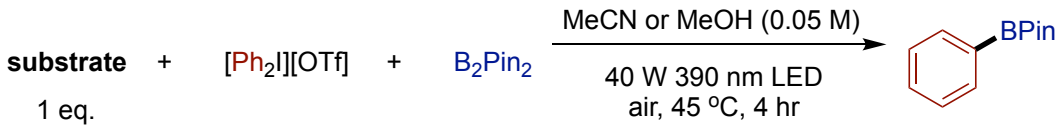

General procedure for substrate Lewis base screen. A magnetic stir bar, substrate (0.05 mol. 1.0 eq.), diphenyliodonium triflate (21 mg, 0.05 mmol, 1.0 eq.), and bis(pinacolato)diboron (25 mg, 0.1 mmol, 2.0 eq.) were added to a 4-mL scintillation vial. MeCN or MeOH(1 mL, 0.05 M) was added, and the vials capped with a Teflon lined screw top cap. The reactions were irradiated by a 40 W 390 nm light at 45 °C for 4 hours. After 4 hours, irradiation was stopped and a 20 µL aliquot was extracted using a microliter syringe and dispensed into a GC vial alongside 50 µL of a 0.04 M mesitylene (0.002 mmol mesitylene, 1 eq. relative to B_2Pin_2) stock solution before dilution to 1.5 mL total volume with EtOAc. This solution was analyzed by GC.

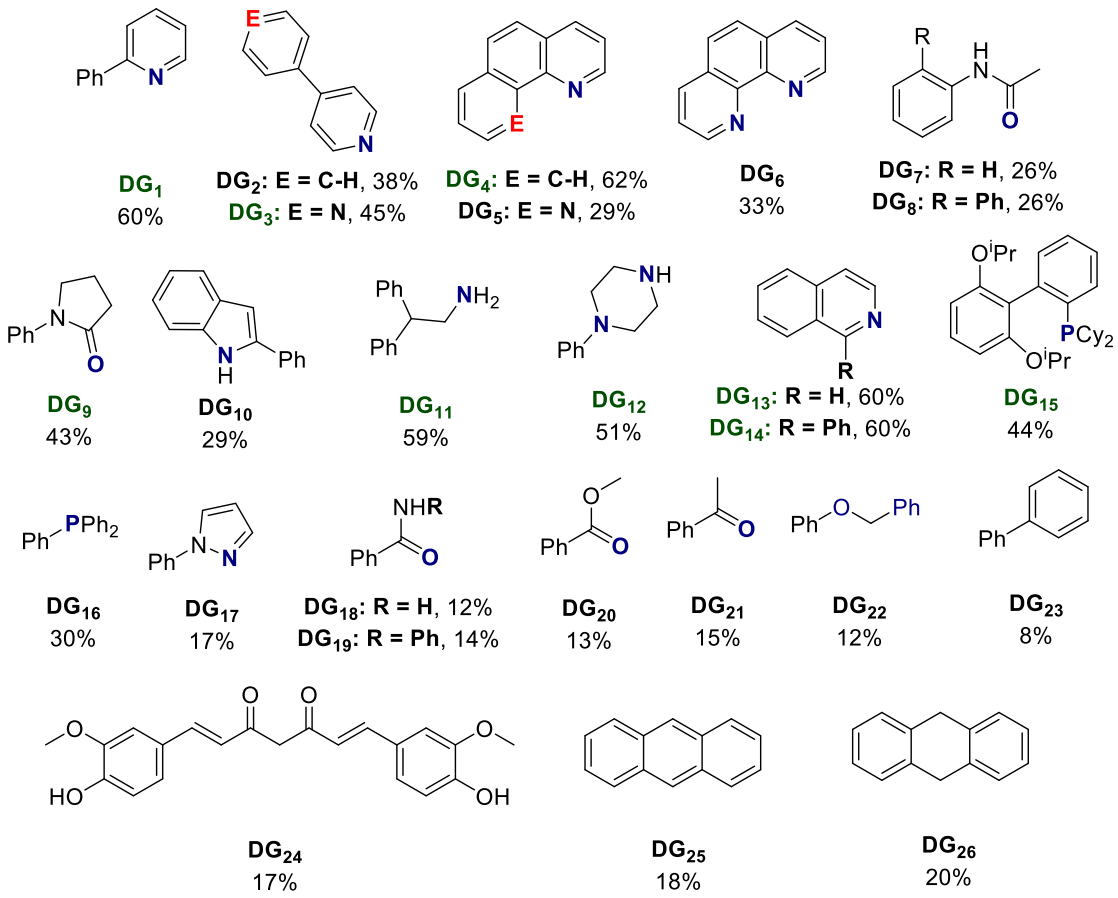

Figure S20. Substrate scope assesses the ability of stoichiometric quantities of Lewis bases to generate aryl radicals from diphenyliodonium triflate in acetonitrile.

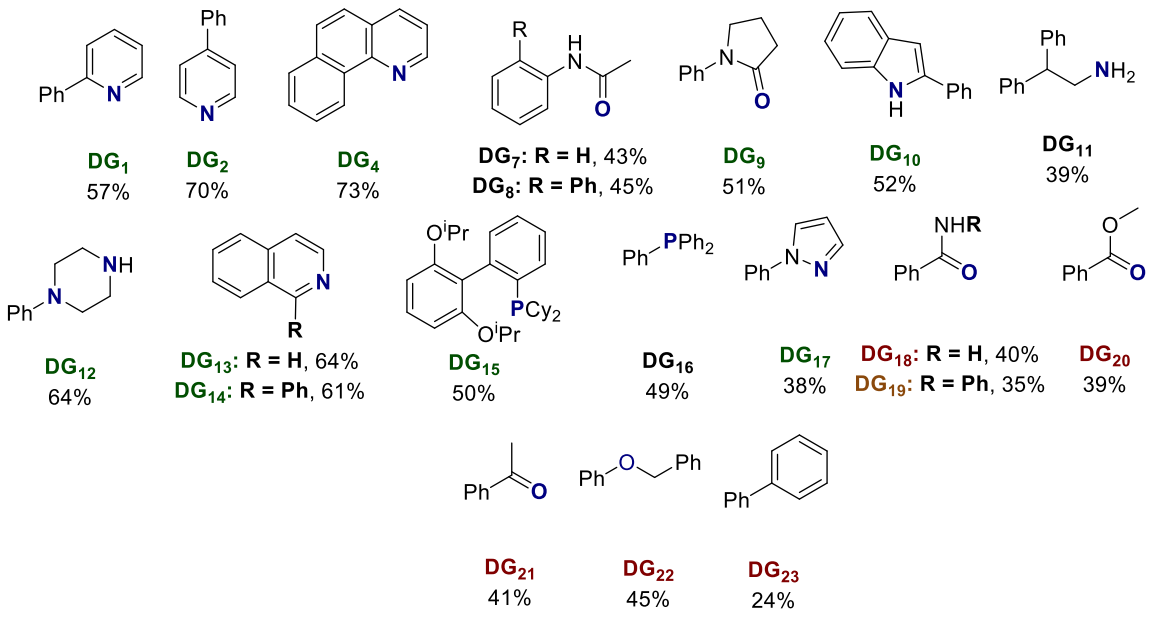

Figure S21. Substrate scope assesses the ability of stoichiometric quantities of Lewis bases to generate aryl radicals from diphenyliodonium triflate in methanol.

D. Initial rate kinetics of 2-arylpyridine and iodonium salt derivatives

General notes: All kinetic reactions were performed under air with a stir rate of 250 rpm, unless otherwise noted.

Reagent Order of B_2Pin_2. To assess whether the concentration of our aryl trapping reagent, B_2Pin_2 impacts the rate of aryl radical capture, we determined the reagent order of B_2Pin_2 using the method of initial rates.

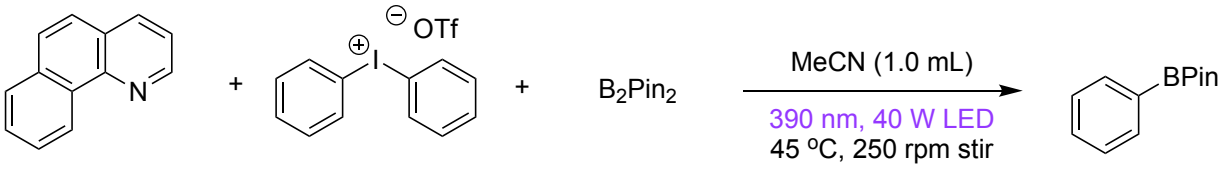

DG_3 0.05 M

2a 0.05 M

0.05-0.2 M

Procedure: A magnetic stir bar and the appropriate amount of B_2Pin_2 (1, 2, 3, or 4 eq. relative to **2a**) was added to a 4-mL scintillation vial. To this vial, 500 µL of a 0.1 M diphenyliodonium triflate stock solution (0.05 mmol **2a**) was added alongside, 500 µL of a 0.1 M benzo[h]quinoline stock solution (0.05 mmol **DG_3**). This vial was sealed with a screw top open cap affixed with a PTFE septum. The reactions were irradiated by a 40 W 390 nm light at 45 °C. At pre-determined timepoints, 20 µL aliquots were extracted using a microliter syringe without turning the LED off or removing the heat. The aliquots were transferred to a GC vial alongside 25, 50, 75 or 100 µL of a 0.04 M mesitylene stock solution (stock: 0.002 mmol mesitylene, 1 eq. relative to B_2Pin_2) before dilution to 1.5 mL total volume with EtOAc. These solutions were analyzed by GC and plotted using excel.

Outcome: Plotting the concentration of B_2Pin_2 against the initial rate demonstrates the zero-order dependence of the aryl borylation reaction on [B_2Pin_2]. This result supports our assertion that radical capture by the boron reagent is fast and that the determined initial rates of radical generation reported hereafter as chemically significant.

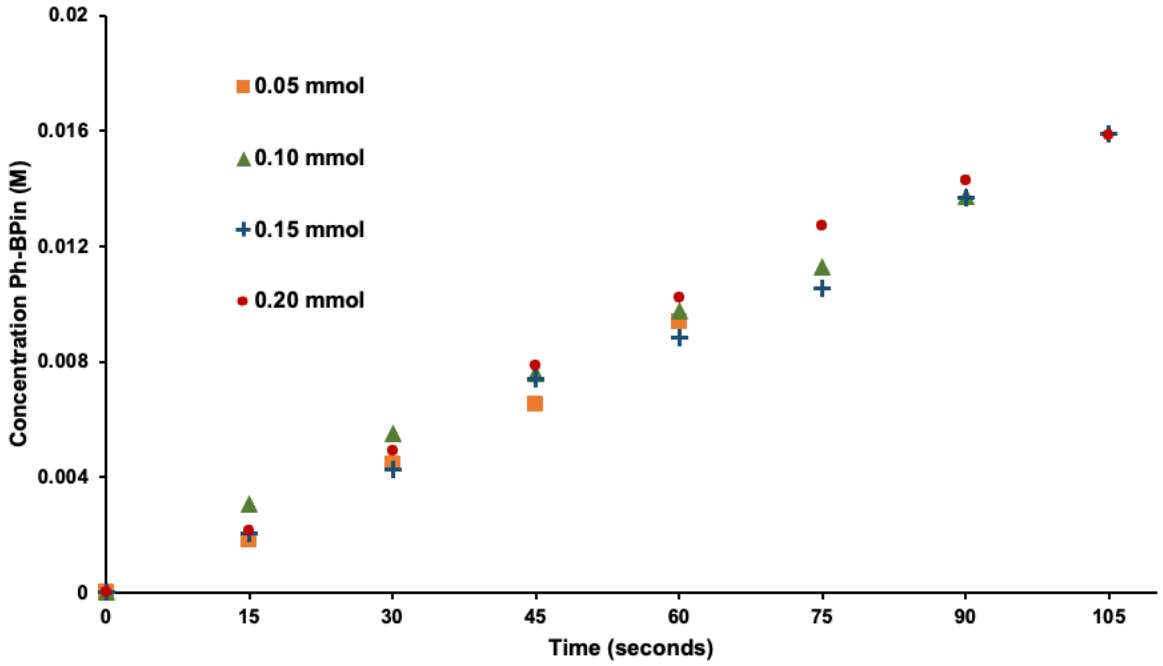

Figure S22. Initial rate time course using concentrations of B_2Pin_2 ranging from 0.1 - 0.4 M.

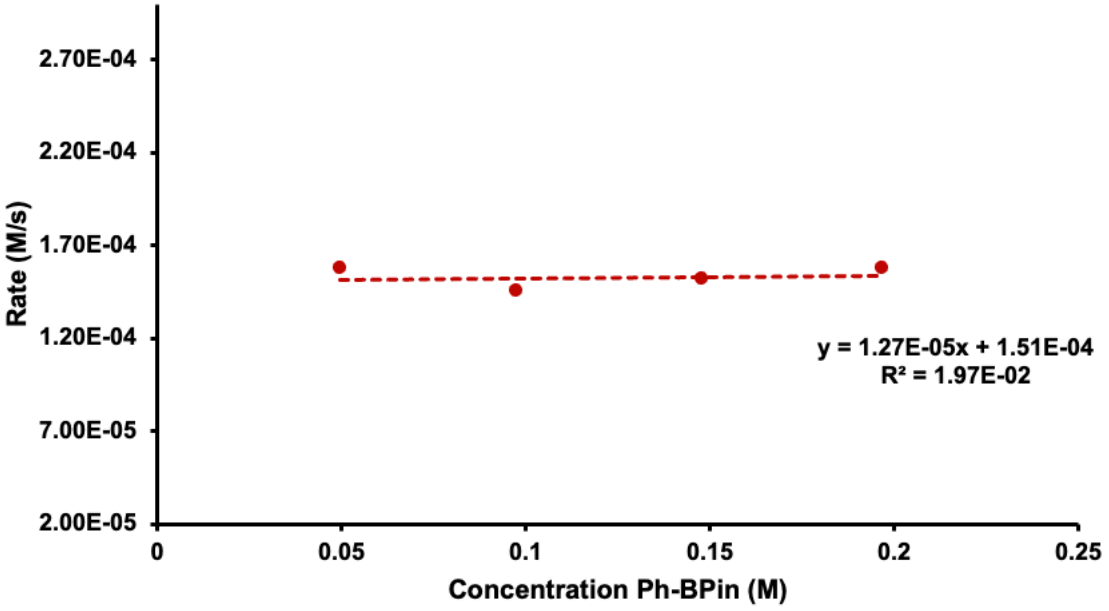

Figure S23. Reagent Order of B_2Pin_2.

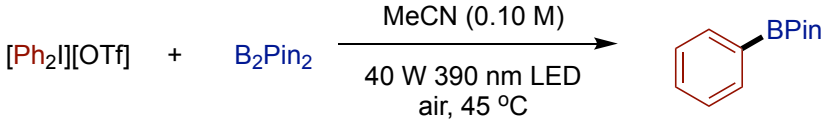

Control reaction procedure. A magnetic stir bar, diphenyliodonium triflate (64 mg, 0.15 mmol, 1.5 eq.), and bis(pinacolato)diboron (25 mg, 0.1 mmol, 1.0 eq.) were added to a 4-mL vial. To this mixture of powders, acetonitrile (1 mL, 0.1 M) was added. The vial was sealed with a screw top open cap affixed with a PTFE septum. The reactions were irradiated by a 40 W 390 nm light at 45 °C. At pre-determined timepoints, 20 µL aliquots were extracted using a microliter syringe without turning the LED off or removing the heat. The aliquots were transferred to a GC vial alongside 50 µL of a 0.04 M mesitylene (0.002 mmol mesitylene, 1 eq. relative to B_2Pin_2) stock solution before dilution to 1.5 mL total volume with EtOAc. These solutions were analyzed by GC and plotted using excel.

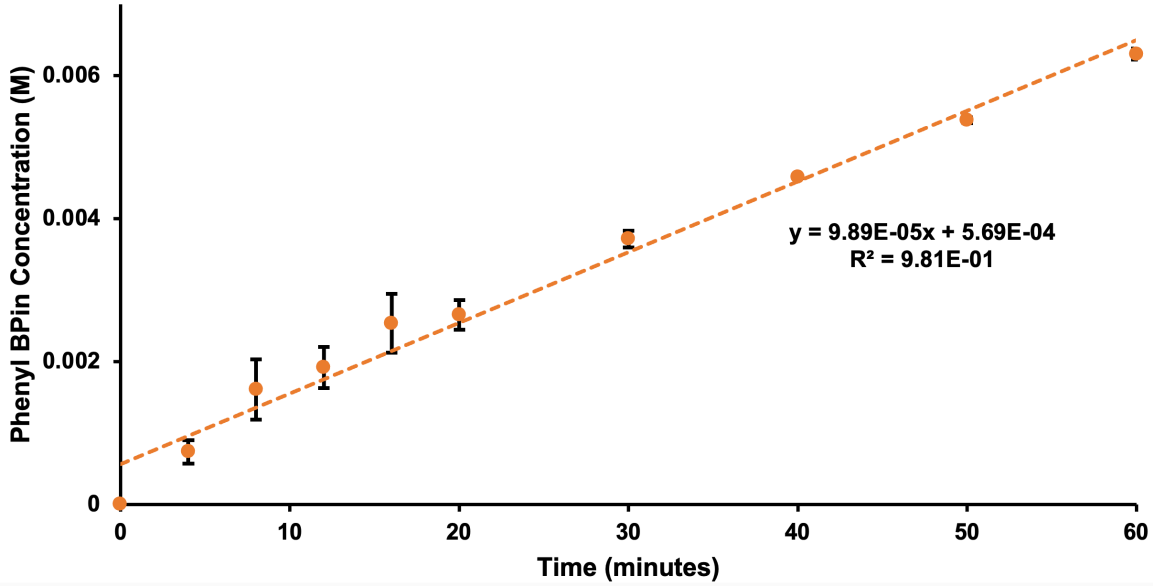

Figure S24. Time course of substrate-free reaction to ascertain the rate of background aryl radical generation.

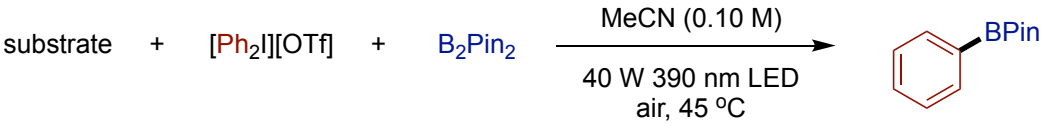

General procedure for collection of kinetic data for pyridine derivatives. A magnetic stir bar, diphenyliodonium triflate (64.5 mg, 0.15 mmol, 1.5 eq.), and bis(pinacolato)diboron (25 mg, 0.10 mmol, 1.0 eq.) were added to a 4-mL scintillation vial. To this mixture of powders, acetonitrile (1 mL, 0.10 M) was added followed by substrate (0.10 mmol, 1.0 eq.). The vial was sealed with a screw top open cap affixed with a PTFE septum. The reactions were irradiated by a 40 W 390 nm light at 45 °C. At pre-determined timepoints, 20 µL aliquots were extracted using a microliter syringe without turning the LED off or removing the heat. The aliquots were transferred to a GC vial alongside 50 µL of a 0.04 M mesitylene (0.002 mmol mesitylene, 1 eq. relative to B_2Pin_2) stock solution before dilution to 1.5 mL total volume with EtOAc. These solutions were analyzed by GC and plotted using excel.

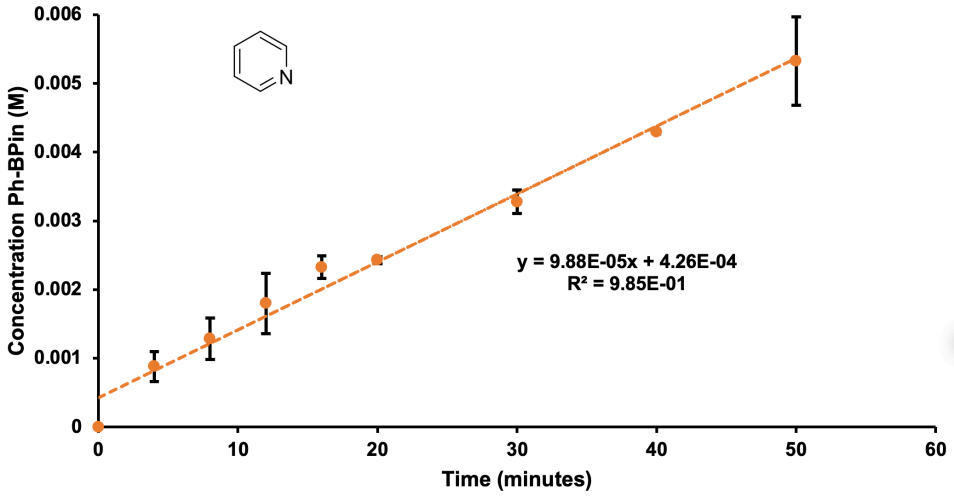

Figure S25. Initial rate time course using pyridine as LB activator.

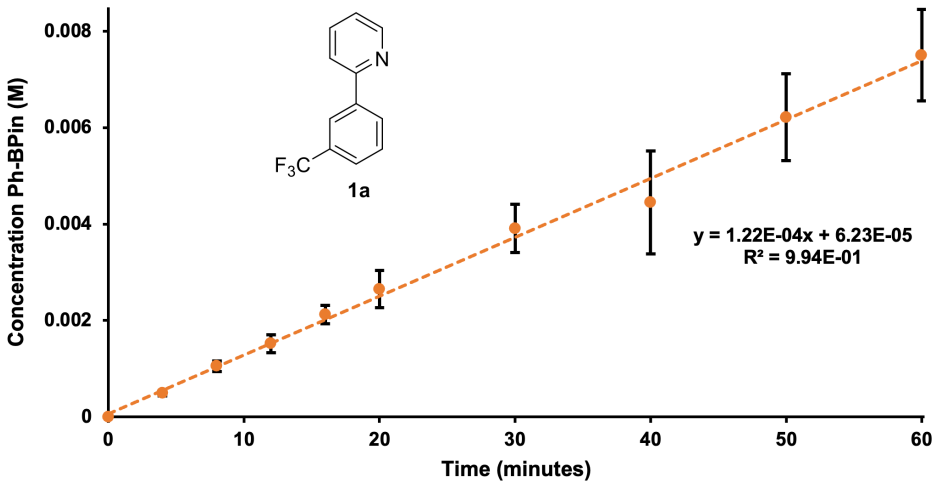

Figure S26. Initial rate time course using 2-(3-trifluoromethylphenyl)phenylpyridine (**1a**) as LB activator.

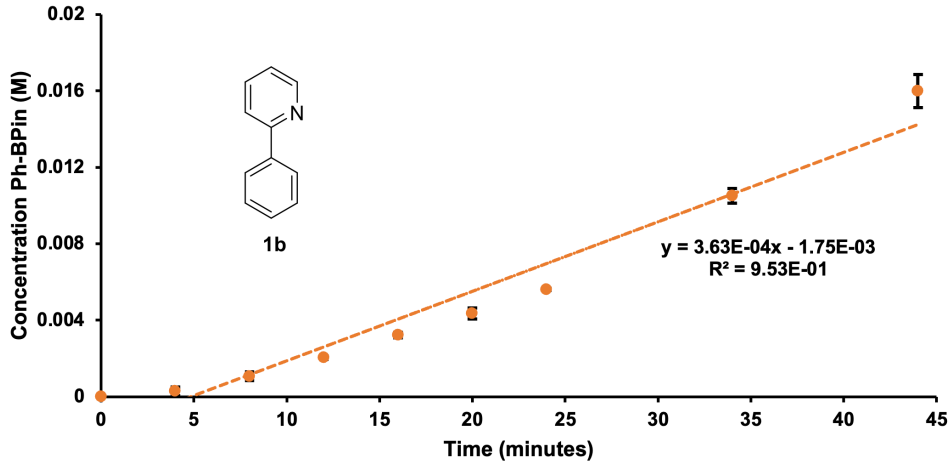

Figure S27. Initial rate time course using 2-phenylpyridine (**1b**) as LB activator.

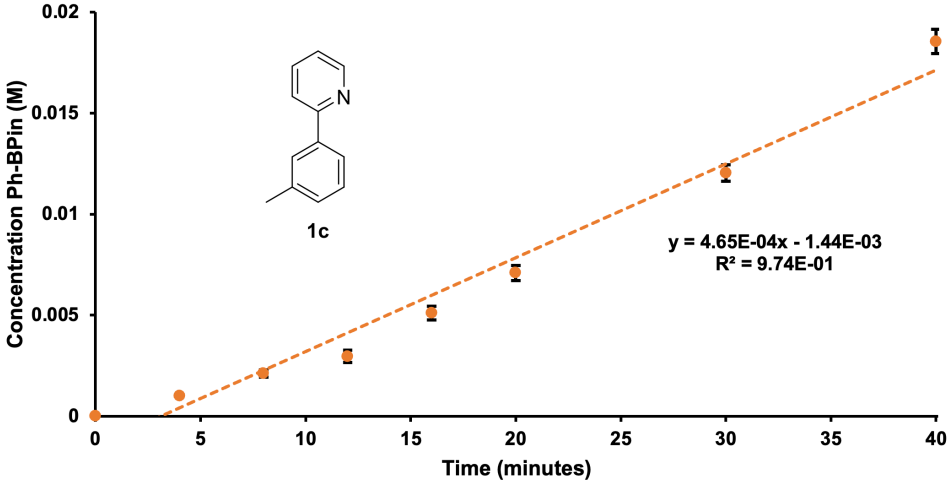

Figure S28. Initial rate time course using 2-(3-methylphenyl)phenylpyridine (**1c**) as LB activator.

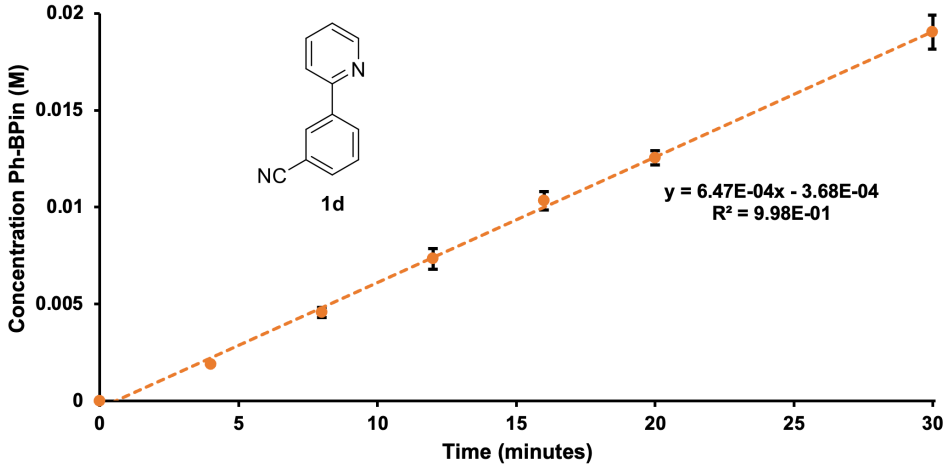

Figure S29. Initial rate time course using 2-(3-cyanophenyl)phenylpyridine (**1d**) as LB activator.

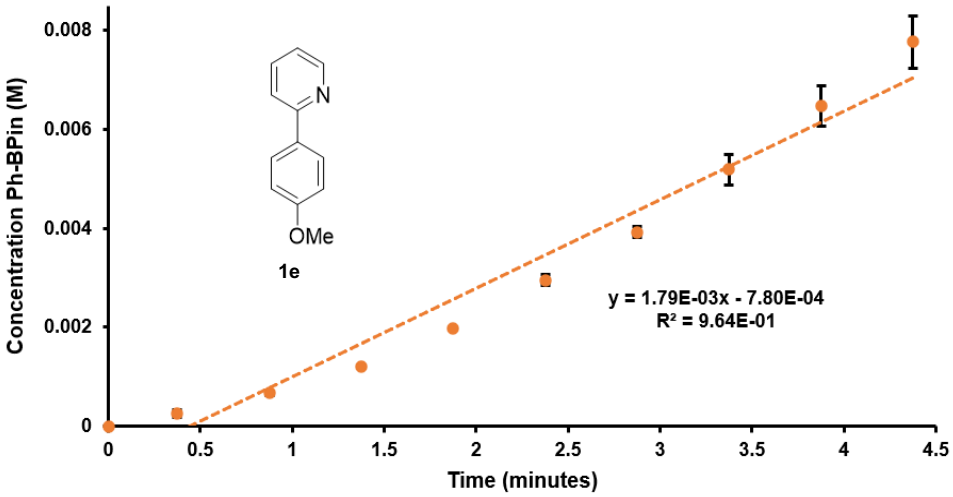

Figure S30. Initial rate time course using 2-(4-methoxyphenyl)phenylpyridine (**1e**) as LB activator.

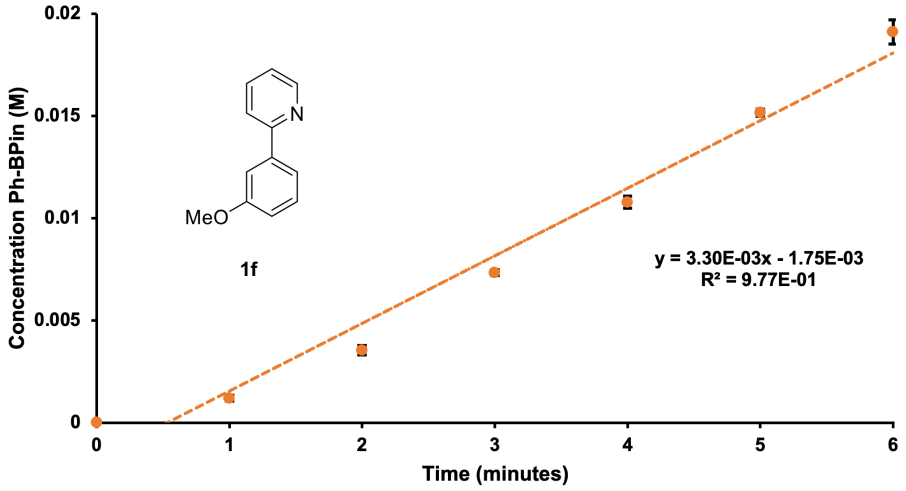

Figure S31. Initial rate time course using 2-(3-methoxyphenyl)phenylpyridine (**1f**) as LB activator.

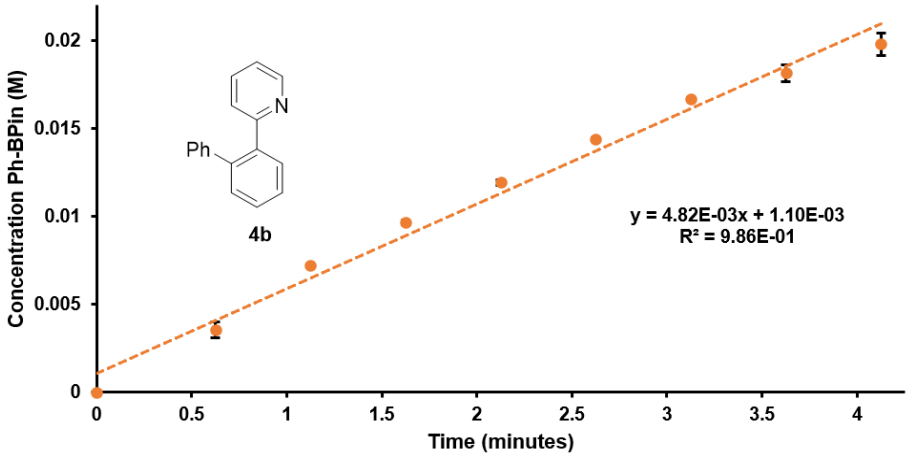

Figure S32. Initial rate time course using 2-(2-phenylphenyl)phenylpyridine (**4b**) as LB activator.

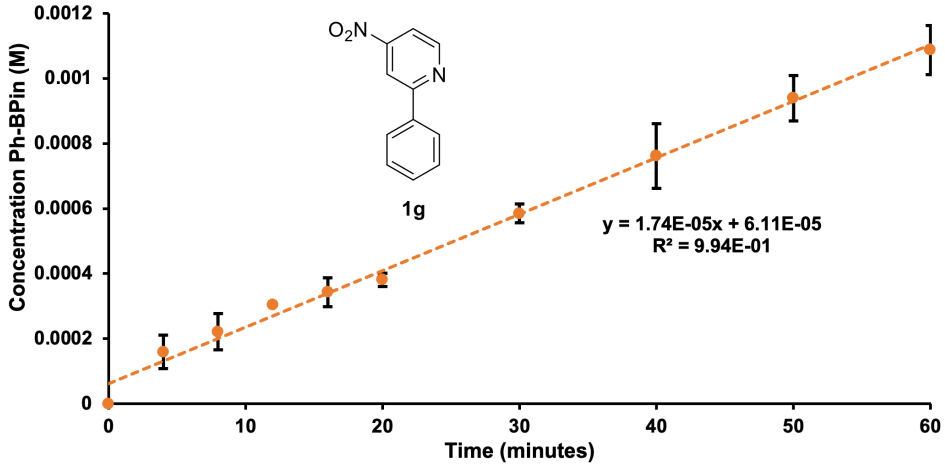

Figure S33. Initial rate time course using 2-phenyl-4-nitropyridine (**1g**) as LB activator.

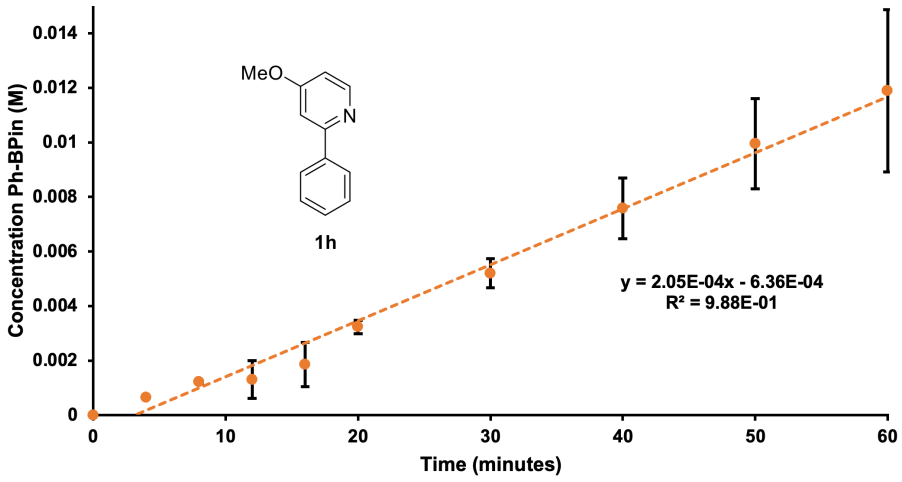

Figure S34. Initial rate time course using 2-phenyl-4-methoxypyridine (**1h**) as LB activator.

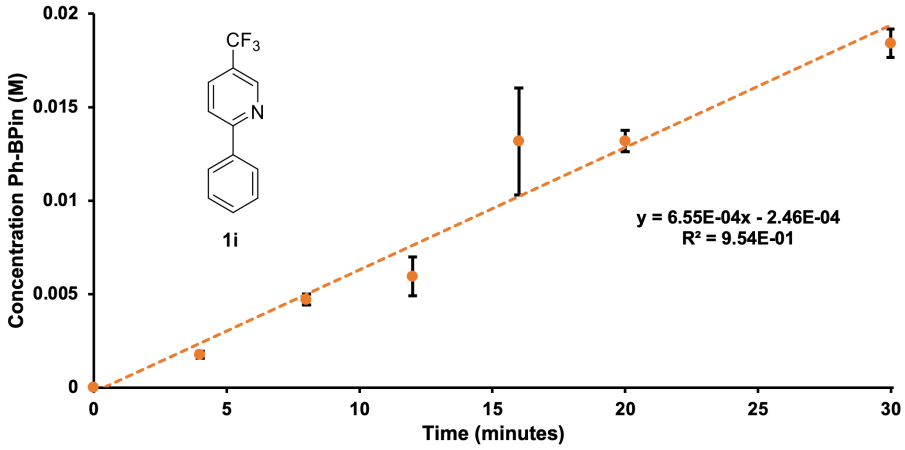

Figure S35. Initial rate time course using 2-phenyl-5-trifluoromethylpyridine (**1i**) as LB activator.

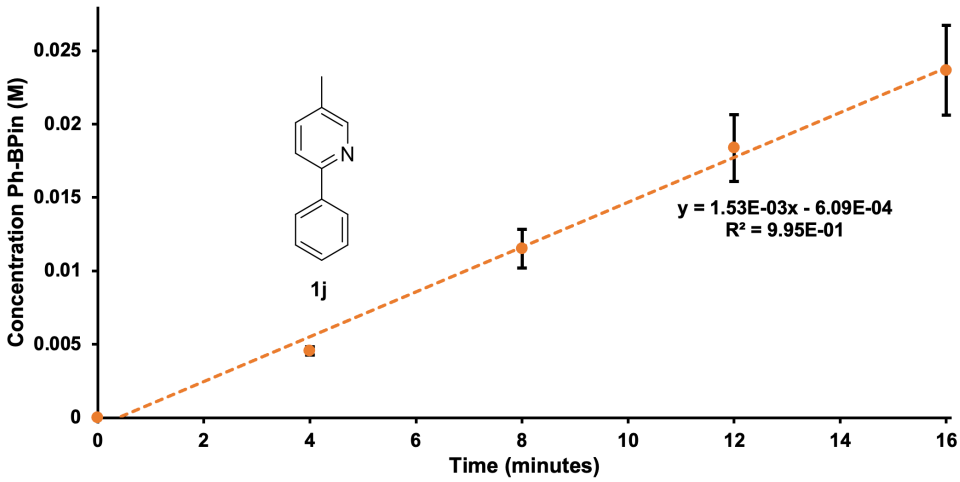

Figure S36. Initial rate time course using 2-phenyl-5-methylpyridine (**1j**) as LB activator.

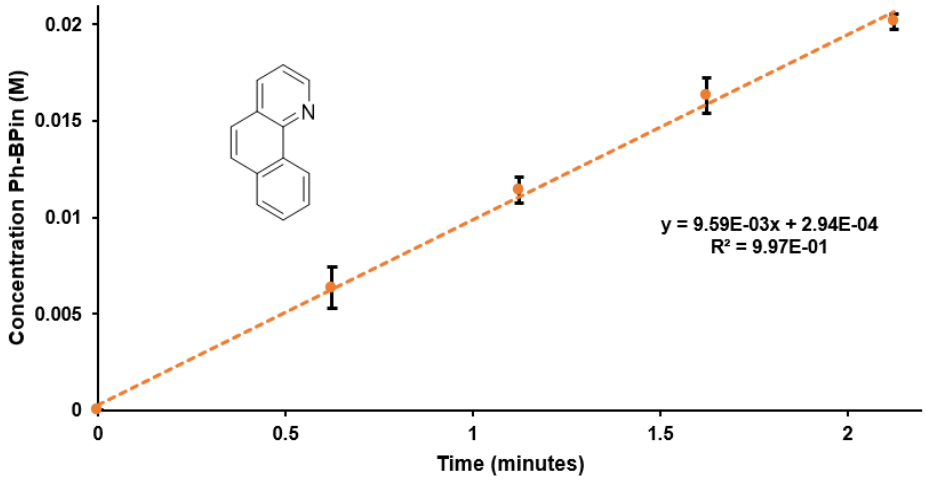

Figure S37. Initial rate time course using benzo[*h*]quinoline (**DG$_4$**) as LB activator.

LB activator	Initial Rate (M/min)	k_{rel}
-	9.89×10^{-5}	1.0
pyridine	9.88×10^{-5}	1.0
1a	1.22×10^{-4}	1.2
1b	3.63×10^{-4}	3.7
1c	4.65×10^{-4}	4.7
1d	6.47×10^{-4}	6.5
1e	1.79×10^{-3}	18.1
1f	3.30×10^{-3}	33.4
4b	4.82×10^{-3}	48.7
1g	1.74×10^{-5}	0.2
1h	2.05×10^{-4}	2.1
1i	6.55×10^{-4}	6.6

1j	1.53 x 10^{-3}	15.5
benzo[*h*]quinoline	9.59 x 10^{-3}	97.1

Table S6. Tabulated initial rate and k_{rel} data.

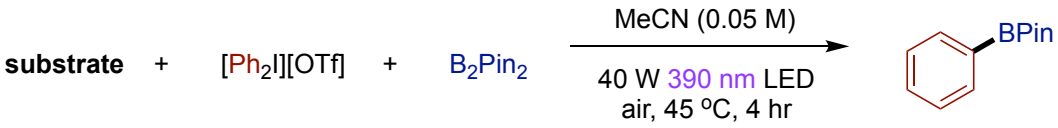

General procedure for pyridine derivative screen. A magnetic stir bar, substrate (0.05 mol. 1.0 eq.), diphenyliodonium triflate (21 mg, 0.05 mmol, 1.0 eq.), and bis(pinacolato)diboron (25 mg, 0.1 mmol, 2.0 eq.) were added to a 4-mL scintillation vial. MeCN or MeOH (1 mL, 0.05 M) was added, and the vials capped with a Teflon lined screw top cap. The reactions were irradiated by a 40 W 390 nm light at 45 °C for 4 hours. After 4 hours, irradiation was stopped and a 20 µL aliquot was extracted using a microliter syringe and dispensed into a GC vial alongside 50 µL of a 0.04 M mesitylene (0.002 mmol mesitylene, 1 eq. relative to B_2Pin_2) stock solution before dilution to 1.5 mL total volume with EtOAc. This solution was analyzed by GC.

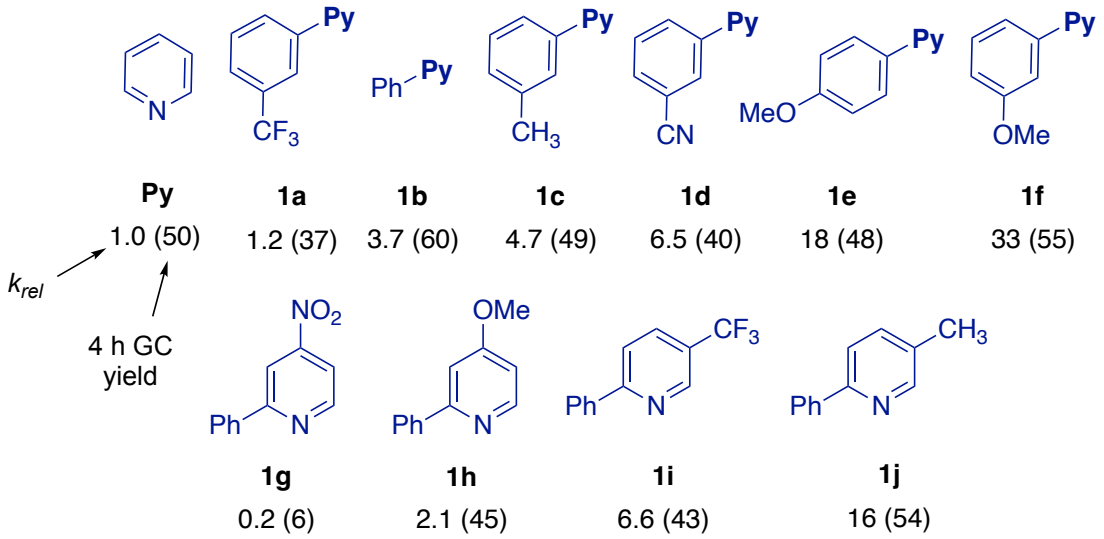

Figure S38. GC yields and relative rates for pyridine derivatives. GC yields are given as an average of 2 runs.

Initial rate kinetics of diaryliodonium salt derivatives

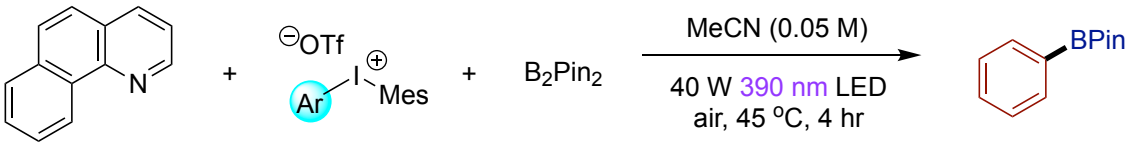

General procedure for collection of kinetic data for diaryliodonium salt derivatives. A magnetic stir bar, diaryliodonium salt (0.05 mmol, 1.0 eq.) was added to a 4-mL scintillation vial. To this, 500 µL of a 0.1 M benzo[*h*]quinoline stock solution was added alongside 500 µL of a 0.2 M bis(pinacolato)diboron stock solution. The vial was sealed with a screw top open cap affixed with a PTFE septum. The reactions were irradiated by a 40 W 390 nm light at 45 °C. At pre-determined timepoints, 20 µL aliquots were extracted using a microliter syringe without turning the LED off or removing the heat. The aliquots were transferred to a GC vial alongside 50 µL of a 0.04 M mesitylene (0.002 mmol mesitylene, 1 eq. relative to B_2Pin_2) stock solution before dilution to 1.5 mL total volume with EtOAc. These solutions were analyzed by GC and plotted using excel.

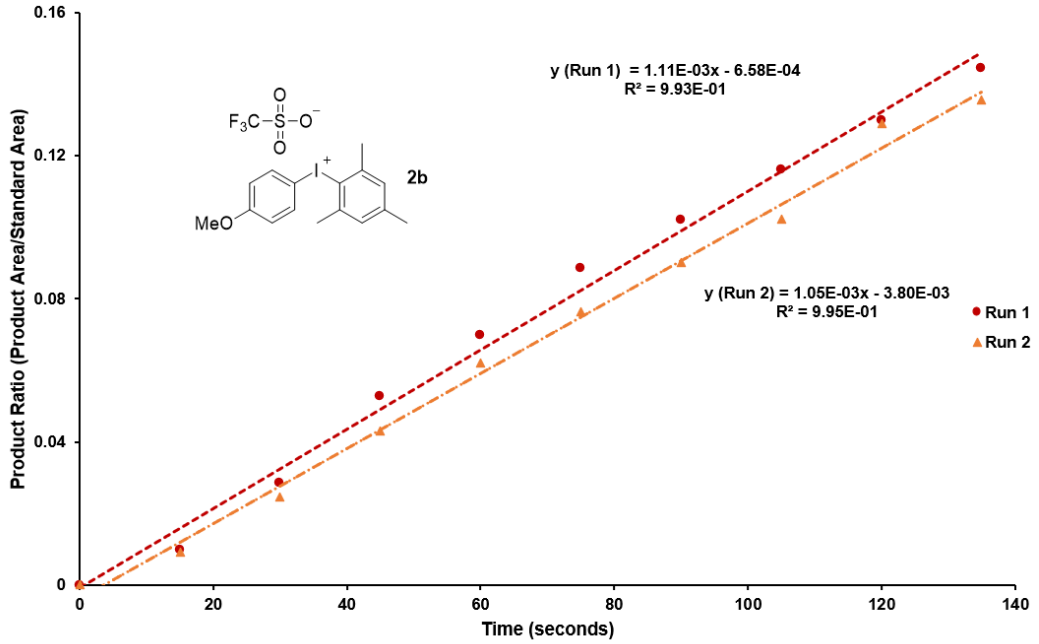

Figure S39. Initial rate time course using 4-methoxyphenylmesityl iodonium triflate (**2b**) as aryl radical source.

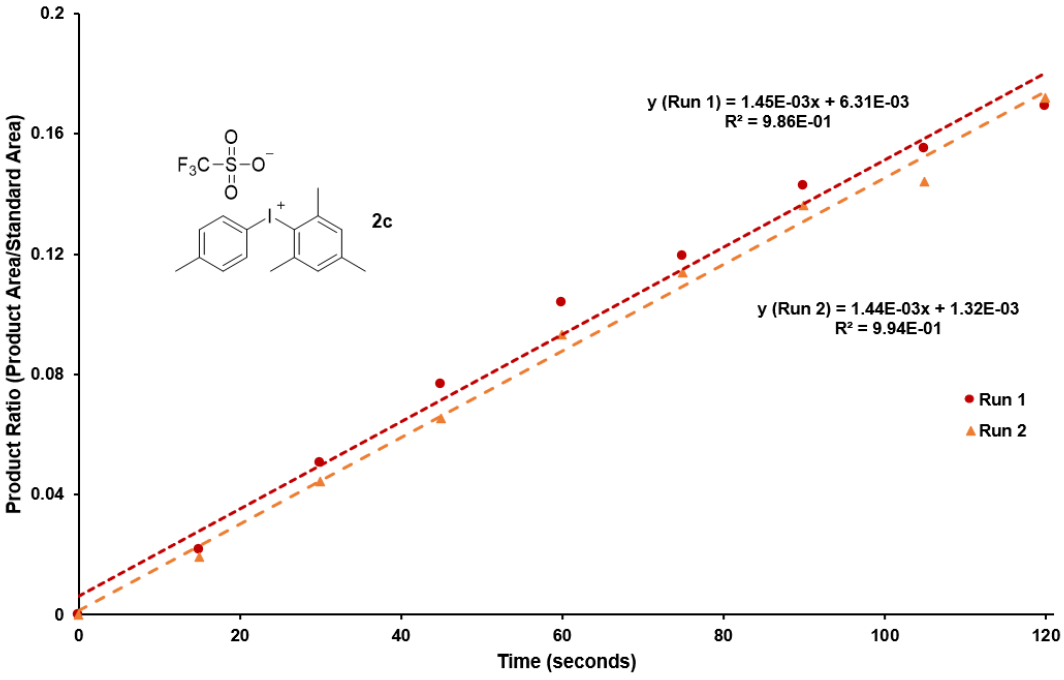

Figure S40. Initial rate time course using 4-methylphenylmesityl iodonium triflate (**2c**) as aryl radical source.

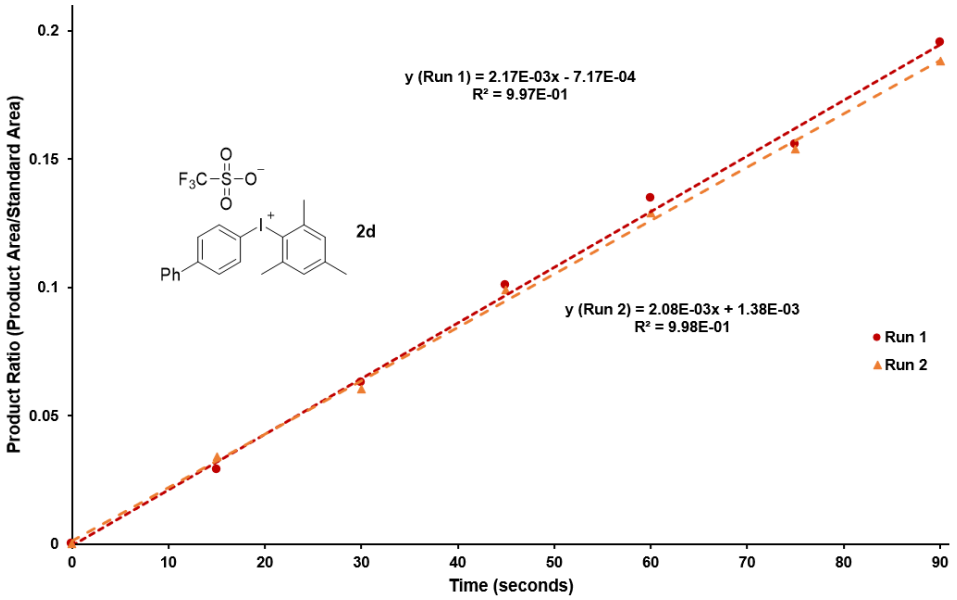

Figure S41. Initial rate time course using 4-biphenylmesityl iodonium triflate (**2d**) as aryl radical source.

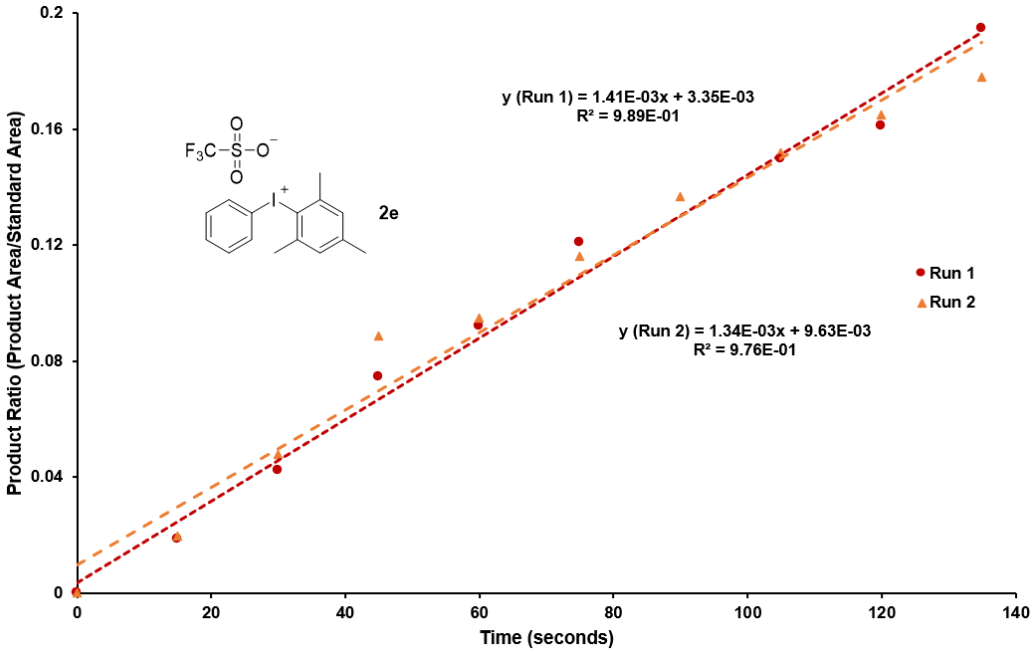

Figure S42. Initial rate time course using phenylmesityl iodonium triflate (**2e**) as aryl radical source.

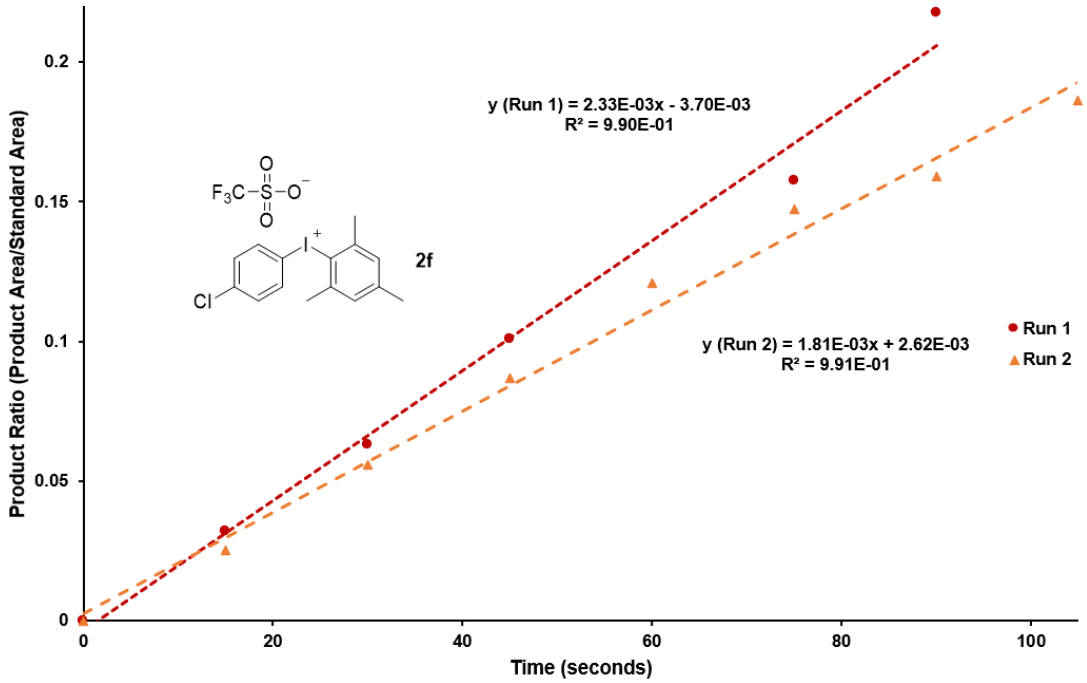

Figure S43. Initial rate time course using 4-chlorophenylmesityl iodonium triflate (**2f**) as aryl radical source.

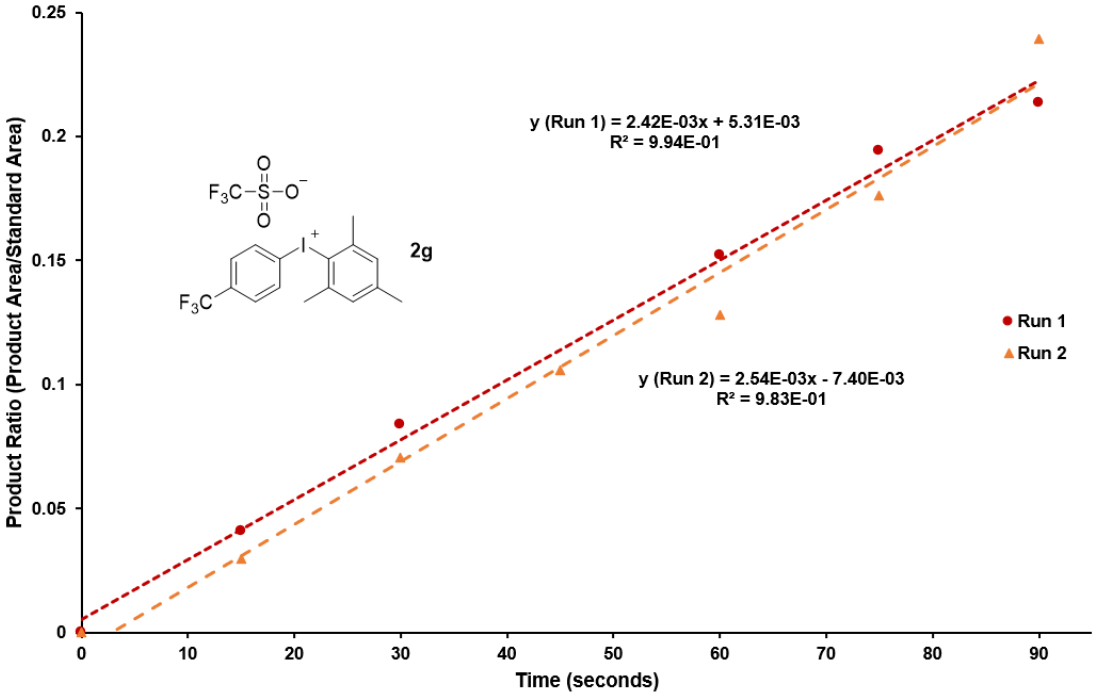

Figure S44. Initial rate time course using 4-trifluoromethylphenylmesityl iodonium triflate (**2g**) as aryl radical source.

Iodonium Salt	Initial rate 1 (area/s)	Initial rate 2 (area/s)	Average initial rate (area/s)
2b	1.11×10^{-3}	1.05×10^{-3}	1.08×10^{-3}
2c	1.45×10^{-3}	1.44×10^{-3}	1.45×10^{-3}
2d	2.17×10^{-3}	2.08×10^{-3}	2.13×10^{-3}
2e	1.41×10^{-3}	1.34×10^{-3}	1.38×10^{-3}
2f	2.33×10^{-3}	1.81×10^{-3}	2.07×10^{-3}
2g	2.42×10^{-3}	2.54×10^{-3}	2.48×10^{-3}

Table S7. Tabulated initial rate data for various iodonium salts.

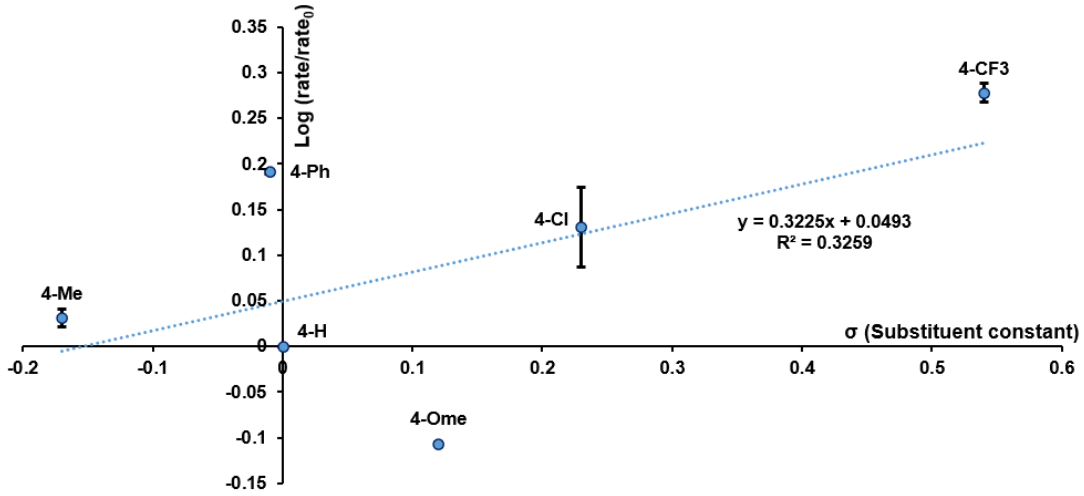

Figure S45. Hammett plot for substituted diaryliodonium salts.

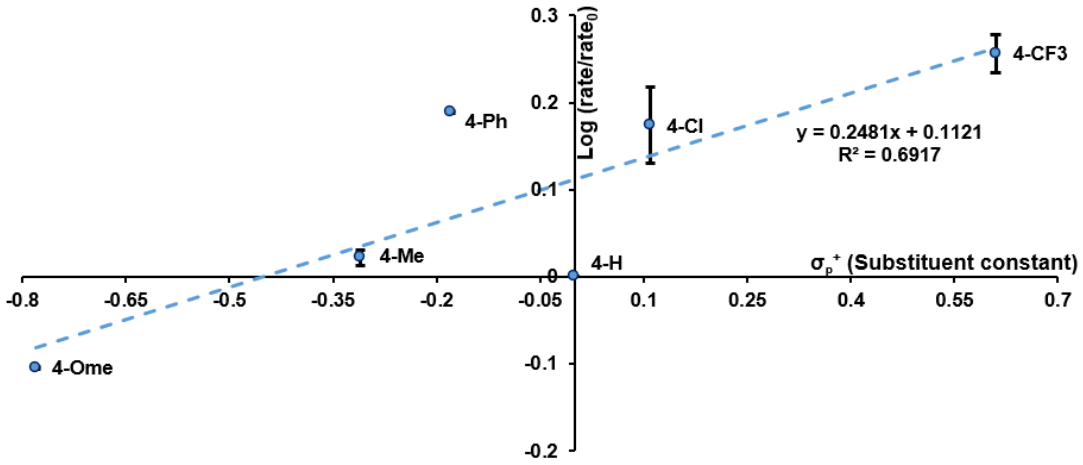

Figure S46. Hammett–Brown plot using σ_p^+ for substituted diaryliodonium salts.

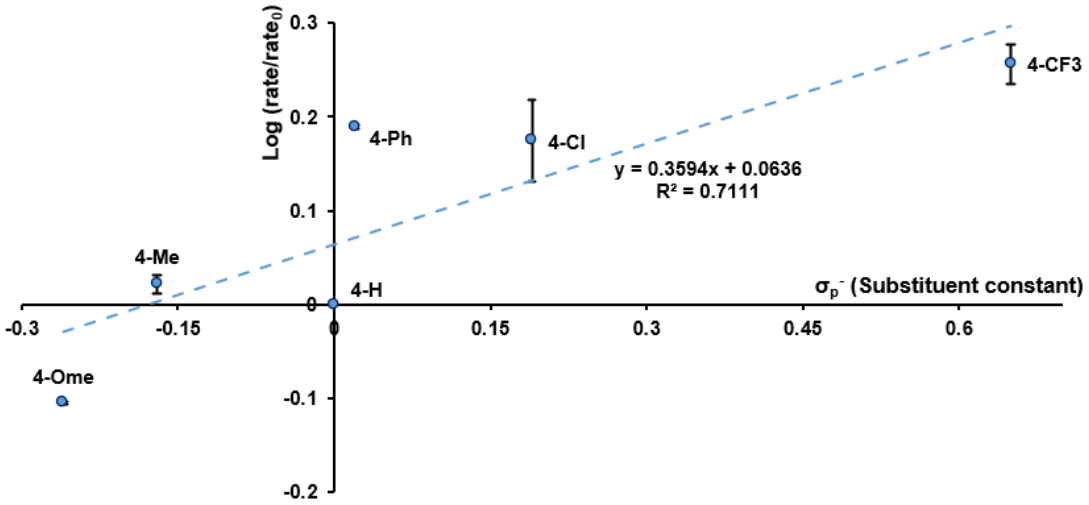

Figure S47. Hammett–Brown plot using σ_p^- for substituted diaryliodonium salts.

Based on these Hammett and Hammett-Brown plots, we can tentatively state that electron-deficient iodonium analogues result in faster radical generation reactions. However, the low correlation of the data to a linear trend suggests there is more information to be gathered and the conclusion may not be so cut and dry as a positive ρ value might suggest. Further experimentation is ongoing to better understand the impact of iodonium salt electronics on radical generation ability.

E. Preliminary mechanistic studies

Synthesis of 1,1,2-triphenylethylene. 1,1,2-triphenylethylene was synthesized following literature procedure.[1] Phenylboronic acid (1.0 mmol, 4.0 eq.), TEMPO (1.0 mmol, 4.0 eq.), potassium fluoride (1.0 mmol, 4.0 eq.), Palladium acetate (0.025 mmol, 10 mol%), styrene (0.25 mmol, 1.0 eq.), and propionic acid (1 mL) were added to a 4 mL vial alongside a stir bar. The reaction was stirred at room temperature for 1 hour. The reaction was then transferred to a separatory funnel where 5 mL of aqueous saturated Na_2CO_3 was added. The mixture was extracted with DCM (3 x 5 mL), dried over Na_2SO_4, and concentrated in vacuo. The crude mixture was purified by column chromatography on silica gel with hexane to afford a light-yellow oil. 81% Yield. ^{1}H NMR (400 MHz, $CDCl_3$): δ 7.35 – 7.28(m, 8H), 7.24 – 7.21 (m, 2H), 7.17 – 7.10 (m, 3H), 7.06 (m, 2H), 6.97 (s, 1H). This NMR agrees with literature data.[1]

Alternative radical trapping reagent. Because alternative aryl borylation strategies have been reported using pyridine derivatives, B_2Pin_2, and purple LEDs,[2] we set out to demonstrate that radical generation was occurring and that it is not contingent upon the presence of diboron reagents. As such, 1,1-diphenylethylene is another common aryl radical trapping reagent used in the literature. So, we elected to substitute B_2Pin_2 with 1,1-diphenylacetylene under our LB-promoted radical generation conditions.

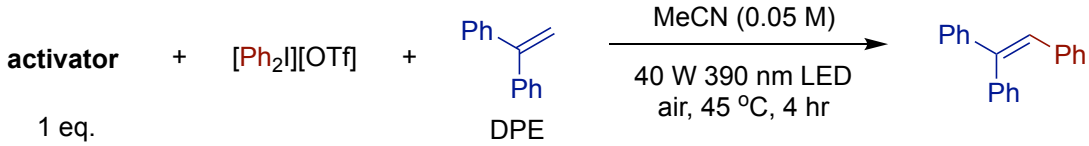

Procedure. Two 4-mL vials were charged with a magnetic stir bar, substrate (0.05 mmol, 1.0 eq.), diphenyliodonium triflate (21 mg, 0.05 mmol, 1.0 eq.), and 1,1-diphenylethylene (18 mg, 0.1 mmol, 2.0 eq.). Acetonitrile (1 mL, 0.05 M) was added, and the vials capped with a Teflon lined screw top cap. The reactions were irradiated by a 40 W 390 nm light at 45 °C for 4 hours. After 4 hours, irradiation was stopped and a 20 µL aliquot was extracted using a microliter syringe and dispensed into a GC vial alongside 50 µL of a 0.04 M

mesitylene (0.002 mmol mesitylene, 1 eq. relative to DPE) stock solution before dilution to 1.5 mL total volume with EtOAc. This solution was analyzed by GC-MS.

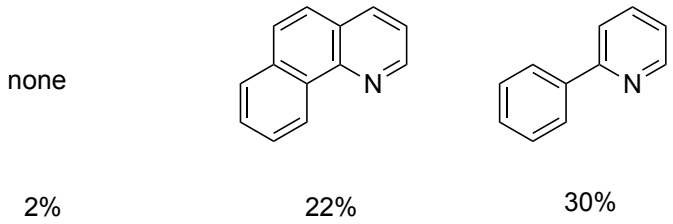

Figure S48. Evaluation of activator efficiency for diaryl alkene arylation.

TEMPO trapping experiments

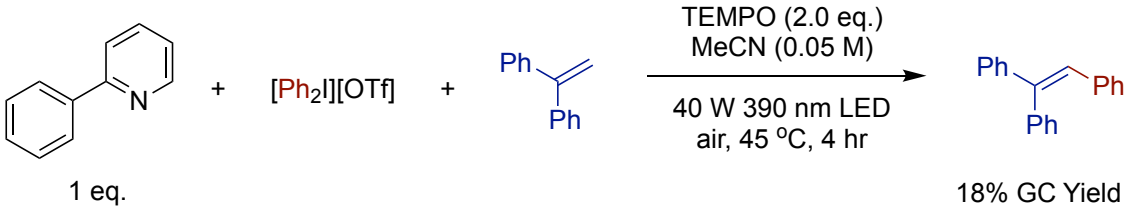

Procedure. Two 4-mL vials were charged with a magnetic stir bar, 2-phenylpyridine (7.8 mg,0.05 mmol, 1.0 eq.), diphenyliodonium triflate (21 mg, 0.05 mmol, 1.0 eq.), 1,1-diphenylethylene (18 mg, 0.1 mmol, 2.0 eq.), and 2,2,6,6-tetramethylpiperidine-1-oxyl (TEMPO) (16 mg, 0.1 mmol, 2.0 eq.). Acetonitrile (1 mL, 0.05 M) was added, and the vials capped with a Teflon lined screw top cap. The reactions were irradiated by a 40 W 390 nm light at 45 °C for 4 hours. After 4 hours, irradiation was stopped and a 20 µL aliquot was extracted using a microliter syringe and dispensed into a GC vial alongside 50 µL of a 0.04 M mesitylene (0.002 mmol mesitylene, 1 eq. relative to trapping reagent) stock solution before dilution to 1.5 mL total volume with EtOAc. This solution was analyzed by GC-MS.

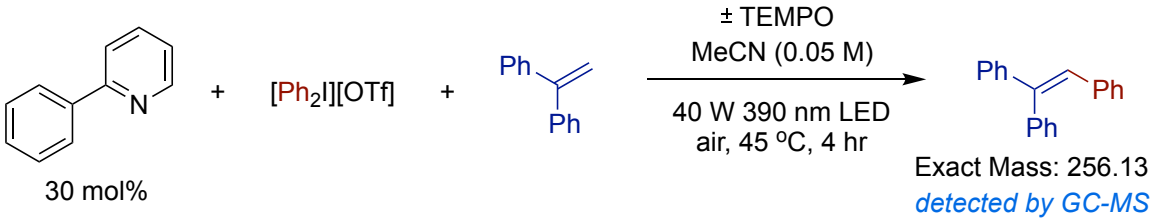

Procedure. Two 4-mL vials were charged with a magnetic stir bar, 2-phenylpyridine (0.015 mmol, 30 mol%), diphenyliodonium triflate (21 mg, 0.05 mmol, 1.0 eq.), and 1,1-diphenylethylene (18 mg, 0.1 mmol, 2.0 eq.). Acetonitrile (1.0 mL, 0.05 M) was added to each vial. To one vial, 2,2,6,6-tetramethylpiperidine-1-oxyl (TEMPO) (16 mg, 0.1 mmol, 2.0 eq.) was added and both vials were sealed with PTFE lined screw caps. The resulting reactions were irradiated by a 40 W 390 nm light at 45 °C under air for 4 hours. After 4 hours, irradiation was stopped. A 20 µL aliquot was extracted using a microliter syringe and dispensed into a GC vial alongside 1.0 mL of ethyl acetate and 50 µL of a 0.04 M mesitylene stock solution. This solution was then analyzed by GC-MS. Uncalibrated GC yield without TEMPO: 57%; Uncalibrated GC yield with TEMPO: 15%.

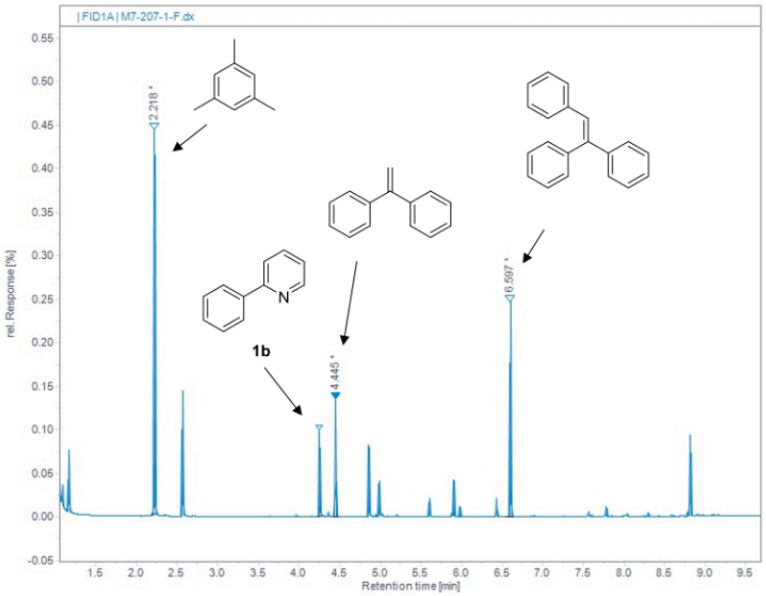

#	Name	Signal description	RT (min)	Area (pA·s)	Area%	Height (pA)	Height%	Amount	Concentration	Start time (min)	End time (min)
1		FID1A	2.218	134.905	48.485	214.430	48.00			2.199	2.238
2		FID1A	4.247	29.512	10.607	47.817	10.70			4.228	4.298
3		FID1A	4.445	37.915	13.627	64.978	14.55			4.409	4.483
4		FID1A	6.597	75.907	27.281	119.470	26.75			6.542	6.645

Figure S49. GC-FID trace of aryl radical trapping by 1,1-diphenylethylene to give 1,1,2-triphenylethylene in the absence of TEMPO.

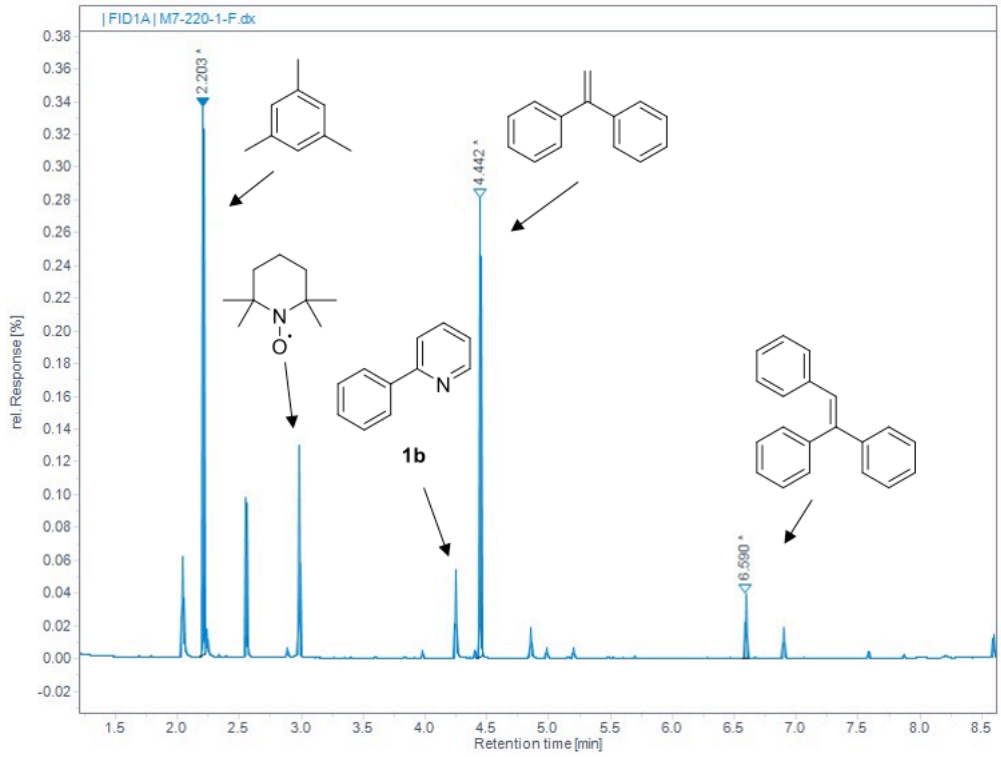

#	Name	Signal description	RT (min)	Area (pA·s)	Area%	Height (pA)	Height%	Amount	Concentration	Start time (min)	End time (min)
1		FID1A	2.203	68.606	49.136	127.674	51.19			2.187	2.221
2		FID1A	4.442	61.257	43.873	106.860	42.84			4.421	4.463
3		FID1A	6.590	9.760	6.990	14.889	5.97			6.565	6.622

Figure S50. GC-FID trace of aryl radical trapping by 1,1-diphenylethylene to give 1,1,2-triphenylethylene with TEMPO.

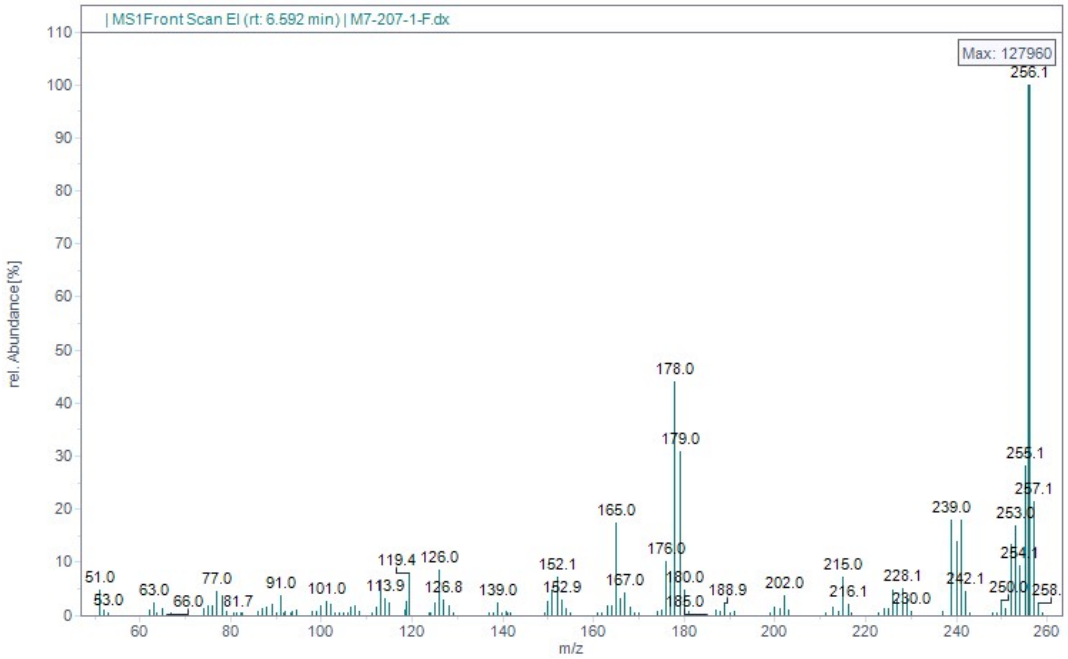

Figure S51. GC-MS of peak corresponding to 1,1,2-triphenylethylene.

1 eq. 16% GC Yield

Procedure. Two 4-mL vials were charged with a magnetic stir bar, 2-phenylpyridine (7.8 mg,0.05 mmol, 1.0 eq.), diphenyliodonium triflate (21 mg, 0.05 mmol, 1.0 eq.), B_2Pin_2 (25 mg, 0.1 mmol, 2.0 eq.), and 2,2,6,6-tetramethylpiperidine-1-oxyl (TEMPO) (16 mg, 0.1 mmol, 2.0 eq.). Acetonitrile (1 mL, 0.05 M) was added, and the vials capped with a Teflon lined screw top cap. The reactions were irradiated by a 40 W 390 nm light at 45 °C for 4 hours. After 4 hours, irradiation was stopped and a 20 µL aliquot was extracted using a microliter syringe and dispensed into a GC vial alongside 50 µL of a 0.04 M mesitylene (0.002 mmol mesitylene, 1 eq. relative to trapping reagent) stock solution before dilution to 1.5 mL total volume with EtOAc. This solution was analyzed by GC-MS.

30 mol% 10% GC yield

Procedure. A 4-mL vial was charged with a magnetic stir bar, 2-phenylpyridine (0.015 mmol, 30 mol%), diphenyliodonium triflate (21 mg, 0.05 mmol, 1.0 eq.), 2,2,6,6-tetramethylpiperidine-1-oxyl (TEMPO) (16 mg, 0.1 mmol, 2.0 eq.), and B_2Pin_2 (25 mg, 0.1 mmol, 2.0 eq.). Acetonitrile (1.0 mL, 0.05 M) was added, and the vial was sealed with PTFE lined screw cap. The resulting reaction was irradiated by a 40 W 390 nm light at 45 °C under

air for 4 hours. After 4 hours, irradiation was stopped. A 20 μL aliquot was extracted using a microliter syringe and dispensed into a GC vial alongside 1.0 mL of ethyl acetate and 50 μL of a 0.04 M mesitylene stock solution. This solution was then analyzed by GC-MS. GC yield = 10%.

Interactions between B_2Pin_2, 1b, and 2a. We used ^{11}B NMR to probe whether any interactions between **1b**, B_2Pin_2, and **2a** occur under our reaction conditions that might lead to aryl radical generation via an EDA complex. First, an ^{11}B NMR spectrum of a 0.1 M B_2Pin_2 solution in CD_3CN was collected. Then, 2-phenylpyridine (0.1 M) was added to the same NMR tube and another ^{11}B spectrum was collected. These spectra were compared the spectrum for a solution of B_2Pin_2, 2-phenylpyridine, and diphenyliodonium triflate (all 0.1 M). The overlay of these three NMR spectra shows no shift in the B_2Pin_2 peak, suggesting against any notable interactions between these components with each other.

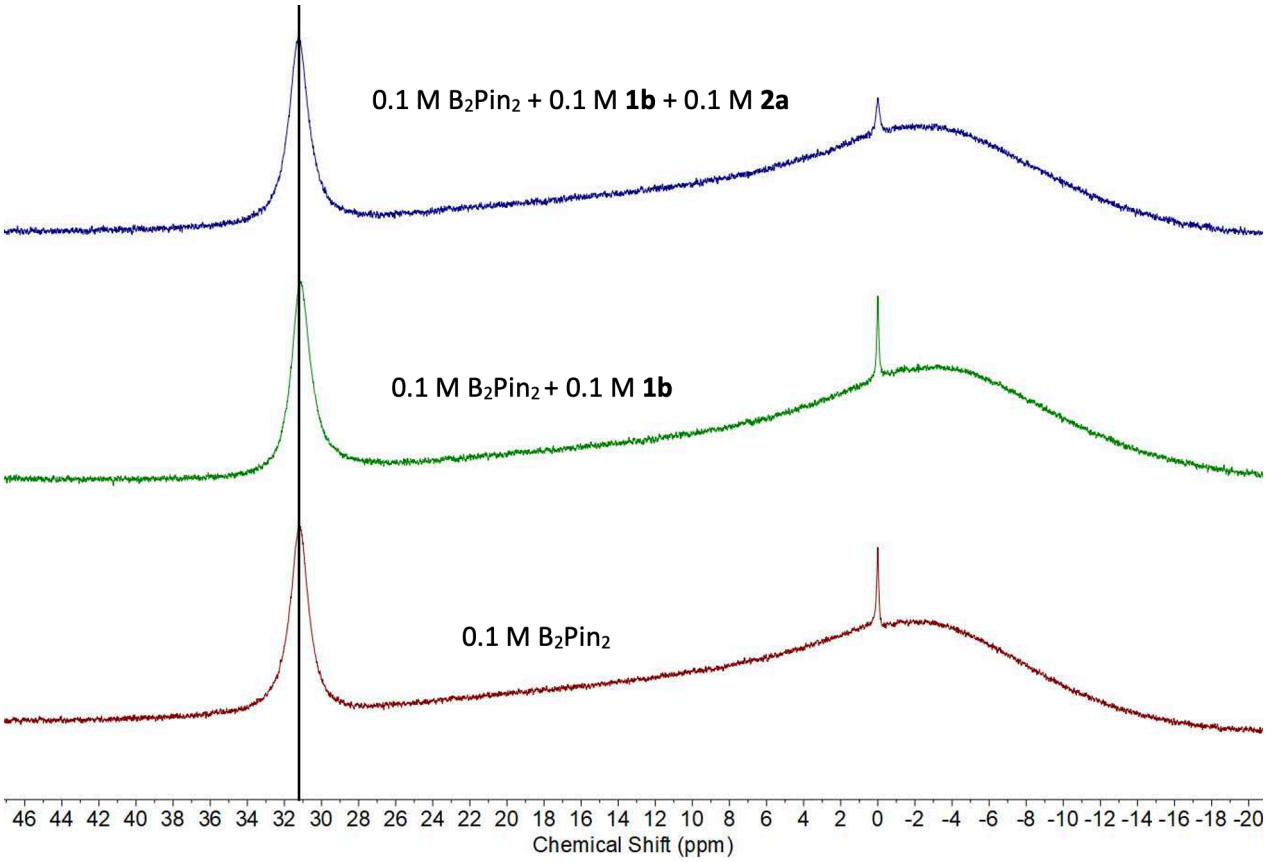

Figure S52. ^{11}B NMR spectra of equimolar concentrations of B_2Pin_2, B_2Pin_2 + **1a**, and B_2Pin_2 + **1a** + **2a**. No change in the B_2Pin_2 resonance is observed. Peak at 0 ppm is the BF_3-Et_2O standard. Broad band at *ca.* -2.0 ppm is the borosilicate glass of the NMR tube.

Interactions between B_2Pin_2 and DG_4. We used ^{11}B VT NMR to confirm that no interactions between DG_4, and B_2Pin_2 occur between -50 °C to 50 °C. A solution of 0.1 M B_2Pin_2 and 0.05 M DG_4 in CD_3OD was collected at room temperature. The operating temperature was then brought down to -50 °C and the solution was allowed to equilibrate for 10 minutes before data acquisition. This procedure was followed for collection of spectral data at -30, 0, 30, and 50 °C.

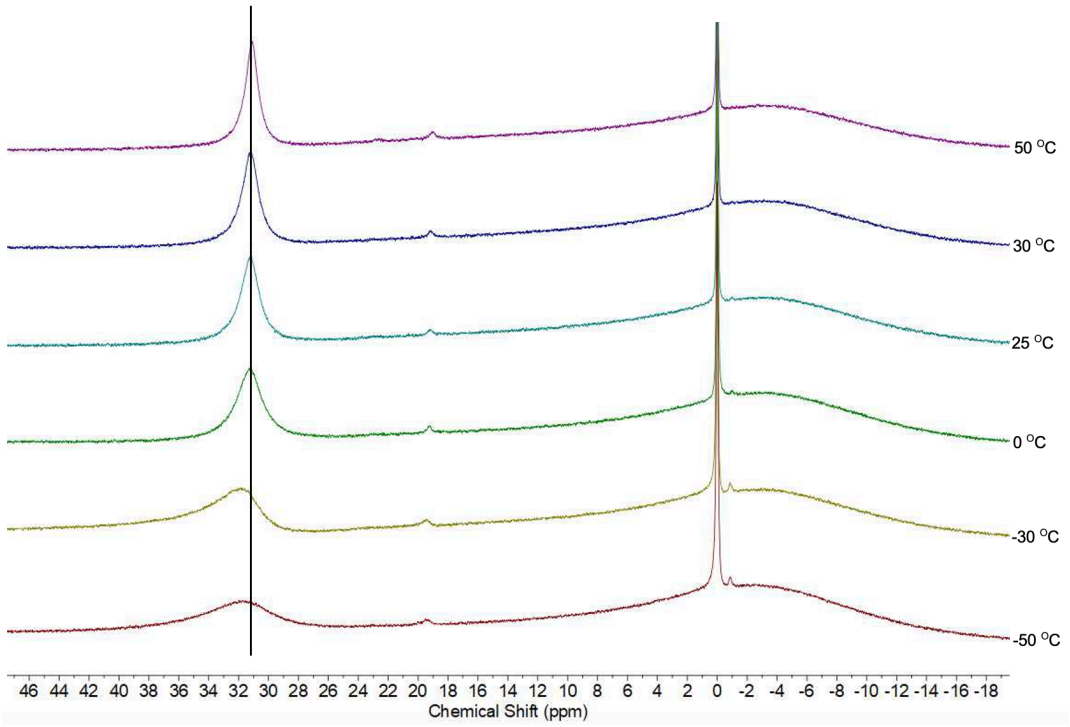

Figure S53. ^{11}B VT NMR spectra of 0.1 M B_2Pin_2 and 0.05 M **DG$_4$**. Peak at +19 ppm is degraded B_2Pin_2. Peak at 0 ppm is the BF_3-Et_2O standard. Broad band at *ca.* -2.0 ppm is the borosilicate glass of the NMR tube.

Low temperature ^{11}B NMR of B_2Pin_2 in MeOH. A solution of 0.1 M B_2Pin_2 in CD_3OD was collected at room temperature. The operating temperature was then brought down to -50 °C and the solution was allowed to equilibrate for 10 minutes before data acquisition.

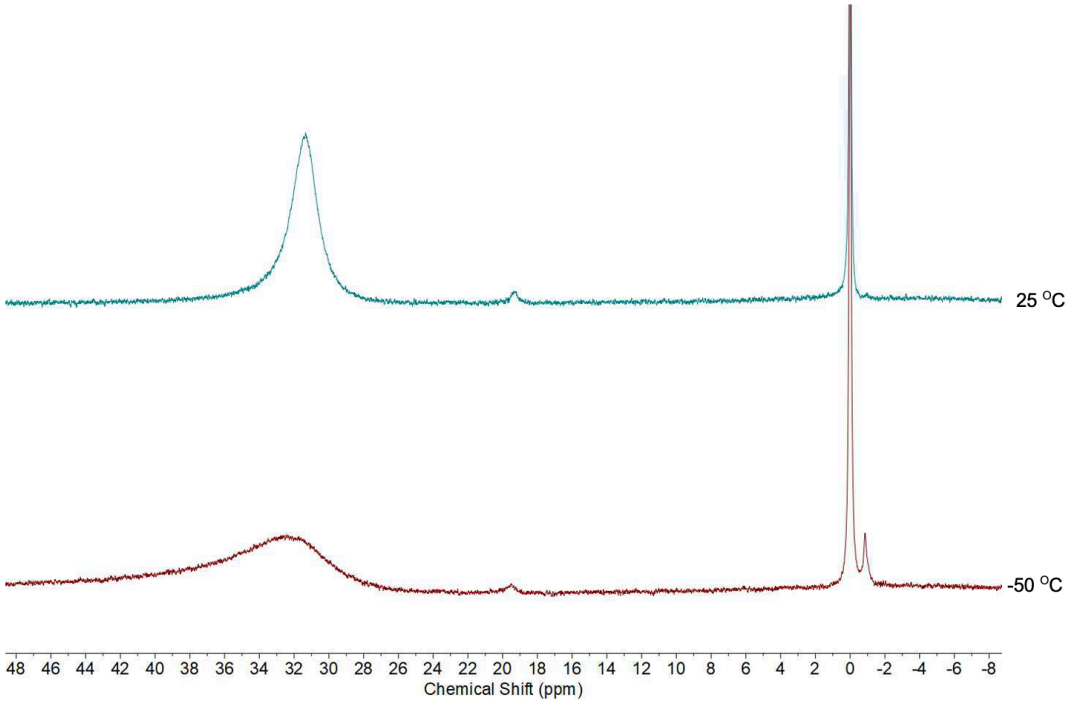

Figure S54. ^{11}B VT NMR spectra of 0.1 M B_2Pin_2. Peak at +19 ppm is degraded B_2Pin_2. Peak at 0 ppm is the BF_3-Et_2O standard. Broad band at *ca.* -1.0 ppm results from a likely MeOH interaction with B_2Pin_2.

Interactions between 1b and 2a. Sanford and co-workers showed that 2-phenylpyridine coordinates to diphenyliodonium salts at temperatures greater than 80 °C with a K_{eq} greater than 100.[3] To determine whether such an interaction is present at 25 °C, various concentrations of solid **2a** were added to a 0.1 M solution of **1b** in 500 mL of CD_3CN. Total volume was kept constant over the course of the experiment. Comparing the ^1H NMR spectrum of pure **1b** with those of **1b** in the presence of increasing concentrations of **2a**, we observed no shift in the C2 proton of **1b**.

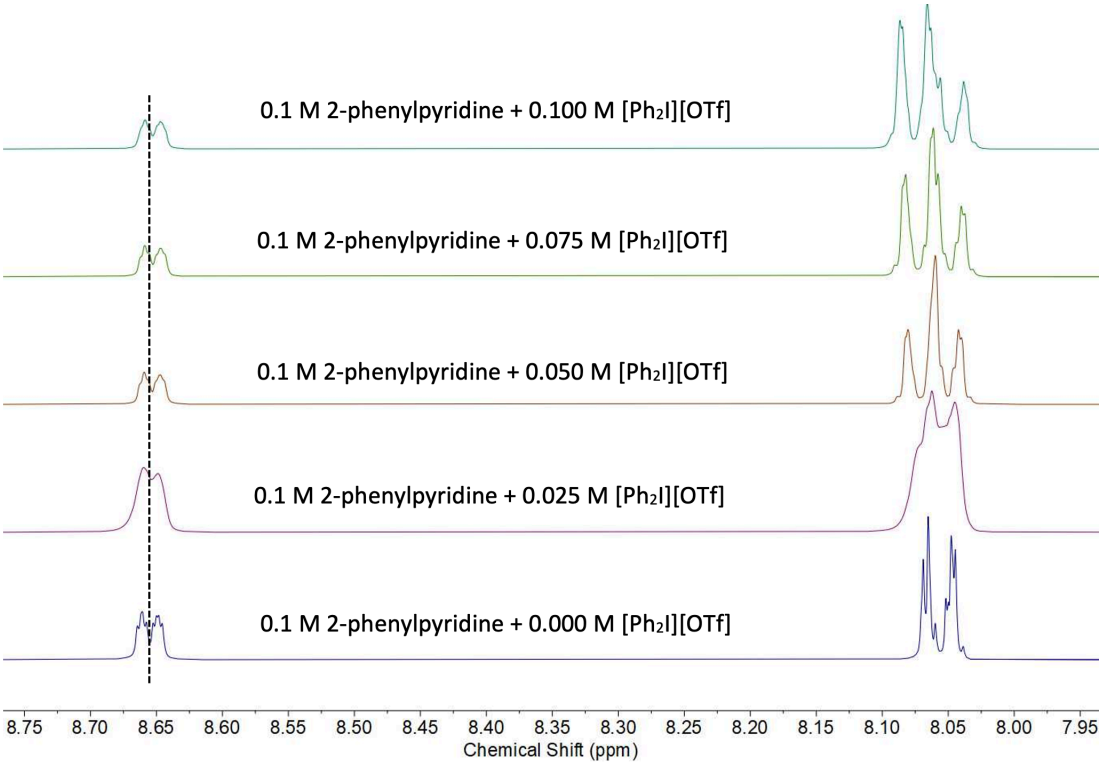

Figure S55. Stacked ^1H NMR spectra of the low-field region demonstrating that increasing concentrations of **2a** do not induce a shift in the C2 H-atom of **1b** at 8.66 ppm.

Interactions between DG_4 and 2a at various temperatures. To probe whether interactions between **DG_4** and **2a** occur at temperatures other than 25 °C, ^1H NMR spectra were collected at various temperatures above and below ambient conditions. A ^1H NMR spectrum of an equimolar solution of **DG_4** (0.05 M) and **2a** (0.05 M) was taken at room temperature. The operating temperature was then brought down to -50 °C. The sample was allowed to equilibrate at the corresponding temperature in the NMR Probe for at least 10 minutes before data acquisition. This procedure was followed for the subsequent temperatures.

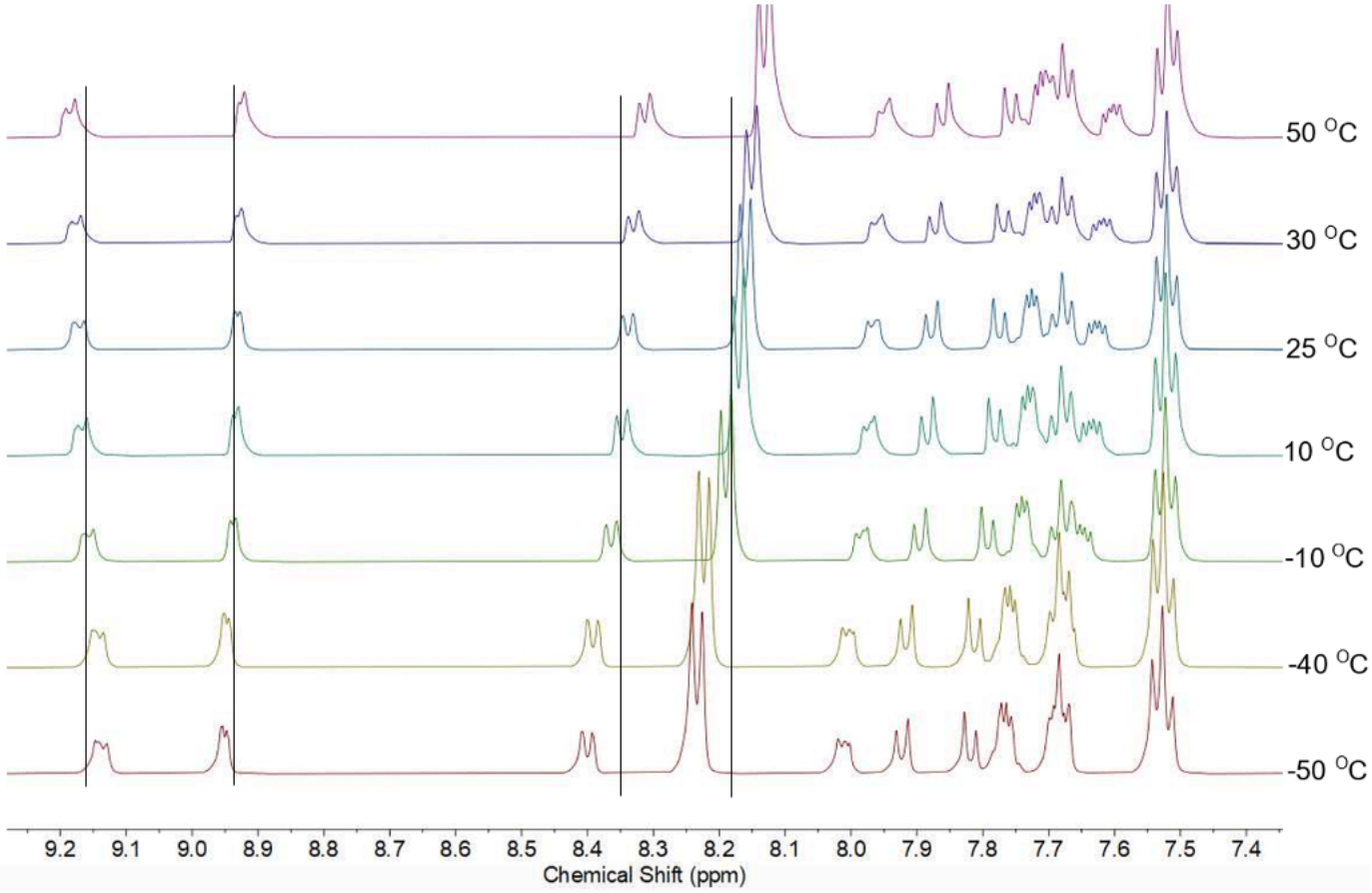

Figure S56. Stacked ^{1}H NMR spectra of the low-field region of an equimolar concentration of **DG$_4$** and **2a**.

The shifting of the resonances of both **DG$_4$** and **2a** made us wonder whether an interaction between the two was the cause. However, the downfield shift of the **DG$_4$** C2-H resonance (9.15 ppm) as temperature increases is opposite what would be expected if an adduct were forming. More typical is the deshielding of this resonance during complexation, which would be more visible at lower temperatures. Because of this odd behavior, we collected VT NMR spectra for both **DG$_4$** and **2a** independently to determine whether the combination of the two reagents was leading to an odd interaction.

VT NMR of DG$_4$ and 2a. To elucidate the origins of the proton shifts, a 0.05 M solution of **DG$_4$** or **2a** were first collected at room temperature. The operating temperature was then brought down to -50 °C. The sample was allowed to equilibrate to this temperature by allowing the sample to sit in the NMR probe for 10 minutes before data acquisition. This protocol was followed for all subsequent temperatures shown in the plot.

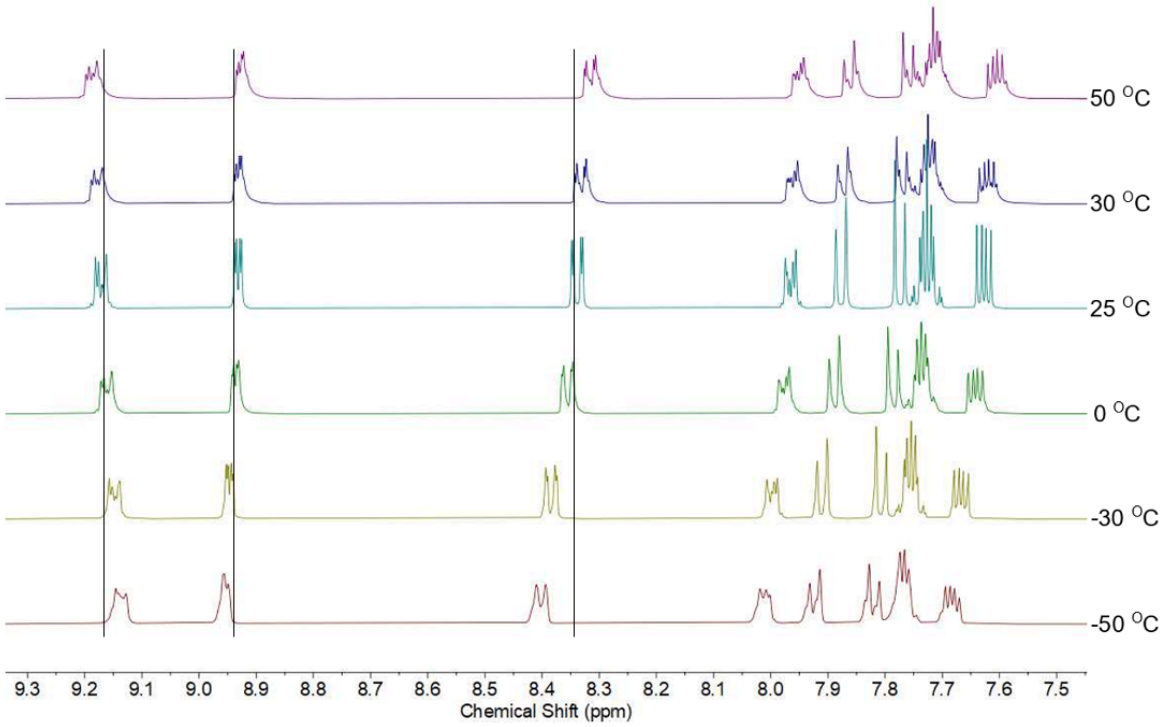

Figure S57. Stacked ^{1}H NMR spectra of the low-field region of an equimolar concentration of **DG$_4$**.

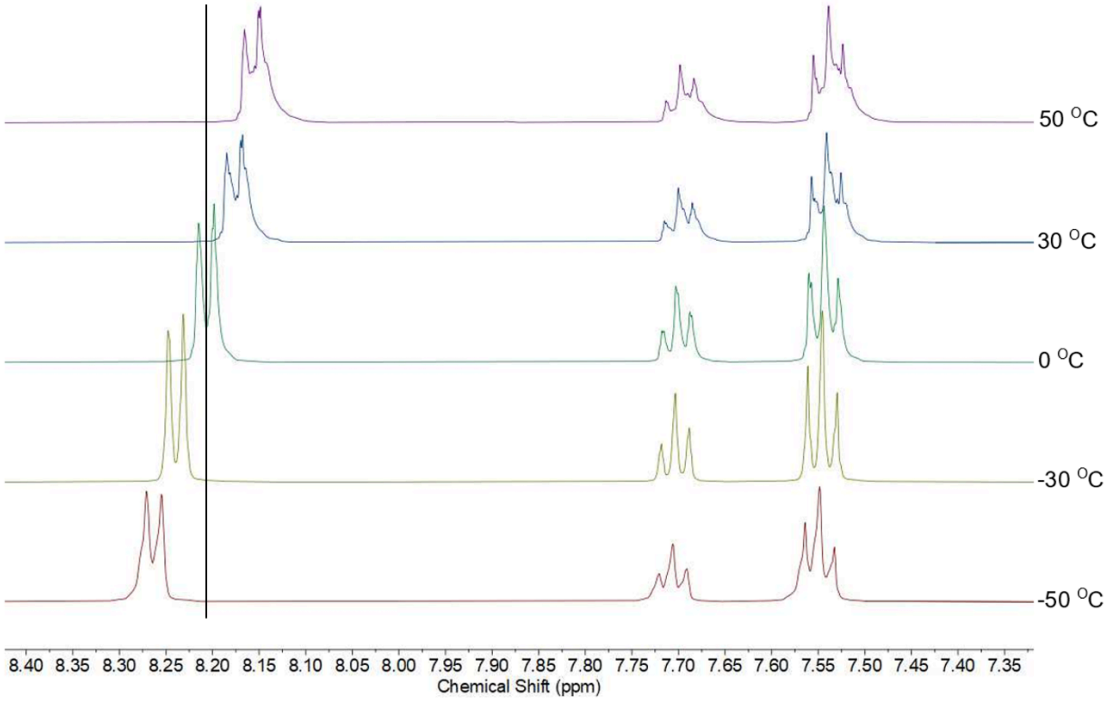

Figure S58. Stacked ^{1}H NMR spectra of the low-field region of an equimolar concentration of **2a**.

From these VT NMR experiments, we can conclude that the observed shifts in the ^{1}H NMR resonances observed when **DG$_4$** and **2a** are combined at various temperatures results from the molecules themselves rather than from any interactions between the species. Therefore, we can definitively state that we do not see any evidence of an EDA adduct by ^{1}H NMR.

Ocular Spectroscopy

Some EDA complexes result in a visible color change. Thus, to probe whether a color change can be visualized by ocular spectroscopy, equimolar mixtures of either **1b** or **DG4** with **2a** were prepared and photographed. All solutions are 0.1 M in MeCN and photographed against a 92 bright piece of copy paper.

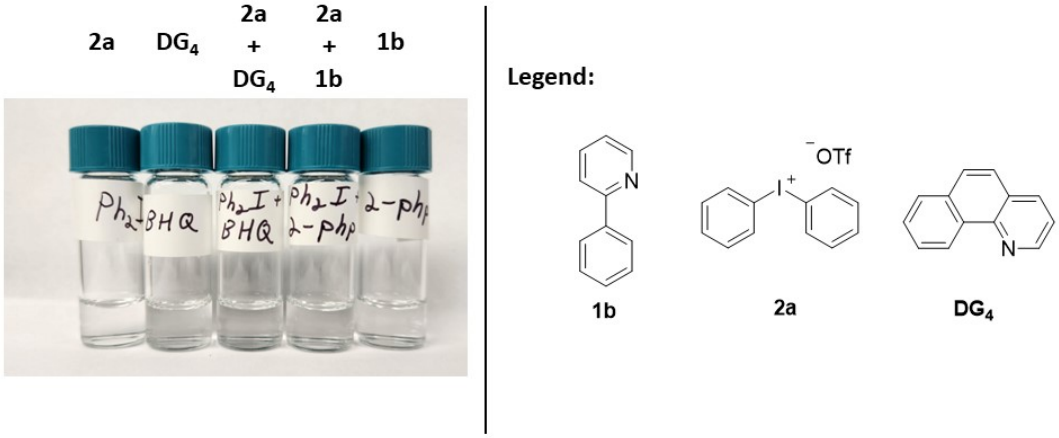

Figure S59. Photographs of mixtures of **1b** or **DG4** with **2a** demonstrating no color changes.

Electron-donor acceptor (EDA) complexes are often proposed for photocatalyst (PC)-free systems that are activated by absorption of visible light. Despite our inability to observe any discrete binding events between **1b** and **2a**, we decided to support the absence of an EDA complex by UV-Vis spectroscopy. EDA complexes show new absorption events by UV-Vis and the absence of new bands suggests against the formation of EDA complexes in our system. In no instance do we see the appearance of any new absorbance bands around 400 nm, which is where we irradiate our radical generation reactions. Therefore, based upon these data and the ^{1}H NMR experiments, we rule out the formation of a discrete EDA complex.

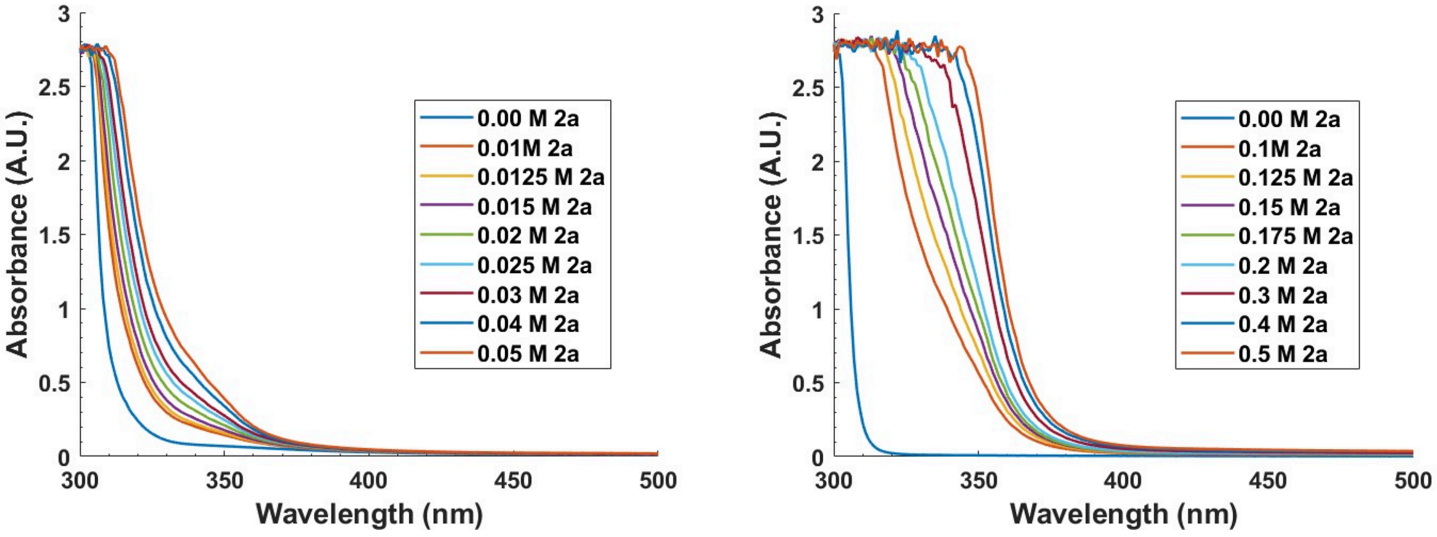

Figure S60. Absorbance spectra of 2-phenylpyridine (**1b**, 0.01 M) with dilute (left) and excessive (right) concentrations of diphenyliodonium triflate (**2a**) in acetonitrile.

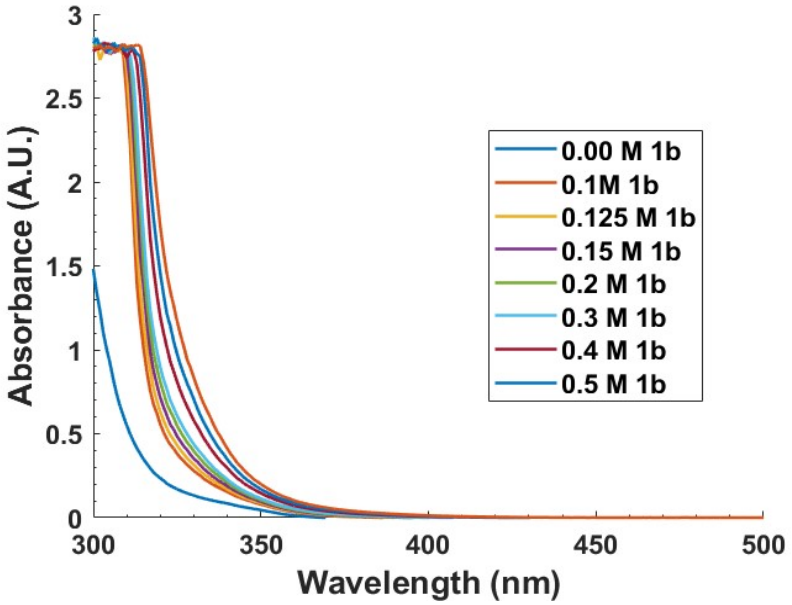

Figure S61. Absorbance spectra of diphenyliodonium triflate (**2a**, 0.01 M) with excessive quantities of 2-phenylpyridine (**1b**) in acetonitrile.

Lastly, to determine whether aryl radical generation can be attributed to absorption by the LB activators, we collected absorbance spectra of each 2-arylpyridine derivative for which we measured its rate of radical generation. For substitution patterns on the flanking ring, 1d displays a significant absorbance at 400 nm, relative to any other derivative, and it accelerated radical generation 6.5x as compared to no additive. However, using 1f as activator resulted in a 33x rate acceleration but it does not show any absorption at wavelengths >350 nm. Based on these two isolated datapoints, we can conclude that direct excitation of LB activator substrates is unlikely to be responsible for their observed impact on radical generation.

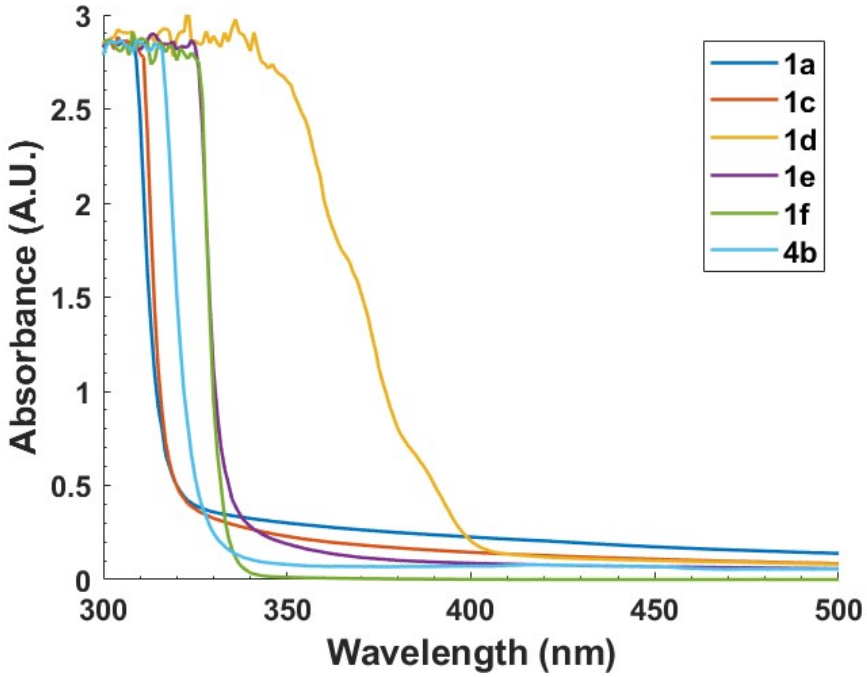

Figure S62. Absorbance spectra were collected for each 2-phenylpyridine derivative featuring a substitution on the flanking phenyl ring. Sample concentrations were each 0.1 M in MeCN.

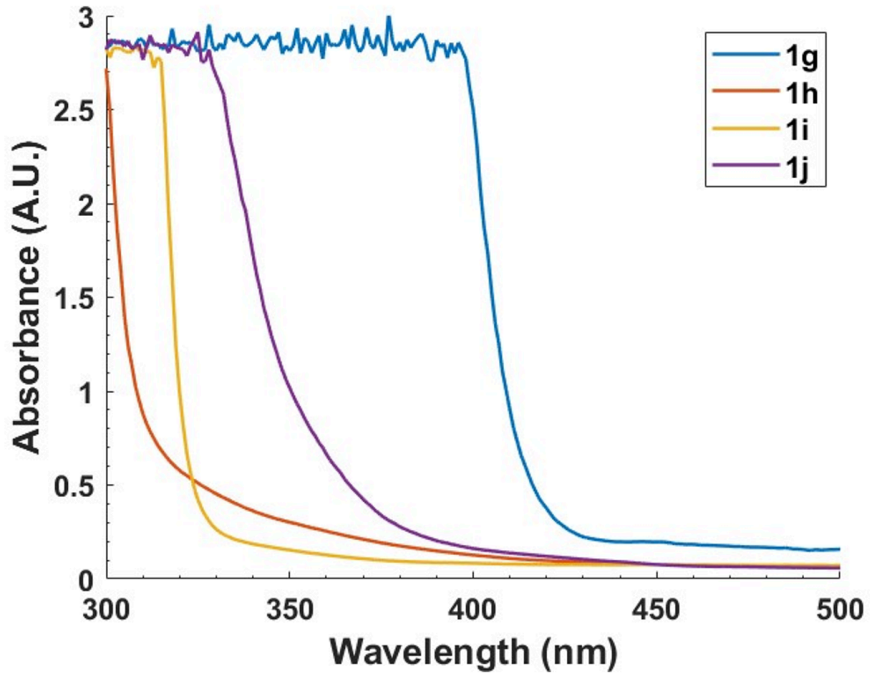

Figure S63. Absorbance spectra were collected for each 2-phenylpyridine derivative featuring a substitution on the pyridine ring. Sample concentrations were each 0.1 M in MeCN.

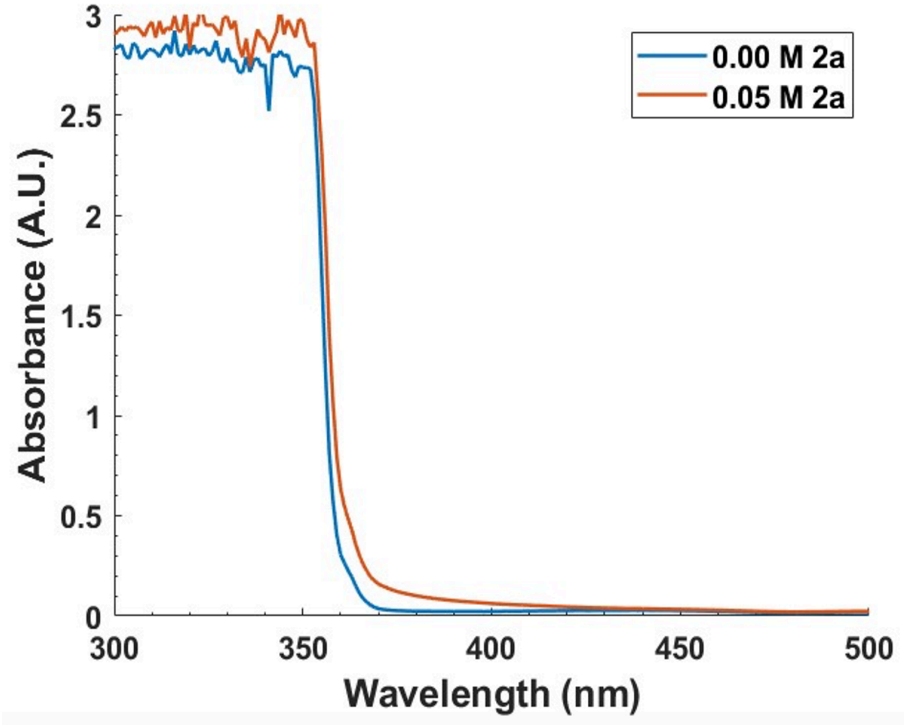

Figure S64. Absorbance spectra collected of benzo[h]quinoline (**DG$_4$**) in the presence of 0 and 0.5 M **2a**. The concentration of benzo[h]quinoline was 0.05 M in MeCN.

F. Optimization of Pd-catalyzed 2-arylpyridine C–H arylation

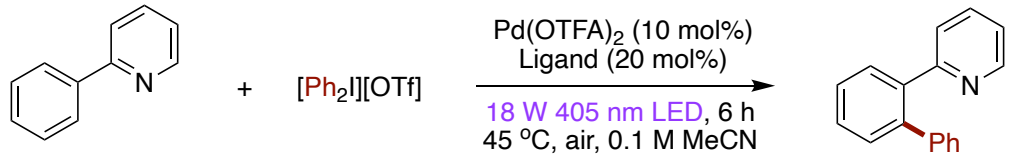

To a 4-mL vial with a magnetic stir bar was added $Pd(OTFA)_2$ (3.3 mg, 0.01 mmol, 10 mol%), ligand (0.02 mmol, 20 mol%), diphenyliodonium triflate (64 mg, 0.15 mmol, 1.5 eq.), and 2-phenylpyridine (15 mg, 0.10 mmol, 1.0 eq.). Acetonitrile (1.0 mL, 0.1 M) was added, and the reaction sealed with a PTFE lined screw cap. The reaction was irradiated by an 18 W 405 nm LED at 45 °C for 6 hours. Upon completion, the crude reaction was analyzed by GC-FID using ^{n}dodecane as the internal standard.

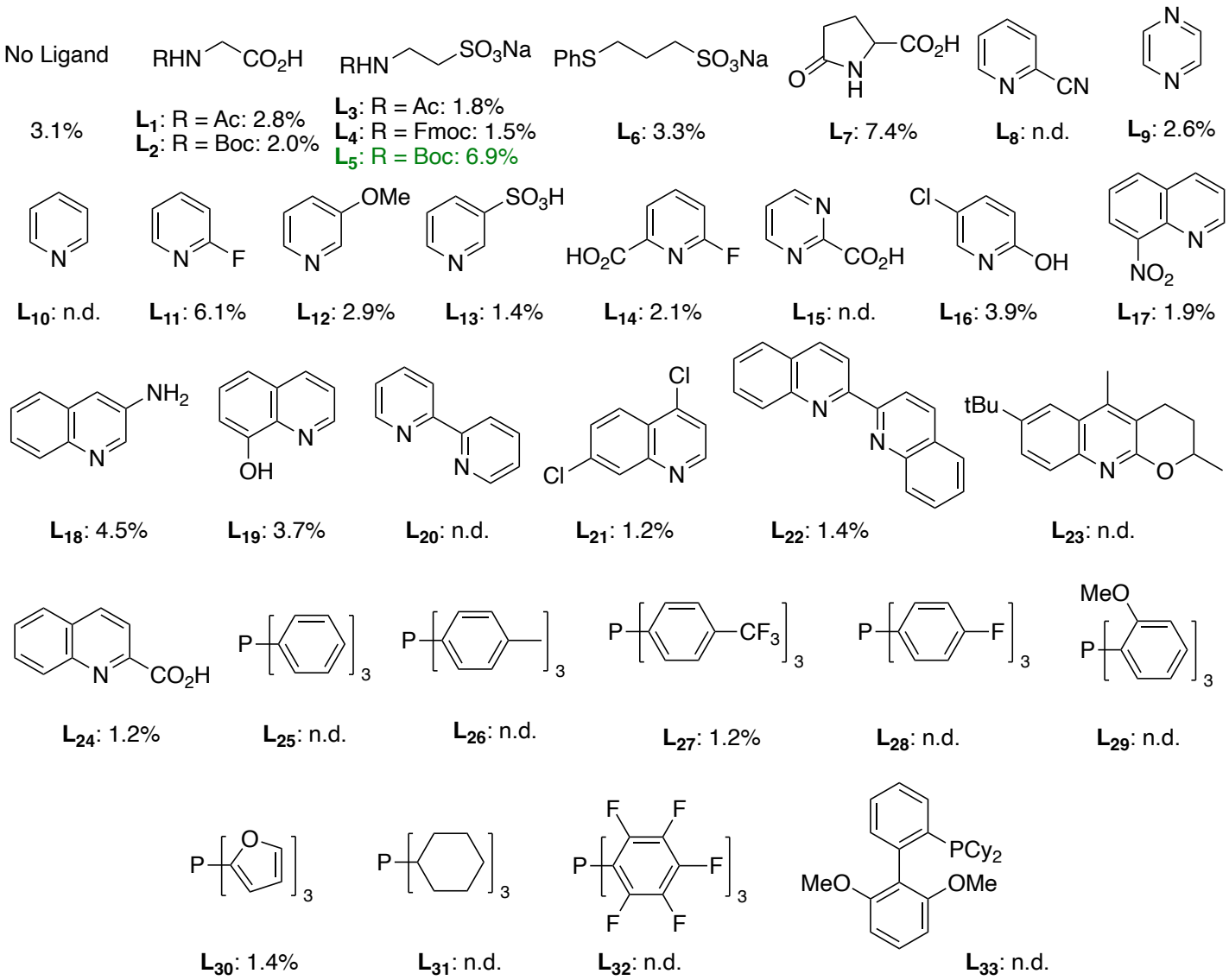

Figure S65. Ligand screen with calibrated GC yields versus ^{n}dodecane provided.

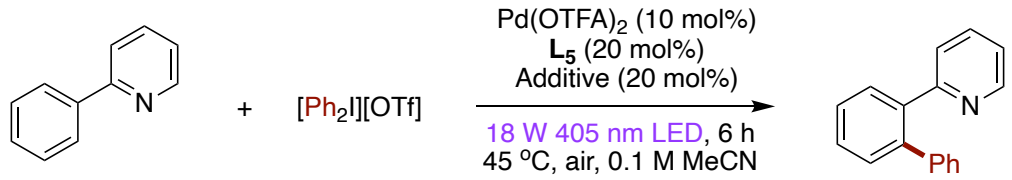

To a 4-mL vial with a magnetic stir bar was added $Pd(OTFA)_2$ (3.3 mg, 0.01 mmol, 10 mol%), **L_5** (4.9 mg, 0.02 mmol, 20 mol%), additive (0.02 mmol, 20 mol%), diphenyliodonium triflate (64 mg, 0.15 mmol, 1.5 eq.), and 2-phenylpyridine (15 mg, 0.10 mmol, 1.0 eq.). Acetonitrile (1.0 mL, 0.1 M) was added, and the reaction sealed with a PTFE lined screw cap. The reaction was irradiated by an 18 W 405 nm LED at 45 °C for 6 hours. Upon completion, the crude reaction was analyzed by GC-FID using ^{n}dodecane as the internal standard.

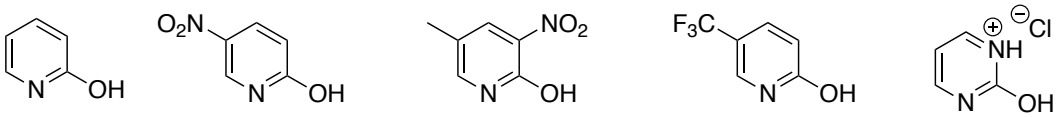

A_1: n.d. **A_2**: 1.6% **A_3**: n.d. **A_4**: n.d. **A_5**: n.d.

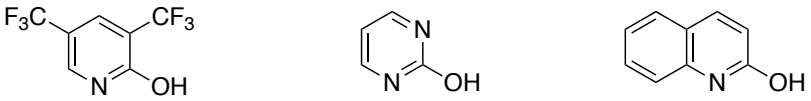

A_6: 3.9% **A_7**: n.d. **A_8**: n.d.

Figure S66. Additive screen with calibrated GC yields versus ^{n}dodecane provided.

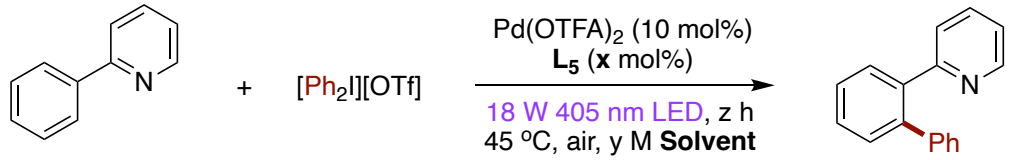

To a 4-mL vial with a magnetic stir bar was added $Pd(OTFA)_2$ (3.3 mg, 0.01 mmol, 10 mol%), **L_5** (x mol%), diphenyliodonium triflate (64 mg, 0.15 mmol, 1.5 eq.), and 2-phenylpyridine (15 mg, 0.10 mmol, 1.0 eq.). Solvent (y M) was added, and the reaction sealed with a PTFE lined screw cap. The reaction was irradiated by an 18 W 405 nm LED at 45 °C for 6 hours. Upon completion, the crude reaction was analyzed by GC-FID using ^{n}dodecane as the internal standard.

Entry	Solvent	Concentration (M)	L_5 loading (mol%)	Time (h)	GC Yield (%)
1	MeCN	0.10	20	6	6.9
2	MeOH	0.10	20	6	1.7
3	HFIP	0.10	20	6	1.8
4	THF	0.10	20	6	n.d.
5	$PhNO_2$	0.10	20	6	3.6
6	DCM	0.10	20	6	1.3
7	Acetone	0.10	20	6	1.0
8	DMF	0.10	20	6	2.2
9	MeCN	0.10	10	6	7.1
10	MeCN	0.10	30	6	25
11	MeCN	0.05	30	6	1.9
12	MeCN	0.20	30	6	32

13	MeCN	0.30	30	6	8.6
13	MeCN	0.20	30	18	57

Table S8. Solvent identity, reaction concentration, ligand loading, and time screens.

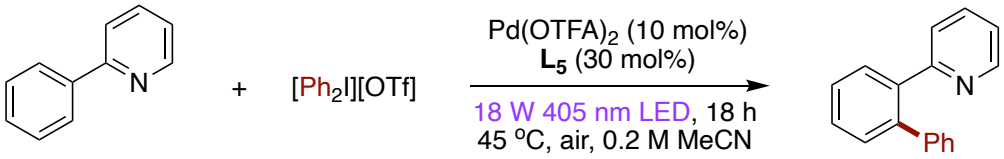

Standard conditions: To a 4-mL vial with a magnetic stir bar was added $Pd(OTFA)_2$ (3.3 mg, 0.01 mmol, 10 mol%), **L_5** (7.2 mg, 0.03 mmol, 30 mol%), diphenyliodonium triflate (64 mg, 0.15 mmol, 1.5 eq.), and 2-phenylpyridine (15 mg, 0.10 mmol, 1.0 eq.). Acetonitrile (0.5 mL, 0.2 M) was added, and the reaction sealed with a PTFE lined screw cap. The reaction was irradiated by an 18 W 405 nm LED at 45 °C for 18 hours. Upon completion, the crude reaction was analyzed by GC-FID using ^{n}dodecane as the internal standard.

Entry	Change from standard conditions	GC Yield (%)
1	No **L_5**	11
2	No Light	n.d.
3	No Pd	n.d.

Table S9. Control reactions as deviations from standard conditions.

Alternative method development: Since minimal activity was observed in the electron poor 2-phenyl-pyridine substrates and significant diarylation was observed in the electron rich 2-phenyl-pyridine substrates multiple methods were explored to address these issues. For the following optimizations, we are no longer using **1b** as substrate to make **3b** and **4b**. Therefore, the calibration curves for **3b** and **4b** cannot be used to give true yields for these alternative substrates. As such, we will use relative ratios for the corresponding products versus ^{n}dodecane. These ratios for the same molecules can be compared to identify which condition modifications are beneficial.

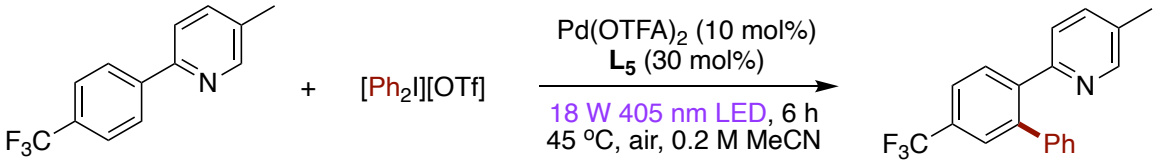

Method optimization for electron deficient FGs. The following general conditions were modified as noted below to determine which changes are beneficial to product formation. To a 4-mL vial with a magnetic stir bar was added $Pd(OTFA)_2$ (3.3 mg, 0.01 mmol, 10 mol%), **L_5** (7.2 mg, 0.03 mmol, 30 mol%), diphenyliodonium triflate (64 mg, 0.15 mmol, 1.5 eq.), and 2-(4-trifluoromethylphenyl)phenyl-5-methylpyridine (24 mg, 0.10 mmol, 1.0 eq.). Acetonitrile (0.5 mL, 0.2 M) was added, and the reaction sealed with a PTFE lined screw cap. The reaction was irradiated by an 18 W 405 nm LED at 45 °C for 18 hours. Upon completion, the crude reaction was analyzed by GC-FID using ^{n}dodecane as the internal standard.

Entry	Change from standard conditions	Ratio pdt/dodecane
1	none	n.d.
2	N_2	0.16
3	0.30 M	0.23
4	0.40 M	0.08

5	2.25 eq. **2a**	0.08
6	1.0 eq. K_2CO_3	0.23
7	1.5 eq. K_2CO_3	0.24
8	2.0 eq. K_2CO_3	0.23
9[a]	1.5 eq. K_2CO_3	0.22

Table S10. Modifications to standard conditions to enable mono-arylation of electron deficient substrates. [a]18 hours.

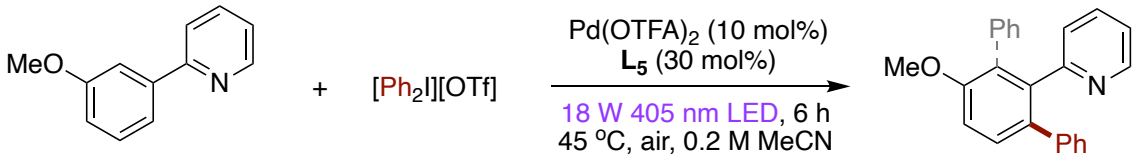

mono-arylation: **4f**
di-arylation: **5f**

Method optimization for electron rich FGs. The major problem was over-functionalization furnishing di-arylation product **5f**. We rationalized that this problem was rooted in the slow dissociation of desired product **4f** from the Pd catalyst before C–H activation occurs again. Therefore, we reasoned that a second ligand added to reactions under standard conditions might facilitate a ligand substitution event to reduce di-arylation. **Standard procedure**: To a 4-mL vial with a magnetic stir bar was added $Pd(OTFA)_2$ (3.3 mg, 0.01 mmol, 10 mol%), $\mathbf{L_5}$ (7.2 mg, 0.03 mmol, 30 mol%), ligand (25 mol%), diphenyliodonium triflate (64 mg, 0.15 mmol, 1.5 eq.), and 2-(4-trifluoromethylphenyl)phenyl-5-methylpyridine (24 mg, 0.10 mmol, 1.0 eq.). Acetonitrile (0.5 mL, 0.2 M) was added, and the reaction sealed with a PTFE lined screw cap. The reaction was irradiated by an 18 W 405 nm LED at 45 °C for 18 hours. Upon completion, the crude reaction was analyzed by GC-FID using ^{n}dodecane as the internal standard.

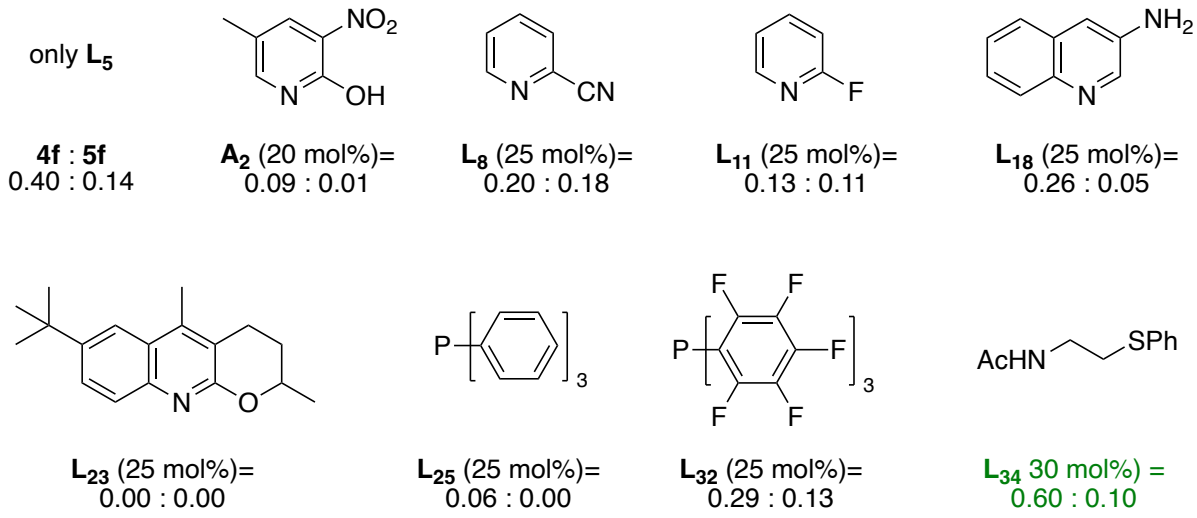

Figure S67. Survey of secondary ligands to minimize di-arylation when electron rich substrates are used. Ratios of **4f** : **5f** are given in reference to ^{n}dodecane.

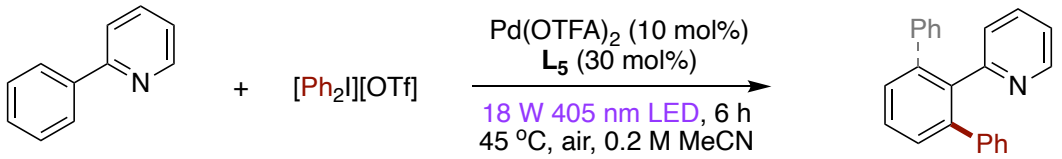

mono-arylation: **4b**
di-arylation: **5b**

Standard procedure: To a 4-mL vial with a magnetic stir bar was added $Pd(OTFA)_2$ (3.3 mg, 0.01 mmol, 10 mol%), **L_5** (7.2 mg, 0.03 mmol, 30 mol%), ligand (25 mol%), diphenyliodonium triflate (64 mg, 0.15 mmol, 1.5 eq.), and 2-phenylpyridine (16 mg, 0.10 mmol, 1.0 eq.). Acetonitrile (0.5 mL, 0.2 M) was added, and the reaction sealed with a PTFE lined screw cap. The reaction was irradiated by an 18 W 405 nm LED at 45 °C for 18 hours. Upon completion, the crude reaction was analyzed by GC-FID using ^{n}dodecane as the internal standard.

Entry	L_5 loading (mol%)	L_{34} loading (mol%)	Ratio 4b/dodecane	Selectivity 4b:5b
1	30	40	0.04	>20:1
2	30	30	0.33	5.1:1
3	30	20	0.31	6.9:1
4	30	10	0.08	9.3:1
5	20	50	0.16	12.6:1
6[a]	20	40	0.51	7.4:1
7	20	30	0.06	7.5:1
8	20	25	0.13	8.9:1

Table S11. Dual ligand loading optimization screen. [a]No differences were observed when reactions run for 18 hours.

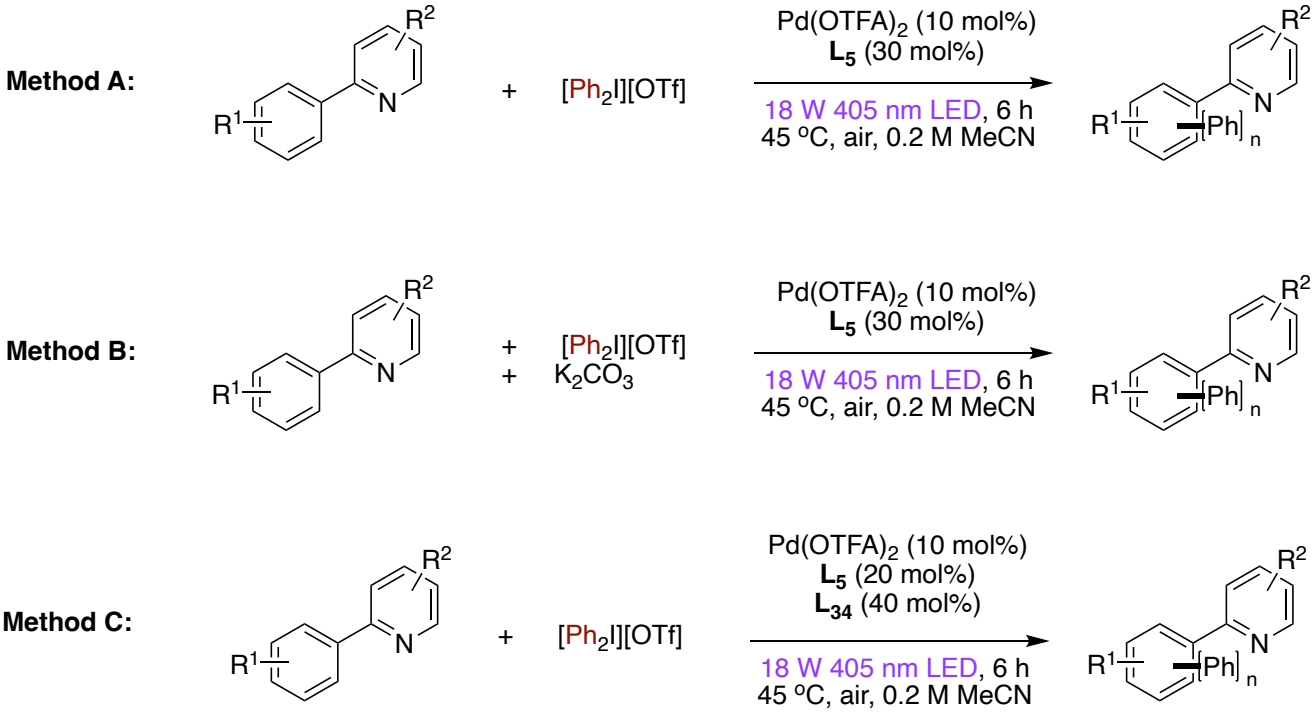

Figure S68. Finalized methods for Pd-catalyzed arylation reactions of 2-arylpyridine molecules.

Entry	Substrate	Method A (pdt/^{n}dodecane)	Method B (pdt/^{n}dodecane)	Method C (pdt/^{n}dodecane)
1	4'-Cl	0.05	0.13	0.04

2	3'-Me	0.47	0.02	0.39[a]
3	3'-CF_3	0.03	0.14	0.03
4	4'-OMe-5-CF_3	0.23	0.11	0.31
5	4'-Ac	0.01	0.14	0.04
6	3'-NHAc	0.26	0.12	0.38
7	5-Me	0.16	0.05	0.25
8	4-NO_2	0.00	0.12	0.03
5	4-OMe	0.11	0.14	0.08
6	4'-CF_3-5-CF_3	0.03	0.13	0.00
7	4'-OMe	0.19	0.02	0.13
8[b]	3'-Cl	0.48	0.00	0.45
9[b]	4'-Ph	0.74	0.00	1.11

Table S12. Method determination for various 2-aryl pyridines using product ratios with respect to [n]dodecane. FG positional location numbers refer to positions on the C2-aryl ring (prime numerals) or on the pyridine ring (numerals). [a]Method C selected due to high quantities of diarylation formed using Method A. [b]Run for 18 hours and using mesitylene as internal standard.

Importantly: The method for any substrate not shown above was hypothesized using trends from these data and the substrate's electronic properties.

G. Synthesis of 2-arylpyridine substrates

General procedure 1 (GP1): The 2-arylpyridine substrates were synthesized according to a modified literature procedure.[4] To a round bottom flask, Na_2CO_3 (21.8 mmol, 7.4 eq.), $Pd(PPh_3)_4$ (0.089 mmol, 3.0 mol%), arylboronic acid (3.88 mmol, 1.2 eq.), and 2-bromopyridine (2.96 mmol, 1.0 eq.) were placed under a nitrogen atmosphere and dissolved in a mixture of pre-degassed toluene (12.5 mL), ethanol (2.5 mL), and H_2O (12.5 mL). The resulting reaction mixture was heated at 80 °C overnight. The next morning, the reaction mixture was cooled to room temperature and quenched with saturated aqueous NH_4Cl. The mixture was extracted using 3 x 20 mL EtOAc. The combined organic extracts were dried over Na_2SO_4, filtered, and concentrated under reduced pressure. The crude mixture was purified by column chromatography on silica gel using mixtures of hexane/EtOAc as the eluent to afford the respective 2-arylpyridine derivatives in analytically pure form.

General procedure 2 (GP2): The 2-arylpyridine substrates were synthesized according to a modified literature procedure.[5] To a round bottom flask, K_2CO_3 (6.40 mmol, 2.0 eq.), $Pd(OAc)_2$ (0.048 mmol, 1.5 mol%), 3-methoxyphenylboronic acid (4.80 mmol, 1.50 eq.), and 2-bromopyridine (3.20 mmol, 1.0 eq.) were placed under a nitrogen atmosphere and dissolved in a degassed 50% aqueous isopropanol solution (25 mL). The reaction mixture was heated at 80 °C overnight. The next morning, the reaction mixture was cooled to room temperature and quenched with aqueous NH_4Cl. The mixture was extracted using 3 x 20 mL EtOAc. The combined organic extracts were dried over Na_2SO_4, filtered, and concentrated under reduced pressure. The crude mixture was purified by column chromatography on silica gel using mixtures of hexane/EtOAc as the eluent to afford the respective 2-arylpyridine derivatives in analytically pure form.

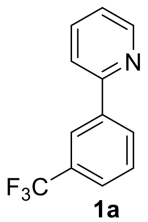

1a

1a. 3'-CF_3-2-phenylpyridine: GP1. 69% yield. Yellow oil. ^{1}H NMR (300 MHz, $CDCl_3$) δ 8.73 (d, *J* = 4.5 Hz, 1H), 8.29 (s, 1H), 8.19 (d, *J* = 7.7 Hz, 1H), 7.87 – 7.72 (m, 2H), 7.68 (d, *J* = 7.9 Hz, 1H), 7.60 (t, *J* = 7.8 Hz, 1H), 7.30 (ddd, *J* = 6.7, 4.8, 1.9 Hz, 1H). The NMR agrees with literature data.[6]

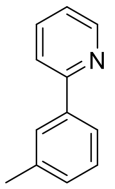

1c

1c. 3'-Me-2-phenylpyridine: GP1. 62% Yield. yellow oil. ^{1}H NMR (300 MHz, $CDCl_3$) δ 8.70 (d, J = 4.5 Hz, 1H), 7.84 (s, 1H), 7.79 – 7.70 (m, 3H), 7.37 (t, *J* = 7.6 Hz, 1H), 7.26-7.20 (m, 3H), 2.47 (s, 3H). The NMR agrees with literature data. [7]

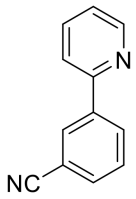

1d

1d. 3'-CN-2-phenylpyridine: GP1. 5:1 Hexane:EtOAc. 87% yield. White solid. ^{1}H NMR (300 MHz, $CDCl_3$) δ 8.70 (s, 1H), 8.30 (d, J = 1.6 Hz, 1H), 8.21 (d, J = 8.0 Hz, 1H), 7.80 (tt, J = 8.0, 2.2 Hz, 1H), 7.72 (dt, J = 8.0, 1.3 Hz, 1H), 7.67 (dt, J = 7.8 Hz, 1.4 Hz, 1H), 7.57 (td, J = 7.9, 2.9 Hz, 1H), 7.30 (m, 1H). The NMR agrees with literature data.[8]

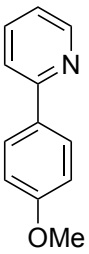

1e

1e. 4'-OMe-2-phenylpyridine: GP2. 20:1 Hexane:EtOAc. 77% yield. White solid. ^{1}H NMR (300 MHz, $CDCl_3$) δ 8.65 (d, J = 4.8 Hz, 1H), 7.99 – 7.92 (m, 2H), 7.76 – 7.64 (m, 2H), 7.18 (ddd, J = 6.7, 4.8, 1.5 Hz, 1H), 7.04 – 6.97 (m, 2H), 3.87 (s, 3H). The NMR agrees with literature data.[7]

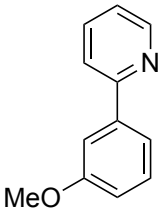

1f

1f. 3'-OMe-2-phenylpyridine: GP2. 20:1 Hexane:EtOAc. 30% yield. Yellow oil. ^{1}H NMR (300 MHz, CDCl3) δ 8.70 (d, J = 4.6 Hz, 1H), 7.79 – 7.69 (m, 2H), 7.60 – 7.52 (m, 2H), 7.39 (t, J = 7.9 Hz, 1H), 7.26 – 7.20 (m, 1H), 6.97 (ddd, J = 8.2, 2.6, 1.0 Hz, 1H), 3.90 (s, 3H). The NMR agrees with literature data.[6]

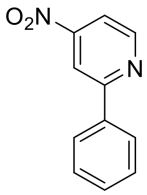

1g

1g. 4-NO_2-2-phenylpyridine: GP1. ~2:1 Hexane:EtOAc. 85% yield. Off white/yellow solid. ^{1}H NMR (400 MHz, $CDCl_3$) δ 8.97 (d, J = 5.4, 1H), 8.44 (s, 1H), 8.08 (d, J = 7.9, 2H), 7.94 (dd, J = 5.4, 1.7 Hz, 1H), 7.58 – 7.50 (m, 3H). The NMR agrees with the single literature source apart from the literature source not properly referencing the solvent peak.[9]

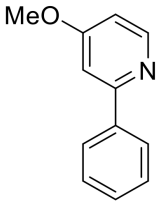

1h

1h. 4-OMe-2-phenylpyridine: GP1. ~5:1 Hexane:EtOAc. 66% yield. Yellow/orange oil. ^{1}H NMR (400 MHz, $CDCl_3$) δ 8.52 (dd, J = 5.9, 3.2 Hz, 1H), 7.98 – 7.92 (m, 2H), 7.50 – 7.38 (m, 3H), 7.23 (t, J = 2.6 Hz, 1H), 6.80 – 6.75 (m, 1H), 3.91 (d, J = 2.9 Hz, 3H). The NMR agrees with literature data.[10]

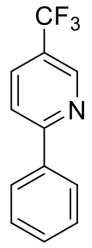

1i

1i. 5-CF_3-2-phenylpyridine: GP1. 88% yield. 20:1 Hexane:EtOAc. White solid. ^{1}H NMR (300 MHz, $CDCl_3$) δ 8.95 (s, 1H), 8.04 (dd, J = 8.0, 2.1 Hz, 2H), 7.99 (dd, J = 8.4, 2.4 Hz, 1H), 7.85 (d, J = 8.4 Hz, 1H), 7.56 – 7.44 (m, 3H). The NMR agrees with literature data.[11]

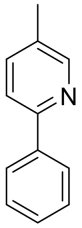

1j

1j. 5-Me-2-phenylpyridine: GP1. 81% yield. Beige solid. ^{1}H NMR (300 MHz, $CDCl_3$) δ 8.53 (s, 1H), 7.97 (d, J = 8.0 Hz, 2H), 7.63 (d, J = 8.0 Hz, 1 H), 7.56 (dd, J = 8.3, 2.2 Hz, 1 H), 7.47 (t, J = 7.7 Hz, 2H), 7.42 - 7.36 (m, 1H), 2.38 (s, 3H). The NMR agrees with literature data.[7]

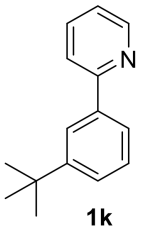

1k

1k. 3'-tBu-2-phenylpyridine: GP1. 79% yield. 20:1 Hexane:EtOAc. Clear liquid. ^{1}H NMR (300 MHz, $CDCl_3$) δ 8.71 (d, J = 4.9 Hz, 1H), 8.04 (t, J = 1.8 Hz, 1H), 7.78 – 7.70 (m, 3 H), 7.47 (dt, J = 8.0, 1.4 Hz, 1H), 7.41 (t, J = 7.7 Hz, 1H), 7.24 – 7.20 (m, 1H), 1.40 (s, 9H). The NMR agrees with literature data.[12]

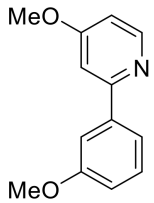

1l

1l. 4-OMe-3'-OMe-2-phenylpyridine: GP1. ~5:1 Hexane:EtOAc 85% yield. Pale yellow oil. ^{1}H NMR (300 MHz, $CDCl_3$) δ 8.50 (dd, J = 5.8, 2.2 Hz, 1H), 7.56 (m, 1H), 7.51 (d, J = 7.6 Hz, 1H), 7.36 (td, J = 7.8, 2.3 Hz, 1H), 7.21 (m, 1H), 6.96 (d, J = 8.5 Hz, 1H), 6.76 (m, 1H), 3.88 (s, 3H), 3.87 (s, 3H). ^{13}C NMR (125 MHz, $CDCl_3$) δ 166.41, 160.03, 159.00, 150.88, 140.98, 129.71, 119.37, 115.13, 112.12, 108.30, 107.07, 55.40, 55.22.

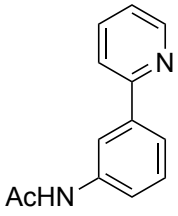

1m

1m. 3'-NHAc-2-phenylpyridine: The following substrate was synthesized according to a modified literature procedure.[13] To a round bottom flask, 3'-NH_2-2-phenyl-pyridine (1.76 mmol, 1.00 eq.) was added with DCM (29 mL). Acetic anhydride (37.3 mmol, 21.2 eq.) was added dropwise to the solution over 5 minutes at room temperature. The solution was allowed to stir for 2 h. Upon completion, solvent was concentrated under reduced pressure. Aqueous $NaHCO_3$ was added, and the solution was extracted 3 x 20 mL with DCM, dried with Na_2SO_4, and concentrated in vacuo. The crude mixture was purified by column chromatography on silica gel using mixtures of 1:5 hexane/EtOAc as the eluent affording a white solid. 86% yield. ^{1}H NMR (400 MHz, $CDCl_3$) δ 8.67 (d, J = 4.8 Hz, 1H), 8.05 (s, 1H), 7.76 – 7.69 (m, 4H), 7.42 (t, J = 8.0 Hz, 2H), 7.26 – 7.21 (m, 1H), 2.18 (s, 3H). The NMR agrees with literature data.[14]

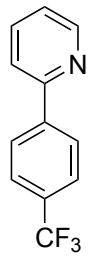

1n

1n. 4'-CF_3-2-phenylpyridine: GP1. 20:1 Hexane:EtOAc. 87% yield. Off white/yellow solid. ^{1}H NMR (300 MHz, $CDCl_3$) δ 8.73 (dt, J = 4.8, 1.4 Hz, 1H), 8.11 (d, J = 8.1 Hz, 2H), 7.86 – 7.67 (m, 4H), 7.30 (ddd, J = 6.7, 4.8, 1.9 Hz, 1H). The NMR agrees with literature data.[15]

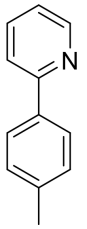

1o

1o. 4'-Me-2-phenylpyridine: GP1. 20:1 Hexane: EtOAc. 83% yield. Yellow oil. ^{1}H NMR (300 MHz, $CDCl_3$) δ 8.68 (d, J = 5.0 Hz, 1H), 7.90 (d, J = 8.3 Hz, 2H), 7.71 (dq, J = 4.0, 1.5 Hz, 2H), 7.28 (d, J = 8.0 Hz, 2H), 7.23 – 7.16 (m, 1H), 2.41 (s, 3H). The NMR agrees with literature data.[7]

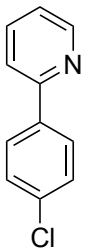

1p

1p. 4'-Cl-2-phenylpyridine: GP2. 62% yield. 20:1 Hexane:EtOAc. White solid. ^{1}H NMR (300 MHz, $CDCl_3$) δ 8.69 (d, J = 5.0, 1H), 7.97 – 7.90 (m, 2H), 7.76 (td, J = 7.6, 1.8 Hz, 1H), 7.70 (d, J = 7.8 Hz, 1H), 7.47 – 7.40 (m, 2H), 7.28 - 7.21 (m, 1H). The NMR agrees with literature data.[16]

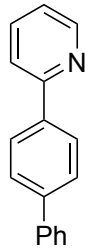

1q

1q. 4'-Ph-2-phenylpyridine: The following substrate was prepared according to a modified GP1. The solvents were changed for degassed THF (4.0 mL) and H_2O (3.0 mL) at 70 °C. 10:1 Hexane:EtOAc. 45% yield. Off-white solid. ^{1}H NMR (300 MHz, $CDCl_3$) δ 8.72 (dt, J = 4.7, 1.3 Hz, 1H), 8.09 (dt, J = 8.6, 2.1 Hz, 2H), 7.79 – 7.76 (m, 2H), 7.72 (dt, J = 8.8, 2.1 Hz, 2H), 7.68 – 7.66 (m, 1H), 7.66 – 7.65 (m, 1H), 7.47 (t, J = 7.7 Hz, 2H), 7.37 (tt, J = 7.3, 1.2 Hz, 1H), 7.27 – 7.23 (m, 1H). The NMR agrees with literature data.[15]

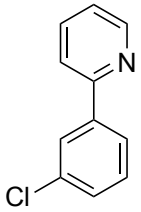

1r

1r. 3'-Cl-2-phenylpyridine: The following substrate was prepared according to a modified patented procedure.[17] A 3-necked flask and condenser was flame-dried and placed under vacuum. Under N_2, Mg (3.96 mmol, 1.50 eq.) and a trace amount of iodine was added. The flask was purged of air (vacuum and N_2 cycle 3x). After the 3rd cycle, diethyl ether (5 mL) was added under N_2 and stirred until the solution became colorless. Upon initial addition of ether, the solution became brown. After stirring for 1.5 h, the solution became a light yellow. A solution of 3-Br-chlorobenzene (2.90 mmol, 1.10 eq.) in ether (10 mL) was added dropwise at a speed at which the reaction mixture refluxes gently over a period of 1 hour. This solution was stirred an additional hour under reflux. The prepared 3-Cl-phenyl-magnesium bromide solution was cannulated into a mixture of 2-bromopyridine (2.64 mmol, 1.00 eq.), $Ni(dppp)_2Cl_2$ (0.00264 mmol, 0.00100 eq.) and ether (10 mL) and gently refluxed for 30 minutes. The mixture was

stirred overnight under reflux. The solution was then allowed to cool to room temperature and was poured into NH_4Cl (aq.) and extracted 3 x 30 mL with DCM. The organic fractions were combined, dried with Na_2SO_4, and concentrated under reduced pressure. The crude mixture was purified by column chromatography on silica gel using mixtures of 10:1 hexane/EtOAc as the eluent affording pale yellow 3'-Cl-2-phenylpyridine. 44% Yield. ^{1}H NMR (300 MHz, $CDCl_3$) δ 8.70 (d, J = 4.8 Hz, 1H), 8.02 (s, 1H), 7.87 (d, J = 7.0 Hz, 1H), 7.77 (t, J = 8.0 Hz, 1H), 7.71 (dd, J = 7.9, 0.9 Hz, 1H), 7.44 – 7.36 (m, 2H), 7.29 – 7.24 (m, 1H). The NMR agrees with literature data.[18]

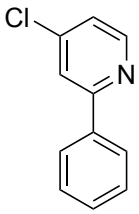

1s

1s. 4-Cl-2-phenylpyridine: GP2. 43% yield. 20:1 Hexane:EtOAc. Pale yellow liquid. ^{1}H NMR (300 MHz, $CDCl_3$) δ 8.59 (d, J = 5.2 Hz, 1H), 7.97 (d, J = 7.7 Hz, 2H), 7.74 (d, J = 1.8 Hz, 1H), 7.52 – 7.42 (m, 3H), 7.25 (dd, J = 5.4, 1.8 Hz, 1H). The NMR agrees with literature data.[19]

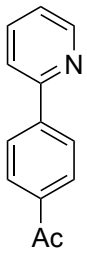

1t

1t. 4'-Ac-2-phenylpyridine: GP1. 44% yield. Off white/brown solid. ^{1}H NMR (400 MHz, $CDCl_3$) δ 8.75 (dt, J = 4.8, 1.4 Hz, 1H), 8.14 – 8.04 (m, 4H), 7.80 (dd, J = 3.6, 1.3 Hz, 2H), 7.29 (s, J = 4.5 Hz, 1H), 2.66 (s, 3H). The NMR agrees with literature data.[20]

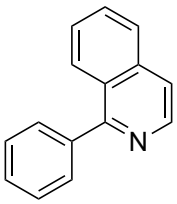

1u

1u. 2-phenylisoquinoline: Phenylisoquinoline was synthesized according to a modified literature procedure.[21] To a 50 mL Schlenk flask, 2-chloroisoquinoline (2.44 mmol, 1 eq.), phenylboronic acid (3.17 mmol, 1.30 eq.), and K_2CO_3 (7.30 mmol, 3 eq.) were added. Under a nitrogen atmosphere, $Pd(PPh_3)_4$ (0.0700 mmol, 3.0 mol%) was added followed by 8.8 mL of a 1:1 mixture of THF/H_2O. The mixture was allowed to reflux at 80 °C for 5 hours, then allowed to cool to room temperature. The mixture was extracted with DCM (3 x 10 mL). The organic layers were combined and washed with 1 M NaOH (aq.). The organic layers were dried over $MgSO_4$, filtered, and concentrated under reduced pressure. The crude mixture was purified by column chromatography on silica gel using mixtures of 6:1 hexane/EtOAc as the eluent to afford pure 1-phenylisoquinoline as an off-white solid. 97% yield. ^{1}H NMR (300 MHz, $CDCl_3$) δ 8.62 (d, J = 5.8 Hz, 1H), 8.11 (d, J = 8.6 Hz, 1H), 7.89 (d, J = 8.3 Hz, 1H), 7.73 – 7.64 (m, 4H), 7.57 – 7.46 (m, 4H). The NMR agrees with the literature data.

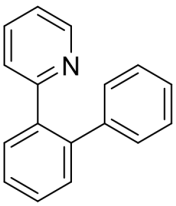

4b

4b. 2'-Ph-2-phenylpyridine. The synthesis of **4b** was from a modified literature procedure.[6] The reaction was performed in a 20 mL vial. In the vial, Palladium dichloride (0.068 mmol, 5 mol%) was added alongside triphenyl phosphine (0.12 mmol, 10 mol%), 2-biphenylboronic acid (1.53 mmol, 1.2 eq.), potassium carbonate (3.74 mmol, 3 eq.) and a magnetic stir-bar. These solids were dissolved in 8 mL (6:2) H_2O:THF solvent mixture. The resulting mixture was then charged with 2-bromopyridine (1.35 mmol, 1.0 eq.). The reaction was stirred at 80°C at 500 rpm overnight. Upon completion, the reaction was allowed to cool to room temperature. The mixture was extracted 3x with DCM (5 mL), dried over $MgSO_4$, and concentrated in vacuo. The crude mixture was purified by column chromatography on silica gel with hexane/EtOAc (10:1) to afford a white solid. 74% yield. ^{1}H NMR (400 MHz, $CDCl_3$): δ 8.64 (m, 1H), 7.70 (m, 1H), 7.47 (m, 3H), 7.38 (td, J = 1.83, 7.80 Hz, 1H), 7.23 (m, 3H), 7.15 (m, 2H), 7.10 (m, 1H), 6.89 (dt, J = 1.0, 7.95 Hz, 1H). This NMR agrees with literature data.[6]

H. Synthesis of iodonium triflate salts

General procedure 3 (GP3): The iodonium salt substrates were synthesized from a modified literature procedure.[22] In a 200 mL round bottom flask, mesitylene (10.0 mmol, 1.11 eq.) was added to a solution of iodoarene (9.00 mmol, 1.00 eq.) and m-CPBA (10.0 mmol, 1.11 eq.) in CH_2Cl_2 (40 mL) and cooled to 0 °C. Trifluoromethanesulfonic acid (15.0 mmol, 1.66 eq.) was added dropwise over 10 minutes, then slowly warmed to room temperature over 2 hours. The solvent was removed under reduced pressure and diethyl ether was added. The solvent was again removed in vacuo and repeated 3x until crystals started to form. After a final addition of diethyl ether, the solution was stored at 4 °C for 2 h, the resulting crystals were filtered and washed with diethyl ether. The solid product was dried under vacuum to yield the diaryliodonium triflates.

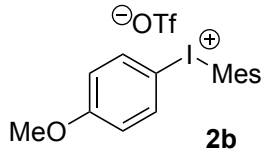

2b

2b. 4-methoxyphenylmesityl iodonium triflate: The following substrate was made according to a literature procedure in a 67% Yield.[23] ^{1}H NMR (125 MHz, $CDCl_3$) δ 7.64 (d, J = 9.1 Hz, 2 H), 7.10 (s, 2 H), 6.93 (d, J = 9.1 Hz, 2 H), 3.82 (s, 3 H), 2.64 (s, 6 H), 2.35 (s, 3H). The NMR agrees with literature data.[23]

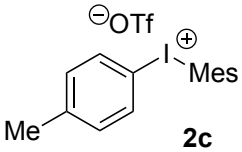

2c

2c. 4-methylphenylmesityl iodonium triflate: 60% Yield. GP3. White Solid. ^{1}H NMR (400 MHz, D_6-DMSO) δ 7.86 (d, J = 8.1 Hz, 2 H), 7.30 (d, J = 8.1 Hz, 2 H), 7.20 (s, 2 H), 2.59 (s, 6 H), 2.33 (s, 3 H), 2.29 (s, 3 H). The NMR agrees with literature data.[22]

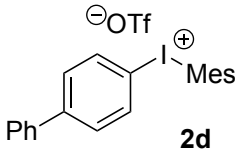

2d

2d. 4-biphenylmesityl iodonium triflate: GP3. White Solid. ^{1}H NMR (400 MHz, $CDCl_3$) δ 7.74 (d, J = 8.7 Hz, 2 H), 7.62 (d, J = 8.7 Hz, 2 H), 7.53 – 7.40 (m, 5 H), 7.15 (s, 2 H), 2.67 (s, 6 H), 2.38 (s, 3 H). The NMR agrees with literature data.[24]

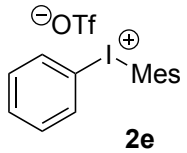

2e

2e. phenylmesityl iodonium triflate: 55% Yield. GP3. White Solid. ^{1}H NMR (400 MHz, $CDCl_3$) δ 7.67 (d, J = 8.2 Hz, 2 H), 7.57 (t, J = 7.6 Hz, 1 H), 7.44 (t, J = 7.9 Hz, 2 H), 7.13 (s, 2 H), 2.63 (s, 6 H), 2.38 (s, 3 H). The NMR agrees with literature data.[25]

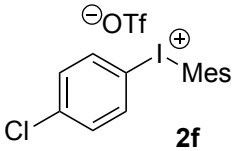

2f

2f. 4-chlorophenylmesityl iodonium triflate: 62% Yield. GP3. Off-white solid. ^{1}H NMR (400 MHz, $CDCl_3$) δ 7.62 (d, J = 8.8 Hz, 2 H), 7.39 (d, J = 8.8 Hz, 2 H), 7.13 (s, 2 H), 2.62 (s, 6 H), 2.37 (s, 3 H). The NMR agrees with literature data.[24]

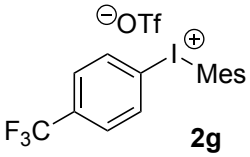

2g

2d. 4-trifluoromethylphenylmesityl iodonium triflate: 40% Yield. GP3. White Solid. ^{1}H NMR (400 MHz, $CDCl_3$) δ 7.81 (d, J = 8.0 Hz, 2 H), 7.66 (d, J = 8.6, 2 H), 7.15 (s, 2H), 2.63 (s, 6 H), 2.39 (s, 3 H). The NMR agrees with literature data.[26]

I. GC-MS characterization and isolation data for 2-arylpyridine arylation products

General procedure 4 (GP4)/Method A: To a 20 mL vial, $Pd(TFA)_2$ (0.0300 mmol, 10.0 mol%), boc-taurine (0.0900 mmol, 30.0 mol%), iodonium salt (0.450 mmol, 1.50 eq.), arylpyridine substrate (0.300 mmol, 1.00 eq.) and acetonitrile (1.5 mL) were added. The reaction was irradiated under an 18 W 405 nm light, while at 45 °C for 18 h. Upon completion, the crude reaction was analyzed by GC-MS with mesitylene as internal standard.

General procedure 5 (GP5)/Method B: To a 20 mL vial, $Pd(TFA)_2$ (0.0300 mmol, 10.0 mol%), boc-taurine (0.0900 mmol, 30.0 mol%), K_2CO_3 (0.450 mmol, 1.50 eq.), iodonium salt (0.450 mmol, 1.50 eq.), arylpyridine substrate (0.300 mmol, 1.00 eq.) and acetonitrile (1.5 mL) were added. The reaction was irradiated under an 18 W 405 nm light, while at 45 °C for 18 h. Upon completion, the crude reaction was analyzed by GC-MS with mesitylene as internal standard.

General procedure 6 (GP6)/Method C: To a 20 mL vial, $Pd(TFA)_2$ (0.0300 mmol, 10 mol%), boc-taurine (0.0600 mmol, 20.0 mol%), *N*-(2-(phenylthio)ethyl)acetamide (0.120 mmol, 40.0 mol%), iodonium salt (0.450 mmol, 1.50 eq.), arylpyridine substrate (0.300 mmol, 1.00 eq.) and acetonitrile (1.5 mL) were added. The reaction was irradiated under an 18 W 405 nm light, while at 45 °C for 18 h. Upon completion, the crude reaction was filtered through basic alumina with MeCN and analyzed by GC-MS with mesitylene as internal standard.

Purification of selected reactions: the crude reaction was concentrated in vacuo and purified by HPLC (0.1 % TFA H_2O/ 0.1 % TFA MeOH). Fractions containing product were concentrated under reduced pressure, then passed through a 50/50 % by mass filter of $MgSO_4/K_2CO_3$ with DCM to afford pure, deprotonated monoarylated arylpyridine product.

2-Arylpyridine Substrate Scope Products

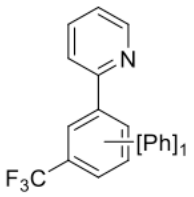

4a

4a. Arylation of 1a with 2a: GP5. 18.0% GC Yield. 18% total arylation. GC-MS(EI) m/z - Calc: 299.1; Exp: 299.1.

RT (min)	Area (pA·s)	Area%
2.259	722.847	41.142
4.248	814.923	46.383
5.904	219.192	12.476

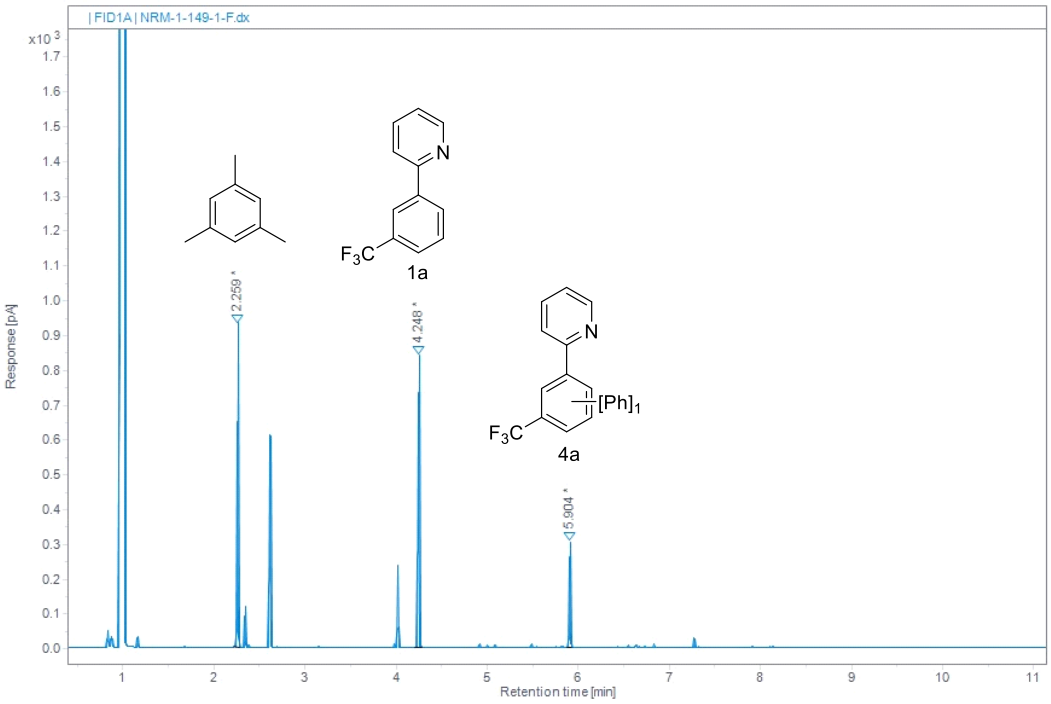

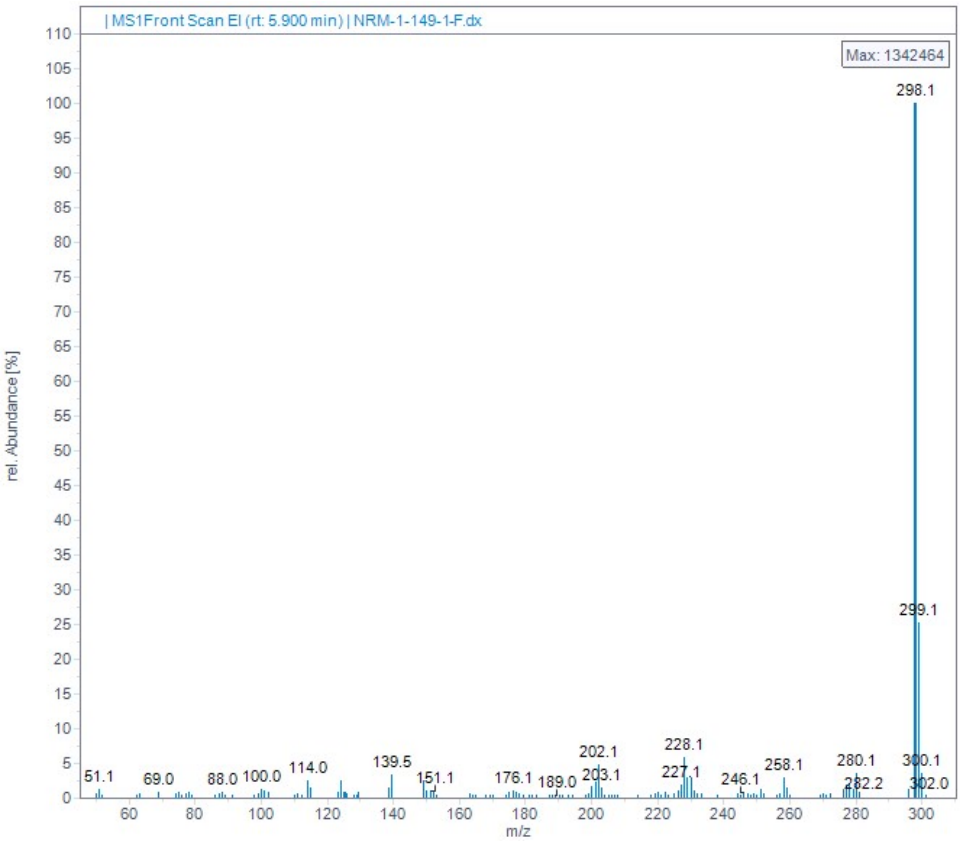

Figure S69. GC-FID trace and peak areas of crude arylpyridine arylation reaction mixture using **2a** (top). Peaks for internal standard (mesitylene), remaining arylpyridine **1a**, and mono-arylated product are highlighted. Mass spectrum of peak exhibiting m/z for mono-arylated product (bottom).

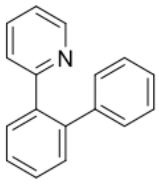

4b

4b. 2'-Ph-2-phenylpyridine: GP6. 46% isolated yield, 51.3% GC Yield. 69% total arylation. ^{1}H NMR (400 MHz, $CDCl_3$) δ 8.63 (dq, J = 4.8 Hz, 1 H), 7.72 - 7.68 (m, 1 H), 7.50 - 7.43 (m, 3 H), 7.42 - 7.34 (td, J = 7.6, 1.9 Hz, 1 H), 7.25 - 7.20 (m, 3 H), 7.18 - 7.13 (m, 2 H), 7.12 - 7.07 (m, 1 H), 6.88 (dt, J = 8.0, 1.0 Hz, 1 H). The NMR agrees with literature data.[15] GC-MS(EI) m/z - Calc: 231.1; Exp: 231.1.

RT (min)	Area (pA·s)	Area%
2.291	5140.131	39.616
4.346	2899.130	22.344
6.119	4302.859	33.163
7.572	632.819	4.877

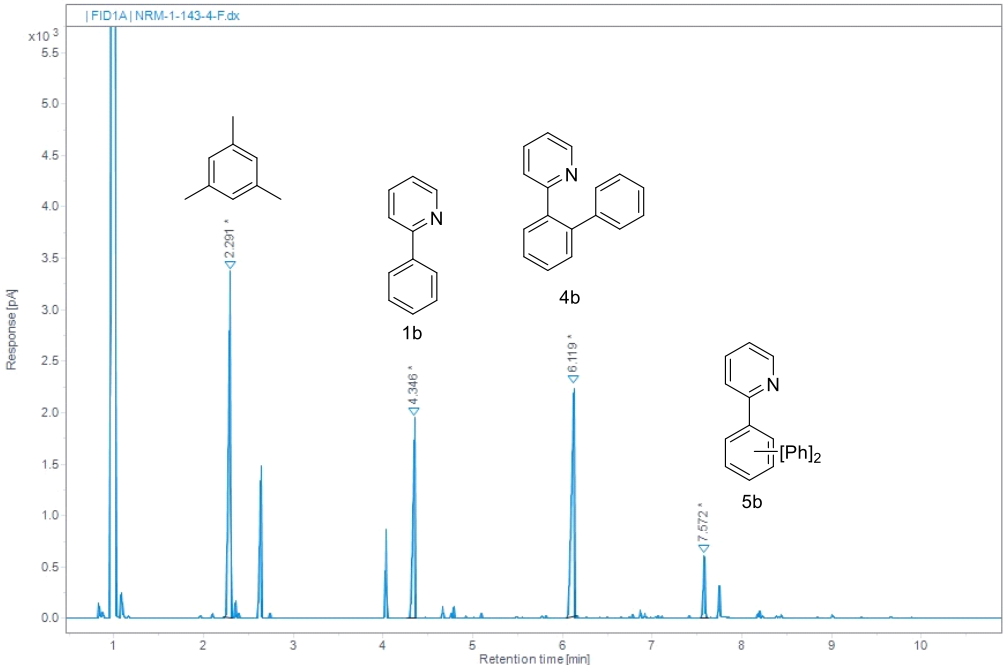

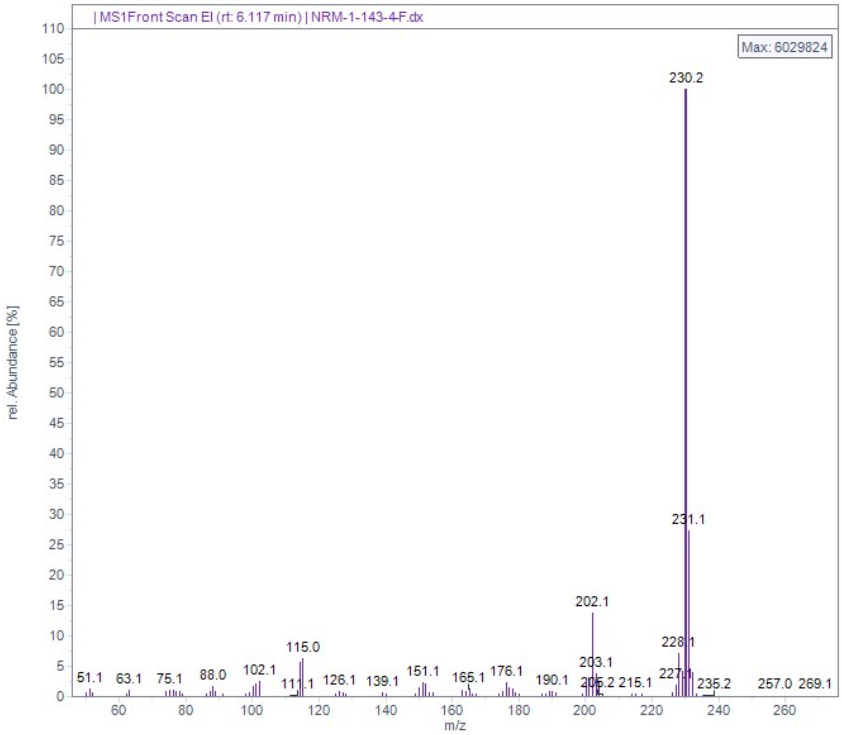

Figure S70. GC-FID trace and peak areas of crude arylpyridine arylation reaction mixture using **2a** (top). Peaks for internal standard (mesitylene), remaining arylpyridine **1b**, and mono- and di-arylated product are highlighted. Mass spectrum of peak exhibiting m/z for mono-arylated product (bottom).

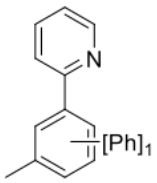

4c

4c. Arylation of 1c with 2a: GP6. 49.2% GC Yield. 49% total arylation. GC-MS(EI) m/z - Calc: 245.1; Exp: 245.1.

RT (min)	Area (pA·s)	Area%
2.248	332.730	40.580
4.686	173.012	21.101
6.390	314.195	38.319

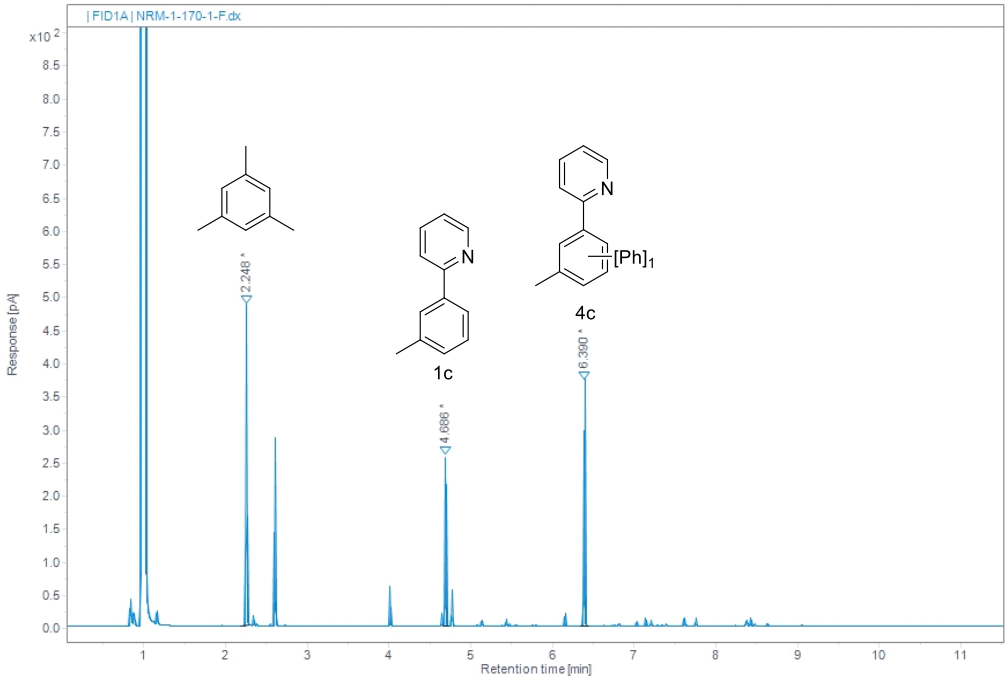

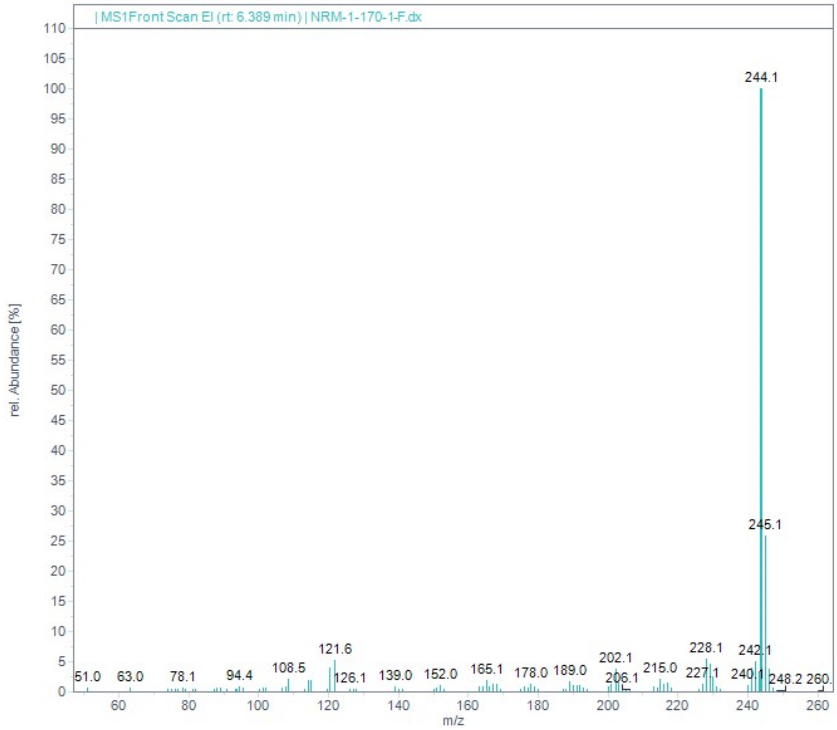

Figure S71. GC-FID trace and peak areas of crude arylpyridine arylation reaction mixture using **2a** (top). Peaks for internal standard (mesitylene), remaining arylpyridine **1c**, and mono-arylated product are highlighted. Mass spectrum of peak exhibiting m/z for mono-arylated product (bottom).

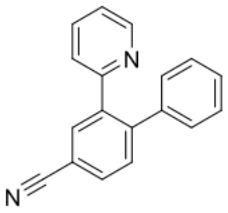

4d

4d. 2'-Ph-5'-CN-2-phenylpyridine: GP5. 9% isolated yield. 10.4% GC Yield. 10% total arylation. ^{1}H NMR (300 MHz, $CDCl_3$) δ 8.66 (d, J = 4.9 Hz, 1H), 8.03 (d, J = 1.8 Hz, 1H), 7.74 (dd, J = 7.9, 1.7 Hz, 1H), 7.54 (d, J = 8.0 Hz, 1H), 7.43 (td, J = 7.7, 2.0 Hz, 1H), 7.30 – 7.27 (m, 3H), 7.19 – 7.12 (m, 3H), 6.87 (d, J = 7.8 Hz, 1H). ^{13}C NMR (125 MHz, $CDCl_3$) δ 157.10, 149.98, 145.22, 140.62, 139.63, 135.77, 134.56, 131.90, 131.47, 129.50, 128.57, 128.00, 125.33, 122.39, 118.77, 111.76 GC-MS(EI) m/z - Calc: 256.1; Exp: 256.1.

RT (min)	Area (pA·s)	Area%
2.227	240.560	43.636
5.425	254.276	46.125
7.069	56.446	10.239

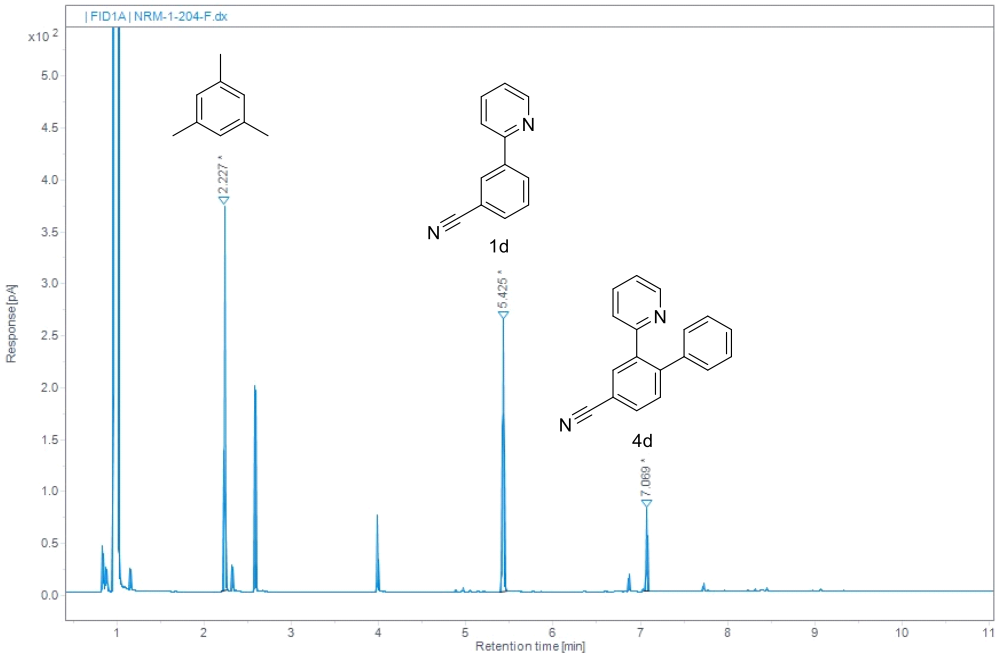

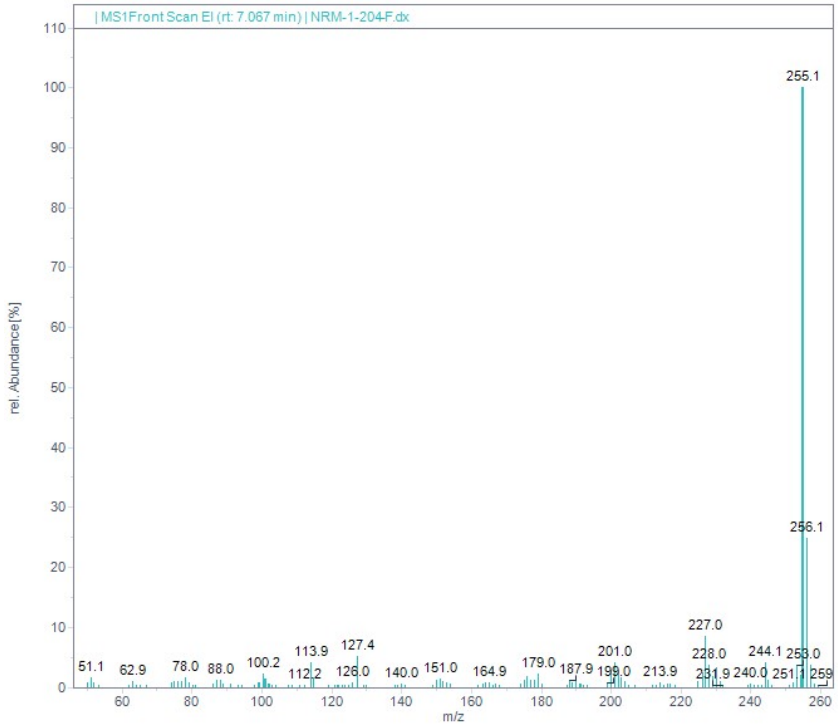

Figure S72. GC-FID trace and peak areas of crude arylpyridine arylation reaction mixture using **2a** (top). Peaks for internal standard (mesitylene), remaining arylpyridine **1d**, and mono-arylated product are highlighted. Mass spectrum of peak exhibiting m/z for mono-arylated product (bottom).

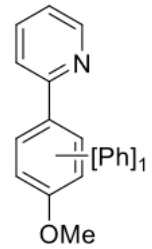

4e. Arylation of 1e with 2a: GP4. 15.6% GC Yield. 16% total arylation. GC-MS(EI) m/z - Calc: 261.1; Exp: 261.1.

RT (min)	Area (pA·s)	Area%
2.268	1874.341	49.574
5.341	1307.678	34.586
6.901	598.909	15.840

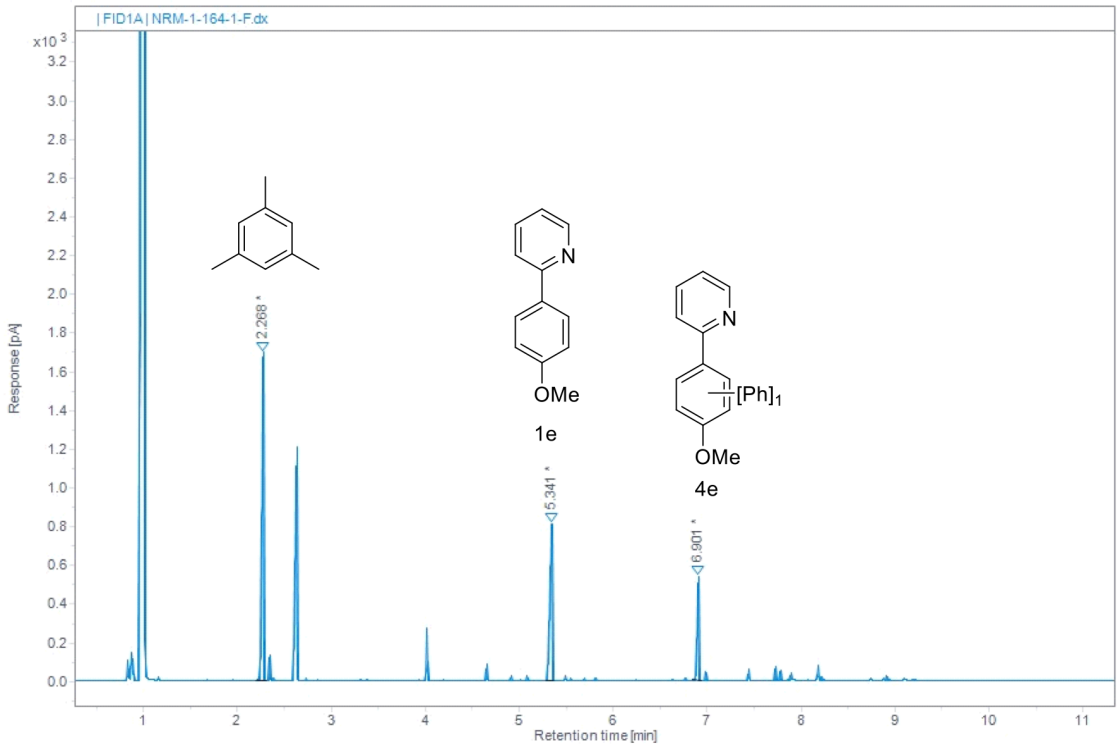

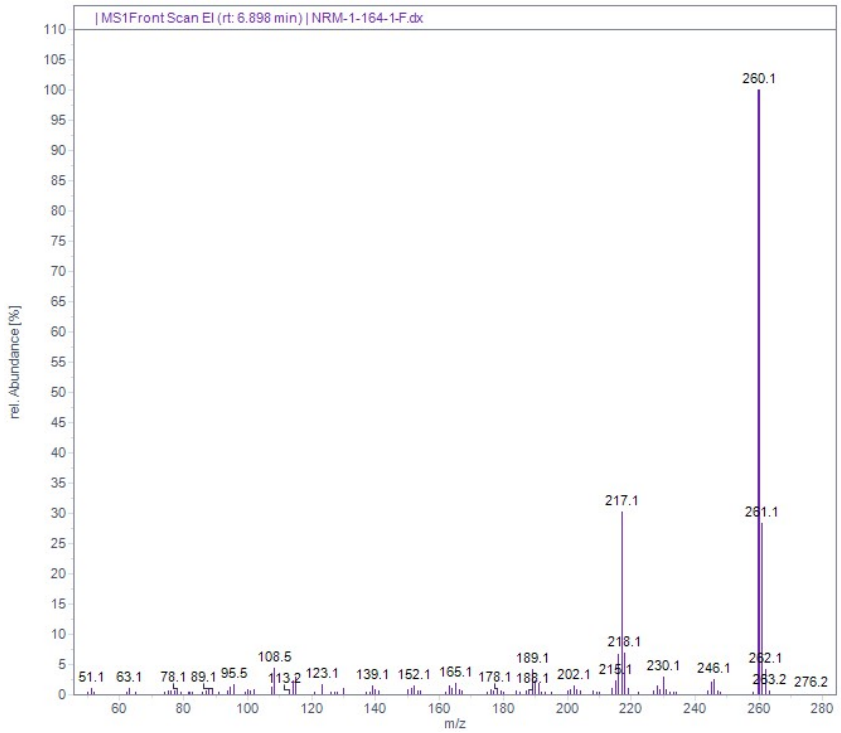

Figure S73. GC-FID trace and peak areas of crude arylpyridine arylation reaction mixture using **2a** (top). Peaks for internal standard (mesitylene), remaining arylpyridine **1e**, and mono-arylated product are highlighted. Mass spectrum of peak exhibiting m/z for mono-arylated product (bottom).

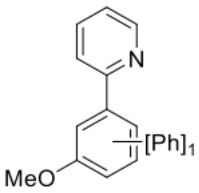

4f. Arylation of 1f with 2a: GP6. 62.0% GC Yield. 76% total arylation. GC-MS(EI) m/z - Calc: 261.1; Exp: 261.1.

RT (min)	Area (pA·s)	Area%
2.273	1434.486	40.175
5.228	359.302	10.063
6.901	1582.842	44.330
7.992	193.963	5.432

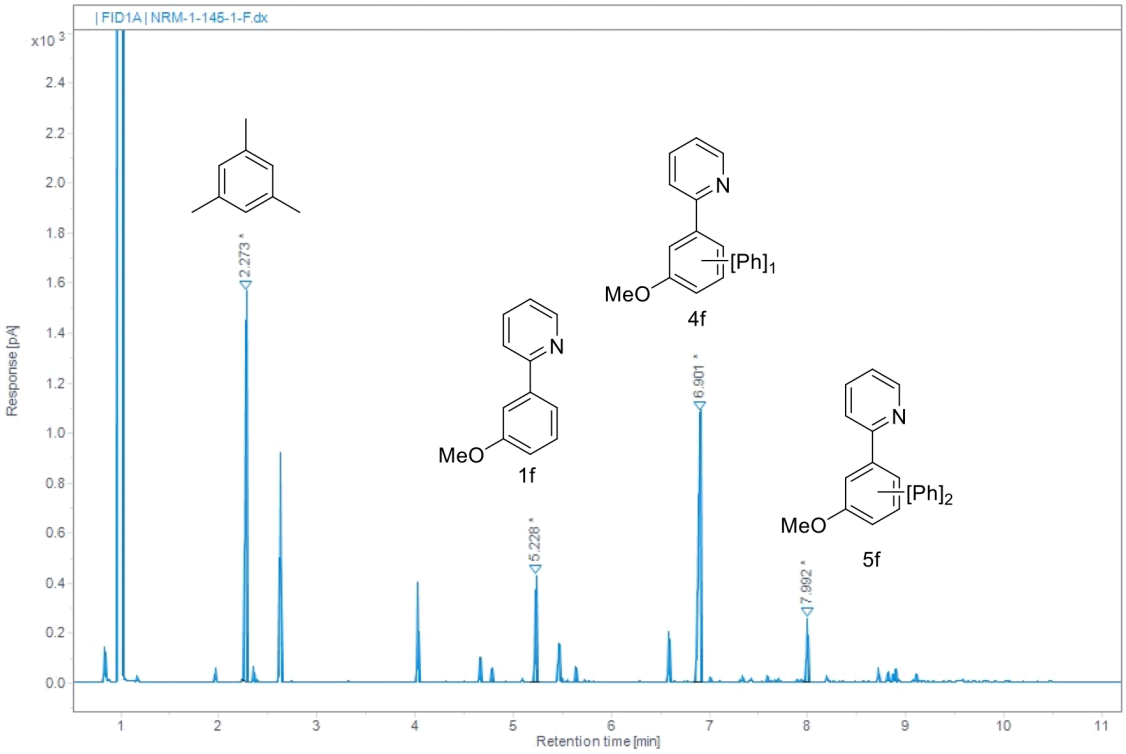

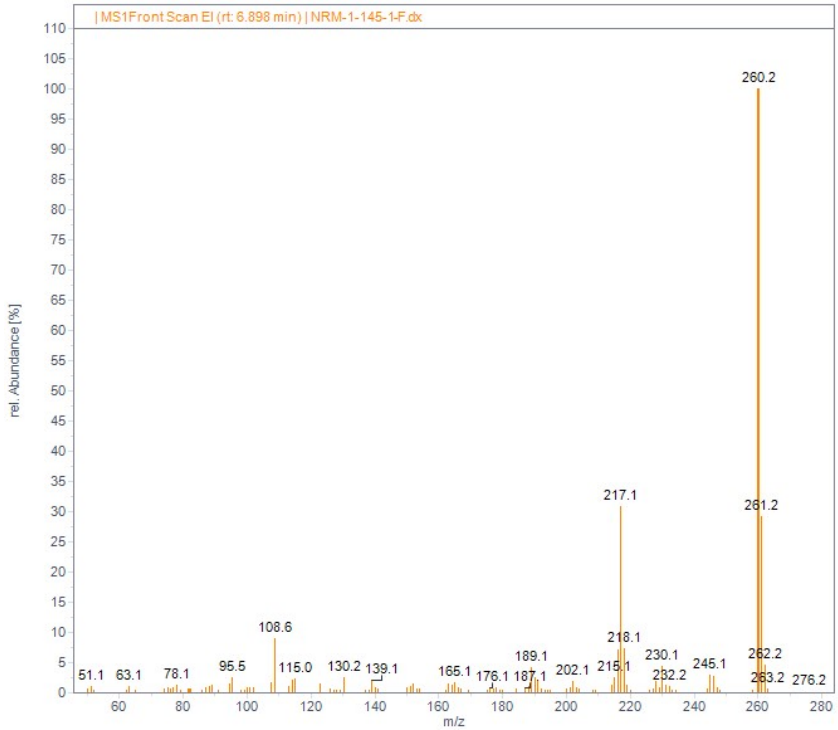

Figure S74. GC-FID trace and peak areas of crude arylpyridine arylation reaction mixture using **2a** (top). Peaks for internal standard (mesitylene), remaining arylpyridine **1f**, and mono- and di-arylated product are highlighted. Mass spectrum of peak exhibiting m/z for mono-arylated product (bottom).

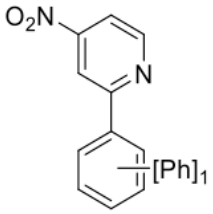

4g

4g. Arylation of 1g with 2a: GP5. 9.7% GC Yield. 10 % total arylation. GC-MS(EI) m/z - Calc: 276.1; Exp: 276.0

RT (min)	Area (pA·s)	Area%
2.067	371.875	56.266
5.073	231.008	34.952
6.625	58.041	8.782

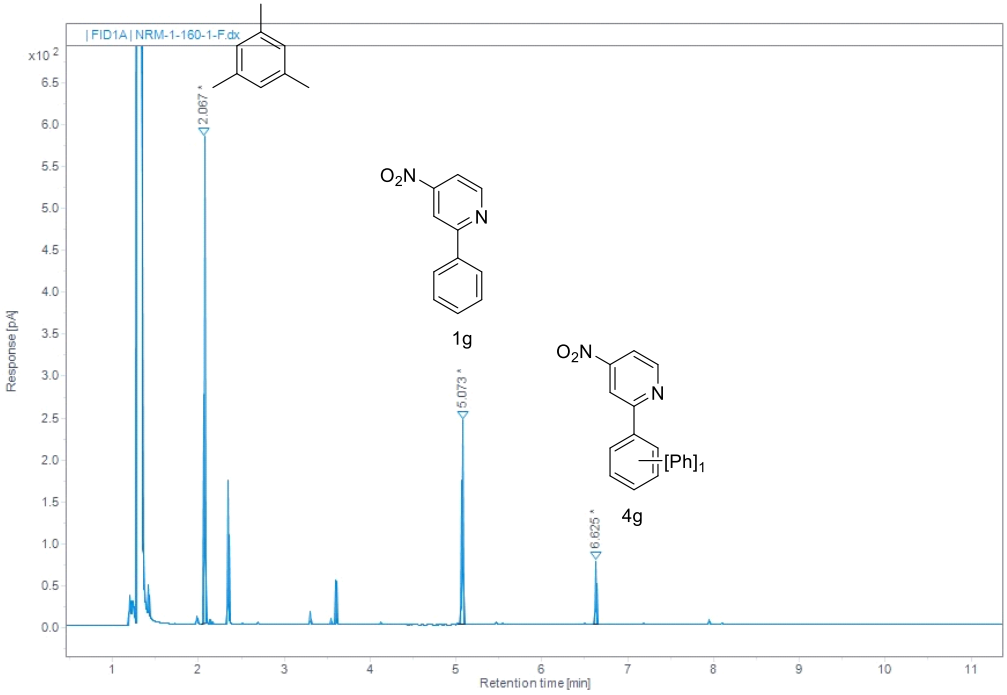

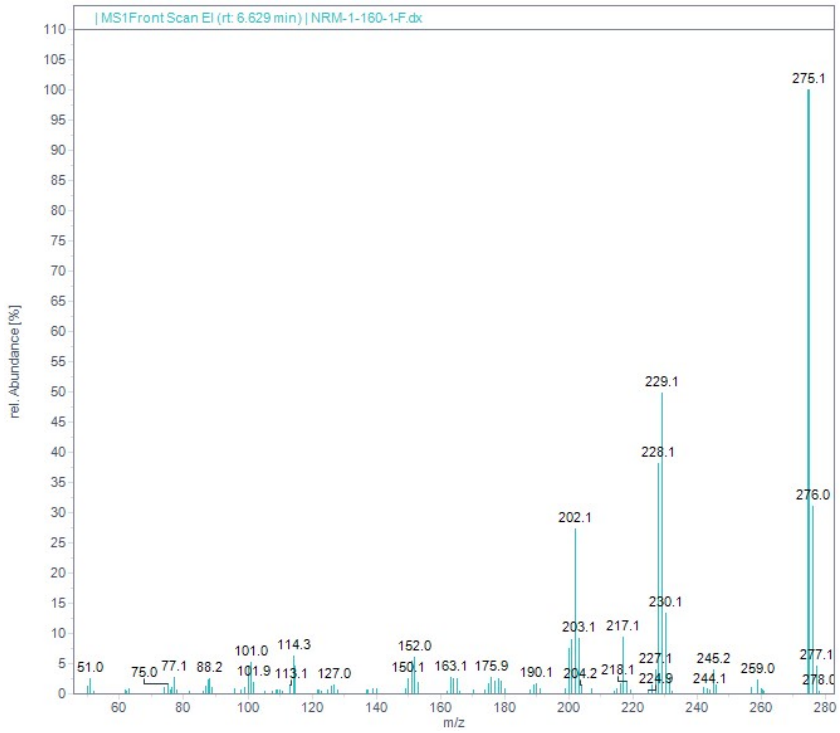

Figure S75. GC-FID trace and peak areas of crude arylpyridine arylation reaction mixture using **2a** (top). Peaks for internal standard (mesitylene), remaining arylpyridine **1g**, and mono-arylated product are highlighted. Mass spectrum of peak exhibiting m/z for mono-arylated product (bottom).

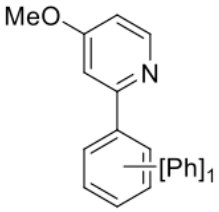

4h

RT (min)	Area (pA·s)	Area%
2.464	693.980	52.717
5.446	428.311	32.536
6.930	194.124	14.746

4h. Arylation of 1h with 2a: GP5. 14.3% GC Yield. 14% total arylation. GC-MS(EI) m/z - Calc: 261.1; Exp: 261.1.

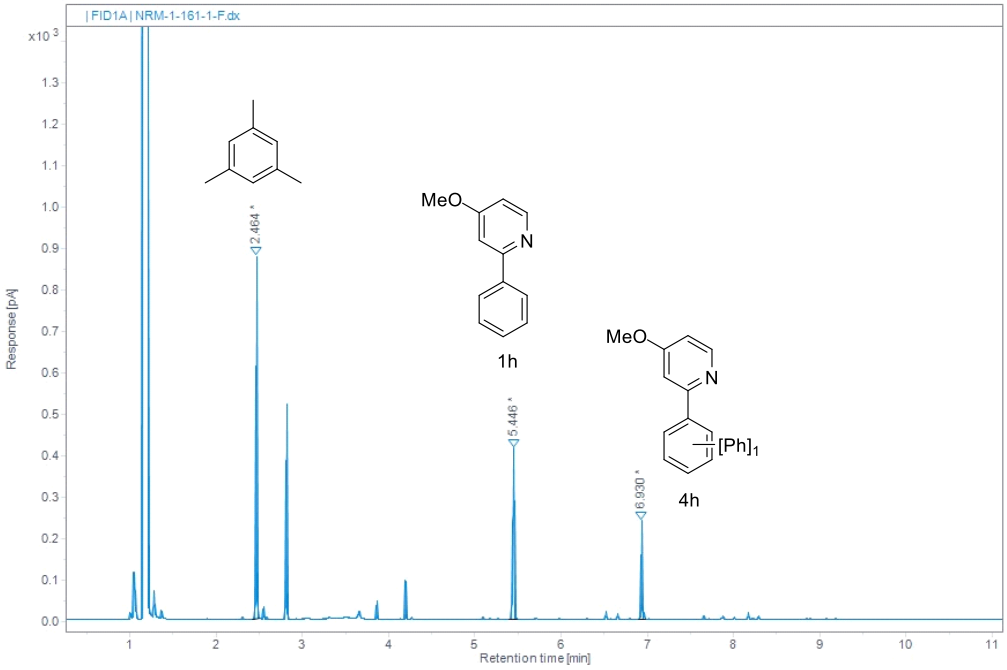

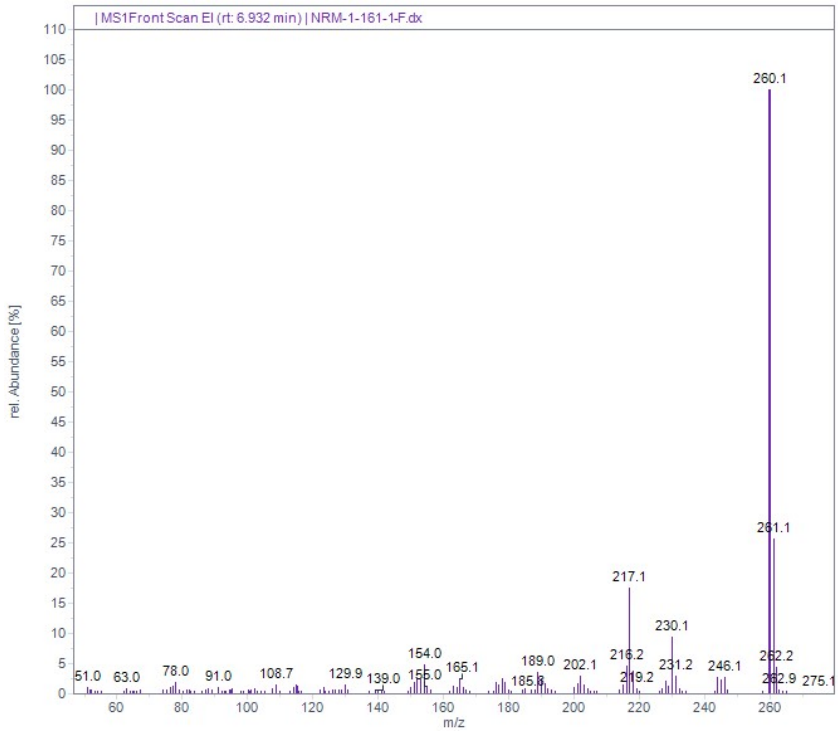

Figure S76. GC-FID trace and peak areas of crude arylpyridine arylation reaction mixture using **2a** (top). Peaks for internal standard (mesitylene), remaining arylpyridine **1h**, and mono-arylated product are highlighted. Mass spectrum of peak exhibiting m/z for mono-arylated product (bottom).

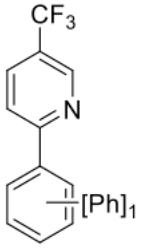

4i

RT (min)	Area (pA·s)	Area%
2.249	428.455	42.265
4.108	309.796	30.560
5.701	248.619	24.525
7.054	26.858	2.649

4i. Arylation of 1i with 2a: GP6. 38.1% GC Yield. 46% total arylation. GC-MS(EI) m/z - Calc: 299.1; Exp: 299.0.

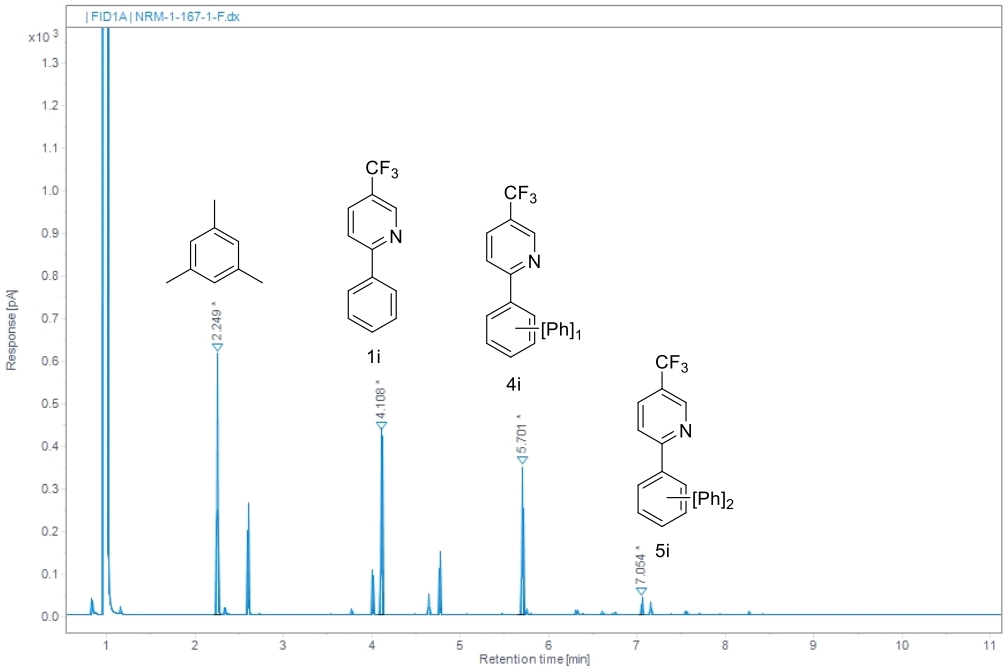

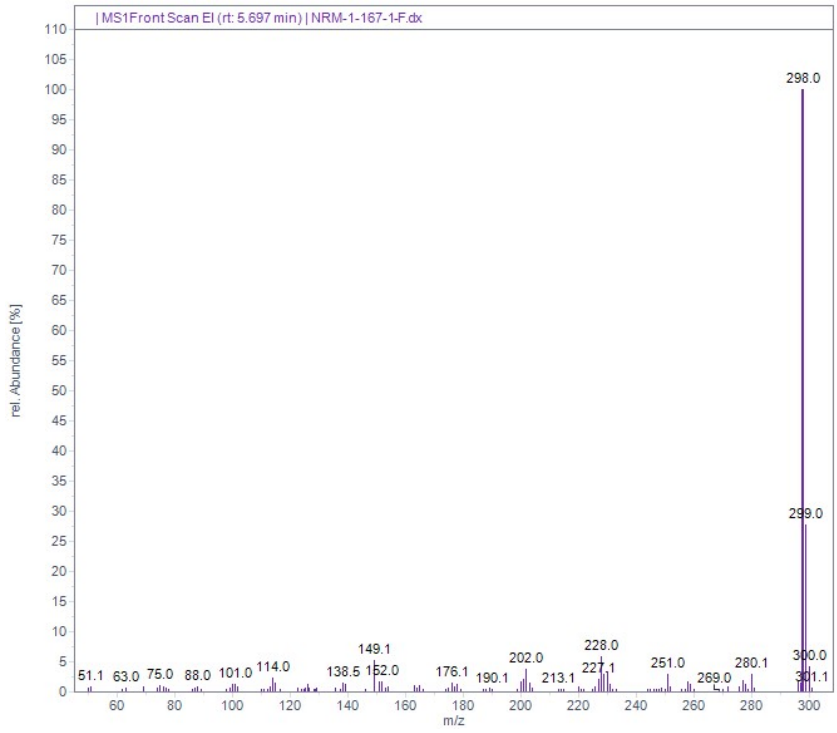

Figure S77. GC-FID trace and peak areas of crude arylpyridine arylation reaction mixture using **2a** (top). Peaks for internal standard (mesitylene), remaining arylpyridine **1i**, and mono-arylated product are highlighted. Mass spectrum of peak exhibiting m/z for mono-arylated product (bottom).

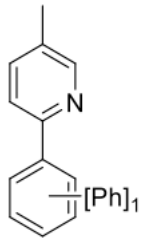

4j

4j. Arylation of 1j with 2a: GP6. 51.5% GC Yield. 66% total arylation. GC-MS(EI) m/z - Calc: 245.1; Exp: 245.1.

RT (min)	Area (pA·s)	Area%
2.249	424.837	38.679
4.757	283.800	25.838
6.401	341.060	31.051
7.709	48.674	4.431

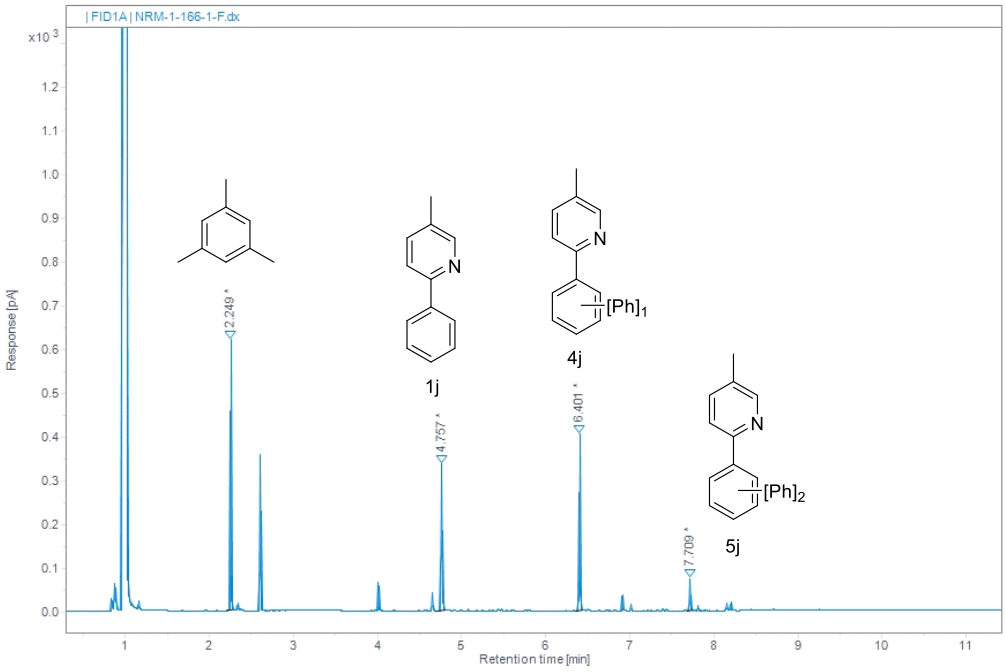

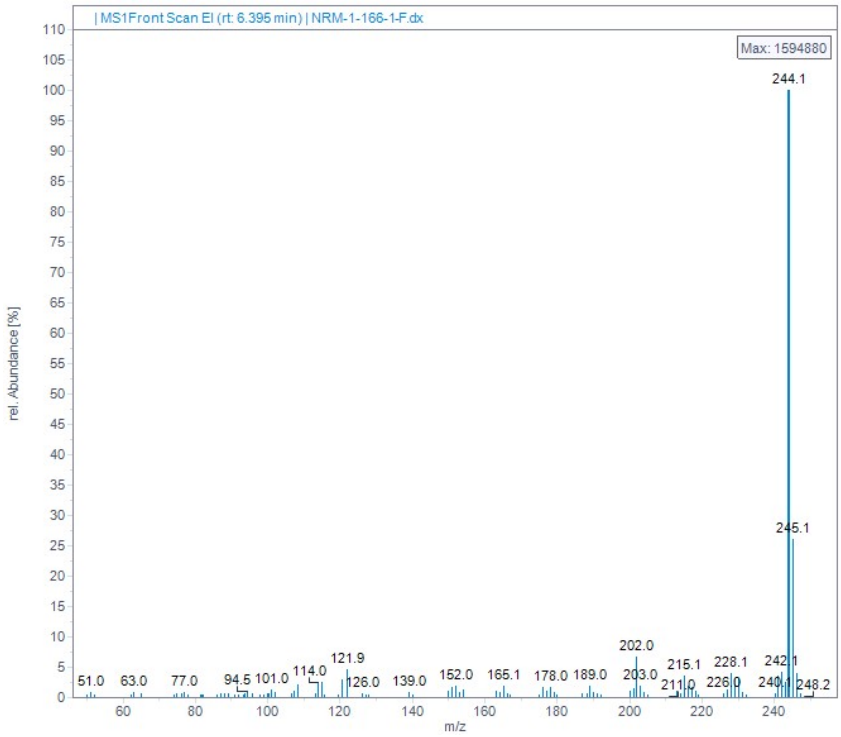

Figure S78. GC-FID trace and peak areas of crude arylpyridine arylation reaction mixture using **2a** (top). Peaks for internal standard (mesitylene), remaining arylpyridine **1j**, and mono- and di-arylated product are highlighted. Mass spectrum of peak exhibiting m/z for mono-arylated product (bottom).

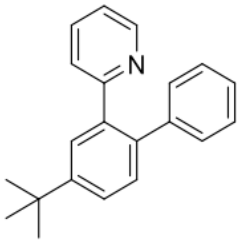

4k

4k. 2'-Ph-5'-tBu-2-phenylpyridine: GP4. 64% isolated yield, 79.6% GC Yield. 80% total arylation. ^{1}H NMR (400 MHz, $CDCl_3$) δ 8.66 (d, J = 4.8, 1 H), 7.70 (d, J = 2.0 Hz, 1 H), 7.51 (dd, J = 8.2, 2.2 Hz, 1 H), 7.40 – 7.35 (m, 2 H), 7.24 – 7.19 (m, 3 H), 7.16 – 7.13 (m, 2 H), 7.12 – 7.08 (m, 1 H), 6.88 (d, J = 8.0 Hz, 1 H), 1.41 (s, 9 H). ^{13}C NMR (500 MHz, $CDCl_3$) δ 150.68, 149.52, 141.37, 137.90, 135.26, 130.38, 129.88, 128.14, 127.47, 126.61, 125.91, 125.74, 121.39, 34.84, 31.52. GC-MS(EI) m/z - Calc: 287.2; Exp: 287.1.

RT (min)	Area (pA·s)	Area%
2.227	179.078	35.739
5.338	67.840	13.539
6.894	254.160	50.723

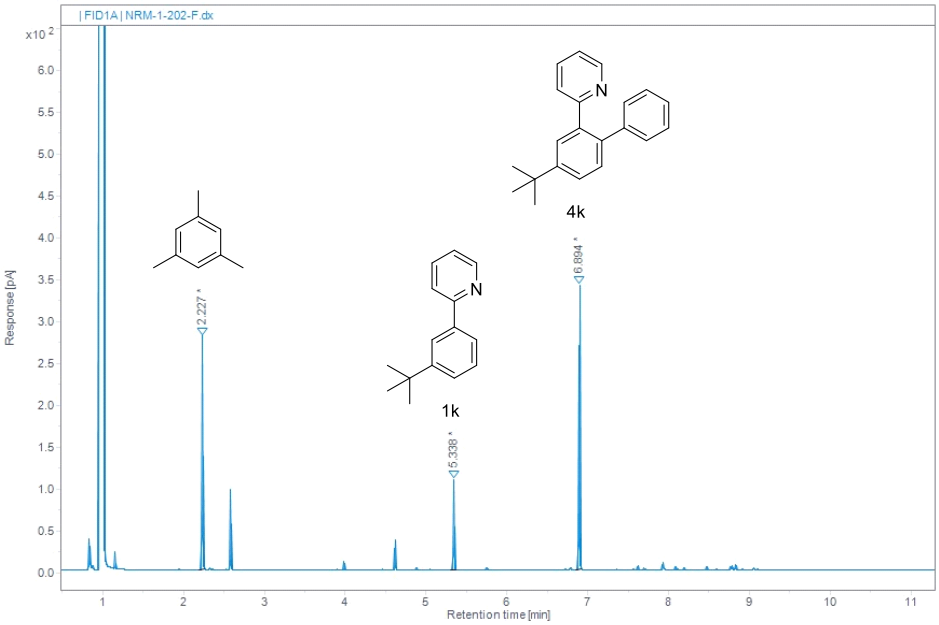

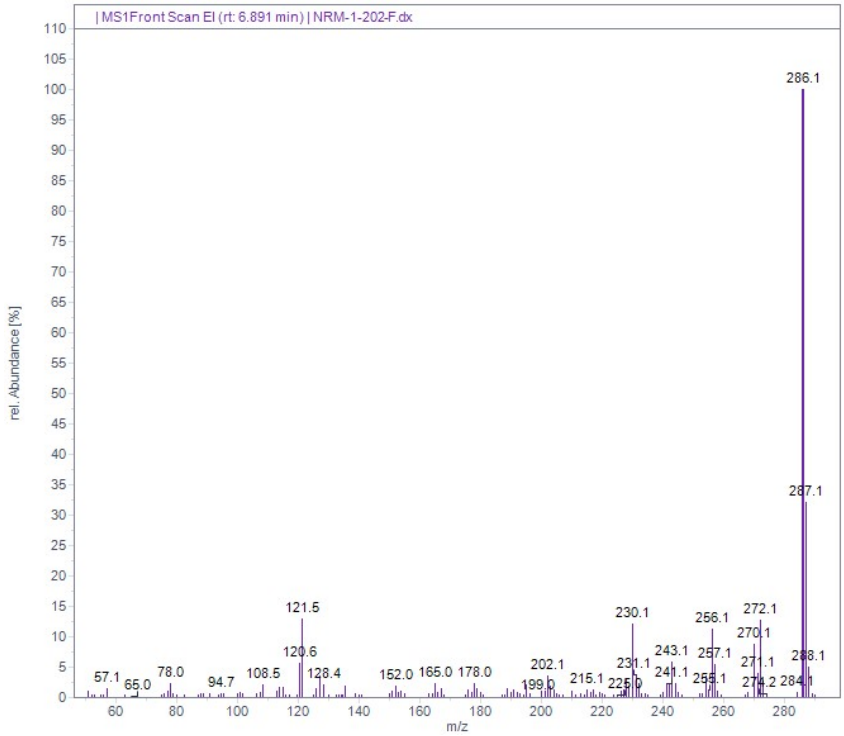

Figure S79. GC-FID trace and peak areas of crude arylpyridine arylation reaction mixture using **2a** (top). Peaks for internal standard (mesitylene), remaining arylpyridine **1k**, and mono-arylated product are highlighted. Mass spectrum of peak exhibiting m/z for mono-arylated product (bottom).

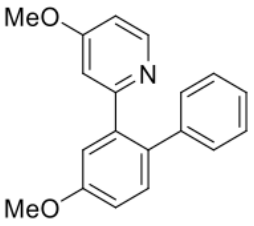

4l

4l. 4-OMe-2'-Ph-5'-OMe-2-phenylpyridine: GP6. 46% isolated yield. 41.1% GC Yield. 50% total arylation. ^{1}H NMR (300 MHz, $CDCl_3$) δ 8.43 (d, J = 5.8 Hz, 1 H), 7.35 (d, J = 8.5 Hz, 1 H), 7.29 (d, J = 2.8 Hz, 1 H), 7.24 - 7.19 (m, 3 H), 7.16 - 7.13 (m, 2 H), 7.02 (dd, J = 8.5, 2.8 Hz, 1 H), 6.65 (dd, J = 5.8, 2.6 Hz, 1 H), 6.37 (d, J = 2.5 Hz, 1 H), 3.90 (s, 3 H), 3.45 (s, 3 H). ^{13}C NMR (125 MHz, $CDCl_3$) δ 164.94, 160.65, 159.17, 150.42, 141.38, 140.61, 133.38, 131.75, 129.86, 128.19, 126.47, 115.23, 114.72, 110.88, 109.16, 55.60, 54.88. GC-MS(EI) m/z - Calc: 291.1; Exp: 291.2.

RT (min)	Area (pA·s)	Area%
2.291	4484.957	43.358
6.169	1770.913	17.120
7.578	3703.408	35.802
8.472	384.785	3.720

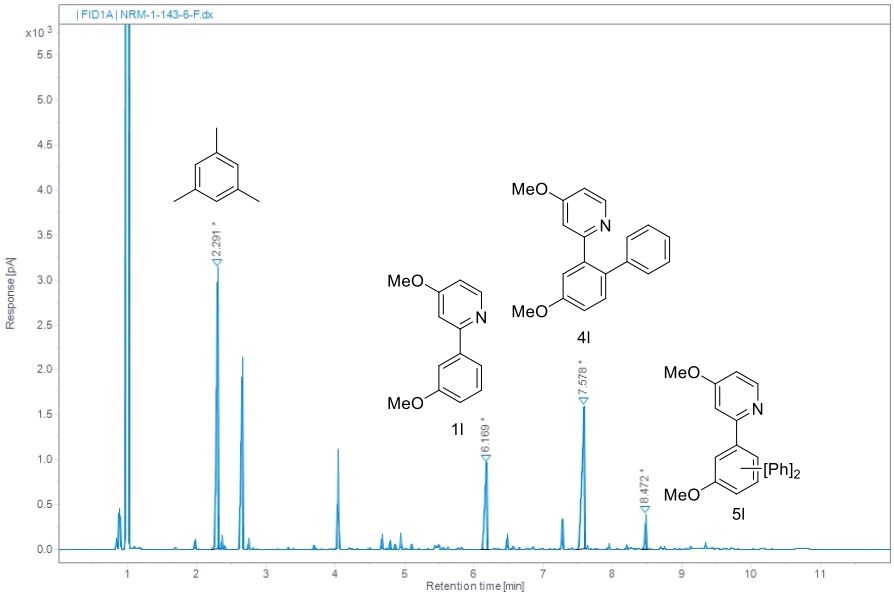

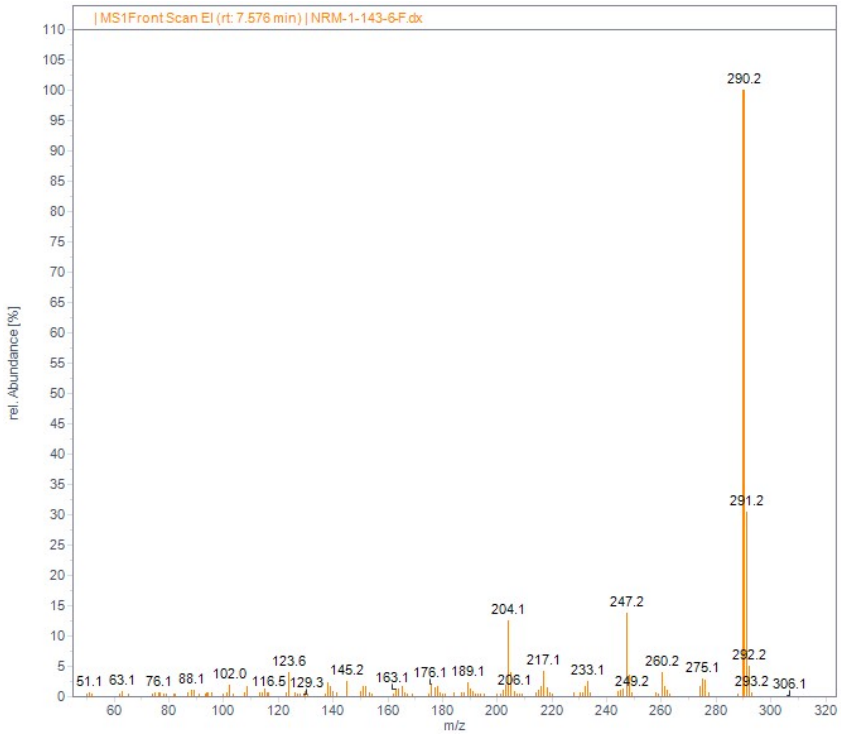

Figure S80. GC-FID trace and peak areas of crude arylpyridine arylation reaction mixture using **2a** (top). Peaks for internal standard (mesitylene), remaining arylpyridine **1l**, and mono- and di-arylated product are highlighted. Mass spectrum of peak exhibiting m/z for mono-arylated product (bottom).

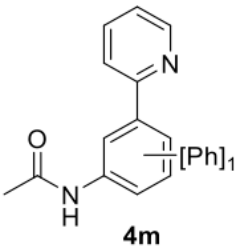

4m

4m. Arylation of 1m with 2a: GP6. 39.8% GC Yield. 92% total arylation. GC-MS(EI) m/z - Calc: 288.1; Exp: 288.1.

RT (min)	Area (pA·s)	Area%
2.257	1124.222	35.450
6.886	372.767	11.754
7.611	848.704	26.762
8.354	367.806	11.598
8.968	457.818	14.436

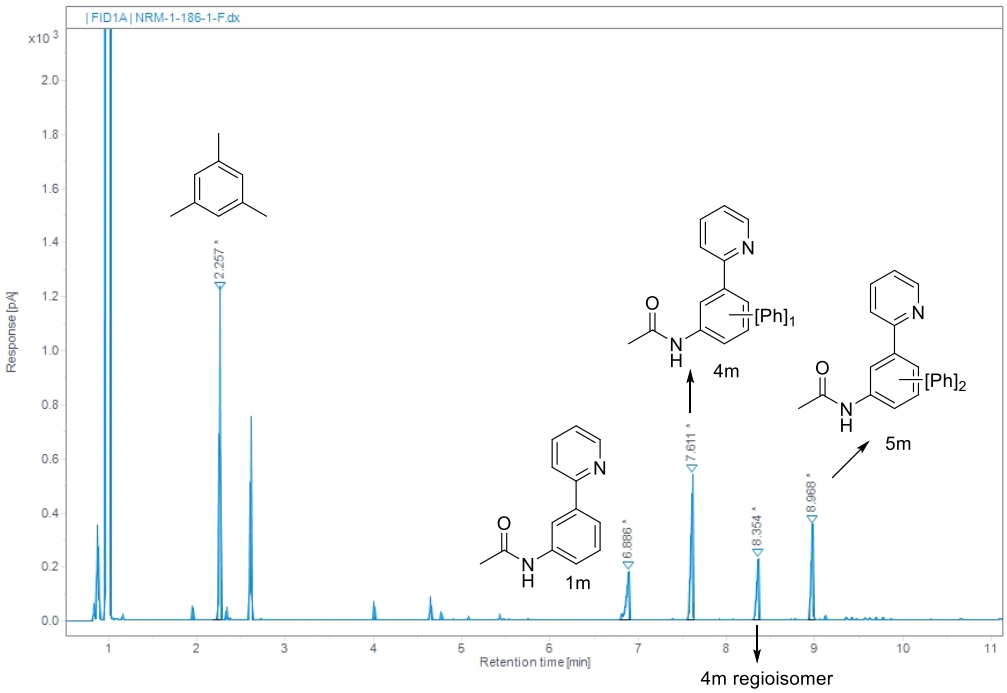

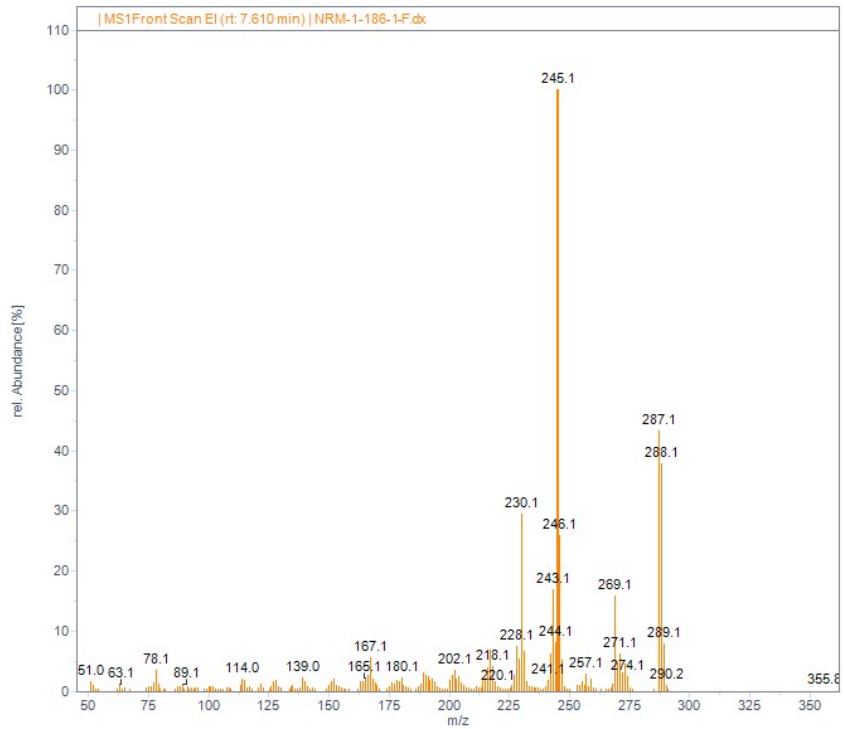

Figure S81. GC-FID trace and peak areas of crude arylpyridine arylation reaction mixture using **2a** (top). Peaks for internal standard (mesitylene), remaining arylpyridine **1m**, and mono- and di-arylated products are highlighted. Mass spectrum of peak exhibiting m/z for major mono-arylated product (bottom).

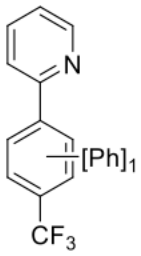

4n

4n. Arylation of 1n with 2a: GP5. 11.3% GC Yield. 11% total arylation. GC-MS(EI) m/z - Calc: 299.1; Exp: 299.1.

RT (min)	Area (pA·s)	Area%
2.075	1182.706	46.751
3.875	1122.433	44.368
5.475	224.679	8.881

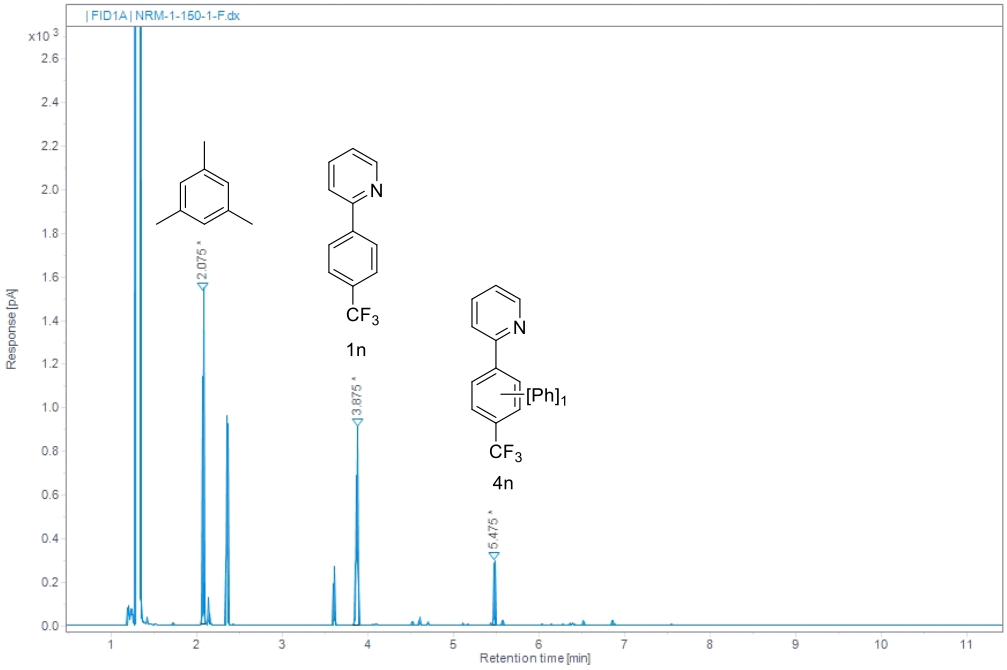

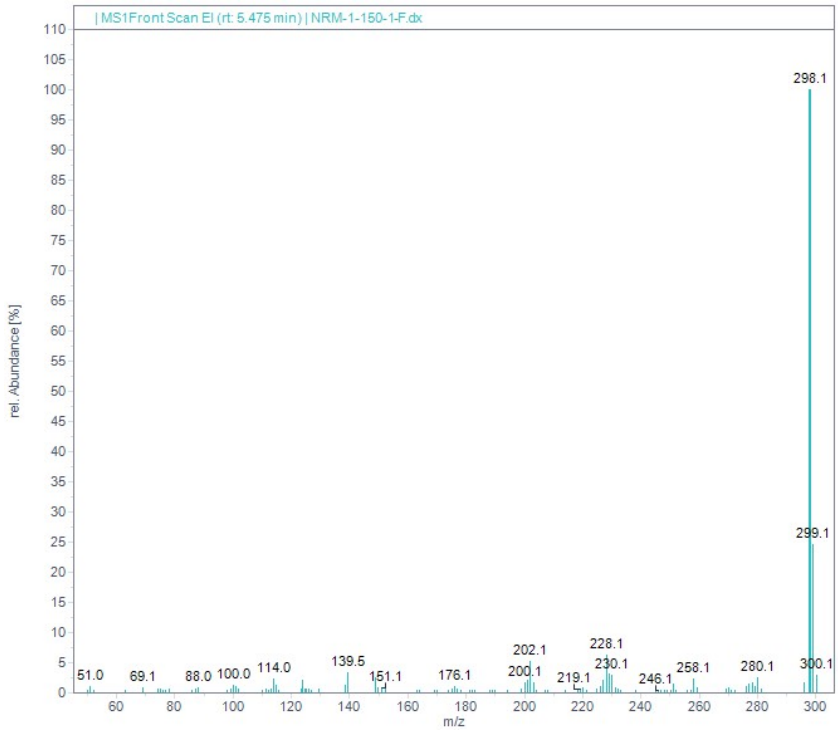

Figure S82. GC-FID trace and peak areas of crude arylpyridine arylation reaction mixture using **2a** (top). Peaks for internal standard (mesitylene), remaining arylpyridine **1n**, and mono-arylated product are highlighted. Mass spectrum of peak exhibiting m/z for mono-arylated product (bottom).

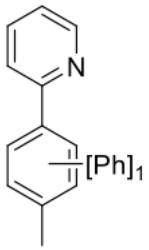

4o

RT (min)	Area (pA·s)	Area%
2.265	1713.070	37.376
4.738	760.885	16.601
6.426	1732.922	37.810
7.780	376.406	8.213

4o. Arylation of 1o with 2a: GP6. 55.1% GC Yield. 79% total arylation. GC-MS(EI) m/z - Calc: 245.1; Exp: 245.1.

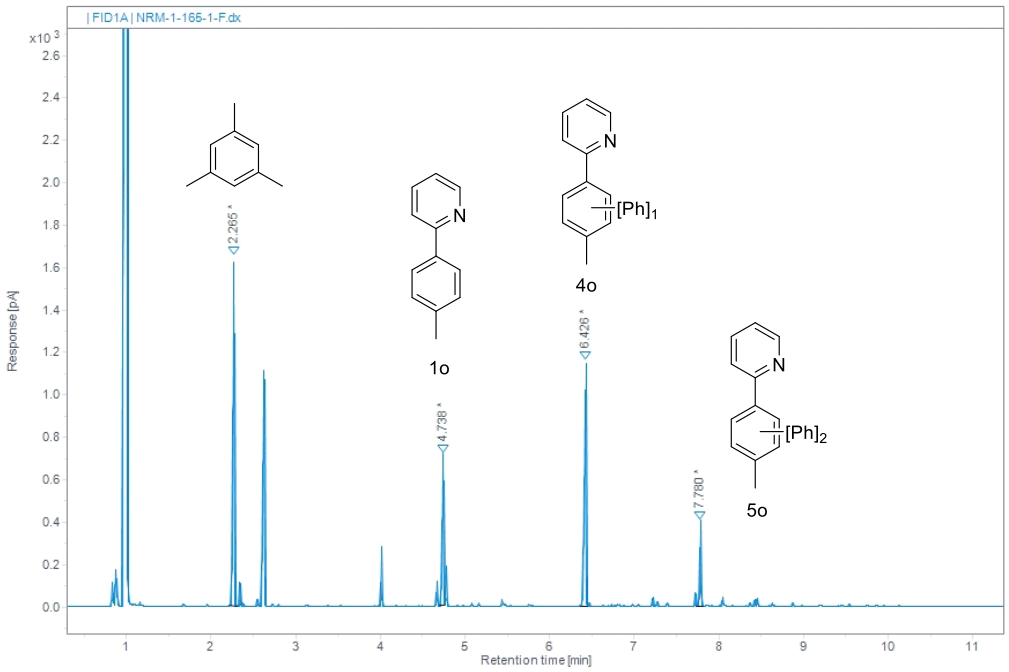

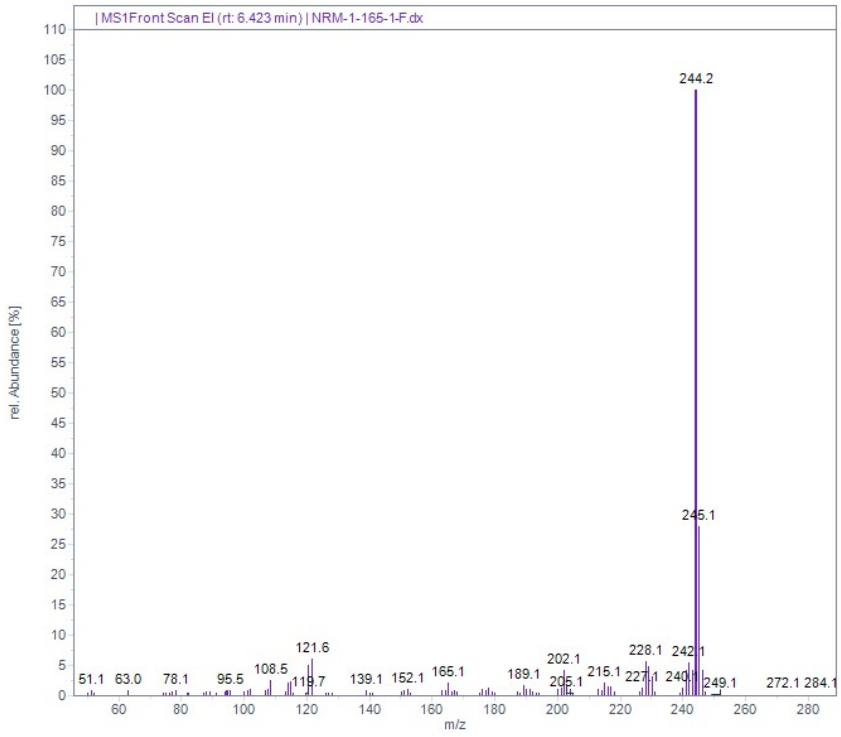

Figure S83. GC-FID trace and peak areas of crude arylpyridine arylation reaction mixture using **2a** (top). Peaks for internal standard (mesitylene), remaining arylpyridine **1o**, and mono- and di-arylated product are highlighted. Mass spectrum of peak exhibiting m/z for mono-arylated product (bottom).

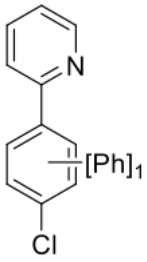

4p

4p. Arylation of 1p with 2a: GP5. 9.2% GC Yield. 9% total arylation. GC-MS(EI) m/z - Calc: 265.1; Exp: 265.1.

RT (min)	Area (pA·s)	Area%
2.265	371.597	49.318
5.035	343.442	45.581
6.688	38.435	5.101

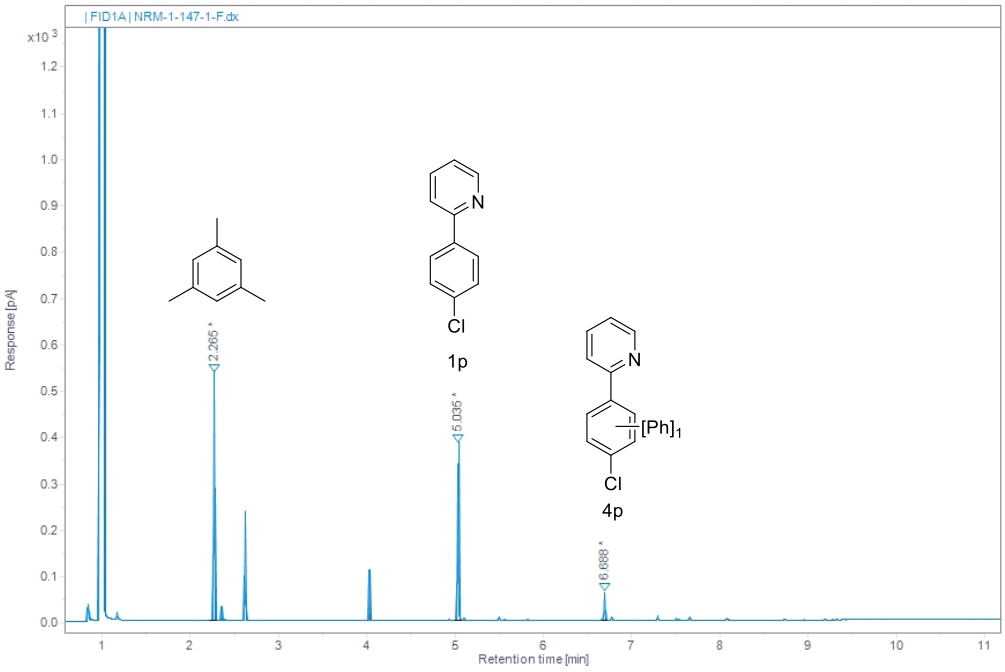

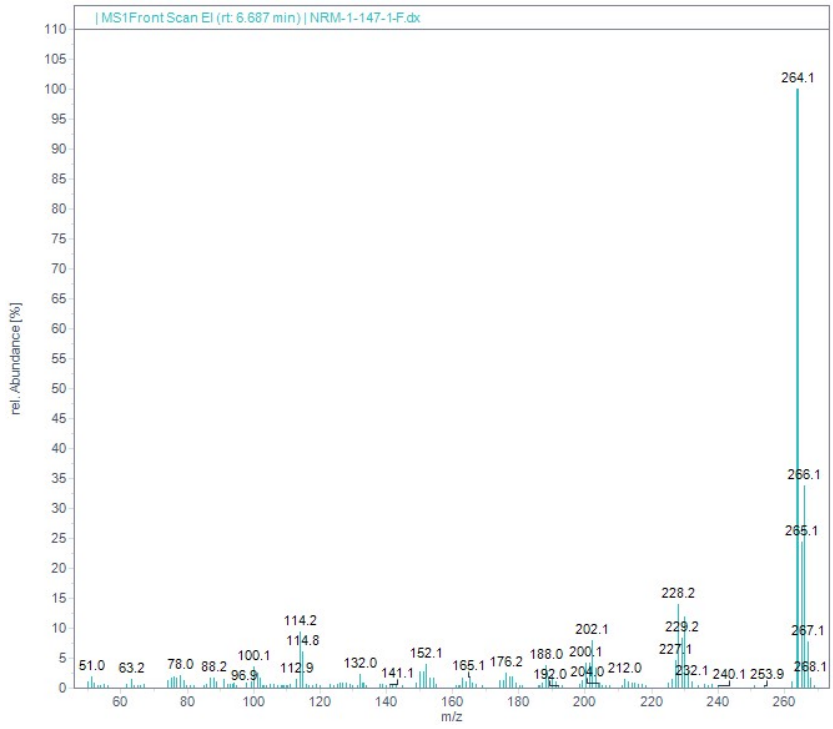

Figure S84. GC-FID trace and peak areas of crude arylpyridine arylation reaction mixture using **2a** (top). Peaks for internal standard (mesitylene), remaining arylpyridine **1p**, and mono-arylated product are highlighted. Mass spectrum of peak exhibiting m/z for mono-arylated product (bottom).

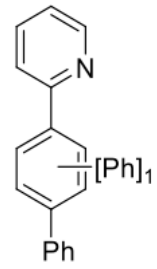

4q

4q. Arylation of 1q with 2a: GP6. 58.1% GC Yield. 76% total arylation. GC-MS(EI) m/z - Calc: 307.1; Exp: 307.1.

RT (min)	Area (pA·s)	Area%
2.230	227.907	39.313
7.007	90.238	15.566
8.367	220.709	38.072
9.637	40.868	7.050

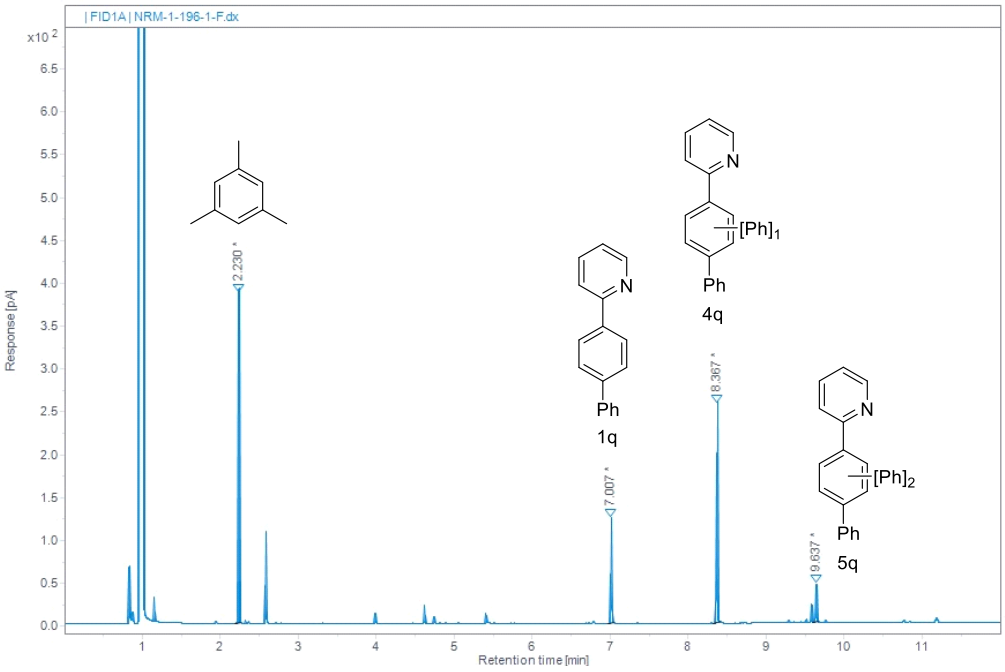

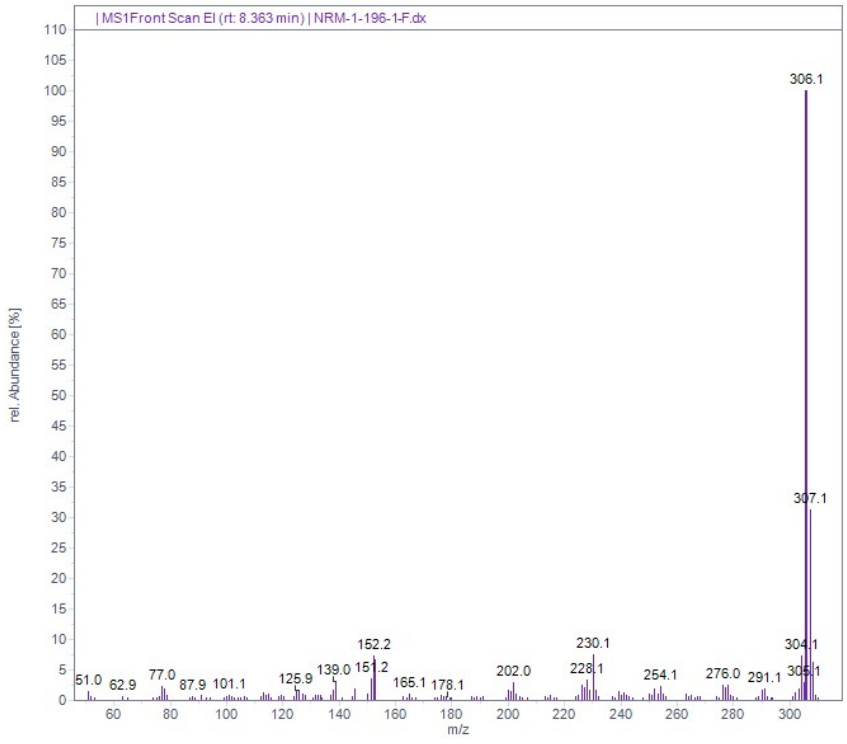

Figure S85. GC-FID trace and peak areas of crude arylpyridine arylation reaction mixture using **2a** (top). Peaks for internal standard (mesitylene), remaining arylpyridine **1q**, and mono- and di-arylated product are highlighted. Mass spectrum of peak exhibiting m/z for mono-arylated product (bottom).

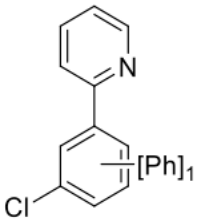

4r

4r. Arylation of 1r with 2a: GP4. 34.9% GC Yield. 43% total arylation. GC-MS(EI) m/z - Calc: 265.1; Exp: 265.0.

RT (min)	Area (pA·s)	Area%
2.229	182.938	47.506
4.969	75.638	19.642
6.660	114.368	29.699
7.886	12.142	3.153

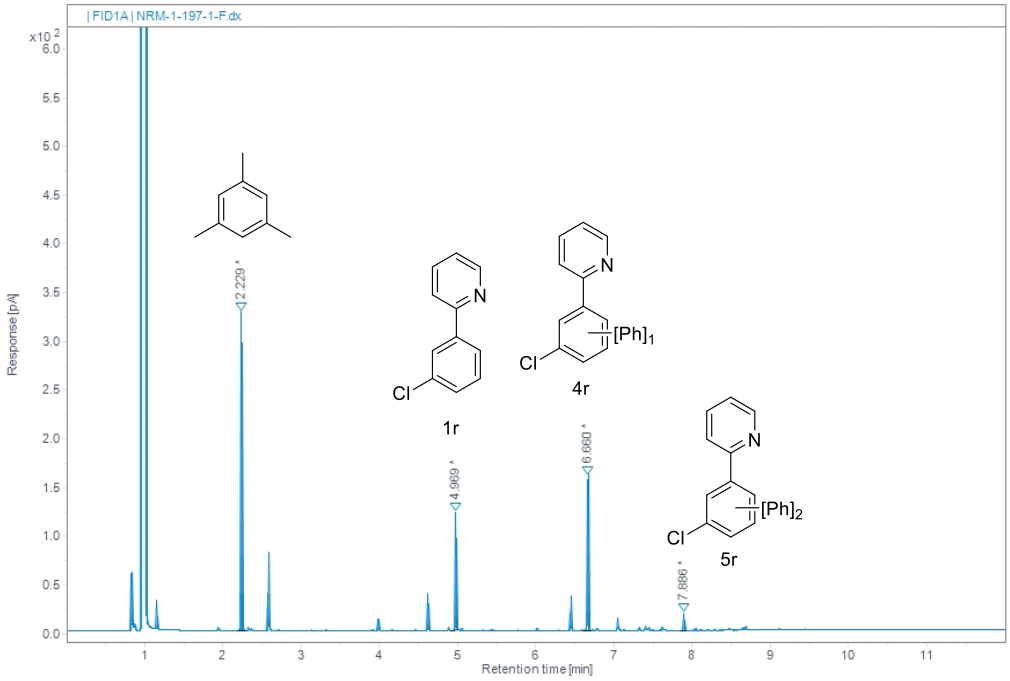

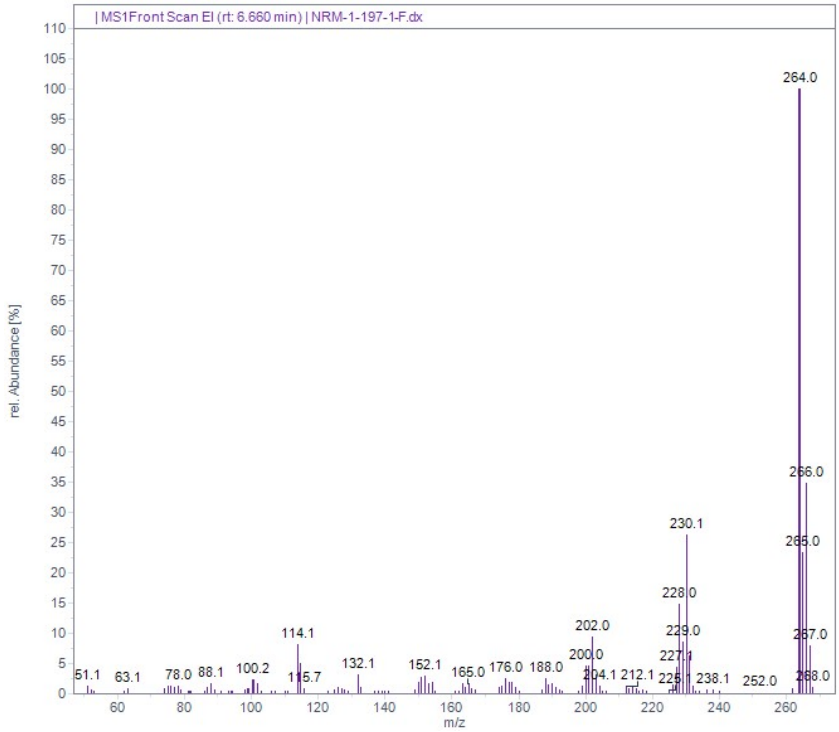

Figure S86. GC-FID trace and peak areas of crude arylpyridine arylation reaction mixture using **2a** (top). Peaks for internal standard (mesitylene), remaining arylpyridine **1r**, and mono- and di-arylated product are highlighted. Mass spectrum of peak exhibiting m/z for mono-arylated product (bottom).

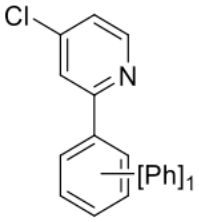

4s

4s. Arylation of 1s with 2a: GP6. 54.0% GC Yield. 82% total arylation. GC-MS(EI) m/z - Calc: 265.1; Exp: 265.0.

RT (min)	Area (pA·s)	Area%
2.232	281.081	41.649
4.773	33.814	5.010
6.386	268.096	39.725
7.715	91.895	13.616

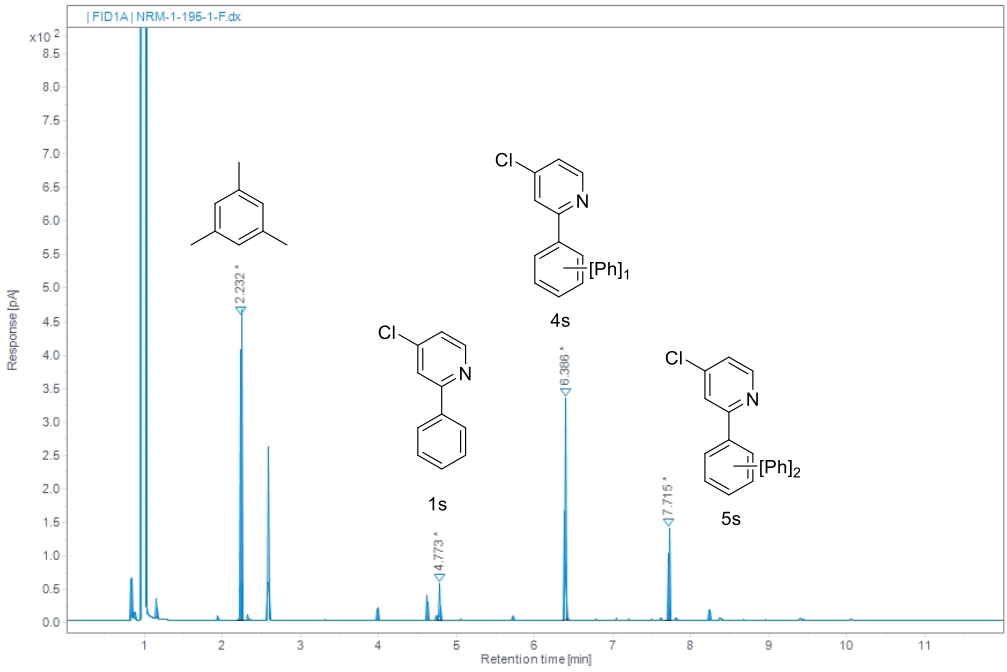

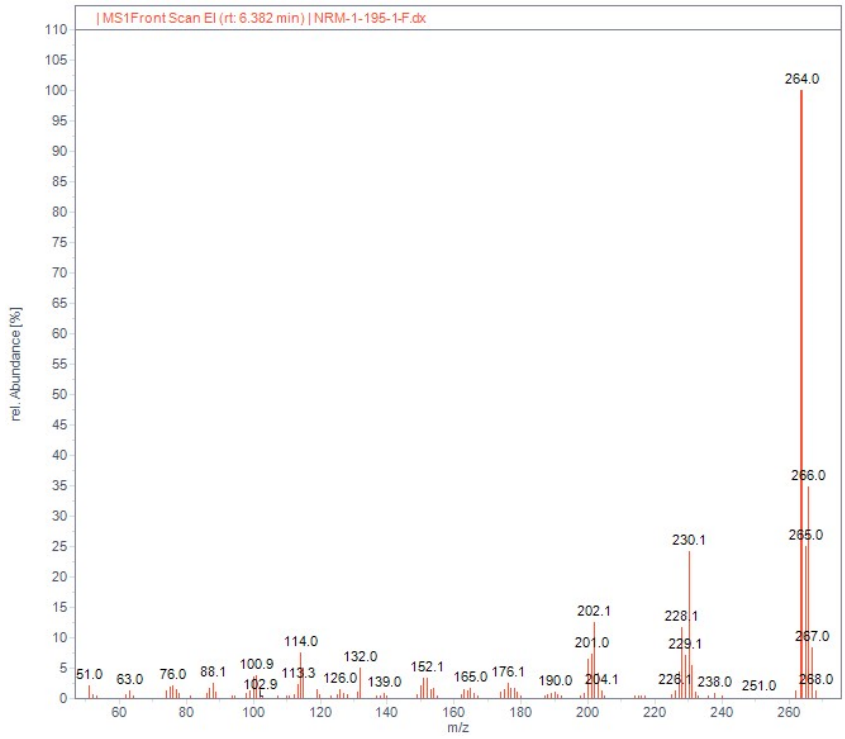

Figure S87. GC-FID trace and peak areas of crude arylpyridine arylation reaction mixture using **2a** (top). Peaks for internal standard (mesitylene), remaining arylpyridine **1s**, and mono- and di-arylated product are highlighted. Mass spectrum of peak exhibiting m/z for mono-arylated product (bottom).

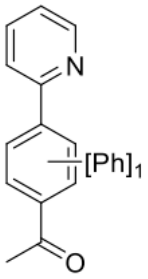

4t

4t. Arylation of 1t with 2a: GP5. 11.0% GC Yield. 11% total arylation. GC-MS(EI) m/z - Calc: 273.1; Exp: 273.1.

RT (min)	Area (pA·s)	Area%
2.262	182.717	44.199
5.873	195.373	47.260
7.362	35.307	8.541

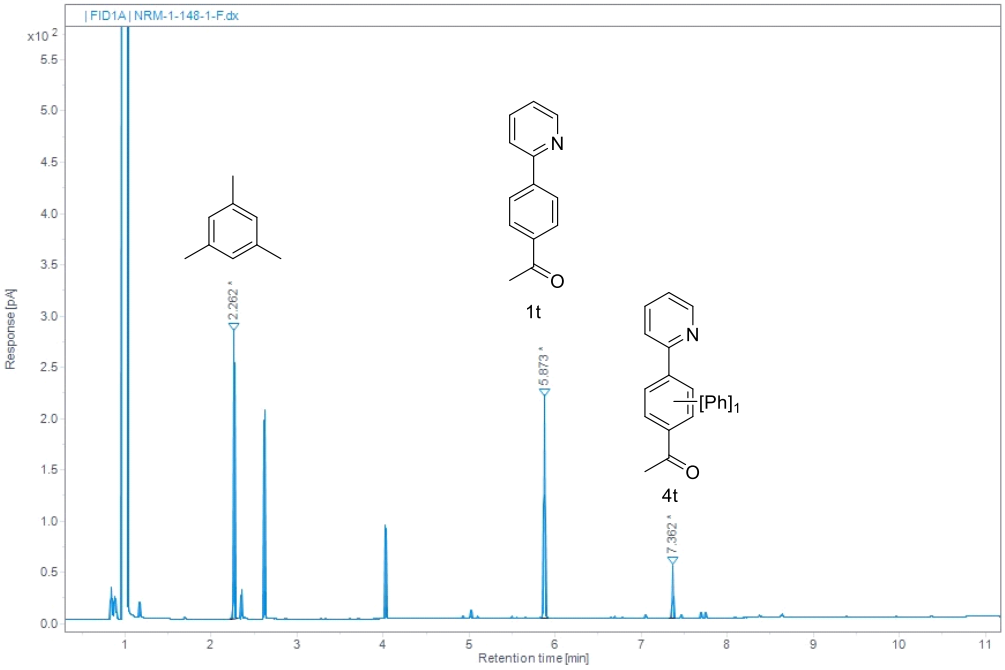

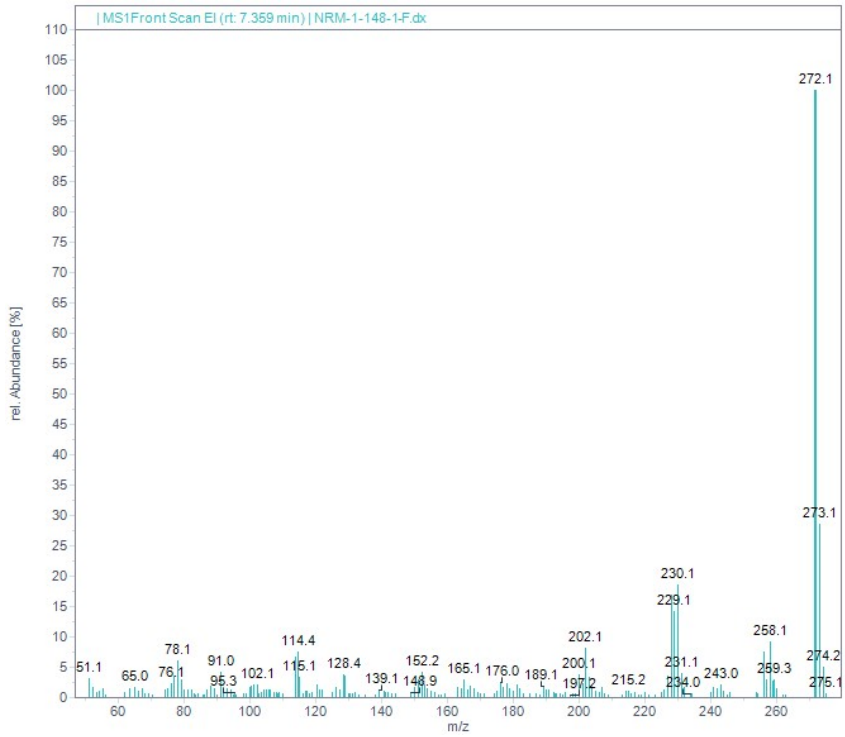

Figure S88. GC-FID trace and peak areas of crude arylpyridine arylation reaction mixture using **2a** (top). Peaks for internal standard (mesitylene), remaining arylpyridine **1t**, and mono-arylated product are highlighted. Mass spectrum of peak exhibiting m/z for mono-arylated product (bottom).

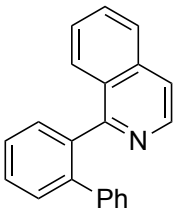

4u

2-(2-phenyl)phenylisoquinoline: To a 4-mL vial, $Pd(TFA)_2$ (0.010 mmol, 10 mol%), bocTaurine (0.030 mmol, 30 mol%), **2a** (0.15 mmol, 1.50 eq.), 2-phenylisoquinoline (0.10 mmol, 1.0 eq.) and methanol (0.5 mL) were added. The reaction was irradiated by an 18 W 405 nm light at 45 °C for 18 hours. The crude reaction was analyzed by GC-MS using mesitylene as internal standard. The title product was purified by HPLC (0.1% TFA H_2O/ 0.1% TFA MeOH). Fractions containing product were concentrated under reduced pressure. The residue was then passed through a 1:1 w/w filter of $MgSO_4/K_2CO_3$ using DCM as eluent to afford analytically pure, 2-(2-phenyl)phenylisoquinoline. 27% yield. ^1H NMR (500 MHz, $CDCl_3$): δ 8.52 (d, J = 5.7 Hz, 1H), 7.73 (d, J = 8.2 Hz, 1H), 7.61 – 7.48 (m, 7H), 7.33 – 7.29 (m, 1 H), 7.09 – 7.04 (m, 2H), 7.02 – 6.97 (m, 3H). The NMR agree with literature data.[27] GC-MS(EI) m/z – Calc: 281.1; Exp: 281.1

RT (min)	Area (pA·s)	Area%
2.201	297.260	39.306
5.928	287.477	38.013
7.298	171.531	22.681

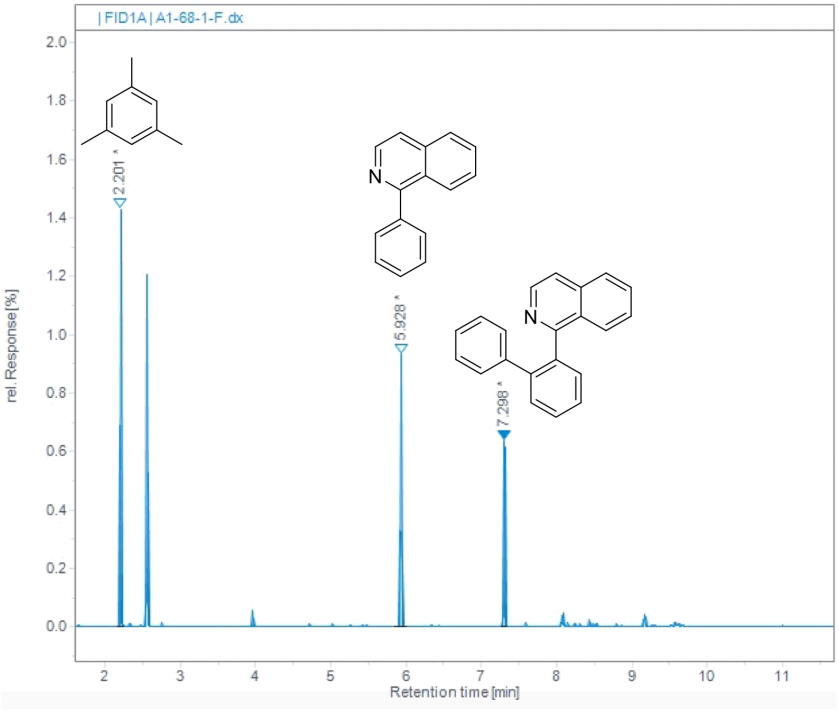

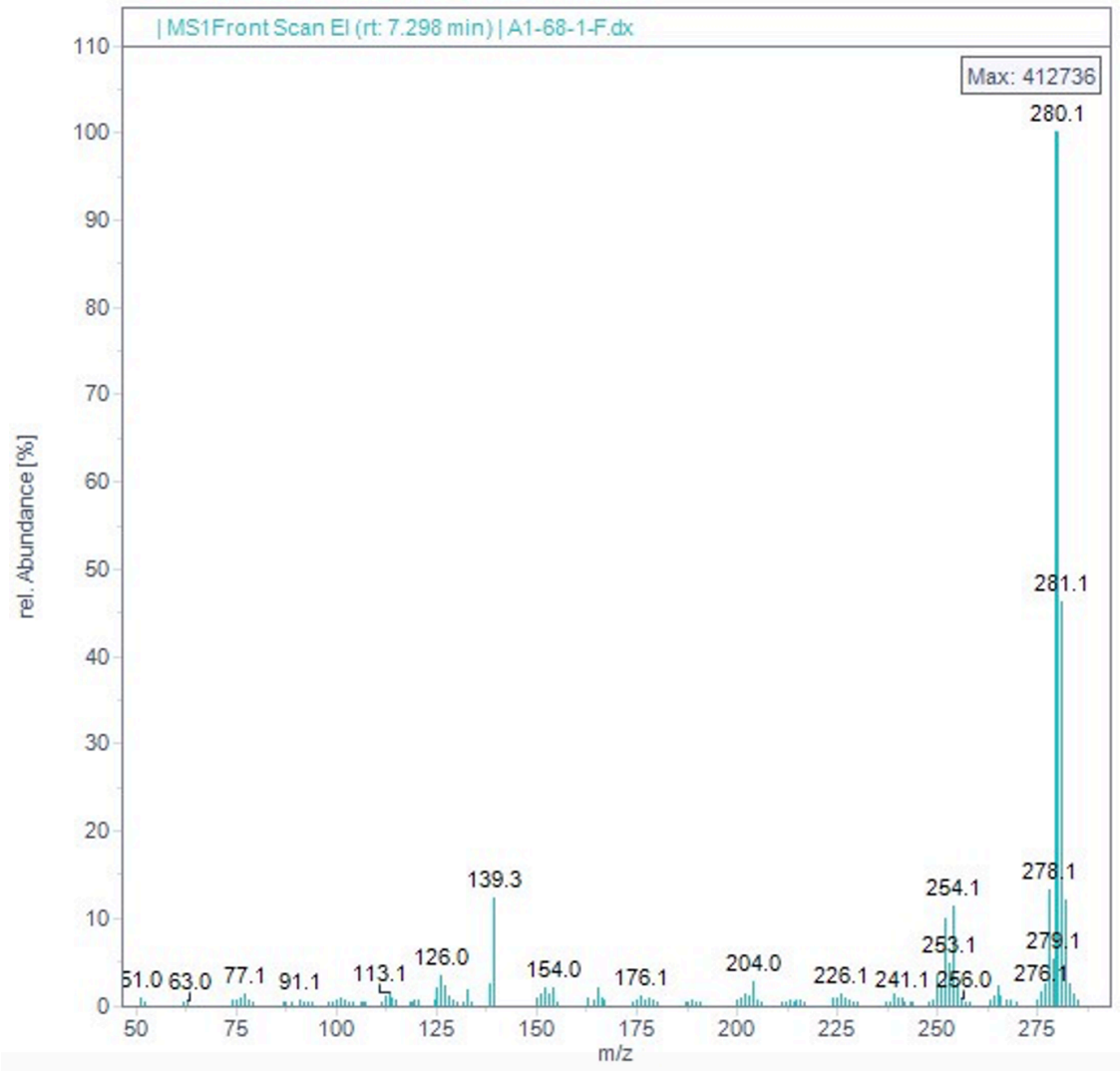

Figure S89. GC-FID trace and peak areas of crude arylpyridine arylation reaction mixture using 2-phenylisoquinoline **1u** (top). Peaks for internal standard (mesitylene), remaining **1u**, and mono-arylated product **4u** are highlighted. Mass spectrum of peak exhibiting m/z for mono-arylated product (bottom).

J. Optimization of Pd-catalyzed acetanilide C–H arylation

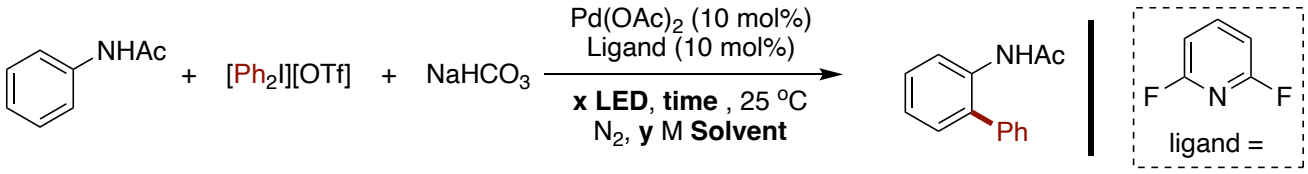

This optimization was performed under an atmosphere of N_2. To a 4-mL vial with a magnetic stir bar was added $Pd(OAc)_2$ (2.2 mg, 0.01 mmol, 10 mol%), 2,6-difluoropyridine (0.85 µL, 0.01 mmol, 10 mol%), $NaHCO_3$ (10 mg, 0.12 mmol, 1.2 eq.), diphenyliodonium triflate (43 mg, 0.10 mmol, 1.0 eq.), and acetanilide (14 mg, 0.10 mmol, 1.0 eq.). Solvent (y M) was added, and the reaction sealed with a PTFE lined screw cap. The reaction was

irradiated by a LED at 25 °C for a specific amount of time. Upon completion, the crude reaction was analyzed by GC-FID using ⁿdodecane as the internal standard.

Entry	Solvent	Concentration (M)	LED wavelength [nm] (power [W])	Time (h)	GC Yield (%)
1	HFIP	0.30	450 (18)	3	5
2	MeOH	0.30	450 (18)	3	1
3	THF	0.30	450 (18)	3	2
4	MeCN	0.30	450 (18)	3	n.d.
5	2,2,2-trifluoroethanol	0.30	450 (18)	3	2
6	Et_2O	0.30	450 (18)	3	n.d.
7	Toluene	0.30	450 (18)	3	1
8	1,4-dioxane	0.30	450 (18)	3	2
9	HFIP	0.30	450 (18)	6	12
10	HFIP	0.30	450 (18)	16	26
11	HFIP	0.50	450 (18)	16	29
12	HFIP	0.50	365 (18)	16	21
13	HFIP	0.50	440 (40)	16	28
14	HFIP	0.50	390 (40)	16	35

Table S13. Solvent identity, reaction concentration, LED parameters, and time screens.

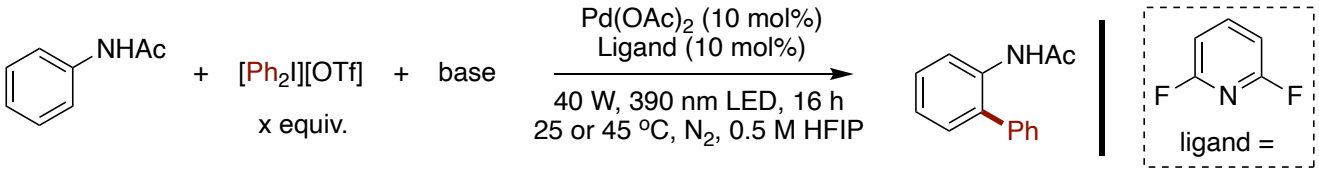

This optimization was performed under an atmosphere of N_2. To a 4-mL vial with a magnetic stir bar was added $Pd(OAc)_2$ (2.2 mg, 0.01 mmol, 10 mol%), 2,6-difluoropyridine (0.85 µL, 0.01 mmol, 10 mol%), base (0.12 mmol, 1.2 eq.), diphenyliodonium triflate (y eq.), and acetanilide (14 mg, 0.10 mmol, 1.0 eq.). HFIP (0.2 mL, 0.5 M) was added, and the reaction sealed with a PTFE lined screw cap. The reaction was irradiated by a 40 W 390 nm LED at 25 or 45 °C for 16 hours. Upon completion, the crude reaction was analyzed by GC-FID using ⁿdodecane as the internal standard.

Entry	2a loading (eq.)	Temperature (°C)	Base identity	GC Yield (%)
1	1.25	25	$NaHCO_3$	31
2	1.50	25	$NaHCO_3$	41
3	1.75	25	$NaHCO_3$	39
4	2.00	25	$NaHCO_3$	39
5	1.50	45	Li_2CO_3	25
6	1.50	45	Na_2CO_3	25
7	1.50	45	$CaCO_3$	19
8	1.50	45	$NaSO_2CF_3$	22
9	1.50	45	$Na_2S_2O_3$	22
10	1.50	45	NaOTf	22
11	1.50	45	NaOTFA	40
12	1.50	45	NaOBz	21
13	1.50	45	K_3PO_4	7
14	1.50	45	KSAc	19
15	1.50	45	$Na_2S_2O_3$	0
16	1.50	45	Cs_2CO_3	17
17	1.50	45	KIO_3	27
18	1.50	45	NEt_3	36

19	1.50	45	$NaHCO_3$	45

Table S14. Iodonium salt loading and base identity screens.

K. Synthesis of acetanilide substrates

All anilines used in this work were commercially available. Substrate *N*-arylacetamides were synthesized according to the following procedures and the characterization data of the resulting acetanilide products were in accordance with literature precedent.[1]

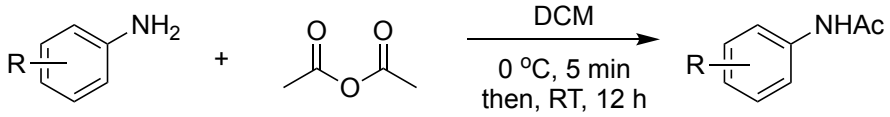

General procedure 7 (GP7): In a 20 mL scintillation vial equipped with a magnetic stir bar, the substituted aniline (2.5 mmol, 1.0 eq.) was dissolved in DCM (10 mL, 0.25 M) under N_2 atmosphere and cooled to 0 °C in an ice bath. To this mixture was added acetic anhydride (3.0 mmol, 1.2 eq.) was added dropwise. The ice bath was removed, and the reaction was left to stir at room temperature for 12 hours. Upon completion, the mixture was washed with 20 mL of a saturated solution of $NaHCO_3$. The organic layer was dried over anhydrous Na_2SO_4, filtered, and the solvent removed under reduced pressure to obtain the crude acetanilide. The crude product was purified by column chromatography on silica gel using mixtures of hexane/EtOAc as eluent to give the analytically pure acetanilides.

General procedure 8 (GP8): In a 20 mL scintillation vial equipped with a magnetic stir bar, the substituted aniline (2.5 mmol, 1.0 eq.) was dissolved in DCM (5 mL, 0.50 M) and cooled to 0 °C in an ice bath. NEt_3 (2.75 mmol, 1.1 eq.) was added followed by acetyl chloride (2.5 mmol, 1.0 eq.) dropwise over 30 minutes. The ice bath was removed, and the reaction was left to stir at room temperature for 3-24 hours, monitoring by TLC for disappearance of the aniline starting material. The mixture was then poured into a separatory funnel and washed with aqueous saturated $NaHCO_3$ (3 x 10 mL), followed by washing with brine (15 mL). The organic layer was dried over anhydrous Na_2SO_4, filtered, and concentrated under reduced pressure to obtain the crude acetanilide. The crude product was purified by column chromatography on silica gel using mixtures of hexane/EtOAc as eluent to give the analytically pure acetanilides.

L. Hammett parameter vs. GC yields of acetanilide arylation

Like we did with 2-phenylpyridine substrates, we sought to display our arylation results as a plot of Hammett parameter versus GC determined total arylation. In this way, trends related to arene substituent effects are readily observed. The standard conditions determined in the previous section was used here, including 2,6-difluoropyridine as ligand for Pd. In this analysis, we observed a negative correlation for arylation of acetanilide substrates **6** as Hammett parameter increases. Here too, the most electron-withdrawing groups like CN or NO_2 afford no detectable arylation products. As with 2-arylpyridine derivatives, the factor limiting application of this methodology to electron-poor acetanilides is most likely cyclopalladation and not aryl radical generation; however, thorough mechanistic investigations are needed before firm conclusions can be drawn. Nevertheless, these results suggest that our light-driven Ar_2I activation approach can be applied broadly to transition-metal-catalyzed C–H arylation reactions even if the substrate doubles as the iodonium salt activator.

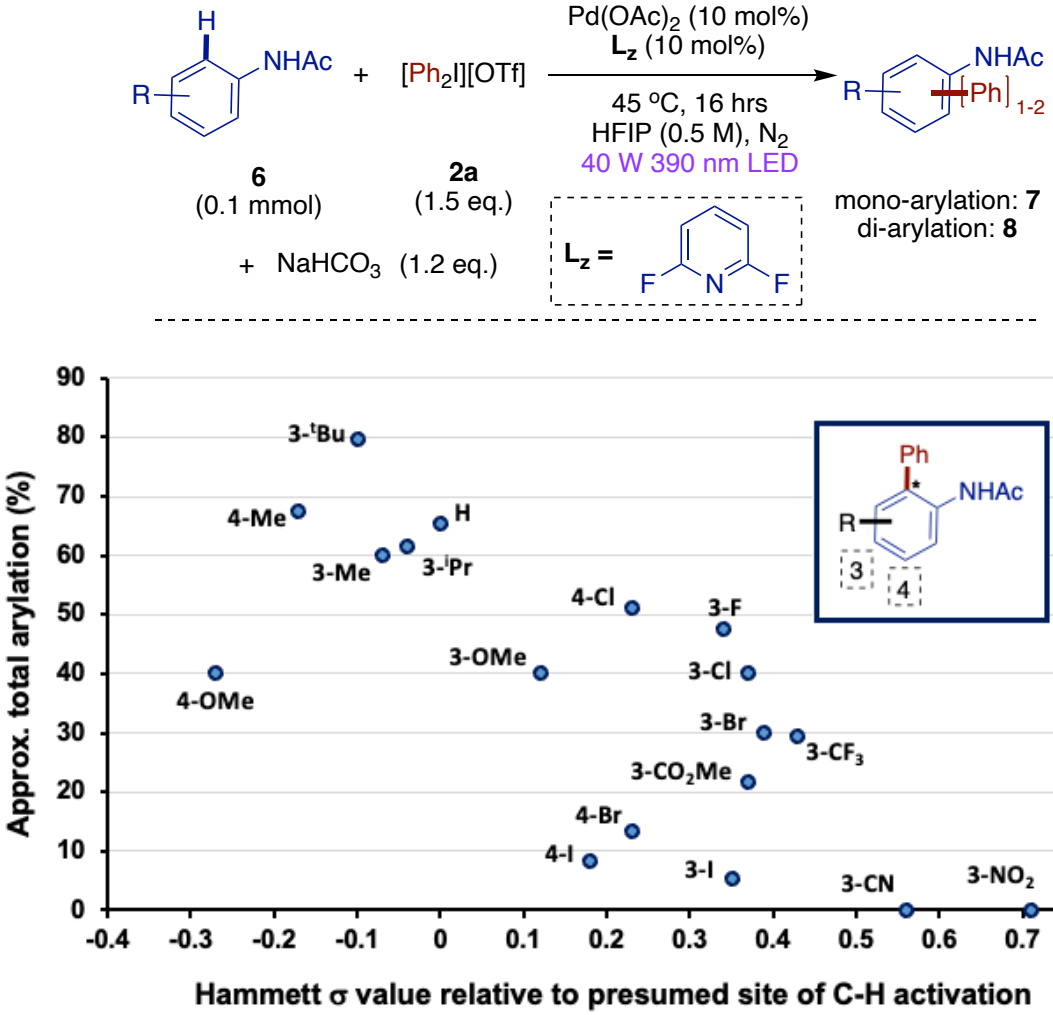

Figure S90. Pd-catalyzed arylation of **6**. Visualization of approximate total arylation observed by GC-FID for a range of **6**. *Presumed site of arylation shown only for Hammett value trend determination. Internal standard was ^{n}dodecane.

M. GC-MS characterization and isolation data for acetanilide arylation products

General procedure 9 (GP9): To a 4-mL vial with a magnetic stir bar was added $Pd(OAc)_2$ (2.2 mg, 0.01 mmol, 10 mol%), 2,6-difluoropyridine (0.9 µL, 0.01 mmol, 10 mol%), $NaHCO_3$ (10 mg, 0.12 mmol, 1.2 eq.), diphenyliodonium triflate (64 mg, 0.15 mmol, 1.5 eq.), and acetanilide (14 mg, 0.10 mmol, 1.0 eq.). HFIP (0.2 mL, 0.5 M) was added, and the reaction sealed with a PTFE lined screw cap. The reaction was irradiated by a 40 W 390 nm LED at 45 °C for 16 hours. Upon completion, the crude reaction was analyzed by GC-FID using ^{n}dodecane as the internal standard.

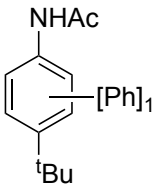

7a. Arylation of 6a with 2a: GP9. Monoarylation 52.9% Total Arylation: 80%. GC-MS(EI) **7a** m/z - Calc: 267.1; Exp: 267.1.

RT (min)	Area (pA·s)	Area%
3.229	325.640	46.661
5.127	64.102	9.185
6.612	243.068	34.829
7.910	65.070	9.324

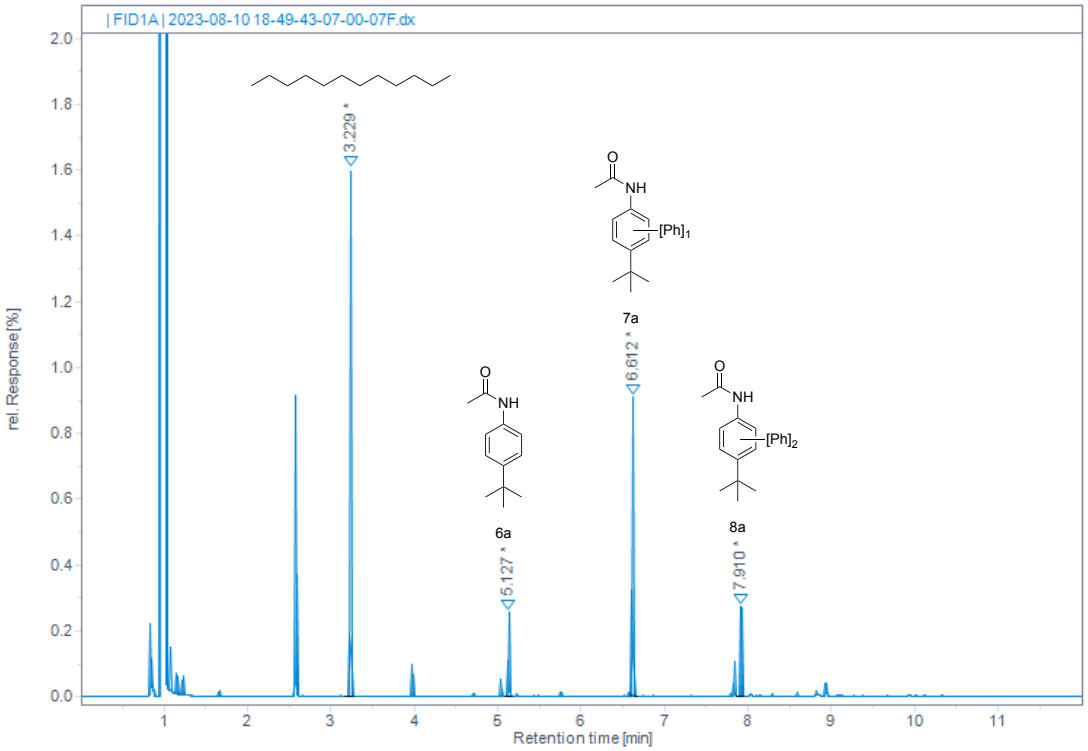

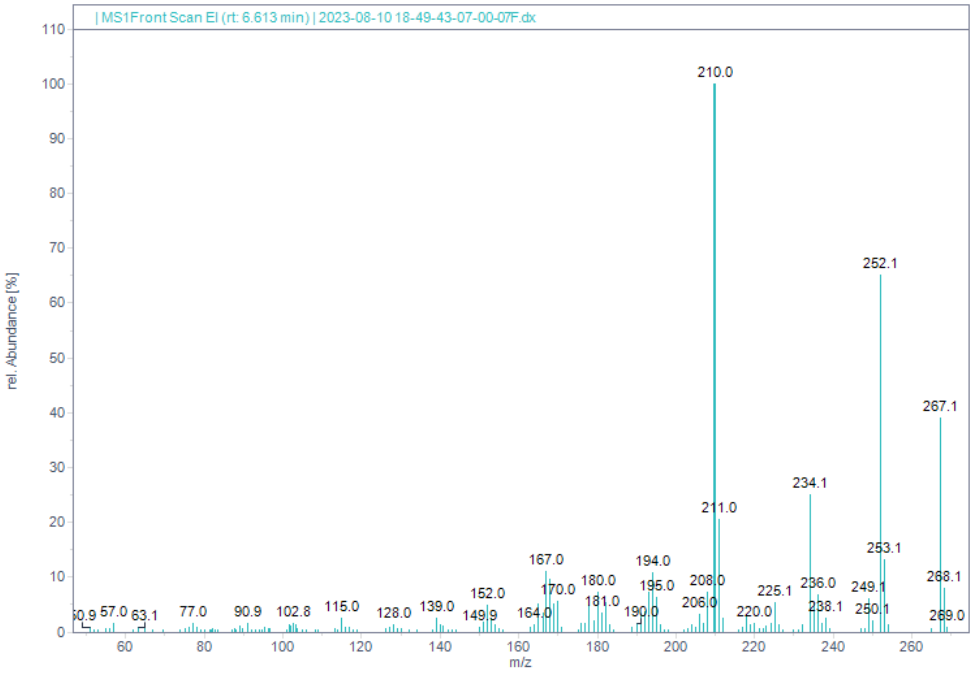

Figure S91. GC-FID trace and peak areas of crude acetanilide arylation reaction mixture (top). Peaks for internal standard (^{n}dodecane), remaining acetanilide **6a**, and mono- and di-arylated product are highlighted. Mass spectrum of peak exhibiting m/z for mono-arylated product (bottom).

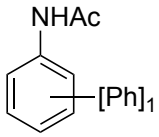

7b. Arylation of 6b with 2a: GP9. Monoarylation: 48.8% Total arylation: 66%. GC-MS(EI) **7b** m/z - Calc: 212.0; Exp: 212.0.

RT (min)	Area (pA·s)	Area%
3.236	659.250	57.963
3.945	83.637	7.354
5.683	309.483	27.211
7.355	84.993	7.473

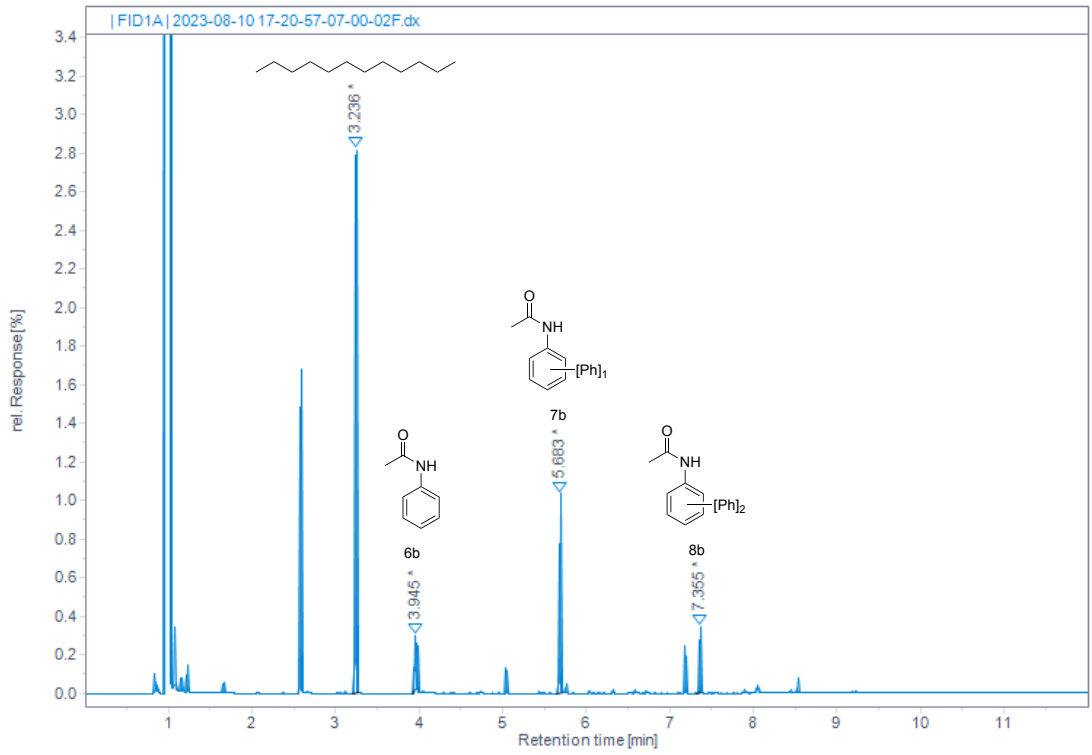

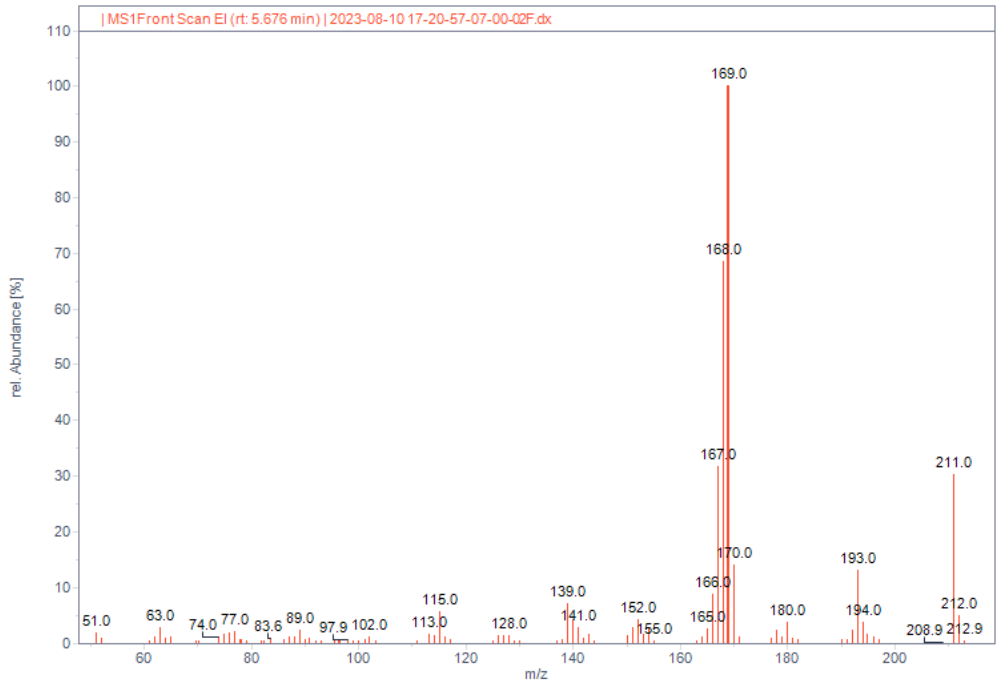

Figure S92. GC-FID trace and peak areas of crude acetanilide arylation reaction mixture (top). Peaks for internal standard (^{n}dodecane), remaining acetanilide **6b**, and mono- and di-arylated product are highlighted. Mass spectrum of peak exhibiting m/z for mono-arylated product (bottom).

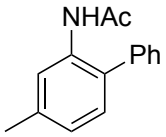

7c. Arylation of 6c with 2a: GP9. Isolated yield on 0.40 mmol of **6c** scale: 57.5%, GC mono-arylation yield: 59.3%; Total arylation: 68%; GC-MS(EI) **7c** m/z - Calc: 225.0; Exp: 225.12.

RT (min)	Area (pA·s)	Area%
3.230	302.347	53.720
4.288	50.162	8.913
5.979	191.680	34.057
7.350	18.634	3.311

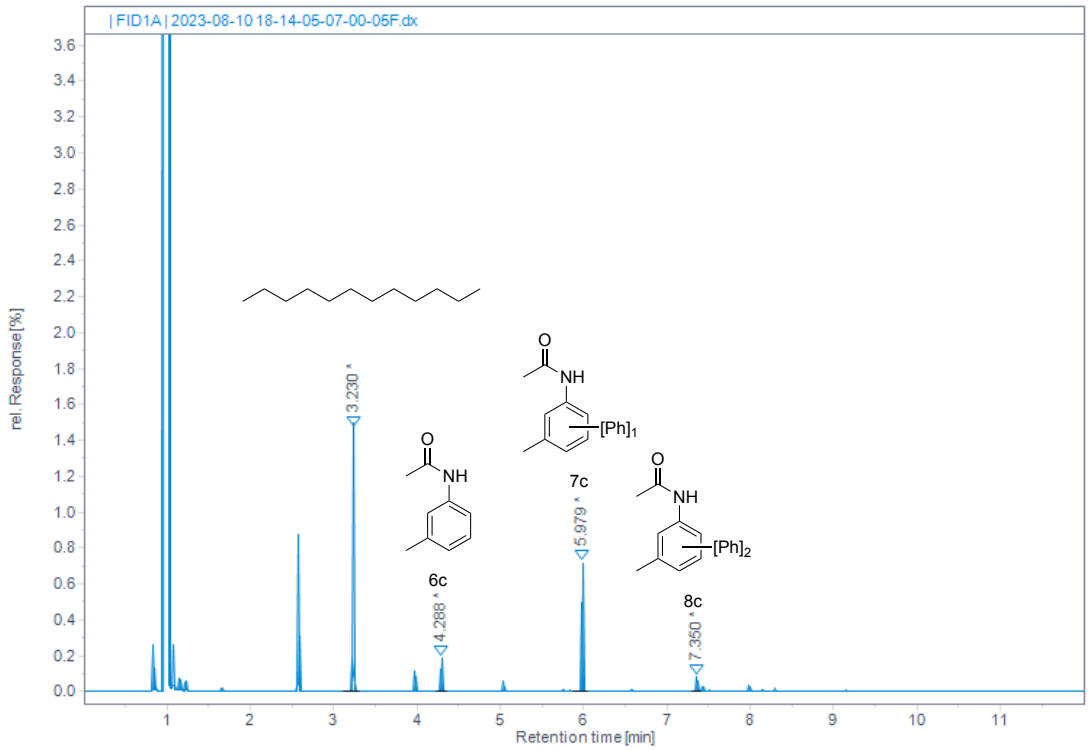

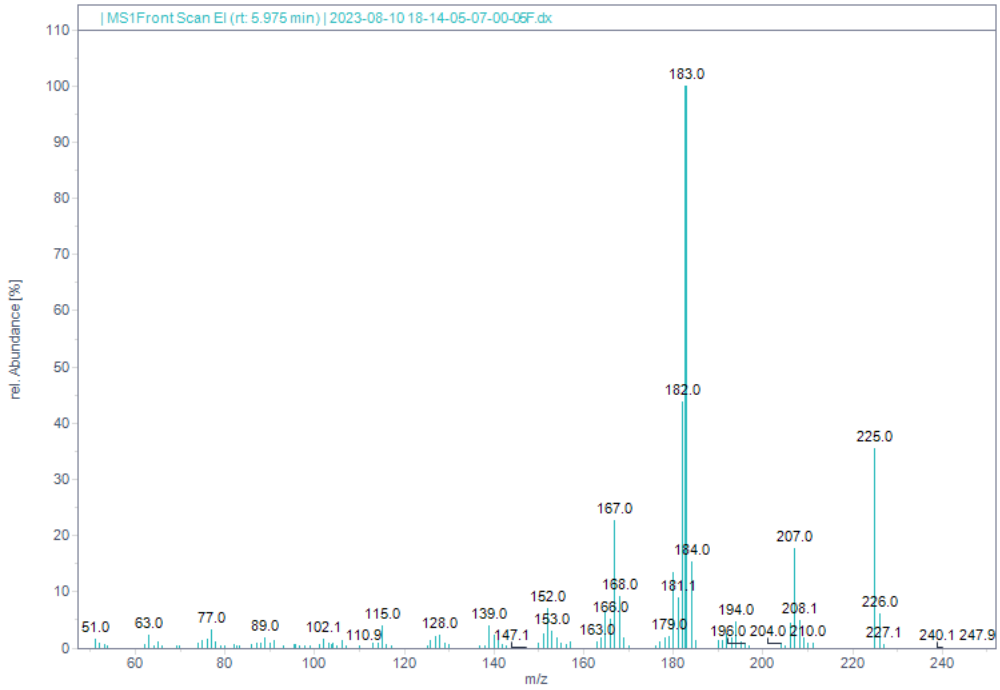

Figure S93. GC-FID trace and peak areas of crude acetanilide arylation reaction mixture (top). Peaks for internal standard (^{n}dodecane), remaining acetanilide **6c**, and mono- and di-arylated product are highlighted. Mass spectrum of peak exhibiting m/z for mono-arylated product (bottom).

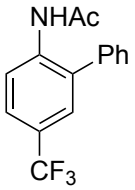

7d. Arylation of 6d with 2a: GP9. Isolated yield on 0.5 mmol of **6d** scale: 16.8%, GC mono-arylation yield: 21.8%; Total Arylation: 30%; GC-MS(EI) **7d** m/z - Calc: 279.1; Exp: 279.1.

RT (min)	Area (pA·s)	Area%
3.220	262.967	57.894
4.061	95.028	20.921
5.485	80.927	17.817
6.819	15.298	3.368

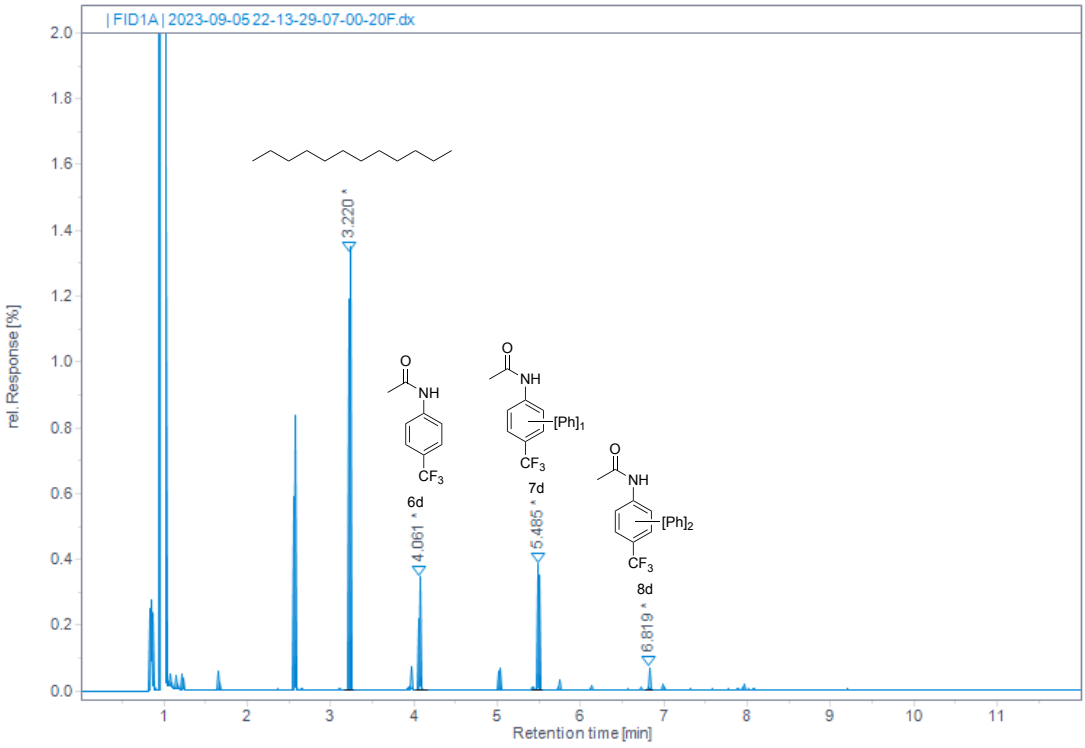

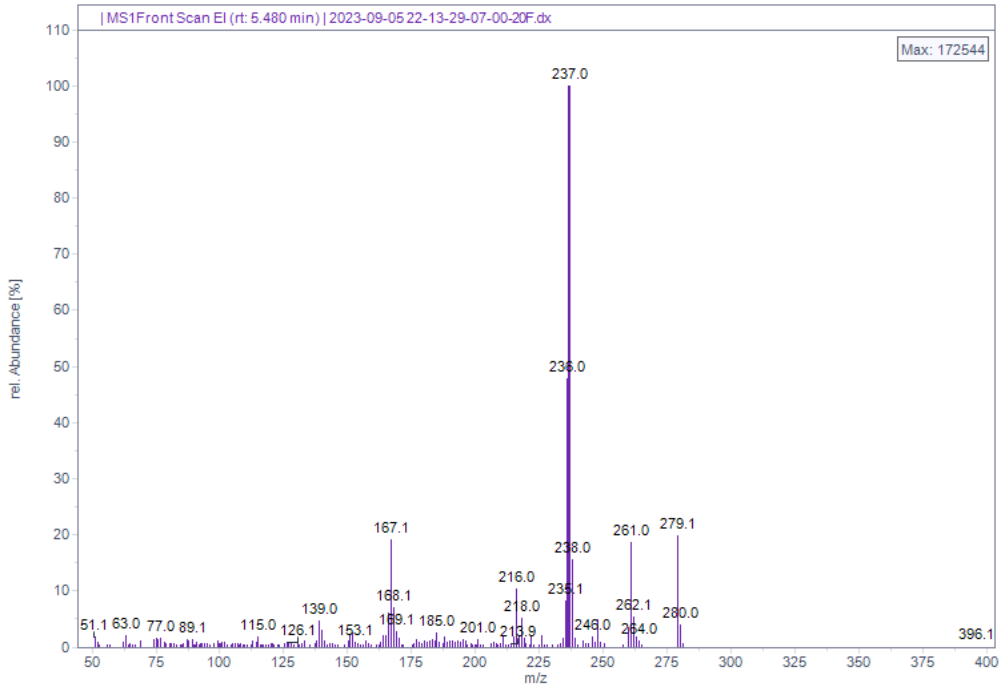

Figure S94. GC-FID trace and peak areas of crude acetanilide arylation reaction mixture (top). Peaks for internal standard (^{n}dodecane), remaining acetanilide **6d**, and mono- and di-arylated product are highlighted. Mass spectrum of peak exhibiting m/z for mono-arylated product (bottom).

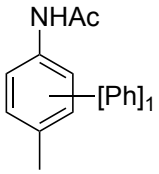

7e. Arylation of 6e with 2a: GP9. Monoarylation: 44.7% Total Arylation: 59%. GC-MS(EI) **7e** m/z - Calc: 225.0; Exp: 225.12.

RT (min)	Area (pA·s)	Area%
3.236	653.052	56.934
4.323	113.915	9.931
6.031	310.653	27.083
7.601	69.412	6.051

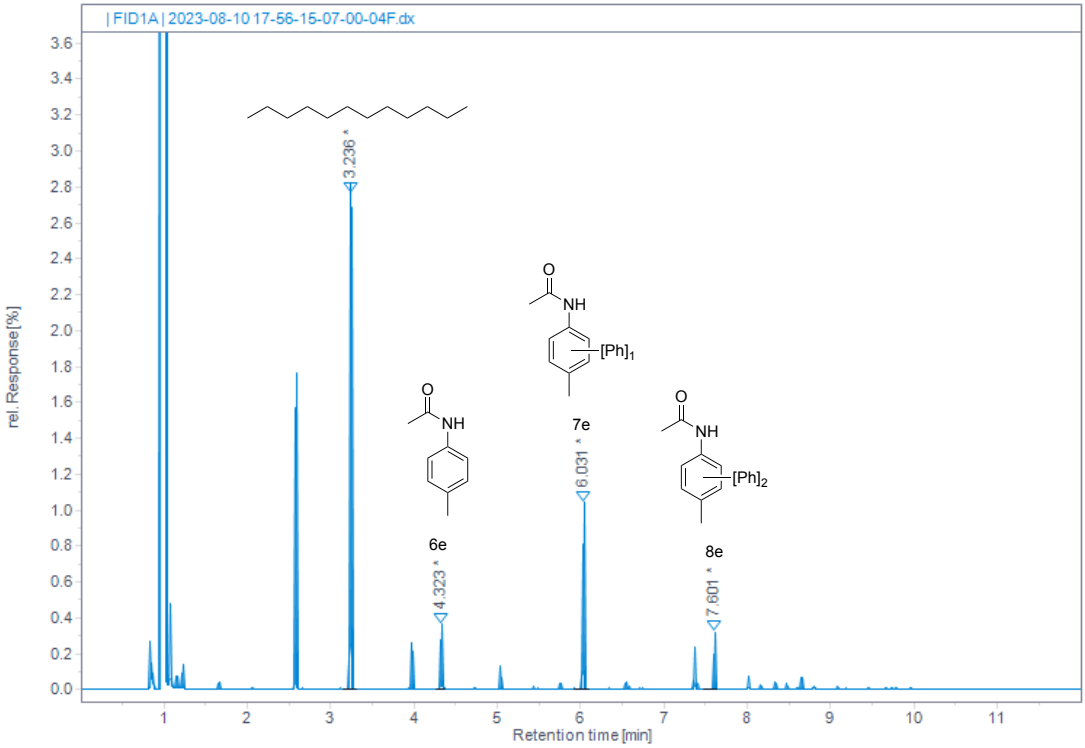

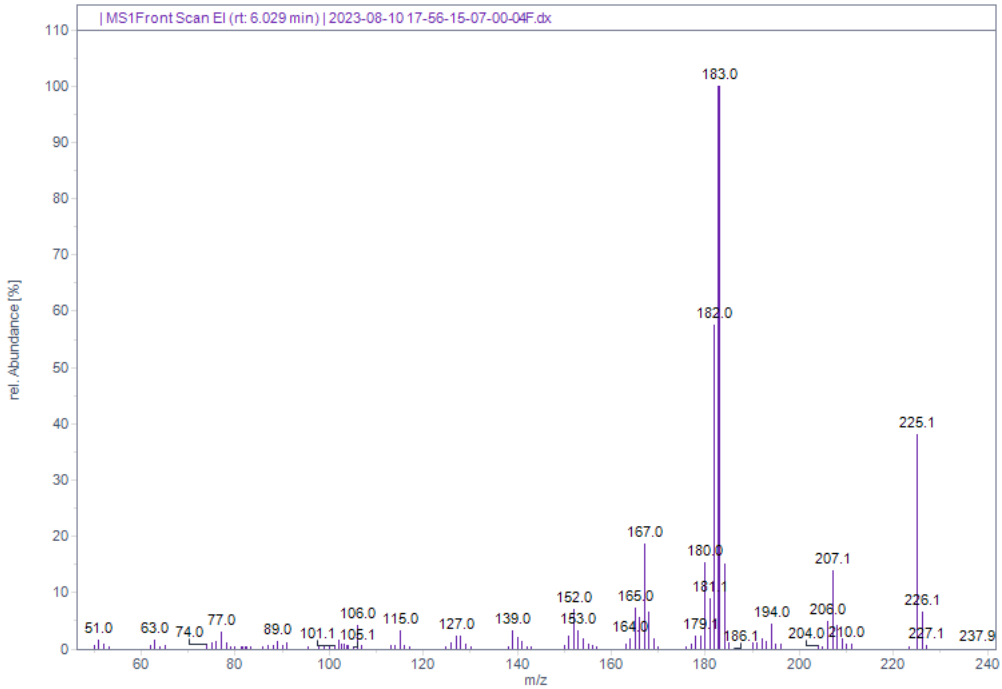

Figure S95. GC-FID trace and peak areas of crude acetanilide arylation reaction mixture (top). Peaks for internal standard (^{n}dodecane), remaining acetanilide **6e**, and mono- and di-arylated product are highlighted. Mass spectrum of peak exhibiting m/z for mono-arylated product (bottom).

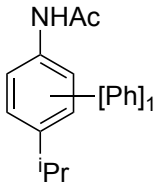

7f. Arylation of 6f with 2a: GP9. Monoarylation: 46.0% Total arylation: 60%. GC-MS(EI) **7f** m/z - Calc: 253.1; Exp: 253.1.

RT (min)	Area (pA·s)	Area%
3.232	539.809	51.657
4.886	143.302	13.713
6.446	304.423	29.132
7.826	57.462	5.499

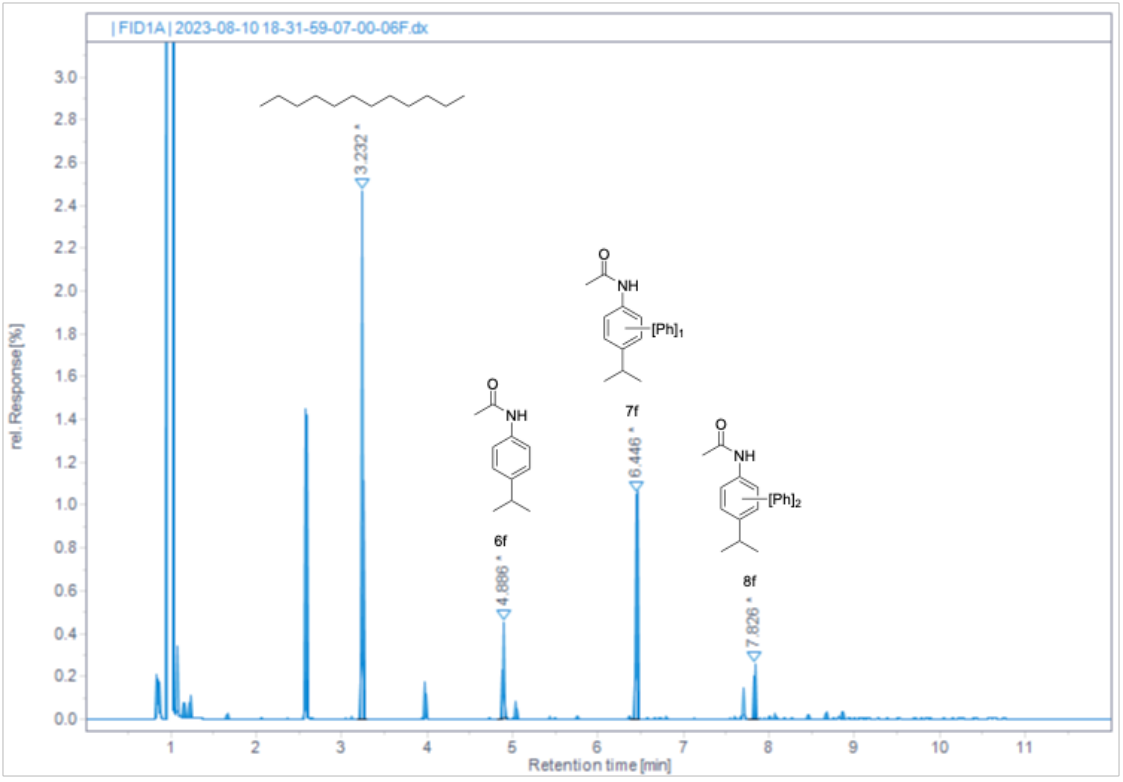

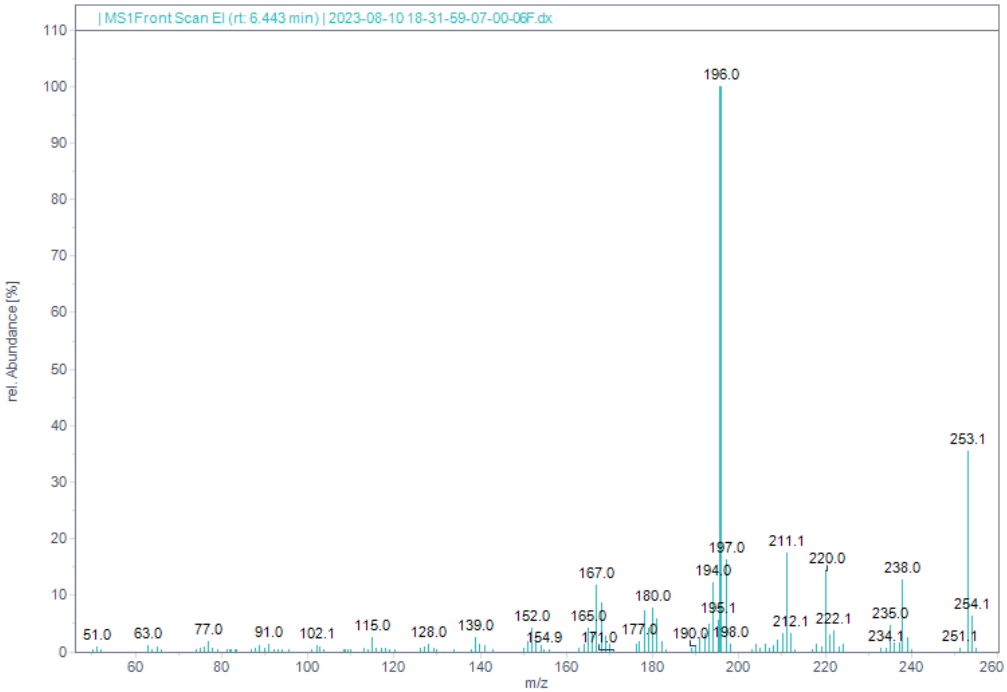

Figure S96. GC-FID trace and peak areas of crude acetanilide arylation reaction mixture (top). Peaks for internal standard (^{n}dodecane), remaining acetanilide **6f**, and mono- and di-arylated product are highlighted. Mass spectrum of peak exhibiting m/z for mono-arylated product (bottom).

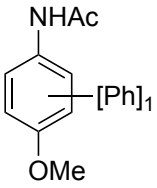

7g. Arylation of 6g with 2a: GP9. Monoarylation: 18.4% Total Arylation: 40%. GC-MS(EI) **7g** m/z - Calc: 241.1; Exp: 241.1.

RT (min)	Area (pA·s)	Area%
3.222	327.348	63.788
4.839	65.723	12.807
6.490	69.054	13.456
7.689	9.499	1.851
7.765	10.764	2.097
7.962	7.451	1.452
8.342	13.757	2.681
8.503	9.586	1.868

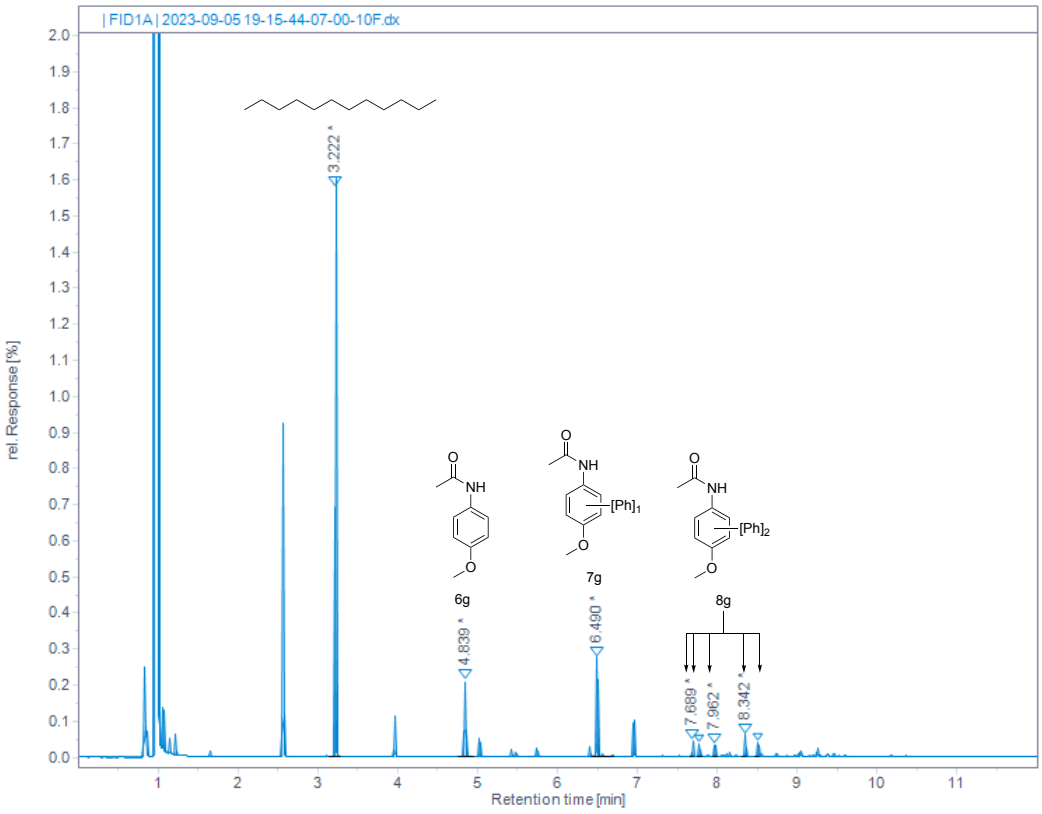

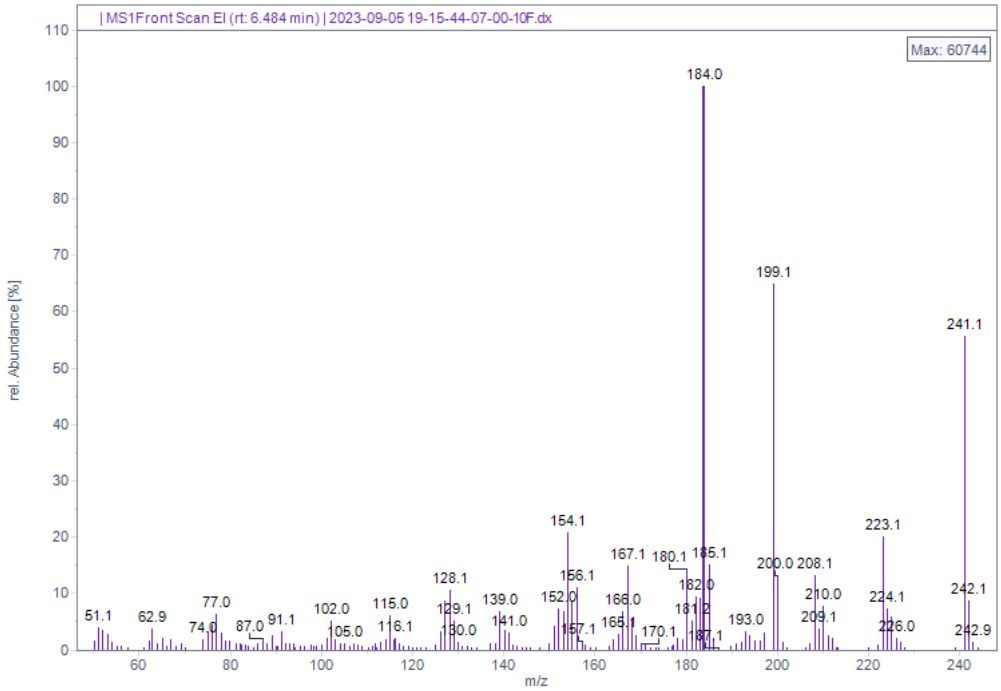

Figure S97. GC-FID trace and peak areas of crude acetanilide arylation reaction mixture (top). Peaks for internal standard (^{n}dodecane), remaining acetanilide **6g**, and mono- and di-arylated product are highlighted. Mass spectrum of peak exhibiting m/z for mono-arylated product (bottom).

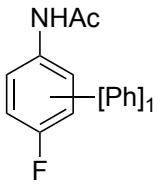

7h. Arylation of 6h with 2a: GP9. Monoarylation: 33.6% Total Arylation: 46%. GC-MS(EI) **7h** m/z - Calc: 229.1; Exp: 229.1.

RT (min)	Area (pA·s)	Area%
3.218	133.513	58.865
3.950	32.180	14.188
5.596	48.642	21.446
7.056	12.479	5.502

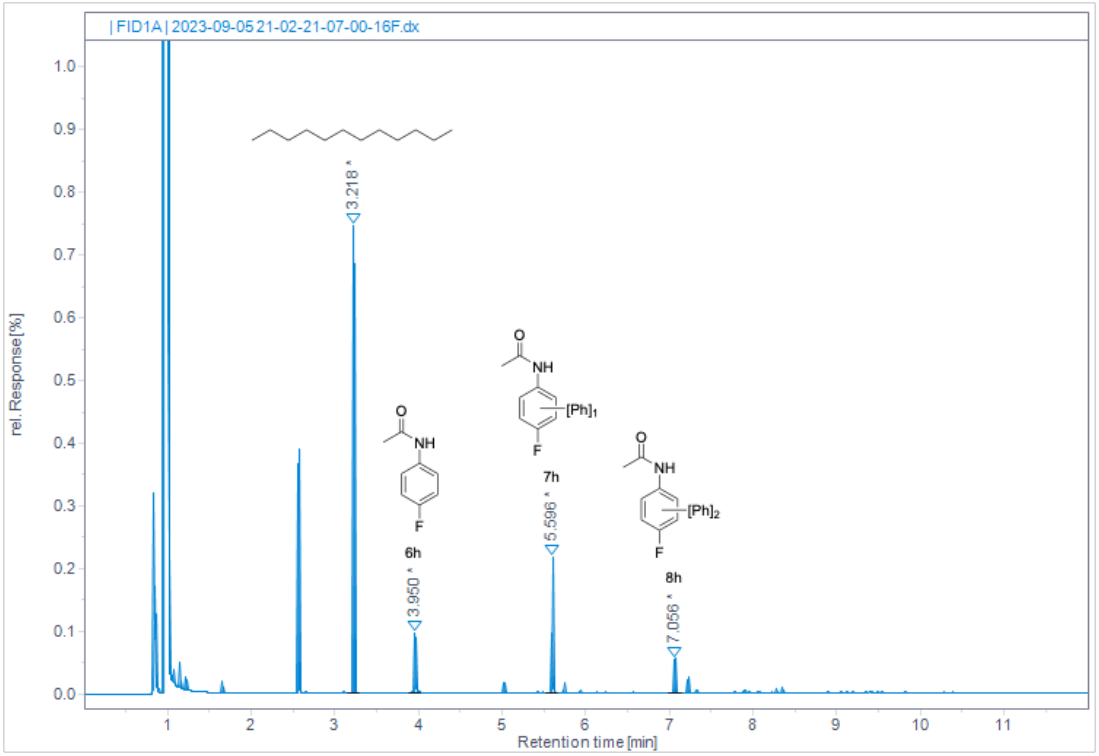

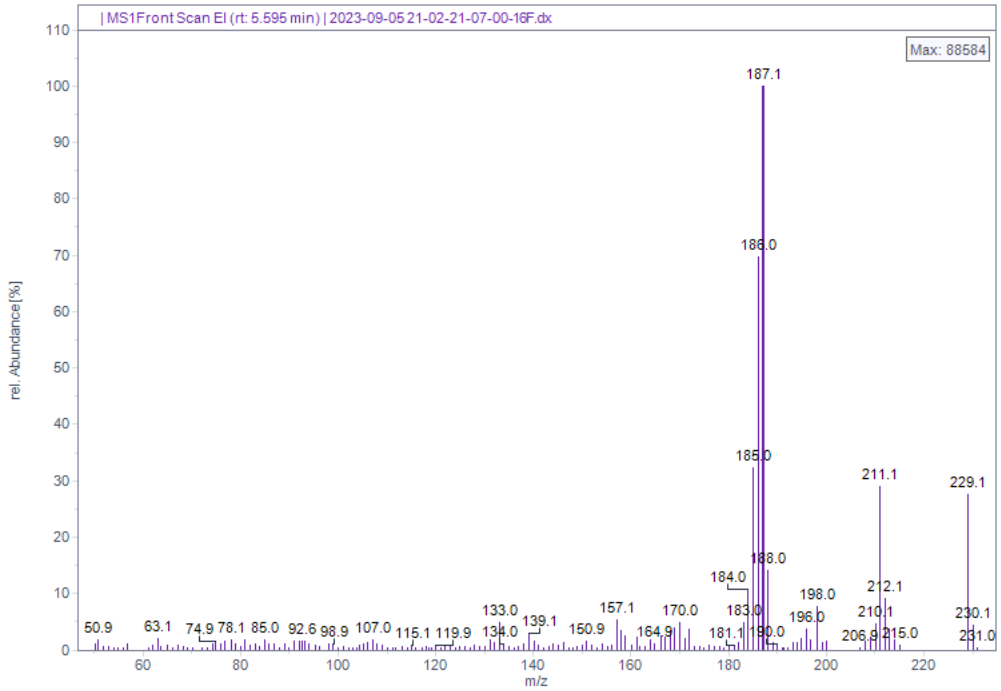

Figure S98. GC-FID trace and peak areas of crude acetanilide arylation reaction mixture (top). Peaks for internal standard (^{n}dodecane), remaining acetanilide **6h**, and mono- and di-arylated product are highlighted. Mass spectrum of peak exhibiting m/z for mono-arylated product (bottom).

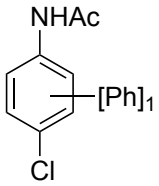

7i. Arylation of 6i with 2a: GP9. Monoarylation: 24.1% Total Arylation: 40%. GC-MS(EI) **7i** m/z - Calc: 245.0; Exp: 245.0.

RT (min)	Area (pA·s)	Area%
3.219	207.998	61.312
4.675	48.629	14.334
6.277	59.015	17.396
7.597	23.606	6.958

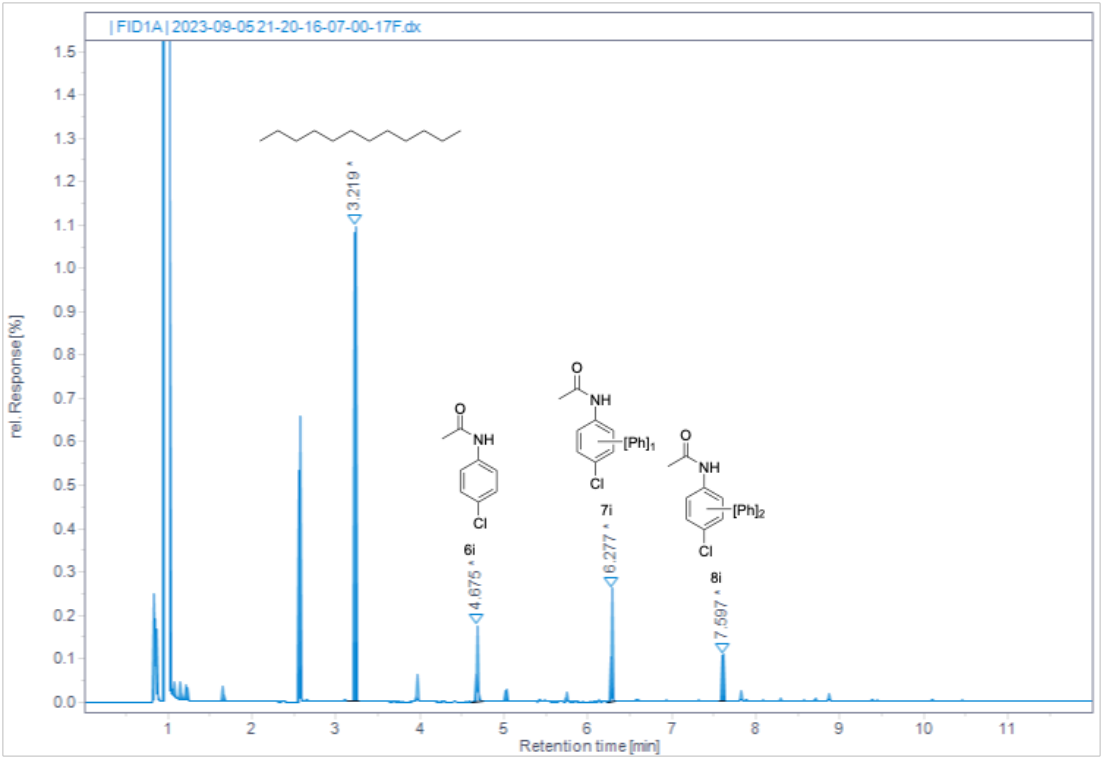

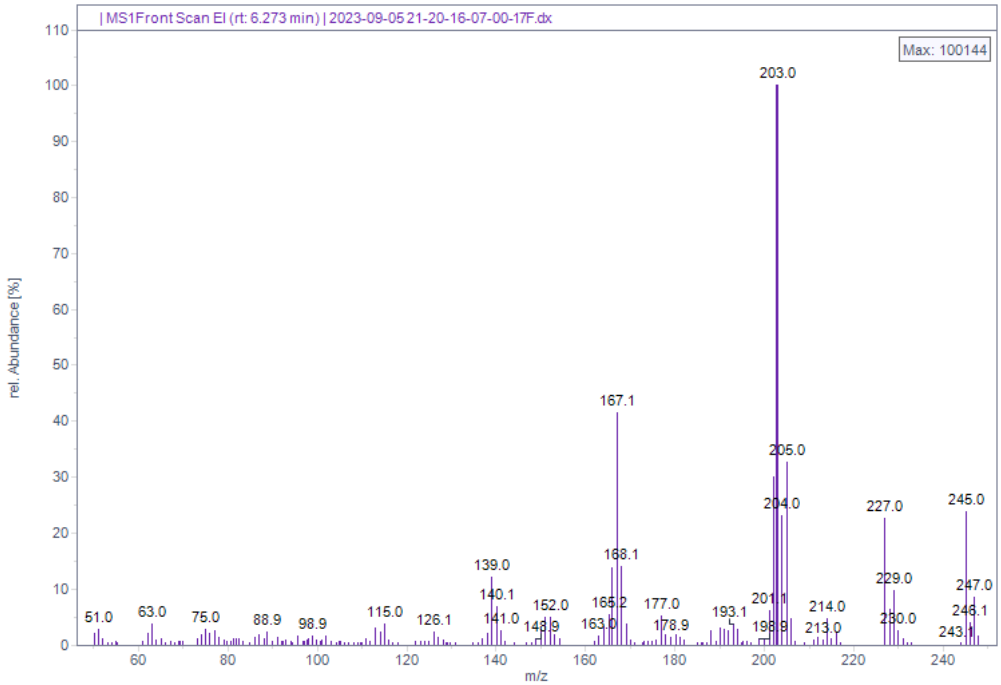

Figure S99. GC-FID trace and peak areas of crude acetanilide arylation reaction mixture (top). Peaks for internal standard (^{n}dodecane), remaining acetanilide **6i**, and mono- and di-arylated product are highlighted. Mass spectrum of peak exhibiting m/z for mono-arylated product (bottom).

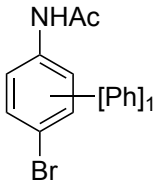

7j. Arylation of 6j with 2a: GP9. Monoarylation: 20.4% Total Arylation: 31%. GC-MS(EI) **7j** m/z - Calc: 289.0; Exp: 289.0.

RT (min)	Area (pA·s)	Area%
3.221	301.391	66.245
5.017	104.999	23.079
6.672	35.125	7.720
7.980	13.449	2.956

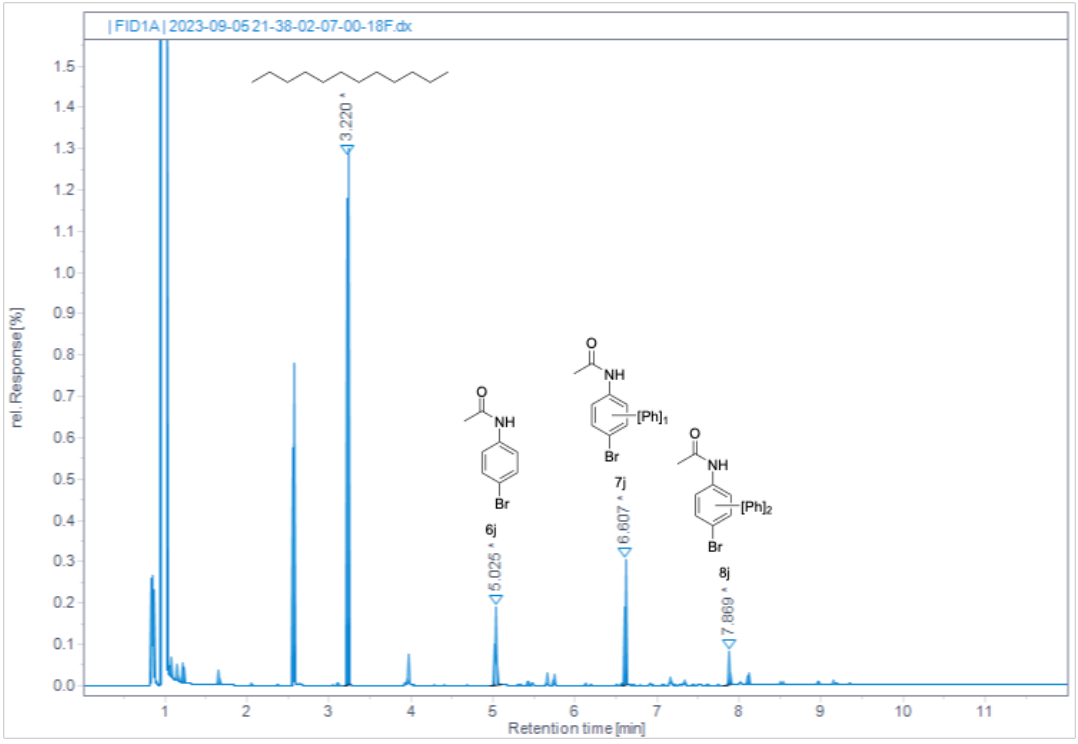

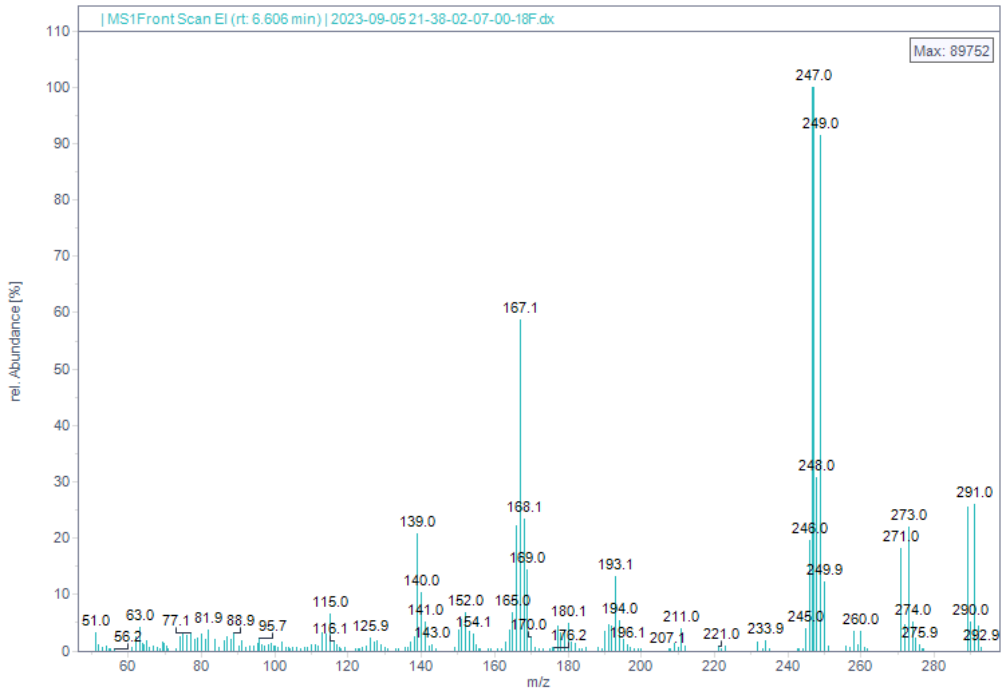

Figure S100. GC-FID trace and peak areas of crude acetanilide arylation reaction mixture (top). Peaks for internal standard (^{n}dodecane), remaining acetanilide **6j**, and mono- and di-arylated product are highlighted. Mass spectrum of peak exhibiting m/z for mono-arylated product (bottom).

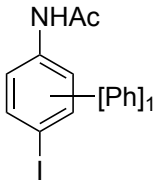

7k. Arylation of 6k with 2a: GP9. Monoarylation: 5.3% Total Arylation: 5.3%. GC-MS(EI) **7k** m/z - Calc: 336.9; Exp: 337.0.

RT (min)	Area (pA·s)	Area%
3.220	235.263	85.437
5.415	26.370	9.576
7.054	13.733	4.987

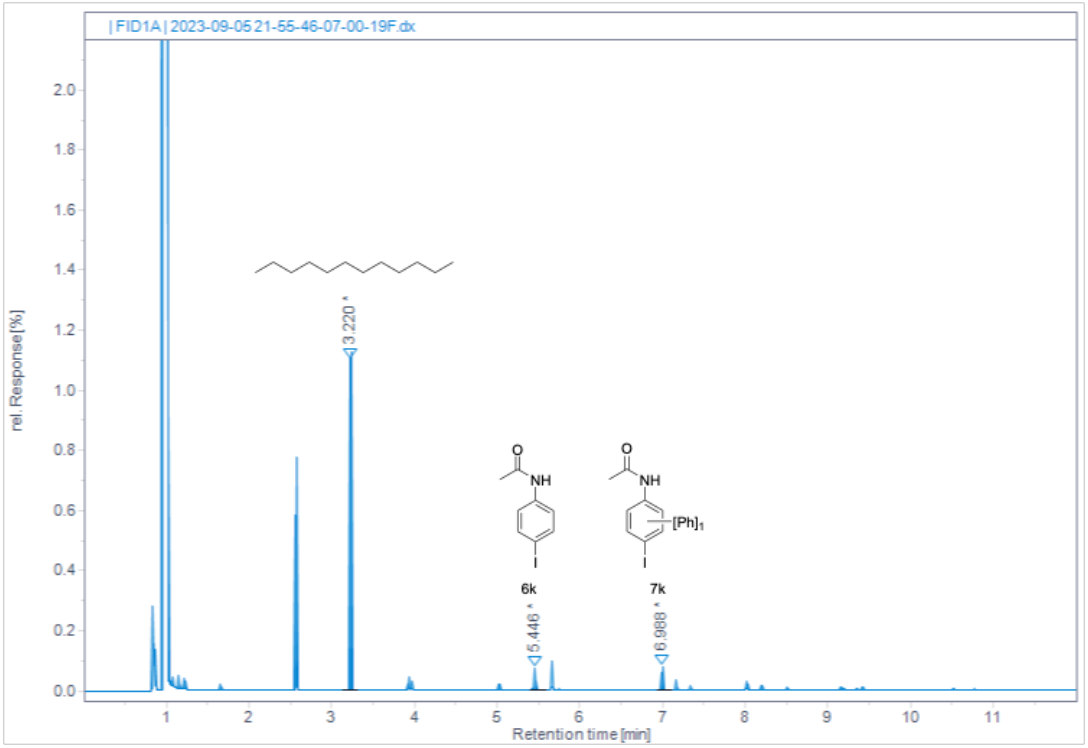

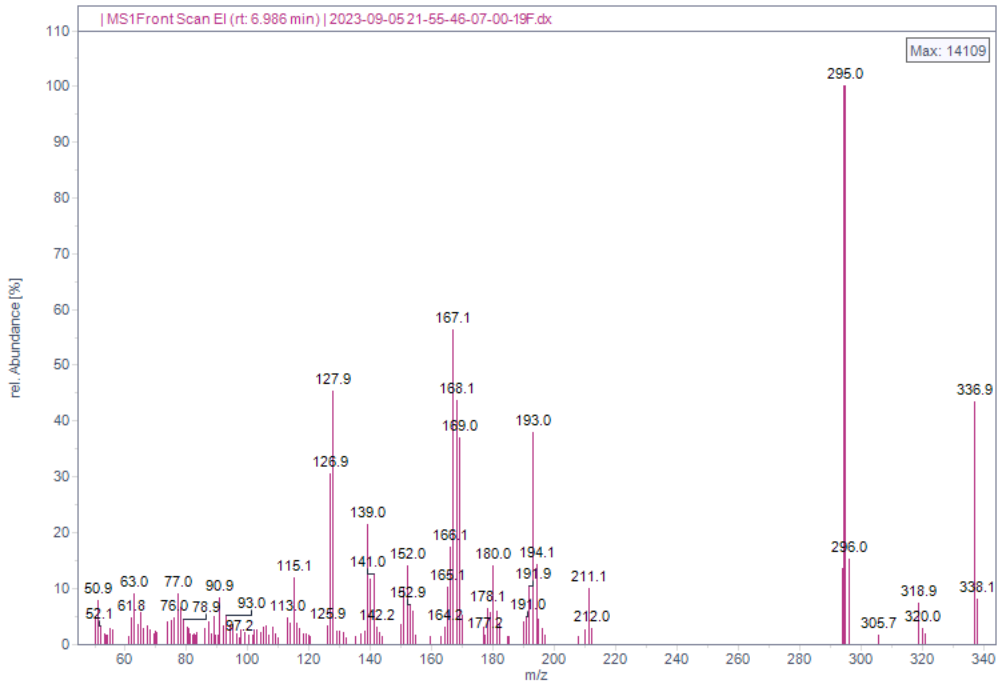

Figure S101. GC-FID trace and peak areas of crude acetanilide arylation reaction mixture (top). Peaks for internal standard (^{n}dodecane), remaining acetanilide **6k**, and mono- and di-arylated product are highlighted. Mass spectrum of peak exhibiting m/z for mono-arylated product (bottom).

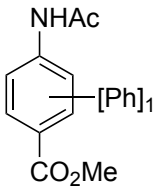

7l. Arylation of 6l with 2a: GP9. Monoarylation: 12.6% Total Arylation: 22%. GC-MS(EI) **7l** m/z - Calc: 269.1; Exp: 269.1.

RT (min)	Area (pA·s)	Area%
3.221	284.433	61.715
5.587	110.742	24.028
7.066	46.672	10.127
8.221	19.036	4.130

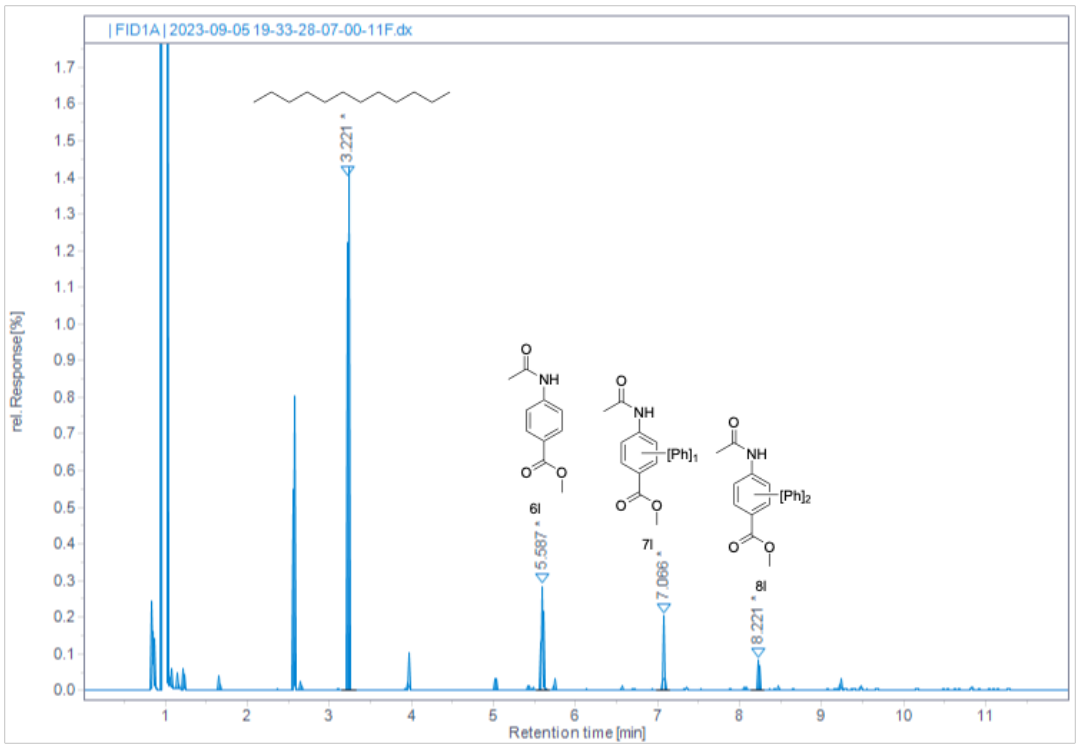

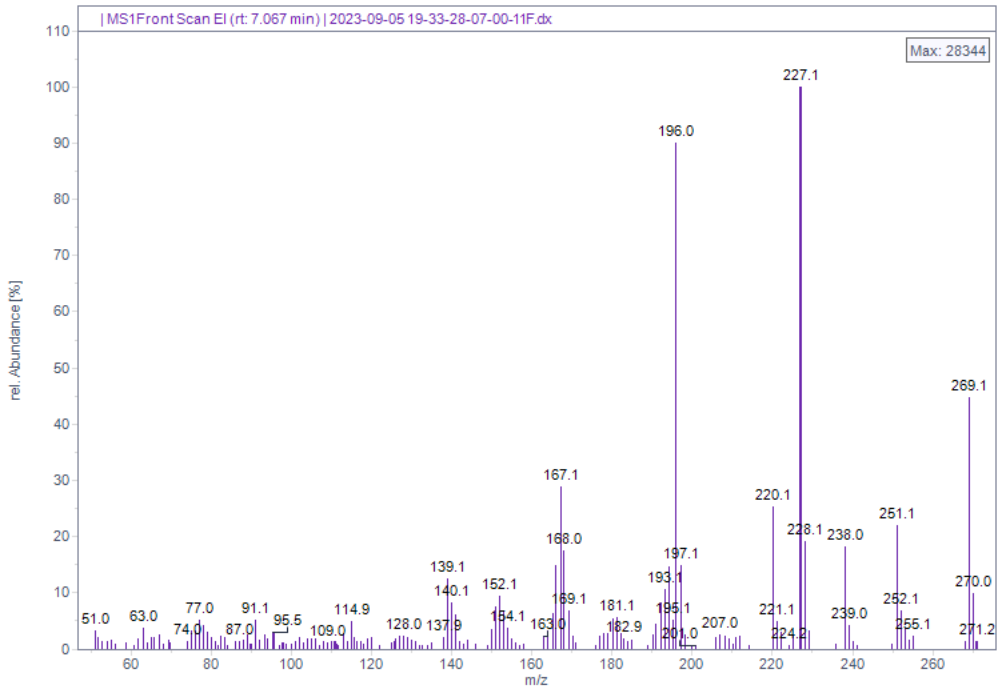

Figure S102. GC-FID trace and peak areas of crude acetanilide arylation reaction mixture (top). Peaks for internal standard (^{n}dodecane), remaining acetanilide **6l**, and mono- and di-arylated product are highlighted. Mass spectrum of peak exhibiting m/z for mono-arylated product (bottom).

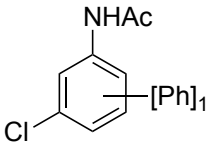

7m. Arylation of 6m with 2a: GP9. Monoarylation: 33.9%. Total Arylation: 49%. GC-MS(EI) **7m** m/z - Calc: 245.0; Exp: 245.0.

RT (min)	Area (pA·s)	Area%
3.221	254.527	59.832
4.666	40.987	9.635
6.347	101.569	23.876
7.701	28.318	6.657

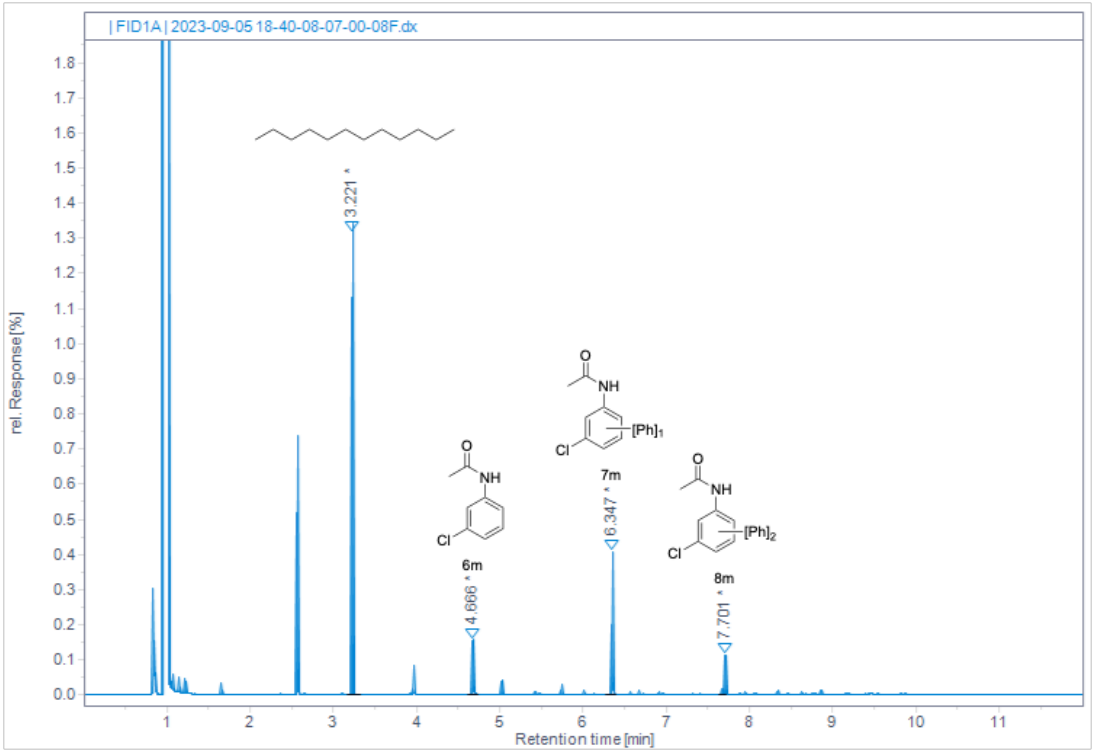

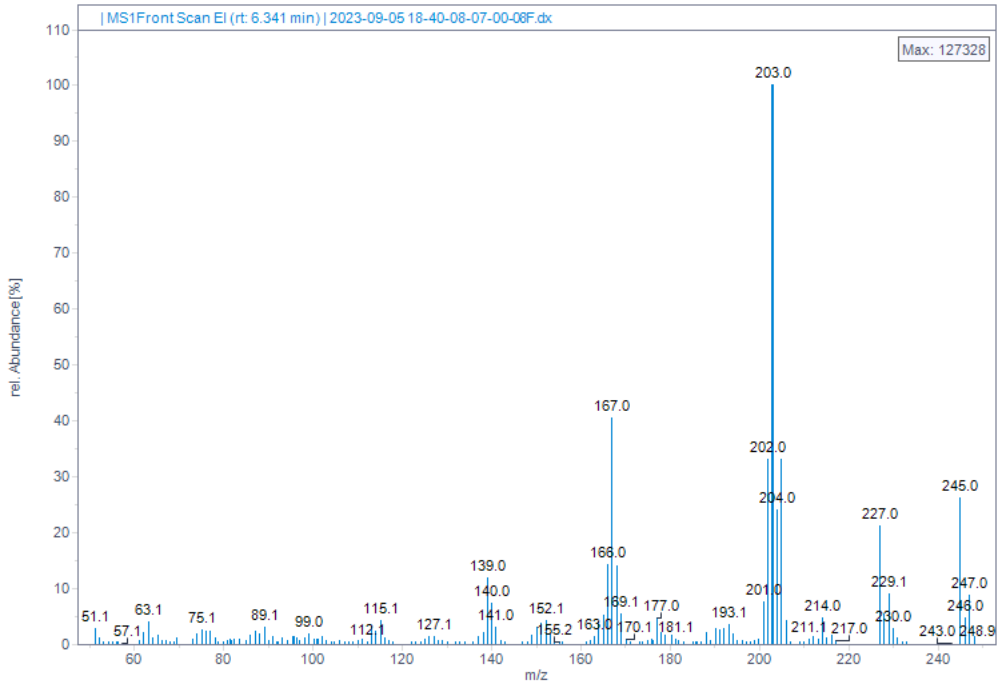

Figure S103. GC-FID trace and peak areas of crude acetanilide arylation reaction mixture (top). Peaks for internal standard (^{n}dodecane), remaining acetanilide **6m**, and mono- and di-arylated product are highlighted. Mass spectrum of peak exhibiting m/z for mono-arylated product (bottom).

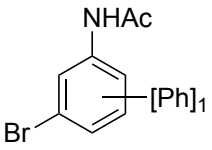

7n. Arylation of 6n with 2a: GP9. Monoarylation: 8.4% Total Arylation: 14%. GC-MS(EI) **7n** m/z - Calc: 289.0; Exp: 289.0.

RT (min)	Area (pA·s)	Area%
3.221	301.391	66.245
5.017	104.999	23.079
6.672	35.125	7.720
7.980	13.449	2.956

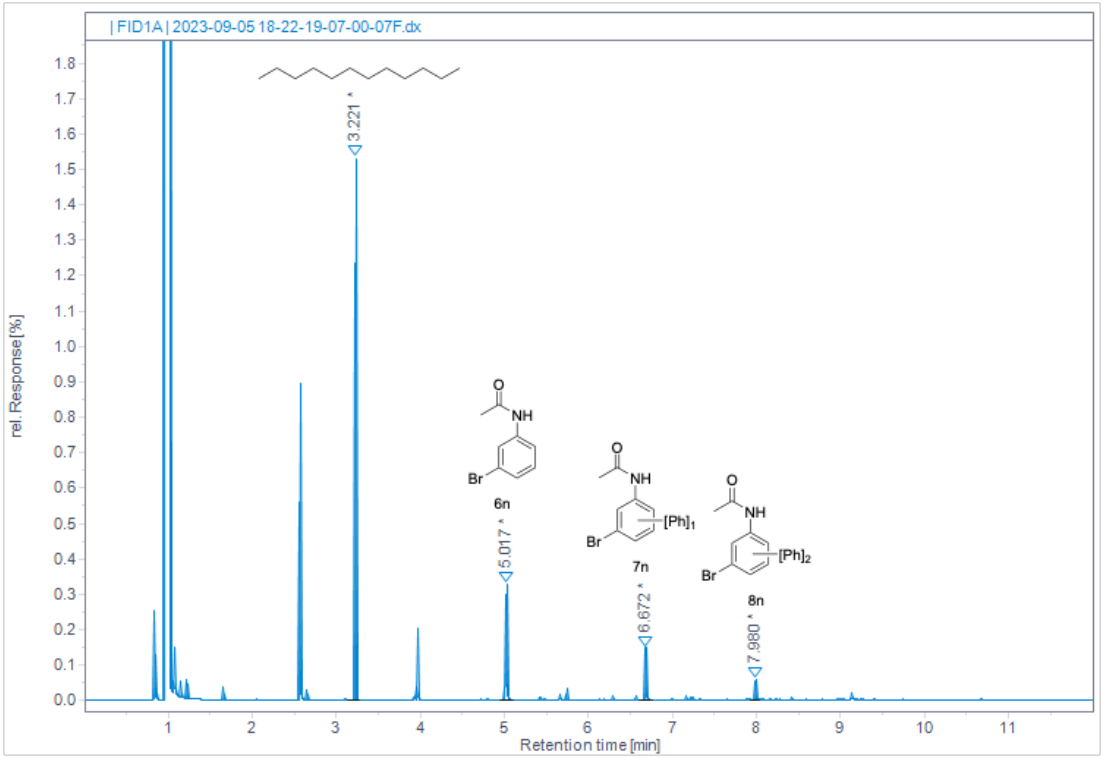

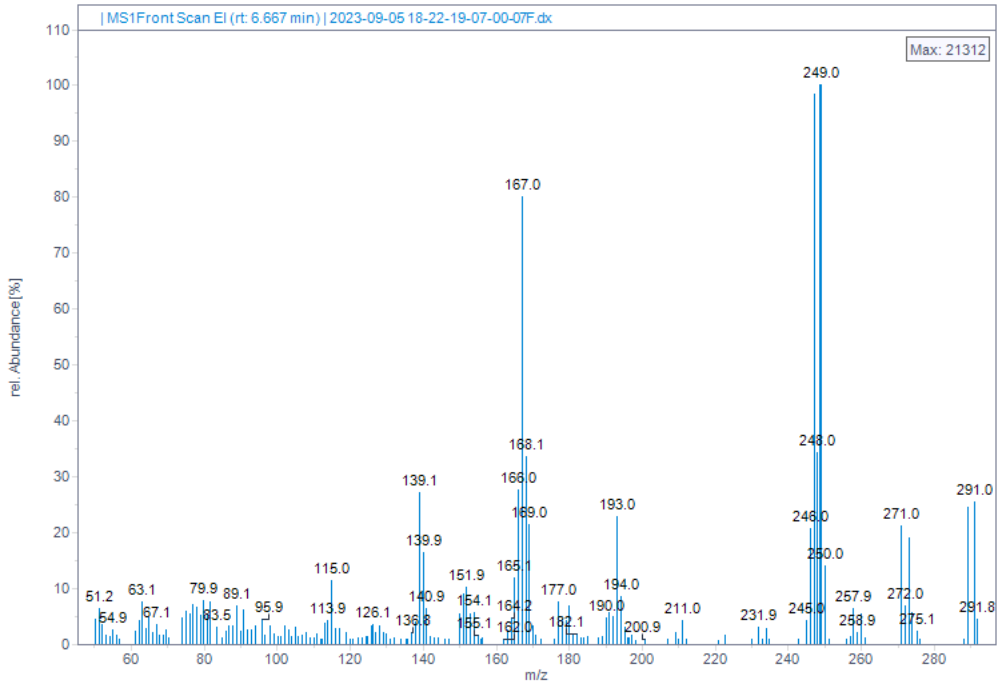

Figure S104. GC-FID trace and peak areas of crude acetanilide arylation reaction mixture (top). Peaks for internal standard (^{n}dodecane), remaining acetanilide **6n**, and mono- and di-arylated product are highlighted. Mass spectrum of peak exhibiting m/z for mono-arylated product (bottom).

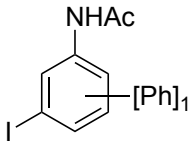

7o. Arylation of 6o with 2a: GP9. Monoarylation: 4.9% Total Arylation: 9% GC-MS(EI) **7o** m/z - Calc: 337.0; Exp: 337.0.

RT (min)	Area (pA·s)	Area%
3.220	235.263	85.437
5.415	26.370	9.576
7.054	13.733	4.987

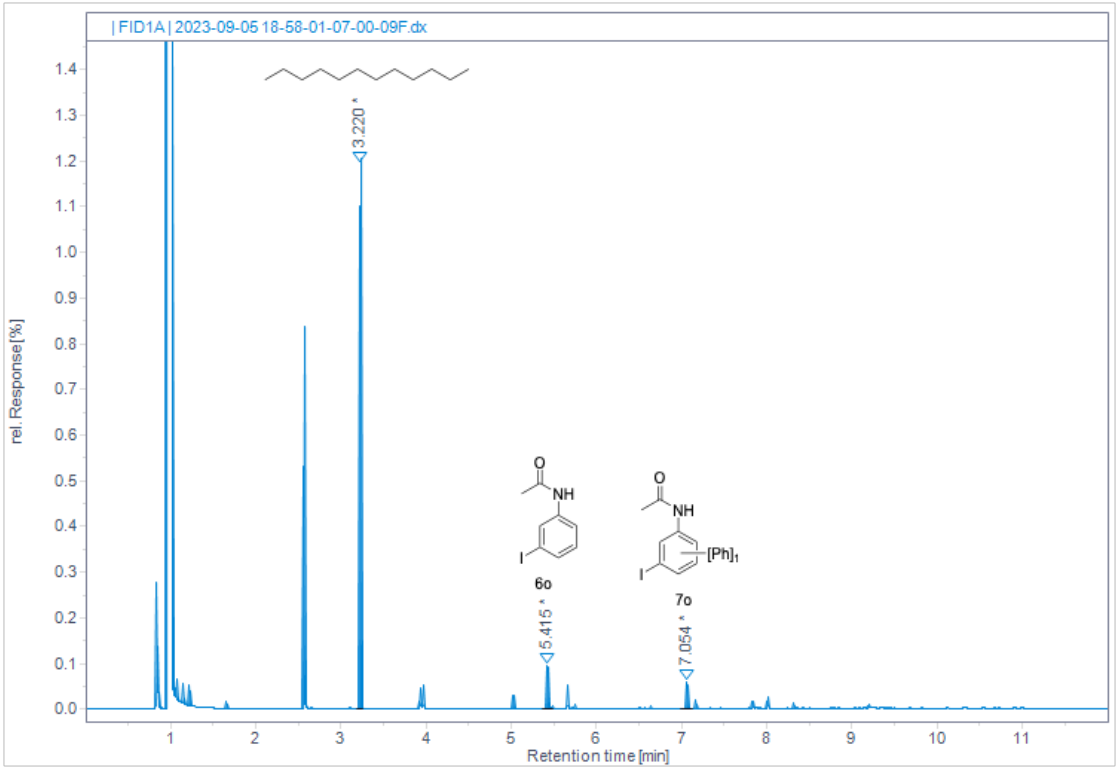

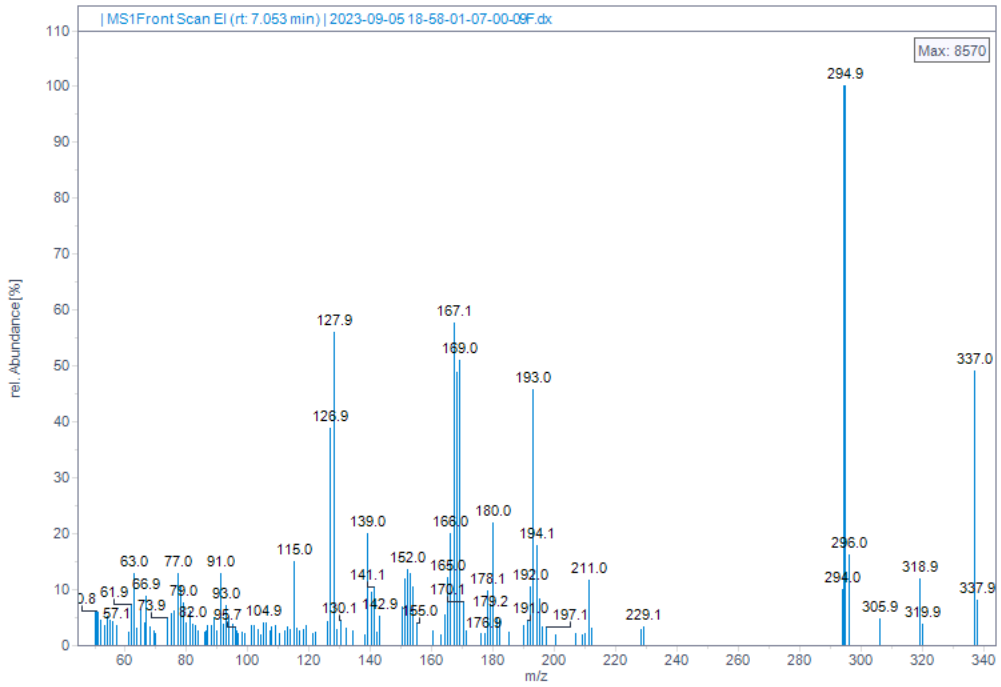

Figure S105. GC-FID trace and peak areas of crude acetanilide arylation reaction mixture (top). Peaks for internal standard (^{n}dodecane), remaining acetanilide **6o**, and mono- and di-arylated product are highlighted. Mass spectrum of peak exhibiting m/z for mono-arylated product (bottom).

N. Proposed mechanism for Pd-catalyzed C–H arylation

Based on all the results provided herein, we propose the following mechanism. Coordination of $\mathbf{L_5}$ to $Pd(OAc)_2$ results in $(\mathbf{L_5})PdX$, which undergoes rapid C-H palladation to give $\mathbf{Pd_a}$. Simultaneously, **1** (more likely product **4** once formed) engages with **2a** to furnish aryl radicals when irradiated by visible light. Herein we propose an energy transfer process. The aryl radical and PhI• react with $\mathbf{Pd_a}$ to give $\mathbf{Pd_c}$ that is primed for reductive elimination of products **4** and $(\mathbf{L_5})$PdOTf. Dissociation of products **4** is a slow process, which enables di-arylation products **5** to form if not forced to dissociate. This is achieved by competitive competition by $\mathbf{L_{34}}$, which creates an off-cycle equilibrium with $(\mathbf{L_5})$PdOTf to close the cycle.

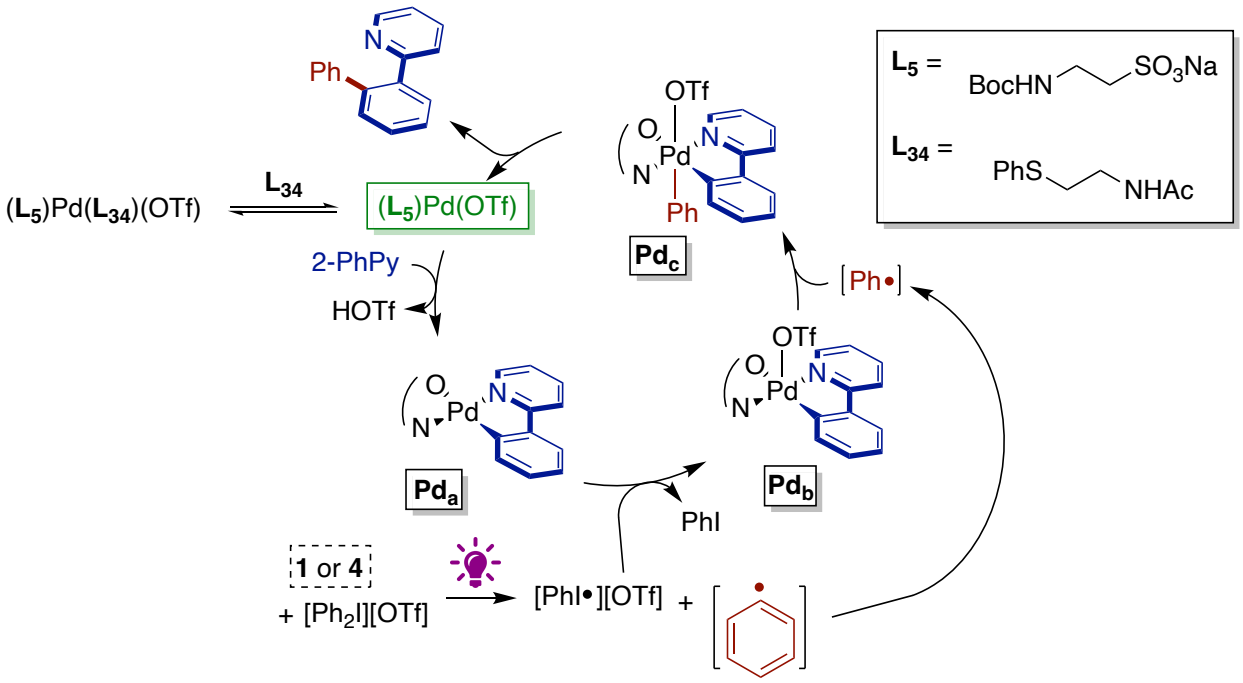

Figure S106. Proposed mechanism incorporating PC-free aryl radical generation and electrophilic palladation of C–H bonds.

O. Computational Study

General. All calculations were carried out using the Gaussian 16 rev. B01 program suite.[28] Geometry optimizations were performed with the M06-2x functional.[29] The def2-TZVP basis set with ECP was used for I[30] and the 6-31+G(d) basis set was used for all other atoms.[31] Frequency calculations at the same level of theory were performed to identify the number of imaginary frequencies (zero for local minima) and to provide the thermal corrections for Gibbs free energy determinations.[32] Single point energy calculations were performed at the def2-TZVP level of theory for all atoms. The relative Gibbs free energies (at 298.15 K) are given in kcal/mol. Optimized structures are illustrated using CYLView.[33]

Correlating adduct stability and halogen bonding to radical generation rate. To date in the literature, association between activator molecules and Ar_2I salts results in strongly colored EDA complexes or detectable halogen bonds by VT NMR studies. Since combinations of LBs in our study do not result in either case, we turned to computational chemistry to determine whether observed radical generations can be attributed to presence of and/or strength of potential halogen bonding interactions. To assess this, we identified minima for 6 LB derivatives, Ph_2I, and adducts for combinations of these components. From these, we extracted the data in Table S15.

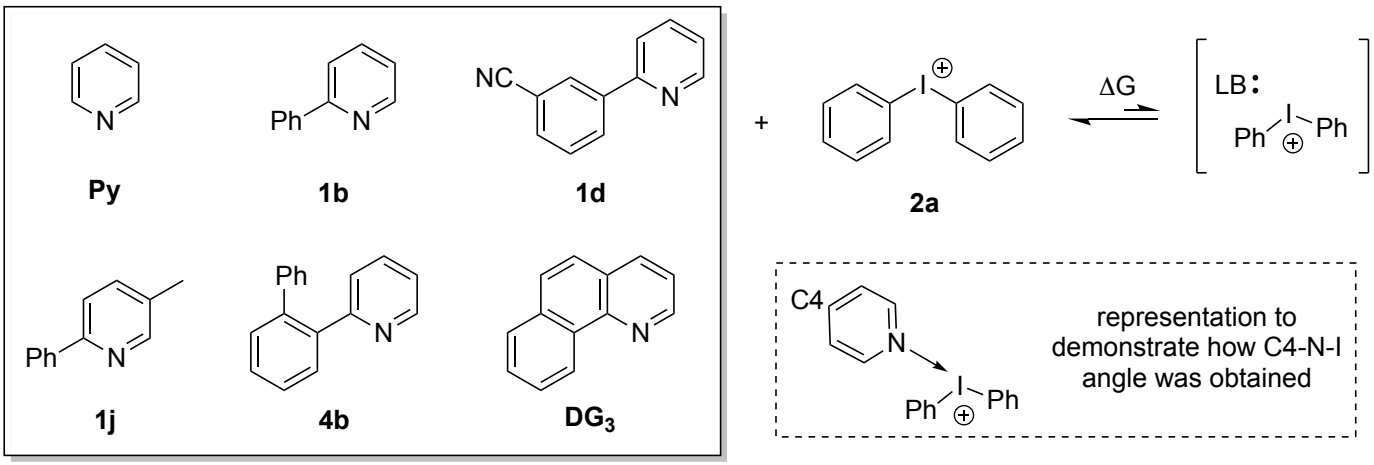

Adduct	Angle (C4-N-I)	k_{rel}	ΔG	K_{eq} (x10^{-3})
Py_2a	173.2	1.0	3.12	5.1
1b_2a	155.5	3.7	2.13	27.6
1d_2a	155.3	6.5	1.04	171.6
1j_2a	155.0	16	-1.24	8186.8
4b_2a	171.0	49	1.72	54.9
DG_4_2a	123.5	97	3.08	5.5

Table S15. Computational determined parameters for pyridine-derivative iodonium salt adduct formation, including notation of experimentally derived k_{rel} values for ease of reference.

After locating the minima for each adduct, we first examined whether a halogen bonding interaction was present. Halogen bonds characteristically show a nearly linear bond angle between the halogen bond donor (I) and halogen bond acceptor (N).[34] The lengths of halogen bonding interactions are variable with ranges up to 3 Å. All N-I distances in our computed structures near this value, so we classified halogen bond strength by how far the directionality of the nitrogen lone pair deviated from 180°. To do this and simplify visualization, the C4-N-I angle was extracted for each adduct and plotted against our experimentally derived k_{rel} (Figure S107). If halogen bond is the sole component enabling photoactivity, C4-N-I angles closer to 180° would give higher reaction rates than C4-N-I angles further from 180°. Instead, no direct link between orientation of N lone pair and reactivity for photolytic radical generation. In fact, the two best activators (**4b** and **DG_4**) are on either end of the spectrum. While **4b** displays a nearly textbook halogen bonding orientation (171° C4-N-I angle), the lone pair of **DG_4** is nearly 60° deviated from linearity, limiting any halogen bonding interactions. N.B. Two different energetic minima were identified for the combination of **DG_4+2a** of which, the depicted interaction was lower in energy. From this preliminary computational analysis, the requirement of a halogen bonding interaction to enable photoactivity in our system is not supported.

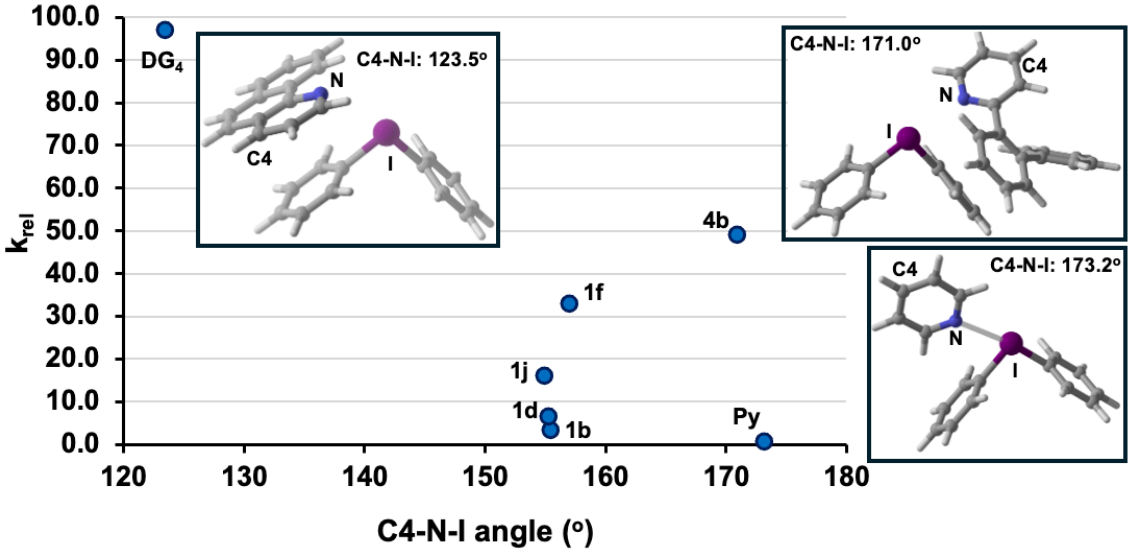

Figure S107. Plot of experimental k_{rel} versus computed C4-N-I angle to assess importance of halogen bonding interaction.

Having looked at the criticality of a discrete halogen bonding interaction for photoactivity, we next turned our attention to the interplay between energetics of adduct formation and rate of radical generation (Figure S108). In PC-free reactivity where EDA complexes are key intermediates, increased favorability of association should necessarily lead to increased reactivity. By this line, less favorable energetics of association should then lead to diminished reactivity. In our case, there is no single extractable trend. On one hand, experimental k_{rel} values <20 generally show that less positive ΔG for **1d** (ΔG = 1.04 kcal/mol) manifested in k_{rel} = 6.5 whereas the most positive ΔG for **Py** (ΔG = 3.12 kcal/mol) resulted in k_{rel} = 1. On the other hand, our best activators do not adhere to this trend. Instead, the least favorable adduct between **2a** and **DG₄** (ΔG = 3.08 kcal/mol) is twice as reactive (k_{rel} = 97) as the doubly favorable adduct between **2a** and **4b** (ΔG = 1.72 kcal/mol, k_{rel} = 49).

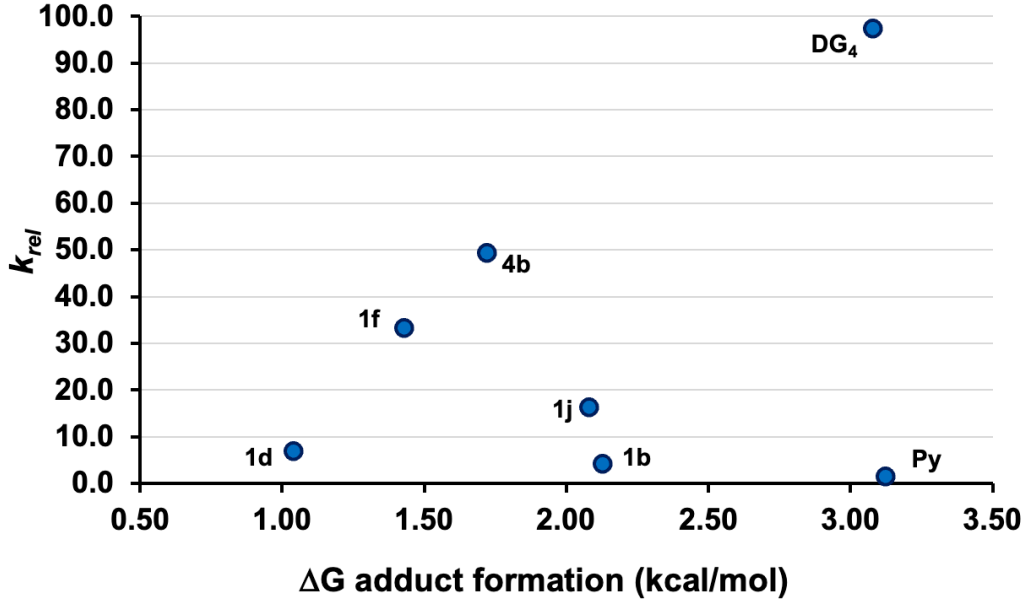

Figure S108. Plot of experimental k_{rel} versus computed ΔG of LB/**2a** adduct formation to assess link between association favorability and reactivity.

Considering the differences in halogen bond capability and adduct stabilities between these two activators, there appears to be another physical property that leads to the heightened activator capabilities of **4b** and **DG₄**. Because the adduct arising from **2a** and **DG₄** is so different from anything else reported in the literature for such

reactivity, we elected to compute the UV-Vis spectrum for this adduct to see whether a new absorption band arises (Figure S109). Computations predict a different absorption band for the adduct; however, the wavelength at which it appears is in the far UV region. While this could be due to the level at which the spectra were predicted (M06-2X/6-31G(d)//def2-TZVP with ECP for I), it could simply not appear near enough to the LED output wavelength to be relevant. That being said, the difference between the predicted band (and its associated tailing) and the reaction irradiation wavelength (390 nm) is similar in magnitude to a recent report on the same topic.[35] From this prediction, it is possible that this adduct is photoactive, but deeper investigations are needed to gather conclusive evidence on the matter.

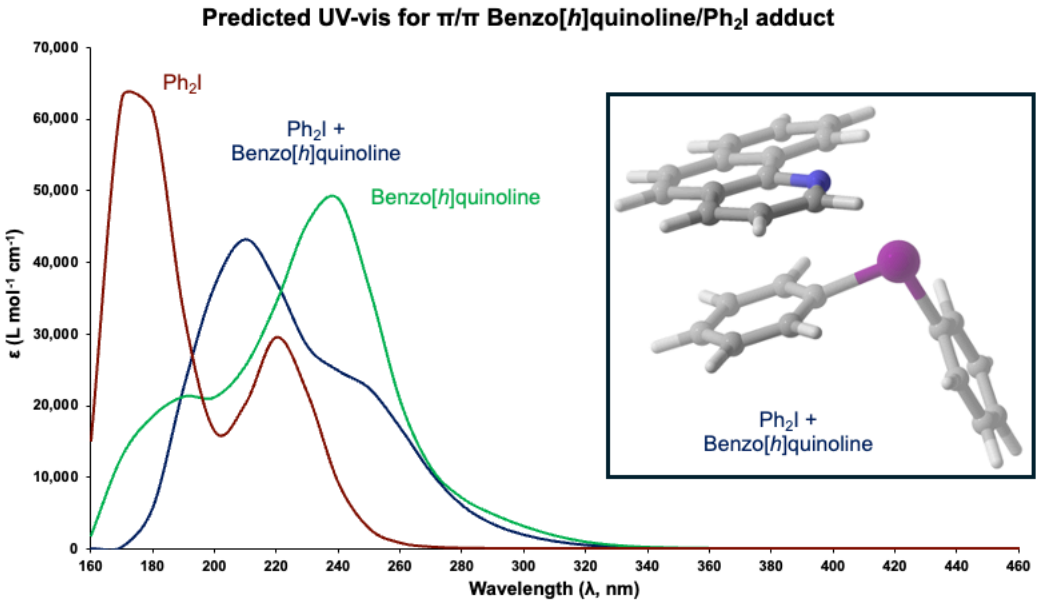

Figure S109. Computed UV-Vis spectra for **2a** (red), **DG$_4$** (green), and the adduct arising from **2a**+**DG$_4$** (blue).

P. Cartesian Coordinates

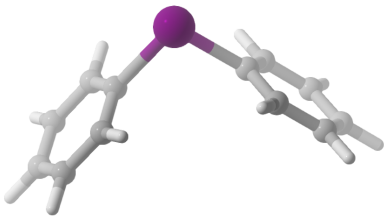

Ph_2I^+
E_{tot} = -760.6519719 a.u.
G_{corr} = 0.141853 a.u.

C	-1.5588020	0.3858930	0.2328710
C	-0.9997500	-0.1018050	1.4099520
H	-1.3927230	0.1742920	2.3823290
C	0.0899920	-0.9651700	1.2974400
H	0.5479460	-1.3620980	2.1973160
C	0.5852230	-1.3133950	0.0406290
H	1.4340640	-1.9850890	-0.0356250
C	0.0006030	-0.8040240	-1.1194150
H	0.3895300	-1.0758140	-2.0951160
C	-1.0886440	0.0627310	-1.0363850
H	-1.5482880	0.4653330	-1.9324380
I	-3.2084880	1.6722930	0.3829840
C	-4.7275680	0.2365360	0.2103770
C	-5.1510990	-0.4165010	1.3639190
H	-4.7217400	-0.1922780	2.3343040
C	-6.1526020	-1.3776140	1.2302330
H	-6.5033500	-1.9048410	2.1112190
C	-6.6992070	-1.6554110	-0.0231610
H	-7.4798920	-2.4034560	-0.1152320
C	-6.2529620	-0.9786310	-1.1584710
H	-6.6812340	-1.1962860	-2.1312290
C	-5.2509670	-0.0138840	-1.0542410
H	-4.8965520	0.5171290	-1.9309400

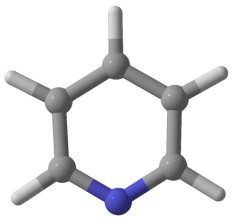

pyridine
E_{tot} = -248.2707062 a.u.

G_{corr} = 0.062439 a.u.

N	-3.1952280	4.3202710	0.9934850
C	-3.0545570	4.7920520	-0.2507630
H	-3.9723220	4.9251170	-0.8186620
C	-1.8223120	5.1064500	-0.8219480
H	-1.7729320	5.4859060	-1.8371520
C	-0.6712940	4.9212280	-0.0601110
H	0.3074710	5.1542760	-0.4686880
C	-0.8020380	4.4308150	1.2367880
C	-2.0809260	4.1473030	1.7138560
H	0.0641650	4.2693630	1.8697880
H	-2.2176570	3.7631600	2.7219460

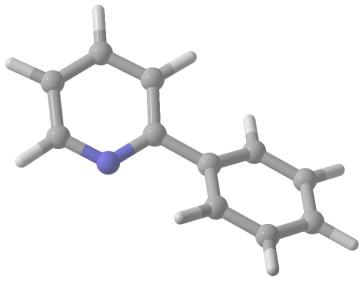

2-phenylpyridine
E_{tot} = -479.3174571 a.u.
G_{corr} = 0.136889 a.u.

N	-3.1326710	3.9955680	0.9047330
C	-2.9768290	4.4647220	-0.3353040
H	-3.8336640	4.3561960	-0.9963540
C	-1.8039700	5.0600890	-0.7957710
H	-1.7348970	5.4200460	-1.8165940
C	-0.7410680	5.1809920	0.0952250
H	0.1892040	5.6506240	-0.2099890
C	-0.8919820	4.7008460	1.3914390
C	-2.1039790	4.1022820	1.7611180
C	-2.3152410	3.5684030	3.1343680
C	-1.2436760	3.0896870	3.8990980
C	-3.6042890	3.5365890	3.6822110
C	-3.8146980	3.0501390	4.9701420
C	-2.7405130	2.5797210	5.7273660
C	-1.4550860	2.5980920	5.1861770
H	-4.4367560	3.9037440	3.0902050
H	-4.8184940	3.0404440	5.3849070
H	-2.9048330	2.1982510	6.7307910
H	-0.6150250	2.2221280	5.7626800
H	-0.0888580	4.8079850	2.1128250
H	-0.2401540	3.0764040	3.4830980

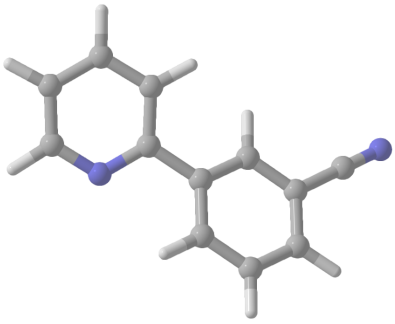

2-(3-cyano)phenylpyridine
E_{tot} = -571.5711222 a.u.
G_{corr} = 0.132807 a.u.

N	-3.1279790	3.9778590	0.8936650
C	-2.9698360	4.4313410	-0.3515100
H	-3.8183070	4.2980900	-1.0183390
C	-1.8027060	5.0413110	-0.8086480
H	-1.7307840	5.3881510	-1.8337710
C	-0.7501400	5.1945920	0.0886880
H	0.1740040	5.6766990	-0.2151070
C	-0.9032570	4.7295300	1.3907070
C	-2.1077710	4.1157010	1.7538880
C	-2.3278520	3.5946120	3.1313970
C	-1.2602910	3.1466580	3.9117070
C	-3.6240400	3.5410260	3.6615500
C	-3.8526160	3.0642550	4.9498410
C	-2.7911160	2.6223330	5.7339120
C	-1.4967240	2.6646440	5.2036650
H	-4.4523690	3.8845240	3.0505920
H	-4.8622420	3.0385820	5.3465730
C	-0.3880740	2.1958710	5.9948220
H	-0.1082680	4.8617530	2.1169230
H	-0.2470550	3.1442790	3.5224600
H	-2.9560570	2.2471610	6.7384180
N	0.5027310	1.8189580	6.6319510

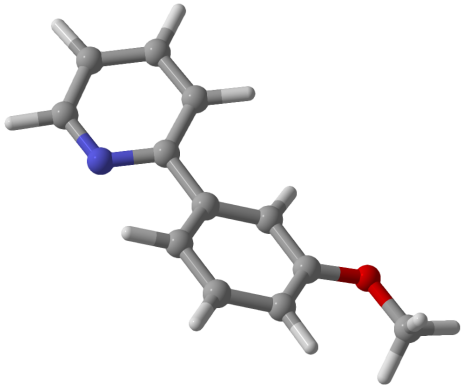

2-(3-methoxy)phenylpyridine
E_{tot} = -593.8449717 a.u.
G_{corr} = 0.166547 a.u.

N	-3.1190530	3.9717900	0.9313880
C	-2.9554000	4.4590040	-0.3007810
H	-3.8051970	4.3528440	-0.9711960
C	-1.7832840	5.0702230	-0.7417490
H	-1.7079600	5.4454450	-1.7566450
C	-0.7294570	5.1871280	0.1604220
H	0.1996690	5.6685510	-0.1295430
C	-0.8880270	4.6869010	1.4481060
C	-2.0985670	4.0740750	1.7977070
C	-2.3197800	3.5192060	3.1620780
C	-1.2514980	3.0362810	3.9159770
C	-3.6154300	3.4788090	3.7008370
C	-3.8149500	2.9709520	4.9776630
C	-2.7480060	2.4875950	5.7416440
C	-1.4611270	2.5206780	5.2004520
H	-4.4477970	3.8529970	3.1149300
H	-4.8158300	2.9480250	5.3989160
O	-0.3490630	2.0689140	5.8409970
H	-0.0925660	4.7889760	2.1785820
H	-0.2396160	3.0224810	3.5215360
H	-2.9327320	2.0938420	6.7342560
C	-0.5116260	1.5263550	7.1421630
H	0.4831700	1.2252690	7.4676700
H	-1.1722120	0.6528080	7.1224630
H	-0.9125190	2.2765700	7.8322970

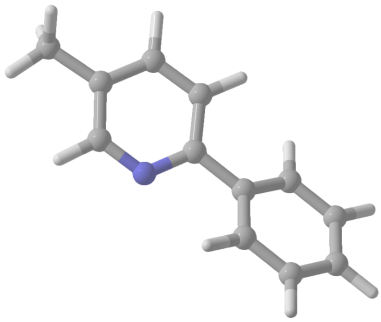

2-phenyl-5-methylpyridine
E_{tot} = -518.6286467 a.u.
G_{corr} = 0.161249 a.u.

N	-3.1368000	3.9740490	0.9779150
C	-2.9791420	4.4442190	-0.2617710
H	-3.8390010	4.3382420	-0.9220380
C	-1.8108040	5.0403030	-0.7415540
C	-1.7056050	5.5438110	-2.1553750
C	-0.7528490	5.1488640	0.1645150
H	0.1801050	5.6169680	-0.1413600
C	-0.8989750	4.6691490	1.4591240
C	-2.1112170	4.0738340	1.8354360
C	-2.3226490	3.5406530	3.2089890
C	-1.2511670	3.0659210	3.9765780
C	-3.6122180	3.5052300	3.7558760
C	-3.8231850	3.0189200	5.0438550
C	-2.7488600	2.5528920	5.8036060
C	-1.4628110	2.5752870	5.2640710
H	-4.4450790	3.8692760	3.1624420
H	-4.8277380	3.0062690	5.4568180
H	-2.9133860	2.1720440	6.8072490
H	-0.6221910	2.2031400	5.8423200
H	-0.0907220	4.7746270	2.1752160
H	-0.2468410	3.0554350	3.5624380
H	-2.6339770	5.3690550	-2.7053680
H	-0.8929280	5.0418120	-2.6902040
H	-1.4960020	6.6181880	-2.1732170

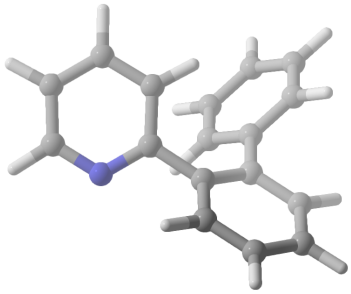

2-(2-phenyl)phenylpyridine
E_{tot} = -710.3583988 a.u.
G_{corr} = 0.211743 a.u.

N	-2.8633540	3.8014530	0.7914240
C	-2.7443310	4.3835600	-0.4068860
H	-3.4180240	4.0219440	-1.1802250
C	-1.8275350	5.3931530	-0.6870180
H	-1.7764110	5.8273600	-1.6797640
C	-0.9941130	5.8261680	0.3425890
H	-0.2724600	6.6204260	0.1764490
C	-1.1048870	5.2270710	1.5911180
C	-2.0490020	4.2083740	1.7758690
C	-2.2350770	3.5630010	3.1088500
C	-1.1584710	3.0932530	3.8876660
C	-3.5384940	3.4712000	3.6128040
C	-3.7872170	2.9535390	4.8803680
C	-2.7213140	2.5137020	5.6649830
C	-1.4238200	2.5806070	5.1652990
H	-4.3585710	3.8325010	2.9987780
H	-4.8047960	2.9003570	5.2555700
H	-2.8994070	2.1077930	6.6563440
H	-0.5956660	2.2043940	5.7604830
H	-0.4753170	5.5399960	2.4183460
C	0.2458760	3.0720270	3.3910010
C	0.5629860	2.4952710	2.1536470
H	-0.2300340	2.0701200	1.5427790

C	1.8812260	2.4568350	1.7057490
H	2.1109770	2.0019510	0.7465360
C	2.9041670	2.9966850	2.4879370
H	3.9315180	2.9694600	2.1369930
C	2.5998580	3.5672470	3.7235550
H	3.3890420	3.9903920	4.3382350
C	1.2797400	3.6008210	4.1727840
H	1.0449030	4.0570280	5.1314480

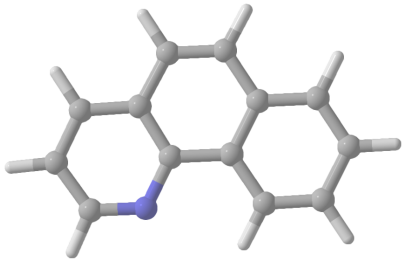

Benzo[*h*]quinoline
E_{tot} = -555.5498623 a.u.
G_{corr} = 0.149824 a.u.

C	-1.9659850	4.4613990	1.6891670
H	-1.0108480	4.6200710	2.1780010
H	-1.3734500	2.5858070	0.7809950
N	-3.3056640	3.0463160	0.2719040
C	-4.3294820	3.9242920	0.3907210
C	-5.5761920	3.6323510	-0.2993910
C	-4.2236210	5.1076530	1.1600010
C	-5.3420150	6.0071990	1.2528890
C	-3.0010640	5.3607110	1.8163540
H	-2.8913420	6.2622800	2.4139860
C	-2.1736620	3.3132290	0.8999060
C	-6.5051020	5.7354240	0.6090830
C	-6.6553420	4.5424640	-0.1838770
C	-7.8688220	4.2619300	-0.8531160
C	-5.7369150	2.4669680	-1.0793190
C	-6.9314260	2.2133400	-1.7242450
C	-8.0070400	3.1173780	-1.6111520
H	-5.2325140	6.9085560	1.8503820
H	-7.3487900	6.4170060	0.6806480
H	-8.6931750	4.9646490	-0.7604230
H	-4.9044570	1.7765320	-1.1613210
H	-7.0441210	1.3134620	-2.3215870
H	-8.9433520	2.9114220	-2.1211960

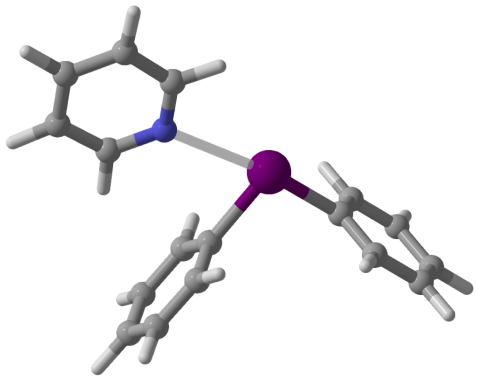

pyridine_Ph_2I^+
E_{tot} = -1008.9369526 a.u.
G_{corr} = 0.223544 a.u.

C	-2.3381880	0.8909540	0.7475370
C	-2.1696710	0.5807390	2.0926620
H	-2.9950450	0.6364240	2.7944830
C	-0.8962390	0.1995650	2.5176540
H	-0.7360620	-0.0466340	3.5621640
C	0.1610210	0.1441460	1.6092650
H	1.1488850	-0.1482540	1.9501060
C	-0.0416120	0.4640720	0.2661910
H	0.7825430	0.4210660	-0.4382510
C	-1.3059790	0.8450480	-0.1836270
H	-1.4709180	1.1043900	-1.2240390
I	-4.2287820	1.5082130	0.0985900
C	-5.0617520	-0.4199200	0.0114270
C	-5.8507500	-0.8569850	1.0731850
H	-6.0415670	-0.2204880	1.9310350
C	-6.3926060	-2.1411650	1.0099960
H	-7.0104900	-2.5004700	1.8265010
C	-6.1400600	-2.9558200	-0.0935730
H	-6.5643570	-3.9538700	-0.1352010
C	-5.3467470	-2.4956950	-1.1457300
H	-5.1531470	-3.1307850	-2.0040720
C	-4.7998710	-1.2137910	-1.1037450
H	-4.1841790	-0.8501610	-1.9205150
N	-2.8028250	3.9210890	0.2532790
C	-3.3711940	4.9405710	-0.4007890
H	-4.2869760	4.7163540	-0.9437730
C	-2.8407710	6.2278460	-0.4053840
H	-3.3395000	7.0192710	-0.9537220
C	-1.6664540	6.4640370	0.3054620
H	-1.2229730	7.4545590	0.3253280
C	-1.0708200	5.4070870	0.9899480
C	-1.6743570	4.1536190	0.9342420
H	-0.1565610	5.5437860	1.5567630
H	-1.2378870	3.3031330	1.4535220

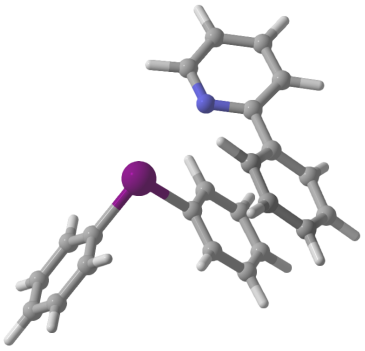

2-phenylpyridine_Ph_2I^+
E_{tot} = -1239.9876446 a.u.
G_{corr} = 0.300345 a.u.

C	-2.4615500	1.0092810	0.8693230
C	-2.2221350	0.2340780	1.9972790
H	-3.0262340	-0.0743660	2.6581150
C	-0.9022730	-0.1264550	2.2658920
H	-0.6844270	-0.7260890	3.1438700
C	0.1285540	0.2987190	1.4277590
H	1.1536450	0.0209460	1.6511470
C	-0.1476430	1.0839430	0.3084360
H	0.6552830	1.4142850	-0.3426110
C	-1.4614120	1.4470270	0.0094370
H	-1.6860840	2.0555560	-0.8606530
I	-4.4462310	1.5552650	0.4495260
C	-5.1421740	-0.4090110	0.1966310
C	-5.8543100	-0.9994180	1.2379530
H	-6.0534210	-0.4623010	2.1596600
C	-6.3086090	-2.3078250	1.0674390
H	-6.8658280	-2.7869490	1.8658070
C	-6.0456250	-2.9928900	-0.1182720
H	-6.4013600	-4.0105470	-0.2431440
C	-5.3295860	-2.3783590	-1.1471520
H	-5.1280540	-2.9132630	-2.0694940
C	-4.8713590	-1.0702110	-0.9996980
H	-4.3168650	-0.5858050	-1.7969030
N	-3.1571320	4.1297560	0.6219930
C	-3.2390880	4.7963430	-0.5339630
H	-4.0663050	4.5242150	-1.1862520
C	-2.3271900	5.7750660	-0.9176710
H	-2.4383180	6.2837100	-1.8685860
C	-1.2794010	6.0697480	-0.0483690
H	-0.5449410	6.8271470	-0.3037230
C	-1.1916990	5.3873640	1.1603380
C	-2.1526000	4.4175900	1.4678340
C	-2.1079900	3.6579470	2.7425830
C	-0.8869090	3.2506460	3.2911310
C	-3.2991170	3.3247780	3.4011340
C	-3.2688220	2.5885900	4.5829080
C	-2.0470890	2.1778020	5.1201990
C	-0.8578570	2.5129970	4.4733550
H	-4.2471980	3.6594880	2.9887610
H	-4.1977140	2.3396350	5.0874220
H	-2.0231100	1.5994500	6.0389270
H	0.0946780	2.1860570	4.8797880
H	-0.4029340	5.6138820	1.8699980
H	0.0422460	3.4798490	2.7758370

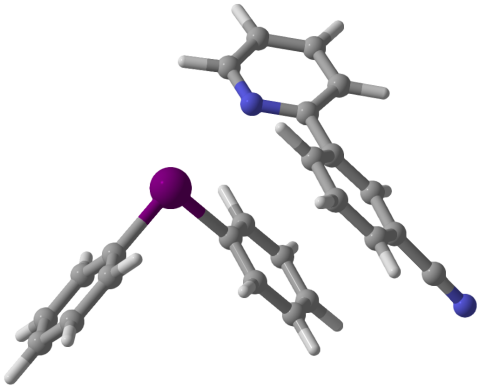

2-(3-cyano)phenylpyridine_Ph_2I^+
E_{tot} = --1332.2424747 a.u.
G_{corr} = 0.295704 a.u.

C	-2.4519880	1.0174300	0.8946140
C	-2.2350680	0.2212840	2.0130060
H	-3.0545750	-0.1162160	2.6399680
C	-0.9187700	-0.1289830	2.3131750
H	-0.7190010	-0.7463610	3.1836480
C	0.1311810	0.3283790	1.5163230
H	1.1529280	0.0603170	1.7658440
C	-0.1231410	1.1312220	0.4039640
H	0.6939520	1.4846490	-0.2165780
C	-1.4324490	1.4826610	0.0723620
H	-1.6389220	2.1025660	-0.7941790
I	-4.4321070	1.5503640	0.4309700
C	-5.1201000	-0.4194970	0.2040320
C	-5.8917530	-0.9706990	1.2239420
H	-6.1411690	-0.4015100	2.1135280
C	-6.3403770	-2.2835180	1.0731620
H	-6.9436210	-2.7336030	1.8547630
C	-6.0121870	-3.0101580	-0.0707060
H	-6.3629770	-4.0313640	-0.1794850
C	-5.2369210	-2.4332460	-1.0783030
H	-4.9849260	-3.0006400	-1.9682390
C	-4.7838250	-1.1212180	-0.9518630
H	-4.1840690	-0.6657690	-1.7332880
N	-3.1708480	4.1680040	0.6123520
C	-3.2544490	4.8366390	-0.5418010
H	-4.0765550	4.5599270	-1.1981130

C	-2.3483380	5.8247300	-0.9182420
H	-2.4609850	6.3355520	-1.8677860
C	-1.3054210	6.1261160	-0.0465870
H	-0.5768800	6.8903920	-0.2977380
C	-1.2139450	5.4394610	1.1604280
C	-2.1694270	4.4637690	1.4574250
C	-2.1242680	3.6929140	2.7263310
C	-0.9070730	3.2454920	3.2394980
C	-3.3112390	3.3789200	3.4017380
C	-3.2868130	2.6251110	4.5727280
C	-2.0762350	2.1651570	5.0840400
C	-0.8912120	2.4807630	4.4103430
H	-4.2562970	3.7405840	3.0062670
H	-4.2129150	2.3940800	5.0885140
H	-2.0444300	1.5665750	5.9881760
C	0.3644770	1.9726670	4.8986200
H	-0.4280750	5.6689340	1.8725940
H	0.0234070	3.4510970	2.7182190
N	1.3740270	1.5543360	5.2821950

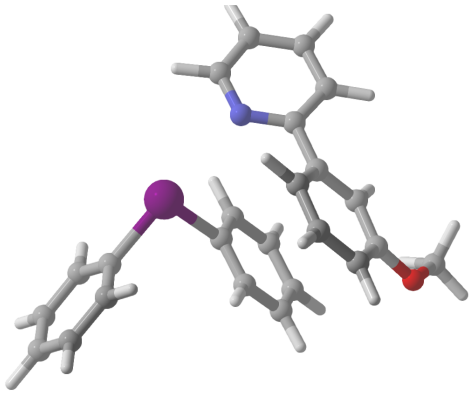

2-(3-methoxy)phenylpyridine_Ph_2I^+
E_{tot} = -1354.5167943 a.u.
G_{corr} = 0.330527 a.u.

C	-2.4318410	1.0271560	0.9629760
C	-2.2445070	0.2730680	2.1147660
H	-3.0759450	-0.0037490	2.7555060
C	-0.9420420	-0.1109830	2.4331440
H	-0.7650160	-0.6960180	3.3303040
C	0.1228710	0.2684930	1.6159110
H	1.1328860	-0.0373640	1.8705210
C	-0.0998100	1.0402920	0.4751070
H	0.7303620	1.3374180	-0.1575840
C	-1.3948830	1.4275170	0.1284540
H	-1.5786250	2.0216870	-0.7608660
I	-4.3948440	1.5751370	0.4509900
C	-5.0816630	-0.3945560	0.2151400
C	-5.8400240	-0.9575150	1.2387640
H	-6.0808550	-0.3957180	2.1354830
C	-6.2860900	-2.2706180	1.0836630
H	-6.8789180	-2.7287650	1.8686030
C	-5.9692510	-2.9873720	-0.0697660
H	-6.3184980	-4.0087130	-0.1825830
C	-5.2074660	-2.4000470	-1.0815220
H	-4.9640500	-2.9596970	-1.9787710
C	-4.7565760	-1.0876590	-0.9492390
H	-4.1664160	-0.6242890	-1.7334430
N	-3.1355940	4.1655550	0.6194760
C	-3.1921310	4.8365130	-0.5354830
H	-3.9848140	4.5445040	-1.2209700
C	-2.2958110	5.8448370	-0.8774230
H	-2.3856740	6.3568050	-1.8288270
C	-1.2911100	6.1644100	0.0327540
H	-0.5704870	6.9450930	-0.1897490
C	-1.2285290	5.4753160	1.2393830
C	-2.1728600	4.4775200	1.5039380
C	-2.1564880	3.7089610	2.7750400
C	-0.9335090	3.2914530	3.3169270
C	-3.3565620	3.3814670	3.4088730
C	-3.3310670	2.6257570	4.5828570
C	-2.1251780	2.1927790	5.1187010
C	-0.9214480	2.5252730	4.4834040
H	-4.2982390	3.7276420	2.9937200
H	-4.2607790	2.3727610	5.0837420
H	-2.0905250	1.5939480	6.0236090
O	0.2085740	2.0390410	5.0586920
H	-0.4735310	5.7176730	1.9800580
H	-0.0122460	3.5266940	2.7951670
C	1.4543570	2.4049980	4.4848890
H	2.2184880	1.9366070	5.1037060
H	1.5846860	3.4926920	4.4970430
H	1.5371790	2.0355590	3.4570400

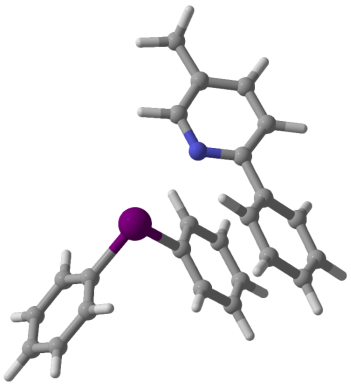

2-phenyl-5-methylpyridine_Ph_2I^+
E_{tot} = -1279.2991986 a.u.
G_{corr} = 0.324996 a.u.

C	-2.4702040	0.9912040	0.9190500
C	-2.2360910	0.2159590	2.0482380
H	-3.0421140	-0.0847320	2.7103070
C	-0.9189460	-0.1544480	2.3165250
H	-0.7051520	-0.7537960	3.1956990
C	0.1146150	0.2603060	1.4763800
H	1.1376180	-0.0254060	1.6994590
C	-0.1561150	1.0459470	0.3560430
H	0.6489390	1.3687430	-0.2962250
C	-1.4671030	1.4197840	0.0579770
H	-1.6880440	2.0298930	-0.8119960
I	-4.4498230	1.5523800	0.4985650
C	-5.1451410	-0.4071220	0.2034640
C	-5.9043960	-1.0015390	1.2083600
H	-6.1396350	-0.4703770	2.1250290
C	-6.3572210	-2.3064350	1.0086450
H	-6.9506940	-2.7886470	1.7785390
C	-6.0452860	-2.9848170	-0.1689680
H	-6.3991470	-4.0001560	-0.3161150
C	-5.2818620	-2.3666240	-1.1609930
H	-5.0419350	-2.8964490	-2.0771030
C	-4.8252890	-1.0614750	-0.9845680
H	-4.2341670	-0.5744750	-1.7537620
N	-3.1553630	4.1080170	0.6907250
C	-3.2496910	4.7749810	-0.4642890
H	-4.0867830	4.5021380	-1.1061680
C	-2.3501060	5.7576490	-0.8773790
C	-2.5117620	6.4709990	-2.1914550
C	-1.2927700	6.0383500	-0.0064140
H	-0.5589470	6.7959030	-0.2707000
C	-1.1865170	5.3587770	1.1996000
C	-2.1430110	4.3896080	1.5253040
C	-2.0824220	3.6302250	2.7990930
C	-0.8542550	3.2248600	3.3331820
C	-3.2645580	3.2937080	3.4721190
C	-3.2185300	2.5568460	4.6530250
C	-1.9897440	2.1487480	5.1758850
C	-0.8092190	2.4871180	4.5148270
H	-4.2183260	3.6264940	3.0713760
H	-4.1408860	2.3054610	5.1682970
H	-1.9534730	1.5701270	6.0940480
H	0.1489020	2.1620750	4.9095530
H	-0.3851240	5.5872650	1.8945870
H	0.0680950	3.4563220	2.8066470
H	-3.3939620	6.1131670	-2.7281110
H	-1.6360760	6.3150140	-2.8292500
H	-2.6190770	7.5492720	-2.0373210

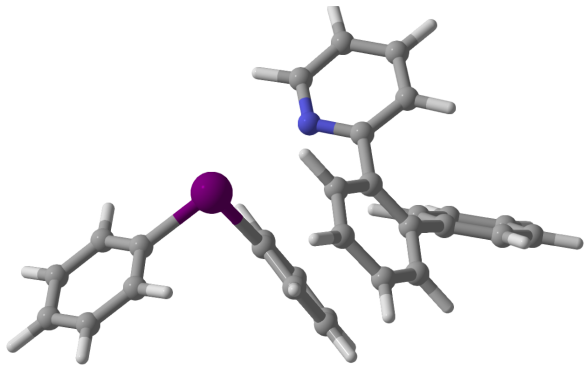

2-(2-phenyl)phenylpyridine_Ph_2I^+
E_{tot} = -1471.0312944 a.u.
G_{corr} = 0.377258 a.u.

C	-0.8442520	-0.5829700	-0.8135430
C	-0.3840770	-1.6430730	-0.0397780
H	-0.5063440	-1.6535430	1.0398800
C	0.2588920	-2.6937730	-0.6952110
H	0.6369890	-3.5286250	-0.1132530
C	0.4238520	-2.6645530	-2.0796910
H	0.9280300	-3.4855890	-2.5793580
C	-0.0402980	-1.5805760	-2.8260640
H	0.0978410	-1.5553930	-3.9021020
C	-0.6849780	-0.5163290	-2.1948300
H	-1.0511070	0.3299620	-2.7667250
I	-1.8983160	0.9573540	0.1400100
C	-3.7746610	0.0241820	-0.0184620
C	-4.1683940	-0.8609740	0.9831090
H	-3.5299180	-1.0655440	1.8368750
C	-5.4098540	-1.4848810	0.8624460
H	-5.7352980	-2.1789260	1.6305170
C	-6.2269280	-1.2162600	-0.2363310
H	-7.1923810	-1.7045560	-0.3220210
C	-5.8124230	-0.3227600	-1.2243900
H	-6.4501770	-0.1143480	-2.0772940
C	-4.5736250	0.3103330	-1.1232520
H	-4.2449300	1.0054200	-1.8890260
N	0.7105260	2.1127010	0.0822990
C	0.7973940	3.1788980	-0.7226790
H	-0.1336260	3.5179670	-1.1718970
C	1.9940760	3.8345330	-0.9895710
H	2.0102710	4.6938320	-1.6505190
C	3.1550110	3.3584490	-0.3817860
H	4.1096360	3.8454860	-0.5542560
C	3.0728720	2.2496910	0.4513590
C	1.8285900	1.6444790	0.6580180
C	1.6782260	0.4642570	1.5555050
C	2.4439010	-0.7069870	1.3933650
C	0.7493950	0.5465690	2.5996430
C	0.5703110	-0.5108450	3.4877600

C	1.3334650	-1.6689840	3.3377370
C	2.2588720	-1.7590960	2.3009370
H	0.1779090	1.4631420	2.7223600
H	-0.1529950	-0.4280930	4.2930020
H	1.2028300	-2.5036000	4.0196830
H	2.8286430	-2.6746260	2.1653350
H	3.9542560	1.8470680	0.9405700
C	3.3891260	-0.8944380	0.2591890
C	2.9941990	-0.6190810	-1.0569850
H	1.9894380	-0.2491200	-1.2502020
C	3.8683870	-0.8297090	-2.1200600
H	3.5408480	-0.6207420	-3.1345790
C	5.1564630	-1.3136410	-1.8828580
H	5.8399320	-1.4747590	-2.7110830
C	5.5594750	-1.5922770	-0.5768240
H	6.5602630	-1.9666130	-0.3831030
C	4.6796000	-1.3883510	0.4861520
H	5.0012740	-1.5984680	1.5031450

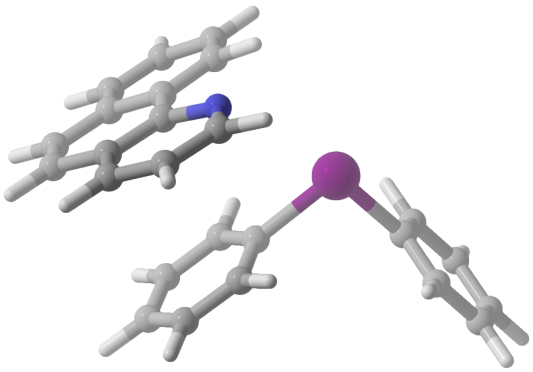

Option A: benzo[*h*]quinoline_Ph_2I^+
E_{tot} = -1316.2178767 a.u.
G_{corr} = 0.312627 a.u.

C	-2.4852540	1.2189020	0.5126290
C	-1.8611200	0.8154210	1.6896640
H	-2.4245090	0.6437150	2.6021060
C	-0.4762920	0.6605270	1.6643930
H	0.0402370	0.3578390	2.5698070
C	0.2393320	0.9097770	0.4920500
H	1.3186680	0.7956890	0.4870520
C	-0.4190900	1.3101120	-0.6698740
H	0.1402160	1.5056850	-1.5790600
C	-1.8054740	1.4725020	-0.6729240
H	-2.3257370	1.7923230	-1.5696800
I	-4.5589360	1.5317220	0.5444800
C	-5.1314400	-0.4642610	0.2428100
C	-5.4318040	-1.2404590	1.3589260
H	-5.3808260	-0.8310820	2.3622930
C	-5.8003590	-2.5694130	1.1494130
H	-6.0394480	-3.1961260	2.0022720
C	-5.8602390	-3.0865340	-0.1447390
H	-6.1484460	-4.1214550	-0.2980900
C	-5.5543530	-2.2833490	-1.2441680
H	-5.6030750	-2.6882210	-2.2496480
C	-5.1857390	-0.9511730	-1.0604870
H	-4.9481440	-0.3197850	-1.9101070
N	-3.2281080	4.2735730	0.9665180
C	-3.0364870	4.7324090	-0.2613650
H	-3.9233820	4.8224760	-0.8855260
C	-1.7742410	5.0794710	-0.7764280
H	-1.6850070	5.4511130	-1.7911470
C	-0.6716170	4.9090180	0.0322490
H	0.3284290	5.1358260	-0.3288260
C	-0.8395370	4.4221630	1.3451180
C	0.2747040	4.1925520	2.2238700
C	-2.1546630	4.1381620	1.7828840
C	-2.3675430	3.6420430	3.1313970
C	0.0811910	3.6881770	3.4685570
C	-1.2414400	3.3925000	3.9537540
C	-3.6605240	3.3814770	3.6342900
C	-3.8286860	2.8509830	4.8988070
C	-2.7083650	2.5745210	5.7078470
C	-1.4378300	2.8509580	5.2444580
H	1.2740420	4.4170840	1.8607830
H	0.9260890	3.4967860	4.1248810
H	-4.5220950	3.6143480	3.0173400
H	-4.8280990	2.6528260	5.2738920
H	-2.8471770	2.1550970	6.6995250
H	-0.5694830	2.6553290	5.8683550

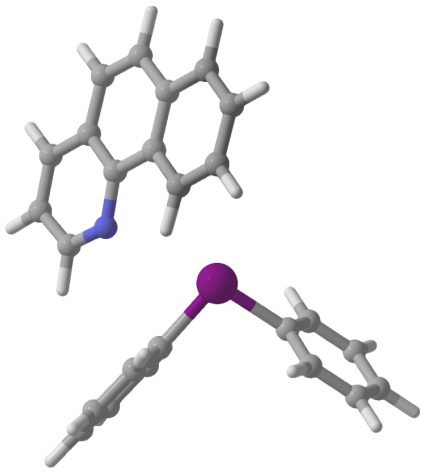

Option B: benzo[*h*]quinoline_Ph_2I^+
E_{tot} = -1316.2123351 a.u.
G_{corr} = 0.310476 a.u.

I	-4.5411960	0.7707960	0.2984150
C	-5.3219320	-1.1413140	0.6638030

C	-5.7551040	-1.4443190	1.9514640
H	-5.6961630	-0.7163810	2.7535840
C	-6.2684630	-2.7207410	2.1840850
H	-6.6132590	-2.9822980	3.1790470
C	-6.3332540	-3.6514220	1.1475780
H	-6.7320970	-4.6424990	1.3381080
C	-5.8904140	-3.3182790	-0.1336340
H	-5.9439910	-4.0443980	-0.9380950
C	-5.3803860	-2.0470580	-0.3924870
H	-5.0377310	-1.7788130	-1.3866340
C	-2.5204070	0.2204320	0.2460150
C	-1.8951770	-0.1298580	1.4379270
H	-2.4332770	-0.1447050	2.3801200
C	-0.5394170	-0.4536440	1.3856960
H	-0.0238540	-0.7311690	2.2991120
C	0.1492580	-0.4082570	0.1726950
H	1.2058210	-0.6539390	0.1445390
C	-0.5088250	-0.0474400	-1.0032920
H	0.0289120	-0.0129650	-1.9450170
C	-1.8668770	0.2723800	-0.9801870
H	-2.3855830	0.5586870	-1.8887740
N	-3.0917370	3.4171760	-0.1033960
C	-4.0102830	4.4090270	0.0105510
C	-5.1510320	4.4098080	-0.8900110
C	-3.8910810	5.4311270	0.9816470
C	-4.9306650	6.4148390	1.1195540
C	-2.7415430	5.4358300	1.7983660
H	-2.6225310	6.2140360	2.5477010
C	-1.7872910	4.4557630	1.6345200
H	-0.8853560	4.4318760	2.2357140
C	-2.0198480	3.4548270	0.6740980
H	-1.3015760	2.6468040	0.5467710
C	-6.0272130	6.3790070	0.3212550
C	-6.1644520	5.3836200	-0.7101780
C	-7.2867570	5.3776380	-1.5695200
C	-5.2633930	3.4893240	-1.9550160
C	-6.3661500	3.5055390	-2.7863300
C	-7.3922080	4.4502800	-2.5861480
H	-4.8199500	7.1803350	1.8826600
H	-6.8177000	7.1159250	0.4350220
H	-8.0636920	6.1231220	-1.4215820
H	-4.4578360	2.7835060	-2.1283240
H	-6.4380670	2.7942750	-3.6033650
H	-8.2575730	4.4565770	-3.2415950

Q. References Cited

1. S. Kirchberg, R. Fröhlich and A. Studer, *Angew. Chem. Int. Ed.*, 2010, **49**, 6877.
2. L. Zhang and L. Jiao, *J. Am. Chem. Soc.*, 2019, **141**, 9124.
3. N. R. Deprez and M. S. Sanford, *J. Am. Chem. Soc.*, 2009, **131**, 11234.
4. J. Y. Kim, S. H. Park, J. Ryu, S. H. Cho, S. H. Kim and S. Chang, *J. Am. Chem. Soc.*, 2012, **134**, 9110.
5. C. Liu and W. Yang, *ChemComm.*, 2009, DOI: 10.1039/B912364D, 6267.
6. J. Martín, E. Gómez‐Bengoa, A. Genoux and C. Nevado, *Angew. Chem. Int. Ed.*, 2022, **61**, e202116755.
7. X. Rao, C. Liu, J. Qiu and Z. Jin, *Org. Biomol. Chem.*, 2012, **10**, 7875.
8. W. Miao, C. Ni, P. Xiao, R. Jia, W. Zhang and J. Hu, *Org Lett*, 2021, **23**, 711.
9. P. Guo, J. M. Joo, S. Rakshit and D. Sames, *J. Am. Chem. Soc.*, 2011, **133**, 16338.
10. C. Yin, K. Zhong, W. Li, X. Yang, R. Sun, C. Zhang, X. Zheng, M. Yuan, R. Li, Y. Lan, H. Fu and H. Chen, *Adv. Synth. Catal.*, 2018, **360**, 3990.
11. J. Liu, Y. Xiao, J. Hao and Q. Shen, *Org. Lett.*, 2023, **25**, 1204.
12. P. Gandeepan, J. Koeller, K. Korvorapun, J. Mohr and L. Ackermann, *Angew. Chem. Int. Ed. Engl.*, 2019, **58**, 9820.
13. Z.-L. Gong and Y.-W. Zhong, *Inorganic Chemistry*, 2016, **55**, 10143.
14. E. Zhang, J. Tang, S. Li, P. Wu, J. E. Moses and K. B. Sharpless, *Chem. Eur. J.*, 2016, **22**, 5692.
15. J. Martín, E. Gómez-Bengoa, A. Genoux and C. Nevado, *Angew. Chem. Int. Ed.*, 2022, **61**, e202116755.
16. P. St. Onge, S. I. Khan, A. Cook and S. G. Newman, *Org. Lett.*, 2023, **25**, 1030.
17. *JP Pat.,* GB2423518, 2006.
18. Y. Li, W. Liu and C. Kuang, *ChemComm.*, 2014, **50**, 7124.
19. J. N. Levy, J. V. Alegre-Requena, R. Liu, R. S. Paton and A. McNally, *J. Am. Chem. Soc.*, 2020, **142**, 11295.
20. Y. Hu, Y. Gao, J. Ye, Z. Ma, J. Feng, X. Liu, P. Lei and M. Szostak, *Org. Lett.*, 2023, **25**, 2975.
21. H. Rhee, T. Kim and J.-I. Hong, *Dalton Transactions*, 2018, **47**, 3803.
22. Á. Sinai, Á. Mészáros, T. Gáti, V. Kudar, A. Palló and Z. Novák, *Org. Lett.*, 2013, **15**, 5654.
23. M. S. McCammant, S. Thompson, A. F. Brooks, S. W. Krska, P. J. H. Scott and M. S. Sanford, *Org. Lett.*, 2017, **19**, 3939.
24. G. Laudadio, H. P. L. Gemoets, V. Hessel and T. Noël, *J. Org. Chem.*, 2017, **82**, 11735.
25. A. F. Fearnley, J. An, M. Jackson, P. Lindovska and R. M. Denton, *ChemComm.*, 2016, **52**, 4987.
26. B. Zhou, W. Hou, Y. Yang, H. Feng and Y. Li, *Org. Lett.*, 2014, **16**, 1322.
27. L. Su, D.-D. Guo, B. Li, S.-H. Guo, G.-F. Pan, Y.-R. Gao and Y.-Q. Wang, *ChemCatChem*, 2017, **9**, 2001.
28. M. J. Frisch, G. W. Trucks, H. B. Schlegel, G. E. Scuseria, M. A. Robb, J. R. Cheeseman, G. Scalmani, V. Barone, G. A. Petersson, H. Nakatsuji, X. Li, M. Caricato, A. V. Marenich, J. Bloino, B. G. Janesko, R. Gomperts, B. Mennucci, H. P. Hratchian, J. V. Ortiz, A. F. Izmaylov, J. L. Sonnenberg, Williams, F. Ding, F. Lipparini, F. Egidi, J. Goings, B. Peng, A. Petrone, T. Henderson, D. Ranasinghe, V. G. Zakrzewski, J. Gao, N. Rega, G. Zheng, W. Liang, M. Hada, M. Ehara, K. Toyota, R. Fukuda, J. Hasegawa, M. Ishida, T. Nakajima, Y. Honda, O. Kitao, H. Nakai, T. Vreven, K. Throssell, J. A. Montgomery Jr., J. E. Peralta, F. Ogliaro, M. J. Bearpark, J. J. Heyd, E. N. Brothers, K. N. Kudin, V. N. Staroverov, T. A. Keith, R. Kobayashi, J. Normand, K. Raghavachari, A. P. Rendell, J. C. Burant, S. S. Iyengar, J. Tomasi, M. Cossi, J. M. Millam, M. Klene, C. Adamo, R. Cammi, J. W. Ochterski, R. L. Martin, K. Morokuma, O. Farkas, J. B. Foresman and D. J. Fox, *Gaussian 16 Rev. B.01*, 2016.
29. Y. Zhao and D. G. Truhlar, *Theor. Chem. Acc.*, 2008, **120**, 215.
30. B. P. Pritchard, D. Altarawy, B. Didier, T. D. Gibson and T. L. Windus, *J. Chem. Inform. Model*, 2019, **59**, 4814.
31. a) G. A. Petersson and M. A. Al‐Laham, *J. Chem. Phys.*, 1991, **94**, 6081; b) G. A. Petersson, A. Bennett, T. G. Tensfeldt, M. A. Al‐Laham, W. A. Shirley and J. Mantzaris, *J. Chem. Phys.*, 1988, **89**, 2193.
32. B. Andrea N. and W. Steven, *Popular Integration Grids Can Result in Large Errors in DFT-Computed Free Energies*, 2019.
33. C. Y. Legault, http://www.cylview.org).
34. G. Cavallo, P. Metrangolo, R. Milani, T. Pilati, A. Priimagi, G. Resnati and G. Terraneo, *Chem. Rev.*, 2016, **116**, 2478.

35. W. Lecroq, P. Bazille, F. Morlet-Savary, M. Breugst, J. Lalevée, A.-C. Gaumont and S. Lakhdar, *Org. Lett.*, 2018, **20**, 4164.